

**How Lichens Work: Functional Aspects of Symbiosis Viewed through Metagenomics and
other Culture-Free Methods**

by

Gulnara Tagirdzhanova

A thesis submitted in partial fulfillment of the requirements for the degree of

Doctor of Philosophy

in

Systematics and Evolution

Department of Biological Sciences
University of Alberta

© Gulnara Tagirdzhanova, 2022

Abstract

Lichens are symbiotic organisms formed around the relationship between a hyphal fungus and a phototrophic unicellular organism, usually a green alga or a cyanobacterium. In addition to the main two partners, lichens often include bacteria and yeasts. Together, the symbiotic partners create architectures that are both fascinating and challenging to study.

In this thesis, I studied how the lichen symbiosis works, and attempted to understand how different symbiotic partners contribute to the symbiotic outcome. I focused primarily on the under-studied yeasts and bacteria of the lichen symbiosis. My other goal was to develop approaches that can be used in the future to better understand lichen symbiosis.

My analyses of metagenomic data generated from lichens gave three main results: 1) I obtained the first genomes of lichen yeasts, thus providing the first direct evidence on their biology and role in the lichen symbiosis. The genomes of the yeasts were smaller than that of the main fungal partner and showed signs of nutrient limitation and scavenging. Compared to the main fungal partner, the genomes of lichen yeasts harboured fewer secondary metabolism gene clusters and pathogenicity signatures, but a larger repertoire of genes potentially involved in the biosynthesis of acidic polysaccharides. 2) I discovered that bacterial communities in lichens are unexpectedly structured, and the majority of bacterial occurrences come from just four families. The two most frequent families, Beijerinckiaceae and Acetobacteraceae, included lineages that I identified as aerobic anoxygenic phototrophs. These bacteria were present in samples across all major lichen groups and geographies. I established that these bacteria are not capable of fixing atmospheric nitrogen, but have biosynthetic pathways for vitamins essential for the eukaryotic symbionts. 3) Finally, I tested a recently published hypothesis that lichen fungi rely on algae for the synthesis of ATP. I showed that contrary to the hypothesis, lichen fungi have not lost a gene essential for

oxidative phosphorylation, and therefore the proposed mechanism of lichen symbiont interdependence is not valid. In addition to my metagenomics work, I developed a protocol for measuring relative abundances of lichen symbionts via ddPCR. Using this method, I tested hypotheses on the role yeasts play in lichens.

This research has significantly expanded our knowledge of lichen yeasts and bacteria, and also provided resources for future exploration. This includes both methods developed during this project, and genomes of lichen symbionts that will be publicly available for future use.

Preface

This thesis contains results of my original work, as well as results of collaborative research.

Some of these results have been published in peer-reviewed journals.

A version of Chapter 2 has been published as Tagirdzhanova, G., Saary, P., Tingley, J. P., Díaz-Escandón, D., Abbott, D. W., Finn, R. D., & Spribille, T. (2021). Predicted input of uncultured fungal symbionts to a lichen symbiosis from metagenome-assembled genomes. *Genome Biology and Evolution*, 13(4), evab047. I was responsible for obtaining the cortex slurry metagenome, genome annotation, comparative genomics analysis, and PCR screening. Paul Saary (EBI-EMBL) did metagenomic assembly and binning. Jeffrey Tingley (Agriculture and Agri-Food Canada) performed a portion of analysis related to Carbohydrate-Active enZymes. David Díaz-Escandón (University of Alberta) calculated the phylogenomic tree. Toby Spribille supervised the project and made the bulk lichen metagenome. All co-authors contributed to writing the manuscript.

A version of Chapter 3 has been published as Tagirdzhanova, G., McCutcheon, J. P. & Spribille, T. (2021) Lichen fungi do not depend on the alga for ATP production: A comment on Pogoda et al. (2018). *Molecular Ecology*, 30(17), 4155-4159. I was responsible for gathering and analyzing data and drafting the manuscript. Toby Spribille supervised the project, and John McCutcheon (Arizona State University) contributed to the study design.

A version of Chapter 4 is intended for publication as: Tagirdzhanova, G., Cameron, E., Saary, P., Garber, A., Stein, L., Finn, R. D., & Spribille, T. Lichen bacterial communities revealed by metagenomics. I gathered data and performed most of the data analysis: occurrence analysis, marker gene screening, genome annotations and functional genomics analyses, etc., unless stated otherwise. Ellen Cameron and Paul Saary (EBI-EMBL) performed metagenomic assembly and

binning, and initial taxonomic assignments, plus a portion of genome annotations. Arkadiy Garber (University of Arizona) annotated iron-related genes. Toby Spribille supervised the project and prepared metagenomic libraries for a portion of the *de novo* sequenced metagenomes. Spencer Goyette and Veera Tuovinen (University of Alberta) contributed to the lab work. Lisa Stein (University of Alberta) and Rob Finn (EBI-EMBL) contributed to the study design.

A version of Chapter 5 is intended for publication as: Tagirdzhanova, G., Cook, J., Vinebrooke, R. & Spribille, T. Linking the abundance of basidiomycete yeasts to the lichen phenotype. I was responsible for the metagenomic analysis, designing and performing the qPCR and ddPCR experiments, assessing lichen morphology and water holding capacity, and data analysis. Jenna Cook (Rolf Vinebrooke lab, University of Alberta) measured vulpinic acid concentration in the samples. Yngvar Gauslaa helped with the interpretation of the water storage experiment. Spencer Goyette and Sophie Dang (University of Alberta) prepared metagenomic libraries. Toby Spribille supervised the project and collected the samples.

When we approach the places where facts and machines are made, we get into the midst of controversies. The closer we are, the more controversial they become. When we go from 'daily life' to scientific activity, from the man in the street to the men in the laboratory, from politics to expert opinion, we do not go from noise to quiet, from passion to reason, from heat to cold. We go from controversies to fiercer controversies.

— Bruno Latour, “Science in Action”

As the man said, for every complex problem there's a simple solution, and it's wrong.

— Umberto Eco, “Foucault's Pendulum”

All things are so very uncertain, and that's exactly what makes me feel reassured.

— Tove Jansson, “Moominland Midwinter”

Acknowledgements

I do not know how common this is, but I started to think about my thesis acknowledgements almost as soon as I started my program: I didn't want to forget anyone. Now writing these lines, I am going through the list I compiled in my head over the last five years; year by year and term by term. It is wild to see how much I have changed over these years, and how much the world has changed. Leaving the regrettable state of the world aside, I wanted to thank everyone who helped me in this journey. My path through the PhD program started with a 7,000 km first step and continued accordingly — through learning a new culture and adjusting to a new language, through a myriad of steep learning curves, through all the highs and all the lows. It wasn't always easy, but it was amazing. This journey has changed me into a person I am now, and I would not trade it for anything.

First of all, I want to thank my supervisor, Toby Spribille. Thank you for giving me the opportunities to learn, grow, and pursue my research interests. Thank you for pushing me to go beyond what I thought I was capable of. I have grown immensely, both as a scientist and as a person, and I feel lucky to have had the chance to learn from you. Thank you for your support and patience during the tough times. Thank you for bringing together the amazing members of the lab, and for all the road trips we had together!

I want to thank John McCutcheon and Warren Gallin, the members of my supervisory committee. Thank you for your support and encouragement, and for all the challenging questions you asked during the committee meetings. I also want to thank Lisa Stein and Joel Dacks, who participated in my candidacy exam, and Betsy Arnold and Janice Cooke, who agreed to be examiners at my defense.

I want to thank all members of the UofA Symbiosis & Evolution Lab: Spencer Goyette, Veera Tuovinen, Amelia Deneka, David Díaz-Escandón, Carmen Allen, Samantha Pedersen, and Alejandro Huereca Delgado. Thank you for being there, for teaching me things, and for all the fun we had together. The years I spent side-by-side with you were wild and will always occupy a special part in my heart. Also thanks to Katherine Drotos, Antoine Simon, and David Nogerius for sharing some of these adventures!

I want to thank my collaborators, without whom this work would not be possible. Special thanks go to Paul Saary, Rob Finn, and Ellen Cameron from the EBI-EMBL. Your contributions were essential to the success of this project, and I feel very lucky for having this opportunity to do science with you.

During the last five years I learned a lot, and I want to thank everyone who took time from their busy schedule and shared with me their expertise: Piotr Lukasik, Sophie Dang, Troy Locke, Vasilis Kokkoris, Sergey Nurk, Yngvar Gauslaa. I, truly, would have never succeeded without your help. I also want to thank the people who helped me with their advice and wisdom when I struggled navigating life in academia and life in general: Lisa Stein, Viktoria Wagner, Trevor Goward, Curtis Björk, Oksana Vernygora.

I want to thank the graduate students of our department, and especially the BGSA execs 2020-2021 and the BGSA EDI group. Special thanks go to Spencer Goyette and Andrew Cook, for luring me into becoming an active member of the graduate student community, which was intimidating at first but very rewarding later.

I want to thank everyone who helped maintain my sanity during tough times. Big thanks to Katya Rozantseva for the friendship. Thanks to Scott Claypool for the coffee and chats. I also

think it would be only fair to thank Ezh the cat, Titus the cat, Kitty the cat, Clara the cat, and Coco the dog, even though they probably aren't going to read these lines.

I want to thank everyone who supported and guided me through my training during the pre-PhD years. I fully appreciate that I would never ever be where I am today without your help. Thanks to Irina Stepanchikova and Dmitry Himelbrandt for introducing me to lichenology and all the opportunities that they gave me for professional growth. Thanks to Eugenia Rysnaya, who taught me to be interested in nature. Big thanks to Alyona Kushnevskaia for encouraging me to take a leap of faith and go on this big adventure. Thank you for believing in me when I did not.

And finally, my biggest thanks go to my family, for always being with me, no matter how many thousands of kilometers separate us. Thanks to my parents, Almira and Mukhammed, for supporting me, and all and any of my academic pursuits. Thanks to my brother, Azat, for always being there for me. Thanks to my future husband, Seidon, for being the safe haven of my life. I love you all and cannot thank you enough.

This research was supported by start-up funds from the Department of Biological Sciences at the University of Alberta and NSERC Discovery Grant granted to Toby Spribille and by funding from Alberta Graduate Excellence Scholarship and Alberta Innovate Graduate Student Scholarship.

Table of Contents

Chapter 1. Introduction	1
Chapter 2. Predicted Input of Uncultured Fungal Symbionts to a Lichen Symbiosis from Metagenome-Assembled Genomes	13
2.1. Abstract	13
2.2. Significance.....	14
2.3. Introduction.....	14
2.4. Results.....	17
2.5. Discussion	30
2.6. Materials and Methods.....	37
References.....	45
Chapter 3. Lichen fungi do not depend on the alga for ATP production	65
3.1. Abstract	65
3.2. Introduction.....	65
3.3. Methods.....	67
3.4. Results.....	70
3.5. Discussion	72
3.6. Supplementary material and data availability.....	74
References.....	74
Chapter 4. Lichen bacterial communities revealed by metagenomics.....	81
4.1. Abstract	81
4.2. Introduction.....	81
4.3. Methods.....	84
4.4. Results.....	91
4.5. Discussion	104
References.....	117
Chapter 5. Linking the abundance of basidiomycete yeasts to the lichen phenotype	192
5.1. Abstract	192
5.2. Introduction.....	192
5.3. Methods.....	195
5.4. Results.....	203
5.5. Discussion	206
References.....	213
Chapter 6. General Conclusions	235
Bibliography	245

List of Tables

Table 2.1. Draft Genome Statistics for the Bulk-Lichen and Cortex-Slurry Metagenomes Following Bin Merging.....	59
Table 4.1. Metagenomic data used in the analysis.....	132
Table 4.2. Details on the metagenomes generated de novo for this study.....	160
Table 4.3. Metagenomes derived from potentially misidentified samples.	161
Table 4.4. Reference genomes from NCBI used for the Rhizobiales phylogenomic tree.	162
Table 4.5. Sequences used as a tblastn query for the screening of Rhizobiales genomes.	175
Table 5.1. Specimens of <i>Bryoria fremontii</i> used in the analysis	220
Table 5.2. Metagenome-assembled genomes used for designing the ddPCR survey.....	224
Table 5.3. Oligonucleotide primers used for PCR.....	225

List of Figures

Fig. 2.1. The assignment of contigs to bins and genomes in the two <i>Alectoria</i> lichen metagenomes.....	60
Fig. 2.2. Maximum likelihood phylogenomic tree based on 42 fungal proteomes and 71 single-copy orthologous loci.....	61
Fig. 2.3. Frequency of association of the three low-abundance partners identified in the cortex-derived metagenome based on PCR-screening of <i>Alectoria</i> lichen thalli paired with a random non- <i>Alectoria</i> lichen and tree bark from the same branch on 32 trees from three localities in BC and AB, Canada.	62
Fig. 2.4. Comparative genomic analysis of the three fungi from <i>Alectoria</i> lichen with closely related genomes.	63
Fig. 2.5. Carbohydrate-active enzymes (CAZymes) in the three fungal MAGs.	64
Fig. 3.1. GC-coverage plots for the four metagenomes produced in this study.	79
Fig. 3.2. Phylogenetic tree of F1F0 ATP synthase subunit C across fungi and bacteria.....	80
Fig. 4.1. Lichen metagenomes arranged by sequencing depth.	176
Fig. 4.2. Maximum likelihood phylogenetic trees of the MAGs.....	177
Fig. 4.3. Co-occurrence networks of lichen symbionts based on presence-absence of MAGs in each metagenome.....	178
Fig. 4.4. Comparing different clustering methods for grouping bacterial genera based on their occurrence profiles in lichen metagenomes.....	179
Fig. 4.5. Comparing different clustering methods for grouping metagenomes based on their bacterial communities.	180
Fig. 4.6. Ordination plot of lichen bacterial communities.	181
Fig. 4.7. CCA ordination plot of bacterial communities in peltigeralean lichens.	182
Fig. 4.8. Number of recovered MAGs as a function of sequencing depth (bp).....	183
Fig. 4.9. Recovery of MAGs of the main two symbionts as a function of sequencing depth. ...	184
Fig. 4.10. Detection of the key groups of symbionts in lichen metagenomes based on three methods of screening: presence of MAGs, presence of rDNA (16S for prokaryotes and 18S for eukaryotes) in the metagenomic assemblies, and presence of rDNA in the raw, unassembled reads.	185
Fig. 4.11. Relative abundances of symbionts in lichen metagenomes.....	186
Fig. 4.12. Comparing different clustering methods for grouping bacterial MAGs based on their KEGG profiles.	187
Fig. 4.13. Taxonomic coherence for the outcomes of three clustering methods: hdbscan, apcluster, and kmeans.	188
Fig. 4.14. Presence of selected pathways and protein complexes in the MAGs of most common lichen bacteria.	189
Fig. 4.15. Maximum likelihood phylogenetic tree of Rhizobiales.	190
Fig. 4.16. Number of genes assigned to each CAZy class per MAG.	191
Fig. 5.1. Specimens of <i>B. fremontii</i>	227
Fig. 5.2. Study design.	228
Fig. 5.3. Examples of images created during the data generation steps.	229
Fig. 5.4. Histograms of the relative abundances of lichen symbionts.	230
Fig. 5.5. The relationship between yeast relative abundance and vulpinic acid concentration. .	231

Fig. 5.6. The relationship between lichen colour type and other characteristics of a lichen sample.	232
Fig. 5.7. Water storage characteristics of <i>B. fremontii</i> in relation to the relative yeast abundance and batch effect.	233
Fig. 5.8. The relationship between sample STM and its colour and vulpinic acid concentration, in the two analyzed batches.	234

Abbreviations

AA	Auxiliary Activity enzyme. A CAZy class.
AAP	Aerobic Anoxygenic Phototrophs. A functional group of bacteria.
ANI	Average Nucleotide Identity. A nucleotide-level similarity index for comparing genomes
ATP	Adenosine Triphosphate
BUSCO	Benchmarking Universal Single-Copy Orthologs. BUSCO is a software for assessing quality of genomic assemblies, based on the presence/absence of universal marker genes (referred to as ‘BUSCO genes’)
CAZy	Carbohydrate-Active enZyme. A database of enzymes involved in synthesis, modification, and breaking-down complex carbohydrates
CCA	Canonical Correspondence Analysis
CE	Carbohydrate Esterase. A CAZy class
ddPCR	droplet digital PCR
DM	Dry Mass
FISH	Fluorescence <i>in situ</i> Hybridization
GH	Glycoside Hydrolase. A CAZy class
GT	Glycosyltransferase. A CAZy class
HMM	Hidden Markov Model
HPLC	High-Performance Liquid Chromatography

ITS	Internal Transcribed Spacer. A locus of ribosomal DNA
MAG	Metagenome-Assembled Genome. A genomic assembly recovered from a binned metagenome
PL	Polysaccharide Lyase. A CAZy class
qPCR	quantitative PCR
rDNA	ribosomal DNA
SA	Surface Area
SFS	Secondary Fungal Symbionts
SMGC	Secondary Metabolism Gene Clusters
SSU	Small Subunit. A locus of ribosomal DNA
STM	Specific Thallus Mass. A proxy of thickness for lichens with hair-like architecture. Calculated as dry weight divided by surface area
WHC	Water Holding Capacity. The amount of water sample can hold, given in mg H ₂ O per cm ² of surface area
WM	Wet Mass

Chapter 1. Introduction

Symbiosis

Symbiosis is a successful evolutionary strategy that shapes life on Earth as we know it. First and foremost, one of the three branches of life, eukaryotes, emerged as a result of symbiosis between multiple prokaryotes (Margulis 1981). This key symbiosis event, however, is far from the only example of a symbiotic association that had planet-scale consequences. Other, more recent, symbioses play important roles in defining ecosystems and channeling the global biogeochemical cycles. The most obvious example here is mycorrhizae, a diverse array of symbioses between plants and fungi. Mycorrhizae are ubiquitous in terrestrial ecosystems and there they regulate cycles of carbon, nitrogen, and phosphorus (van der Heijden et al. 2015). Other examples include: nitrogen-fixing bacterial symbionts in plants (nitrogen cycle; Herridge et al. 2008), photosynthetic symbionts in corals and other invertebrates (carbon cycle; Yellowlees et al. 2008), and chemoautotrophic symbionts in marine animals (sulfur cycle; Cavanaugh 1983). In fact, a big portion of animal species — notably, not all, see Hammer et al. (2019) — engage in a symbiosis with their microbial symbionts, and the symbionts have shaped the evolution of the animal kingdom (Zilber-Rosenberg & Rosenberg 2008, McFall-Ngai 2013). Symbioses are typically based on a flow of goods and services between partners that benefits at least one of them. The examples of goods and services are diverse. They include nutrition: e.g. organic carbon “traded” by a plant for phosphorus (Wyatt et al. 2014); essential amino acids that bacterial symbionts provide to their insect host (McCutcheon et al. 2009); and digestion aided by gut microbiota (Brune 2014). They include protection: e.g. bacterial symbionts in insects that ward off pathogens via antibiotics and predators via toxins (Van Arnem et al. 2018), and even bioluminescent bacteria that conceal the shadow of their bobtail-squid host (Ruby & McFall-

Ngai 1992). “Symbiotic phenotypes”, i.e. new traits that emerge as a direct result of a symbiosis, are a big source of evolutionary innovation (Margulis & Fester 1991).

The term symbiosis encompasses thousands of relationships that differ in size, complexity, and the cost-benefit ratio for the partners. Previously, all symbioses were classified into strict categories — mutualisms, commensalisms, and parasitisms — based on how the benefits and costs are split between the partners (Sapp 2010). However, now the habit of giving a symbiont one label might come to an end. Costs and benefits of a symbiotic relationship are highly context-dependent (Keeling & McCutcheon 2017), and a symbiont that is neutral in one context can become harmful in another (Casadevall & Pirofski 2014). How closely symbiotic partners depend on each other also varies between different symbioses — and this variation can also be context dependent (Chomicki et al. 2020). In this thesis, I use the term “symbiosis” in the broad sense, i.e. spanning the whole spectra from mutualism to parasitism and from facultative to obligate relationships.

Lichens

Among symbioses, algal-fungal symbioses known as lichens occupy a somewhat special place. De Bary (1879) is often credited with coining the term symbiosis, which he used to describe lichens. Two years prior, Frank (1877) used the term “symbiotismus”, which he also applied to lichens. De Bary and Frank did not discover the nature of lichens: a decade earlier Schwendener (1869) showed that lichen bodies contain both fungal and algal cells. De Bary (1879) reframed this discovery, claiming that the fungus and the alga engage in a special relationship, a symbiosis. At first, such coexistence was considered a rare exception — but over time it became recognized as the rule (Smith & Douglas 1987).

The classic model of lichen symbiosis recognizes two partners: the main fungus (sometimes called “mycobiont”) and the phototrophic partner, typically a unicellular green alga or a cyanobacterium (Nash 1996). As early as the 1920s, it became clear that in addition to the two main partners, lichens often have a suite of other organisms associated with them (Spribille et al. 2020). These organisms included bacteria and additional fungal partners, both in the hyphal form and as yeasts. Historically, these organisms received far less attention than the two dominant symbionts. Yeasts were first identified as a consistent part of the symbiosis only in 2016 (Spribille et al. 2016, Tuovinen et al. 2019), after high-throughput sequencing facilitated their detection. Bacteria were first detected as early as 1926 (Cengia Sambo 1926), but became a subject of extensive research only recently. To this day, bacteria and yeasts are often considered to be external to the lichen symbiosis, and whether they should be seen as integral part of the symbiosis remains debated.

Historically, lichen symbiosis has been viewed as a nutritional symbiosis — the assumption now complicated by new data and new hypotheses (Spribille et al. 2022). Under the nutritional model, the phototrophic partner supplies the fungus with sugars, and the fungus, in turn, creates the symbiotic body to host (or, depending on the point of view, to capture) algal cells (Ahmadjian 1993). Drew and Smith (1967) first demonstrated the flow of sugars from the phototroph to the fungus. However, several lines of evidence — not least the subsequent work by the same authors — called into question whether the transported goods are actually used for nutrition (Smith 1979). Understanding how the players interact with each other — is it a syntrophy or a service industry? — requires understanding the goods and services available; these things are intricately linked. Much of my thesis focuses on the players, but also on the goods and services.

In addition, the symbionts, long assumed to be two, seem to be increasing in number as we apply new technologies to interrogating who is there (Grimm et al. 2021). How lichen bacteria and additional fungi, including the yeasts, fit into the model of the lichen symbiosis is a major knowledge gap, however the cases of lichen bacteria and lichen yeasts are notably different.

In the case of lichen bacteria, biologists have been hypothesizing about their potential contributions to the symbiosis for almost a century (Henkel & Yuzhakova 1936, Iskina 1938). Until recently, most information on lichen bacteria came from culturing studies, which now are sidelined by various metaomics approaches (e.g. metagenomics, metatranscriptomics, etc.) (Schneider et al. 2011, Grube et al. 2015, Grimm et al. 2021). The recent studies generated a plethora of new information and several hypotheses about the role of lichen bacteria (e.g. their potential in recycling lichen biomass or fixing nitrogen for the eukaryotic symbionts). However, they are mostly limited to a handful of model species, and we do not know to which extent the conclusions from these studies can be generalized to the lichens as a whole.

In the case of lichen yeasts, the knowledge gap is even wider. Prior to the start of this project, we knew very little about the biology of lichen yeasts: basically, we knew that they exist in the specific parts of lichen bodies and which taxonomic groups they belonged to. One piece of evidence — which, in fact, led to the discovery of lichen yeasts — suggested that the yeasts are linked to the secondary metabolite profile of the lichen (Spribille et al. 2016), raising the question of whether the yeasts can affect the lichen phenotype. This question remains to be solved, and much remains to be discovered about the role yeasts play in the symbiosis.

Arguably, these knowledge gaps partially arise from one feature of the lichen symbiosis. Unlike other symbioses, lichen symbiosis resulted in a new body plan. Lichen bodies consist of cells of multiple symbiotic partners: hyphae of the main fungal partner, cells of the phototrophic partners

(green algae or cyanobacteria), and, at least in some cases, bacteria and other fungi, including yeasts (Spribille et al. 2020). Among the symbionts, only some have a simple form of multicellularity, i.e. filamentous growth known for the main lichen fungi (Nagy et al. 2018) and some cyanobacteria (Kardish et al. 1989). The rest of the symbionts are unicellular. However, coming together they can produce symbiotic architectures that are large, stable, three-dimensional, and have no analogue among non-symbiotic relatives of the symbiont (while other fungi can create multicellular structures, e.g. fruiting bodies, multicellular vegetative structures, like we find in lichens, are exceedingly rare). Lichens present a unique case of complex multicellularity that has arisen from interactions of genetically different partners.

Lichen architectures vary in structure and complexity (Nash 1996). Broadly, they can be split into two categories. Crusts (or microlichens) are relatively simple and two-dimensional; they closely adhere to their substrate or are immersed in it. In contrast, macrolichens are three-dimensional and usually have stratified bodies organized into several “tissues”. The “tissues” usually include cortex — a layer that acts as exoskeleton providing lichen body with structure and isolating the interior from the surrounding environment (Spribille et al. 2020). Cortex is biofilm-like and is defined by its extracellular matrix — a set of substances that are secreted into the extracellular space by the symbionts and that together act as glue cementing cells into a single rigid layer (see Fig. 2 in Spribille et al. 2020). The integration of individual symbionts into the symbiotic architectures is so thorough, that for 200 years these architectures had been treated as biological species, and as such lichen symbioses were assigned names and ecological traits, and (see Nash 1996).

This amalgamation of symbiotic partners into a single body is not only the most interesting feature of the lichen symbiosis. It is also a source of methodological challenges. Lichen

symbionts often do not grow well in the lab, and to this day scientists have had limited success in recreating lichens *de novo* from axenic cultures. Performing experiments on lichens is hard. An alternative would be to use *in situ* methods, such as metagenomics. Using these methods, we can interrogate intact lichen samples from nature without the need to recreate lichens in the lab.

However, applying metagenomics to lichens brings new challenges. Lichen samples contain cells of numerous organisms, many of which have never been isolated in culture. For many of them, we did not have a sequenced genome prior to this project. In addition, many of them are eukaryotic and as such possess large and complex genomes. Finally, different organisms are present in lichens in uneven abundances, which makes it harder to get enough sequencing data to capture low-abundance symbionts. These factors combined make it highly nontrivial to disentangle lichen metagenomic data and produce usable genomes of individual partners, which can be used for downstream analysis. Another approach, alternative to metagenomics, can come from quantification symbionts and linking abundances of individual symbionts to phenotypic traits of the lichen symbioses. Similar studies often use staining and/or PCR-based quantification and have been done on other symbioses, both mutualistic and parasitic (e.g., Maciá-Vicente et al. 2009, Engel et al. 2015, Qian et al. 2018).

Research gaps addressed in this thesis

In this thesis, I focus on composition and functioning of lichen symbiosis, with the specific focus on the under-studied yeasts (Chapters 2 and 5) and bacteria (Chapter 4). I use metagenomics (Chapters 2–4) and other *in situ* methods (Chapter 5), which relied on intact lichen samples. This allowed me to achieve my goals and meet the methodological challenges mentioned above.

In Chapter 2, I aim to bridge the knowledge gap related to the biology of lichen yeasts and the nature of their relationship to the main fungus of the lichen symbiosis. In this chapter, I present

the first genomes of lichen yeasts, which I obtained from a “cortex slurry” sample created from a lichen. I compare the yeasts' genomes to the genome of the main fungal partner and other fungal genomes, and use the results to generate hypotheses about the role the yeasts play in lichens. I also screen samples of the model lichens from several locations to establish whether the yeasts are stably associated with the studied lichen.

In Chapter 3, I use metagenome-assembled genomes of the main fungal partner to stress-test a recently published hypothesis. I check whether lichen fungi indeed have lost an essential gene required for oxidative phosphorylation, which would place them into total dependence on other symbionts.

In Chapter 4, I aim to bridge the knowledge gap related to the lack of a systematic survey of bacteria in lichens. To that end, I perform a large-scale reanalysis of lichen metagenomic data. I analyze the composition of lichen symbioses and patterns of occurrence of different lineages. I also use genomes to characterize bacterial symbionts and predict their role in the symbiosis. Finally, I investigate how depth of sequencing affects the outcome of metagenomic analysis.

In Chapter 5, I report an experimental framework I set up to test some of the hypotheses formulated in Chapter 2. Using a novel ddPCR protocol, I measure the abundance of lichen yeasts and use these data to test two hypotheses: First, that the yeasts are linked to the secondary metabolite profiles of *Bryoria fremontii* lichens, or more specifically that the yeast abundance correlates with the concentration of vulpinic acid. And second, that yeasts make lichens more hygroscopic.

References

- Ahmadjian, V. (1993). *The lichen symbiosis*. John Wiley & Sons.
- Brune, A. (2014). Symbiotic digestion of lignocellulose in termite guts. *Nature Reviews Microbiology*, *12*(3), 168–180.
- Casadevall, A., & Pirofski, L. A. (2014). Microbiology: ditch the term pathogen. *Nature*, *516*(7530), 165–166.
- Cavanaugh, C. M. (1983). Symbiotic chemoautotrophic bacteria in marine invertebrates from sulphide-rich habitats. *Nature*, *302*(5903), 58–61.
- Cengia Sambo, M. (1926). Ancora della polysimbiosi nei licheni ad alghe cianoficee. 1. Batteri simbiotici. *Atti della Società Italiana di Scienze Naturali e del Museo Civico di Storia Naturale in Milano*, *64*, 191–195.
- Chomicki, G., Kiers, E. T., & Renner, S. S. (2020). The evolution of mutualistic dependence. *Annu. Rev. Ecol. Evol. Syst.*, *51*(1), 409-432.
- De Bary, A. (1879). Die Erscheinung der Symbiose. In *Die Erscheinung der Symbiose*. De Gruyter.
- Drew, E. A., & Smith, D. C. (1967). Studies in the physiology of lichens: VIII. Movement of glucose from alga to fungus during photosynthesis in the thallus of *Peltigera polydactyla*. *New Phytologist*, *66*(3), 389–400.
- Engel, P., Bartlett, K. D., & Moran, N. A. (2015). The bacterium *Frischella perrara* causes scab formation in the gut of its honeybee host. *MBio*, *6*(3), e00193-15.

- Frank, A.B. 1877. Über die biologischen Verhältnisse des Thallus einiger Krustenflechten *Beitr. Biol. Pflanz.* 2: 123–200.
- Grimm, M., Grube, M., Schiefelbein, U., Zühlke, D., Bernhardt, J., & Riedel, K. (2021). The lichens' microbiota, still a mystery?. *Frontiers in Microbiology*, 12, 714.
- Grube, M., Cernava, T., Soh, J., Fuchs, S., Aschenbrenner, I., Lassek, C., ... & Berg, G. (2015). Exploring functional contexts of symbiotic sustain within lichen-associated bacteria by comparative omics. *The ISME journal*, 9(2), 412–424.
- Hammer, T. J., Sanders, J. G., & Fierer, N. (2019). Not all animals need a microbiome. *FEMS Microbiology Letters*, 366(10), fnz117.
- Henkel, P. A., Yuzhakova, L. A. (1936). Azotfiksiruyuschie bakterii v lishaynikah [nitrogen-fixing bacteria in lichens]. *Izv Biol Inst Permsk Gos Univ*, 10, 9–10.
- Herridge, D. F., Peoples, M. B., & Boddey, R. M. (2008). Global inputs of biological nitrogen fixation in agricultural systems. *Plant and Soil*, 311(1), 1–18.
- Kardish, N., Kessel, M., & Galun, M. (1989). Characterization of symbiotic and cultured Nostoc of the lichen *Nephroma laevigatum* Ach. *Symbiosis*, 7, 257–266.
- Keeling, P. J., & McCutcheon, J. P. (2017). Endosymbiosis: the feeling is not mutual. *Journal of Theoretical Biology*, 434, 75–79.
- Iskina, R. E. (1938). K voprosu ob azotfiksiruyushchikh bakteriyakh v lishaynikakh (On the question of nitrogen-fixing bacteria in lichens). *Izvestiya Permskogo Nauchno-Issledovatel'skogo Instituta*, 11, 133–140.
- Maciá-Vicente, J. G., Jansson, H. B., Talbot, N. J., & Lopez-Llorca, L. V. (2009). Real-time PCR quantification and live-cell imaging of endophytic colonization of barley (*Hordeum*

vulgare) roots by *Fusarium equiseti* and *Pochonia chlamydosporia*. *New Phytologist*, 182(1), 213-228.

Margulis, L. (1981). *Symbiosis in cell evolution: Life and its environment on the early earth*. Freeman, San Francisco.

Margulis, L., & Fester, R. (Editors). 1991. *Symbiosis as a source of evolutionary innovation, speciation and morphogenesis*. MIT Press, Cambridge

McCutcheon, J. P., McDonald, B. R., & Moran, N. A. (2009). Convergent evolution of metabolic roles in bacterial co-symbionts of insects. *Proceedings of the National Academy of Sciences*, 106(36), 15394–15399.

McFall-Ngai, M., Hadfield, M. G., Bosch, T. C., Carey, H. V., Domazet-Lošo, T., Douglas, A. E., ... & Wernegreen, J. J. (2013). Animals in a bacterial world, a new imperative for the life sciences. *Proceedings of the National Academy of Sciences*, 110(9), 3229–3236.

Nagy, L. G., Kovács, G. M., & Krizsán, K. (2018). Complex multicellularity in fungi: evolutionary convergence, single origin, or both? *Biological Reviews*, 93(4), 1778–1794.

Nash, T. H. (Ed.). (1996). *Lichen biology*. Cambridge University Press.

Qian, L., Jia, F., Jingxuan, S., Manqun, W., & Julian, C. (2018). Effect of the secondary symbiont *Hamiltonella defensa* on fitness and relative abundance of *Buchnera aphidicola* of wheat aphid, *Sitobion miscanthi*. *Frontiers in Microbiology*, 9, 582.

Ruby, E. G., & McFall-Ngai, M. J. (1992). A squid that glows in the night: development of an animal-bacterial mutualism. *Journal of Bacteriology*, 174(15), 4865–4870.

Sapp, J. (2010). On the Origin of Symbiosis. In *Symbioses and Stress* (pp. 3–18). Springer, Dordrecht.

- Schneider, T., Schmid, E., de Castro Jr, J. V., Cardinale, M., Eberl, L., Grube, M., ... & Riedel, K. (2011). Structure and function of the symbiosis partners of the lung lichen (*Lobaria pulmonaria* L. Hoffm.) analyzed by metaproteomics. *Proteomics*, *11*(13), 2752–2756.
- Schwendener, S. (1869). *Die Algentypen der Flechtengonidien*. Basel, Switzerland: Universitaetsbuchdruckerei.
- Smith, D. C. (1979). Is a lichen a good model of interactions in nutrient-limited environments? In: Shilo M, ed. *Strategies of microbial life in extreme environments: report of the Dahlem Workshop on Strategy of Life in Extreme Environments, Berlin, 1978, November 20–24*. Weinheim, Germany: Verlag Chemie, 291–301.
- Smith, D. C., & Douglas, A. E. (1987). *The Biology of Symbiosis* London: Edward Arnold.
- Spribille, T., Resl, P., Stanton, D. E., & Tagirdzhanova, G. (2022). Evolutionary biology of lichen symbioses. *New Phytologist*, *234*(5), 1566–1582.
- Spribille, T., Tagirdzhanova, G., Goyette, S., Tuovinen, V., Case, R., & Zandberg, W. F. (2020). 3D biofilms: in search of the polysaccharides holding together lichen symbioses. *FEMS Microbiology Letters*, *367*(5), fnaa023.
- Spribille, T., Tuovinen, V., Resl, P., Vanderpool, D., Wolinski, H., Aime, M. C., ... & McCutcheon, J. P. (2016). Basidiomycete yeasts in the cortex of ascomycete macrolichens. *Science*, *353*(6298), 488–492.
- Tuovinen, V., Ekman, S., Thor, G., Vanderpool, D., Spribille, T., & Johannesson, H. (2019). Two basidiomycete fungi in the cortex of wolf lichens. *Current Biology*, *29*(3), 476–483.
- Van Arnem, E. B., Currie, C. R., & Clardy, J. (2018). Defense contracts: molecular protection in insect-microbe symbioses. *Chemical Society Reviews*, *47*(5), 1638–1651.

van der Heijden, M. G., Martin, F. M., Selosse, M. A., & Sanders, I. R. (2015). Mycorrhizal ecology and evolution: the past, the present, and the future. *New Phytologist*, *205*(4), 1406–1423.

Wyatt, G. A., Kiers, E. T., Gardner, A., & West, S. A. (2014). A biological market analysis of the plant-mycorrhizal symbiosis. *Evolution*, *68*(9), 2603–2618.

Yellowlees, D., Rees, T. A. V., & Leggat, W. (2008). Metabolic interactions between algal symbionts and invertebrate hosts. *Plant, Cell & Environment*, *31*(5), 679–694.

Zilber-Rosenberg, I., & Rosenberg, E. (2008). Role of microorganisms in the evolution of animals and plants: the hologenome theory of evolution. *FEMS Microbiology Reviews*, *32*(5), 723–735.

Chapter 2. Predicted Input of Uncultured Fungal Symbionts to a Lichen Symbiosis from Metagenome-Assembled Genomes

A version of this chapter has been published as Tagirdzhanova, G., Saary, P., Tingley, J. P., Díaz-Escandón, D., Abbott, D. W., Finn, R. D., & Spribille, T. (2021). Predicted input of uncultured fungal symbionts to a lichen symbiosis from metagenome-assembled genomes. *Genome Biology and Evolution*, 13(4), evab047.

2.1. Abstract

Basidiomycete yeasts have recently been reported as stably associated secondary fungal symbionts of many lichens, but their role in the symbiosis remains unknown. Attempts to sequence their genomes have been hampered both by the inability to culture them and their low abundance in the lichen thallus alongside two dominant eukaryotes (an ascomycete fungus and chlorophyte alga). Using the lichen *Alectoria sarmentosa*, we selectively dissolved the cortex layer in which secondary fungal symbionts are embedded to enrich yeast cell abundance and sequenced DNA from the resulting slurries as well as bulk lichen thallus. In addition to yielding a near-complete genome of the filamentous ascomycete using both methods, metagenomes from cortex slurries yielded a 36- to 84-fold increase in coverage and near-complete genomes for two basidiomycete species, members of the classes Cystobasidiomycetes and Tremellomycetes. The ascomycete possesses the largest gene repertoire of the three. It is enriched in proteases often associated with pathogenicity and harbors the majority of predicted secondary metabolite clusters. The basidiomycete genomes possess ~35% fewer predicted genes than the ascomycete and have reduced secretomes even compared with close relatives, while exhibiting signs of nutrient limitation and scavenging. Furthermore, both basidiomycetes are enriched in genes coding for enzymes producing secreted acidic polysaccharides, representing a potential

contribution to the shared extracellular matrix. All three fungi retain genes involved in dimorphic switching, despite the ascomycete not being known to possess a yeast stage. The basidiomycete genomes are an important new resource for exploration of lifestyle and function in fungal–fungal interactions in lichen symbioses.

2.2. Significance

Many lichen symbioses have been recently shown to contain low-abundance secondary fungal symbionts in the form of basidiomycete yeasts. Here, we present the first annotated genomes of the secondary fungal symbionts and compare them with the genomes of the dominant fungus of the symbiosis. Lichen yeast genomes are among the smallest 5% in fungi, but possess the machinery for secreted polysaccharide profiles and phosphate scavenging functions not found in the dominant fungal symbiont.

2.3. Introduction

Culture-independent molecular methods have been a game changer for working with mutualistic symbioses, which are often recalcitrant to laboratory experimentation. Not only have such methods led to the discovery of previously unknown symbionts (e.g., Matsuura et al. 2018), they have also permitted us to explore their functional potential (e.g., Karimi et al. 2018). Lichen symbioses were long considered to consist entirely of a fungus and one or two photosynthesizing partners, usually a chlorophyte alga and/or a cyanobacterium, based on what could be interpreted with confidence using traditional microscopy. Despite evidence of additional associated microbes, including both bacteria and fungi, from culturing studies as early as the 1930s (Lenova and Blum 1983), it was only through shotgun sequencing that the stable and constant association of basidiomycete secondary fungal symbionts (SFSs) was discovered in lichen symbioses, especially those formed by members of the ascomycete family Parmeliaceae (Spribille et al.

2016; Tuovinen et al. 2019). These partners had not only evaded previous detection by culturing but also by amplicon sequencing with common primers (Spribille et al. 2016).

The inability to isolate SFSs has not only made them hard to detect, it has also left their relationship to the lichen difficult to test. In the lichen system in which they were first detected, the *Bryoria tortuosa* symbiosis, their abundance correlated positively with the visible production of the secondary metabolite vulpinic acid in the shared extracellular matrix between the core ascomycete symbiont and the yeasts. The close association with a secondary metabolite and the tight integration of yeasts into the extracellular matrix led us to hypothesize a role in contributing to secondary metabolism and/or in secreting polysaccharides into the extracellular matrix (Spribille et al. 2020). Perhaps not exclusive of these possibilities, other authors have suggested that SFSs may be parasites. The two main groups of SFSs, members of the basidiomycete orders Cyphobasidiales and Tremellales, were both known in lichens prior to their discovery as yeasts by their fertile, hyphal forms. These are rare but easier to spot than yeasts, in the form of gall-like protrusions on lichen thalli (Tuovinen et al. 2019, 2021). Their relationship to known mycoparasites has led others to suspect that they parasitize the core ascomycete symbiont (Millanes et al. 2016). That being said, we are not aware of any direct evidence of mycoparasitism, such as fungal–fungal haustoria, from lichen SFSs. We have, however, shown one of them (*Tremella*) to enmesh algal cells (Tuovinen et al. 2019).

It became evident in our original metatranscriptome study of SFSs that determining the nature of SFS interactions with the other members of the lichen system would not be trivial. In studies that have used raw mRNA extracts from whole lichens (Spribille et al. 2016, Tuovinen et al. 2019), the much lower cell abundance of the yeasts resulted in Illumina flow cell being swamped by cDNA from the more abundant core symbionts. The problem of core symbiont DNA driving

down secondary symbiont coverage also manifests itself when sequencing metagenomic libraries. The ability to recover SFS reads declines as less flow cell space is dedicated to a whole library and appears to stand in direct relationship to declining coverage of the core symbionts. For instance, when the ascomycete symbiont is sequenced at $5\times$ coverage, SFSs may not be detected at all in many cases (Lendemer 2019), even in lichen symbioses in which they are readily demonstrable at high frequency using endpoint PCR screening (Černajová and Škaloud 2019; Mark et al. 2020).

Even if deeper coverage is obtained, other hurdles have stood in the way of assembling complete and comparable eukaryotic genomes from metagenomic samples. Although microbial eukaryotes constitute a significant fraction of biodiversity and have recently gained more attention (Delmont et al. 2018; West et al. 2018), the recovery of high-quality metagenomic assembled eukaryotic genomes has been limited by the bioinformatic challenges presented by the larger genome size and complexity (e.g., repetitive regions and varied nucleotide composition). Solving these challenges could provide a powerful tool set to 1) interrogate the lichen system both for other stably associated symbionts, as well as 2) provide initial prognoses of the gene repertoires and potential complementarities of the genomes involved.

The present study had two specific goals. First, we set out to obtain high coverage genome assemblies for previously unobtainable low abundance partners from wild lichen material. We accomplished this by sequencing a metagenome both from whole lichen material as well as from slurry derived from dissolved lichen EPS. Second, we set out to predict the gene repertoires of the two SFSs associated in high frequency with the *in vivo* lichen and contrast them to the genome of the dominant fungal partner based entirely on metagenome-derived data sets. For this portion of the study, we focused on three aspects of their biology relevant for the lichen

symbiosis: 1) potential contributions of the SFSs to the lichen symbiosis, including production of polysaccharide matrix and secondary metabolites, nutrient scavenging and lipid deposition; 2) trophic lifestyle of the SFSs and their relationship to the “core” fungus; and 3) the detection of potential signal for mutualistic versus antagonistic interactions between the fungi in the symbiosis. The findings run up against new limitations, but substantially extend our knowledge of the potential capabilities of the SFSs.

2.4. Results

2.4.1. Extraction of Symbiont Genomes from Metagenomic Data

We generated metagenomes from two samples of *Alectoria sarmentosa*: One from pulverized bulk lichen material, and the other from pelleted sediment obtained by soaking a thallus in hot water (cortex slurry). We assembled each metagenome separately (Table S1). In order to separate symbiont genomes within metagenomes, we binned (or grouped) contigs using tetranucleotide frequency patterns and sequence coverage. For each bin, we assigned provisional taxonomic identifications by drawing 200 proteins at random and deriving taxon predictions from UniProt (see Materials and Methods). Next, we generated estimates of completeness and contamination for each bin as putative metagenome-assembled genomes (MAGs) and plotted the contigs as GC-coverage plots (Fig. 2.1A and B). *Ab initio* binning and taxon assignment led to the recognition of two large eukaryotic genomes in the bulk lichen metagenome, corresponding to an ascomycete fungus and chlorophyte alga; and five in the cortex slurry, one from an ascomycete fungus, two from basidiomycete fungi, and two from bacteria (Table 2.1). Of the two basidiomycete MAGs, one had completeness estimates varying, dependent on the tools employed, from 83.9% to 97.7%, the other from 83.4% to 90.7%. Estimated contamination rates were all below 1% (Table 2.1). The algal MAG was nearly complete but had a contamination

rate of 80% (Table S2); no algal MAG was recovered from the cortex slurry. Each of these MAGs was recovered as a single bin.

The highest coverage MAG in both metagenomes belonged to an ascomycete (Table S2). However, the bin identified as the core ascomycete MAG in both of the metagenomes had completeness of only 80–92%, as reported by different tools, despite high coverage (Table S3). That being said, we noticed several bins arranged at near-identical coverage to the ascomycete bin in the GC-coverage plots, forming a more or less linear cloud, ranging in GC content from ~30% to 55% (Fig. 2.1A and B). To explore the possibility that these additional bins also belonged to, and would complete, the ascomycete MAG, we inferred their taxonomy. For each of the eight bins, the inferred lineage was Ascomycota (Table S2). Merging these four bins (Fig. 2.1C and D) improved completeness for the ascomycete MAG to around 98% whereas not significantly impacting estimated contamination (by <1%; Table 2.1). For the downstream analysis, we treated the merged bins as a single MAG.

2.4.2. Symbiont Genomes from *Alectoria* Metagenomes

The cortex-slurry metagenome yielded five nearly complete MAGs, three fungal and two bacterial (Table 2.1). In order to refine the taxonomic placement of the fungal MAGs, we performed a phylogenomic analysis based on 71 single copy orthologs identified in 38 published fungal genomes and all the fungal MAGs from both metagenomes. Using this approach, we placed the ascomycete MAG from both metagenomes in the class Lecanoromycetes, confirming its identity as the dominant fungus of the lichen symbiosis (Fig. 2.2). For clarity, this fungus, which formally carries the name *A. sarmentosa* under the code of nomenclature, will be hereafter called the “lecanoromycete” whereas the lichen itself will be referred to as the “*Alectoria* lichen.” The remaining two MAGs resolved within the basidiomycete classes

Cystobasidiomycetes and Tremellomycetes, respectively (Fig. 2.2). The cystobasidiomycete is an exact match for a known, unnamed *Cyphobasidium* species previously detected by PCR from *Alectoria* lichen (hereafter *Cyphobasidium*; Fig. S1). The tremellomycete is newly detected in the *Alectoria* lichen and is sister to *Biatoropsis usnearum*, a member of *Tremella s.lat.* (hereafter *Tremella*; Millanes et al. 2011) (Fig. S2). Using CheckM (Parks et al. 2015), both bacterial MAGs isolated from the cortex-slurry metagenome were assigned to *Granulicella* (Acidobacteria; Table S4).

The use of cortex slurries led to a significant change in symbiont DNA, and considerably increased the relative abundance of secondary symbionts. In the bulk-lichen metagenome, both *Cyphobasidium* and *Tremella* were also present, as was shown by the presence of their rDNA sequences. But their coverage was insufficient for them to be assembled and recovered as identifiable bins. Coverage of a contig containing the ITS of *Cyphobasidium* was 336 times lower than that of the dominant fungus; for *Tremella* the ratio was 1:184. In the cortex-slurry metagenome, the same ratios were 1:4 for *Cyphobasidium* and 1:5 for *Tremella*, constituting an 84-fold and 36-fold coverage increase, respectively.

The basidiomycete MAGs were less than half as large as the lecanoromycete MAG (Table 2.1); GC content was 38% for the lecanoromycete and 51–52% for the basidiomycetes. *De novo* genome annotation resulted in 9,407 protein-coding gene models for the main fungus, 6,095 for *Cyphobasidium*, and 6,038 for *Tremella* (Table S5). A gene prediction based on known orthologs could be modeled for only a portion of them (64–71%; see Materials and Methods). A large suite of functional elements was shared between ascomycete and basidiomycete (Fig. S3).

2.4.3. Constancy of Association

Only one of the two basidiomycete fungi and none of the bacteria had previously been reported as *Alectoria* lichen symbionts. In order to assess whether these occur as stably associated symbionts, we used PCR to screen for their presence in 32 thalli of *Alectoria* lichens from three locations in eastern BC and western AB. In each case, the sampled *Alectoria* thallus was sampled together with a randomly chosen, adjacent lichen symbiosis and adjacent bare bark on the same tree. All *Alectoria* thalli contained at least one SFS; most contained both *Cyphobasidium* and *Tremella* (Fig. 2.3, Tables S6 and S7).

Most sequences of *Cyphobasidium* and *Tremella* from *Alectoria* lichens, including sequences extracted from the metagenomes, were recovered in known lichen-associated clades of these two genera (Figs. S4 and S5). Most *Cyphobasidium* from *Alectoria* formed a clade mixed only with *Cyphobasidium* from closely related *Bryoria* lichens (clade 1, Fig. 2.3, Fig. S4); a few sequences came from clade 2, made up by Cyphobasidiales from other lichen symbioses. In *Tremella* from *Alectoria*, by contrast, a much larger percentage of samples drew from a clade shared with other lichen symbioses: Half of the sequences formed their own clade (clade 1, Fig. 2.3, Fig. S5), whereas half came from the clade 2, which also constituted the majority of the sequences we obtained from other lichens. The sequenced MAGs of *Cyphobasidium* and *Tremella* belong to clade 1 on their respective trees (Figs. S4 and S5).

Both SFS lineages also occurred in some other lichens, and occasionally in bark samples. By contrast, we found *Granulicella* in only one *Alectoria* thallus (Fig. 2.3), but 12 bark extractions. We concluded that this bacterium is not stably associated with the *Alectoria* lichen and excluded it from further analyses.

2.4.4. The Basidiomycete MAGs Are Similar to Closely Related Genomes but Have Smaller Secretomes

As a “sanity check,” we compared all three of our MAGs with genomes sequenced from cultures of closely related species. All three MAGs were similar to related genomes in gene count, assembly size and GC content (Fig. 2.4, Table S8). The MAG of the *Alectoria* lichen lecanoromycete compared with five other lecanoromycete genomes, all of which are lichen fungal symbionts, exhibited numbers of Carbohydrate Active enZymes (CAZymes), secondary metabolite gene clusters (SMGC) and secreted proteins close to average among the six genomes (354 CAZymes, 57 SMGC, and 374 secreted proteins in the *Alectoria* lichen lecanoromycete vs. 346 CAZymes, 54 SMGC, and 372 secreted proteins on average; Fig. 2.4).

The basidiomycete fungi from the *Alectoria* lichen were similar to their close relatives in the SMGC and CAZyme profiles (Fig. 2.4). All twelve studied genomes, with one exception, harbored several putative SMGCs belonging to nonribosomal peptide synthetases (NRPS) and terpene classes. *Tremella* from the *Alectoria* lichen was the only genome to include a polyketide synthase (PKS) cluster. Numbers of CAZymes in both basidiomycetes were close to average (322 in *Cyphobasidium* and 356 in *Tremella* vs. 344 on average). We compared CAZyme profiles of fungi with different ecology (e.g., plant pathogens and mycoparasites) but failed to detect any lifestyle-dependent pattern (Table S9). The most notable difference is in the size of secretomes, which were smaller in both of the lichen-associated basidiomycetes compared with their relatives. This observation is unlikely to be fully explained by potential incompleteness of the MAGs, as not only the number of genes identified as secreted, but also their percentage across all genes were lower in the MAGs than in the related genomes (2.8% in *Cyphobasidium*

vs. 3.4% on average among Pucciniomycotina; 2.4% in *Tremella* vs. 2.7% on average among Tremellales).

2.4.5. The Three Fungal Genomes Show Evidence of Different Cell Wall and Secreted Polysaccharide Profiles

Our genomic evidence was consistent with data on cell walls of fungi related to the three studied species. Putative chitin and β -1,3-glucan synthases (*GAS1*, *CHS1*, *CHS2*, *CHS3*, *CHS5*, *CHS7*; Lesage et al. 2004, 2005) found in the lecanoromycete matched the reports of chitin and glucan (reviewed by Spribille et al. 2020). The cell walls of *Cryptococcus neoformans*, a close relative of *Tremella*, are built by α -1,3 and β -1,3-glucans, chitin, and chitosan (Doering 2009). In the *Tremella* MAG we identified genes involved in biosynthesis of all of these polysaccharides: Putative α -1,3-glucan synthase *AGS1*, β -1,3-glucan synthase *FKS1* (Lesage et al. 2004), chitin synthases (*CHS1*, *CHS2*, *CHS3*, *CHS5*, *CHS7*; Lesage et al. 2005), as well as putative chitin deacetylase *CDA2*, which catalyzes deacetylation of chitin into chitosan (Martinou et al. 2003). For the class Cystobasidiomycetes, only the monosaccharide composition of the cell wall is known (Takashima et al. 2000). The presence of putative β -1,3-glucan synthase *FKS1* and putative chitin synthases (*CHS1*, *CHS2*, *CHS3*, *CHS7*) in the *Cyphobasidium* MAG suggested that the cell wall composition includes β -1,3-glucans and chitin.

The extracellular polysaccharides reported from lichens similar to *Alectoria* include variously-linked glucans (β -1,3; β -(1,3),(1,4); α -(1,3),(1,4)) and heteromannans, predominantly with α -1,6-mannan backbones (Spribille et al. 2020). We identified genes potentially involved in the synthesis of these polysaccharides in all three fungi. Putative β -1,3-glucan synthases were found in all three MAGs. Based on this, all three fungi seemed equally likely to produce β -(1,3),(1,4)-glucans. By contrast, only the lecanoromycete and *Tremella* possessed putative α -1,3-glucan

synthase *AGSI*, even though all three fungi had an enzyme making putative α -1,4 bonds (*GSYI*). The lecanoromycete was also unique in containing proteins similar to those from the mannan polymerase complex II, which synthesizes α -1,6-mannan backbone in multiple ascomycete fungi (e.g., Henry et al. 2016). Although all three MAGs encoded some GT32 enzymes known to be involved in α -1,6-mannan biosynthesis, the lecanoromycete had more than either of the basidiomycetes (Fig. S7).

The genomic data predicted the synthesis of several acidic polysaccharides not yet reported from lichens. First, glucuronoxylomannan (GXM) is a polysaccharide known from *Cryptococcus* (e.g., Zaragoza et al. 2009) and, in the form of a GXM-like polysaccharide that includes fucose, in non-lichen *Tremella* (de Baets and Vandamme 2001). Both *Tremella* and *Cyphobasidium*, but not the lecanoromycete, contained homologues of all so-called CAP genes (*CAP10*, *CAP59*, *CAP60*, and *CAP64*), which play a role in capsule synthesis in *Cryptococcus* (Zaragoza et al. 2009). Only *CAP10* (CAZy family GT90) was present in the lecanoromycete. It also possessed four proteins assigned to the same GT69 family as *CAP59* and *CAP60* (Fig. 2.5A). Consistent with a fucose-containing polysaccharide, both basidiomycete MAGs but not the ascomycete code for putative GDP-L-fucose synthase *GER1* (1.1.1.271). Second, we also found two GT families involved in heparan sulfate biosynthesis, GT47 and GT64, in the basidiomycete MAGs (Fig. S7). Currently, the only fungal GT47 enzyme is reported from *C. neoformans* (Geshi et al. 2018). GT64s have been reported from other fungi only a few times (Chang et al. 2016). As heparan sulfate production is not known from any fungus, it may play a role in producing an acidic polysaccharide that displays different monosaccharide composition of linkages, as suggested by Grijpstra (2008) for cryptococcal GT47. Third, the inferred ability of the lecanoromycete to

produce glucuronic acid stood in contrast to previous reports where uronic acids were reported missing from cultures of some lecanoromycetes (Honegger and Bartnicki-Garcia 1991).

2.4.6. The Lecanoromycete Genome Codes for More Degradative Enzymes That Target Plant Polysaccharides than Either SFS (Fig. 2.5B)

Among GH5 predicted to be secreted by the lecanoromycetes and *Cyphobasidium*, we identified enzymes from subfamilies GH5_7 (β -mannanases) and GH5_5 (β -1,4-glucanases). Fig. 2.5C shows a GH5 family tree that was used to infer functions of the GH5 from the studied MAGs. These enzymes were identified as targeting plant polysaccharides, because the corresponding substrates (β -mannans and β -1,4-glucans, such as cellulose) are components of the plant cell wall (Burton et al. 2010) and not known to be produced by the studied fungi. It is possible that these enzymes are used to hydrolyze components of the algal cell wall, which was shown to contain polysaccharides with these structures (Centeno et al. 2016). The lecanoromycete MAG was the only one to code for a putative secreted glucanase or xyloglucanase from the GH12 family (Fig. 2.5A and B), which might target cellulose and is known to be upregulated in lecanoromycete-alga coculturing experiments (Kono et al. 2020), and a secreted β -mannanase or β -1,4-glucanase from the GH45 family. Some secreted auxiliary activity CAZymes (AA) belonged to families likewise involved in digesting plant polymers through oxidative processes: AA3 (active on cellobiose and lignin) in all three secretomes and AA9 (active on cellulose) in the lecanoromycete secretome. The lecanoromycete MAG also coded for a putative secreted cutinase (carbohydrate esterase CE5, Pfam accession PF01083), which targets plant cuticle (Nakamura et al. 2017; Fig. S7 and Table S10).

2.4.7. The Lecanoromycete Genome Codes for More Secondary Metabolite Clusters than Either SFS

Alectoria lichen produces usnic acid, α -alectoronic acid and barbatic acid (Brodo and Hawksworth 1977). Both α -alectoronic and barbatic acid are biosynthetically related compounds derived from the polyketide orsellinic acid. Orsellinic acid has been linked to a Group I nonreducing Type I PKS (Liu, Zhang, et al. 2015), an apparent ortholog of which was present in the lecanoromycete (62% identity over 99% query cover). Usnic acid is a dibenzofuran derived from orsellinic acid, though evidence has recently been advanced to suggest a nonreducing PKS gene cluster including methylphloracetophenone synthase and methylphloracetophenone oxidase correlates with the upregulation of usnic acid (Abdel-Hameed et al. 2016). An orthologue of this PKS cluster, too, was found in the lecanoromycete (84% identical over 99% cover). One SM cluster was predicted to produce a siderophore. In the *Alectoria* lichen, the majority of SM clusters and all but one PKS cluster were found in the lecanoromycete (Fig. 2.4, Table S5). We found far more SMGCs than there are known secondary metabolites in the *Alectoria* lichen (57 SMGCs vs. three secondary metabolites).

Among SMGCs predicted for the lecanoromycete, two showed similarity to characterized clusters producing toxins. In a NRPS cluster, the core biosynthetic gene was similar to one from the aspirochlorine gene cluster, a mycotoxin known from *Aspergillus* (57% identity of the amino acid sequence, over 95% query coverage). A terpene gene cluster showed similarity to the gene cluster producing PR-toxin (62% identity, over 97% query coverage), a mycotoxin from *Penicillium*. A gene similar to fusarin synthase was assigned to the same cluster (46% identical over 93% query cover).

We found fewer predicted SMGCs in *Cyphobasidium* and *Tremella* (Fig. 2.4). All but one SMGC found in the basidiomycetes were NRPS and terpene clusters. A Type III PKS cluster predicted in *Tremella* was the only PKS cluster in the basidiomycetes.

2.4.8. SFSs Genomes Predict Nutrient Limitation and Scavenging

Putative secreted phosphorus-scavenging enzymes are more numerous in the basidiomycete MAGs than in the lecanoromycete (Table S10). Both basidiomycete secretomes contain purple acid phosphatase-like proteins, a type of acid phosphatase known mostly from plants and some ascomycete fungi: Two proteins in *Cyphobasidium* (Pfam accession PF16656 and PF14008) and one in *Tremella* (PF14008). Histidine phosphatase superfamily branch 2 contains some enzymes that break down nucleotides and phytic acid. These enzymes are secreted by fungi for scavenging phosphorus from extracellular sources (Rigden 2008). We found two similar proteins (PF00328) in *Tremella* and one in the lecanoromycete. The three fungi had a similar set of putative phosphate transporters (*PHO84* and *PHO91*), but in *Tremella* *PHO84* appeared duplicated.

The *Tremella* MAG lacked some nutrient assimilation enzymes, suggesting it is auxotrophic. Through KEGG annotation, we found key enzymes (nitrate transporter, nitrate reductase, and nitrite reductase) in the nitrogen assimilation pathway in the lecanoromycete and *Cyphobasidium*, but *Tremella* lacked all three. This is consistent with reports that some members of Tremellales are unable to assimilate nitrate or nitrite as nitrogen sources (Lee et al. 2011).

2.4.9. The Lecanoromycete Exhibits More Pathogenic Features than Either Basidiomycete

Numerous studies have undertaken to connect fungal lifestyle to genomic signatures (e.g., Pellegrin et al. 2015). The leading candidates that have been studied are proteases,

polysaccharide lyases, glycoside hydrolases (GH) and lipases. Each of these is represented in all three of the *Alectoria* lichen fungal genomes, in differing proportions. The lecanoromycete secretome contained twice as many proteases as that of *Tremella* and almost three times as many as in *Cyphobasidium* (Fig. 2.4, Table S5). This increase is proportional to the secretome size. Only the lecanoromycete contained trypsin-like proteases (MEROPS family S1) (Fig. S8), associated with pathogenic fungi regardless of their host (Dubovenko et al. 2010). Subtilisin proteases (S8), known to be involved in mycoparasitism (Fan et al. 2014) were present in a greater number in the lecanoromycete MAG, but only *Tremella* subtilisins were predicted to be secreted.

In endophytes and plant pathogens, fungalyisin, a metalloprotease (M36), plays a role in suppressing host defenses by cleaving chitinases released by the plant in response to fungal infection (Zuccaro et al. 2011, Sanz-Martín et al. 2016). Both *Tremella* and the lecanoromycete MAGs encoded fungalyisin, but only the lecanoromycete fungalyisin was predicted to be secreted (Fig. S8). The lecanoromycete also was the only fungus to have two other secreted proteins that in fungi suppress chitin-triggered immune response: *LysM* domain-containing protein (PF01476), which binds to chitin to mask it from host immune systems (Kombrink and Thomma 2013); and a chitin-binding protein (PF00187; Table S10).

The numbers of putative secreted lipases predicted in the three fungi are low. The lecanoromycete secretome contained three lipases assigned to four Pfam families (accessions PF01764, PF01735, PF03893, and PF13472, respectively) whereas the basidiomycete MAGs encoded one secreted lipase-like protein each (Table S10). A phospholipase-like domain PLA2_B (PF04800) found in *Tremella* was also present in the lecanoromycete. A GDSL-like lipase/acylhydrolase (PF00657) was found only in *Cyphobasidium*. Secreted lipases, whereas

known from mutualistic fungi (Chen et al. 2018), are thought to contribute to pathogen virulence (Pellegrin et al. 2015).

The only secreted protease inhibitor, from MEROPS family I51, was encoded in the *Cyphobasidium* MAG. Members of this family act as inhibitors of serine carboxypeptidases Y (S10), of which the lecanoromycete possessed the largest number that were predicted as secreted, though they were predicted from all three fungi.

2.4.10. We Found No Evidence of Any of the Fungi Targeting Polysaccharides Produced Exclusively by Other Fungal Partners

For all three fungi, the majority of secreted GH appeared to be active on polysaccharides synthesized by the same fungus, including β -glucanases (GH128, GH16, GH17, GH132, GH152, some GH5) and chitinases (GH18; Fig. 2.5B). The same two MAGs that encoded putative α -1,3-glucan synthase, *Tremella* and the lecanoromycete, were predicted to secrete α -1,3-glucanase (GH71). Similarly, all CAZy families targeting acidic polysaccharides (GH28, GH105, polysaccharide lyase PL14) were predicted to be secreted by the basidiomycetes, which are predicted to synthesize acidic polysaccharides. We did not identify any GHs that definitively target polysaccharides produced by other fungal members of the symbiosis in any pairwise combination.

2.4.11. All Three Fungi Possess Predicted Polyol Transporters

In each of the three fungi, we found a protein highly similar to characterized D-sorbitol/D-mannitol/ribitol transporters (BLASTp e-value < 1e-140). All three proteins were assigned to PF00083 (Sugar [and other] transporter). All three possessed several transmembrane domains, though only the protein from *Cyphobasidium* possessed twelve transmembrane domains, as is

typical for sugar transporters (Leandro et al. 2009), whereas proteins from the lecanoromycete and *Tremella* had seven and eight, respectively.

2.4.12. We Cannot Rule Out or Confirm That Any of the Fungi Are Oleaginous

As both basidiomycetes have relatives within the same class that produce large amounts of lipids (oleaginous fungi; Sitepu et al. 2014), we examined the MAGs for the presence of genes known to be involved in lipid production following Beopoulos et al. (2009) and Adrio (2017). In fact, from all three fungi we predicted most of the enzymes required for being oleaginous: 1) enzymes involved in lipid biosynthesis initiation: AMP deaminase *AMD1*, ATP-citrate lyase *ACLI*, malic enzyme *MAE1* (also called *MDHI*), and acetyl-CoA carboxylase *ACC*; 2) fatty acid synthases *FAS1* and *FAS2*; and 3) enzymes involved in triacylglycerol synthesis: glycerol-3-phosphate acyltransferase (*SCT1*, EC 2.3.1.15 identified by KEGG Pathway annotation), lysophosphatidic acid acyltransferase (*SLC1*, EC 2.3.1.51), phosphatidic acid phosphohydrolase (*PAP*, EC 3.1.3.4), and diacylglycerol acyltransferases *DGAI* and *LROI* (EC 2.3.1.158). However, the key enzyme for steryl ester synthesis, sterol O-acyltransferase (*ARE1* and *ARE2*, EC 2.3.1.26), was predicted only for the lecanoromycete and *Cyphobasidium*.

2.4.13. All Three Fungi Have Machinery for Dimorphic Switching

In the three fungi, we searched for the homologs of genes regulating dimorphic switching in other fungi, originally characterized from *Candida albicans*, the yeast-to-hypha switching of which is well characterized (Sudbery 2011). Dimorphic switching in fungi is controlled through *cAMP/PKA* and *MAPK* pathways (Borges-Walmsley and Walmsley 2000). In all three fungi, we found the key enzymes involved in this process: Adenylate cyclase *CYR1*, small G proteins *RAS2*, *GPA2*, and *CDC42*, protein kinase A *PKA*, p21-activated kinase *STE20*, and elements of *MAPK* cascade *STE11*, *STE7*, and *STE2*. Downstream targets of the signaling pathways are

transcriptional factor pathways (Borges-Walmsley and Walmsley 2000). The only protein identified as associated with the yeast-form growth in the lecanoromycete from Park et al. (2013) was a C2H2-type zinc finger transcription factor (Jeong et al. 2015), a type of transcription factor common across eukaryotes (Wolfe et al. 2000). We found multiple C2H2 zinc finger domain-containing proteins (PF00096) in all three fungal MAGs. Similar proteins had been already reported as dimorphic transition regulators in other fungi (Hurtado and Rachubinski 1999), and a C2H2-type zinc finger transcription factor was reported before as a suppressor of hyphal growth in *C. albicans* (Murad et al. 2001). Of transcription factors suppressing hyphal growth, two (*RFG1*, identified through KEGG annotation, and *TUPI1*) were predicted in the lecanoromycete and *Tremella* (Kadosh and Johnson 2001). Among other genes playing the same role, *NGRI* was predicted in *Tremella*, and *SSN6* and *TEC1* (identified through KEGG annotation) were predicted in *Cyphobasidium*. Transcription factors promoting hyphal growth were predicted from all three MAGs with the lecanoromycete having the most: *SKN7* and *CRZ1* in all three fungi, *STE12* in the lecanoromycete and *Tremella*, *ACE2* in the lecanoromycete and *Cyphobasidium*, *EFG1*, *CSR1* and *UME6* in the lecanoromycete, and *FLO8* in *Cyphobasidium*.

2.5. Discussion

Our study is the first to provide genome annotations of SFSs in a lichen and the first to compare and contrast the potential of primary and secondary fungal symbionts. The genomes of SFSs we describe here possess far fewer genes than the lecanoromycete, and rank within the smallest 5% of 1,737 sequenced fungal genomes to date (<https://mycocosm.jgi.doe.gov/fungi/fungi.info.html>, last accessed February 8, 2021). Though genomic data will ultimately need to be complemented with other lines of evidence, patterns of gene enrichment and secretion provide clear evidence of divergent function and inform previous hypotheses of lifestyle among the three fungi in the

Alectoria lichen. These results are furthermore robust to the possibility of false absence of one or few genes. Two of the three MAGs, the lecanoromycete and *Cyphobasidium*, are >97% complete; the *Tremella* MAG is only ~90% complete, but still within the threshold commonly used in metagenomics (Bowers et al. 2017) and high compared with other published eukaryotic MAGs (Delmont et al. 2018). It is therefore unlikely that, for example, CAZyme profiles of the fungi will significantly change.

2.5.1. Potential Contributions of the Fungal Partners

Even with these limitations, however, three clear patterns stand out from our comparison of the three genomes. First, our data are consistent with the theory that SFSs produce secreted polysaccharides that can contribute to the extracellular matrix. Most lecanoromycete-derived lichens possess α -1,6-mannans (Spribille et al. 2020), a common product of ascomycetes (Leal et al. 2010), and our genomic data confirmed that these can be produced by the lecanoromycete. It is however not clear if or to what extent α -1,6-mannans account for the extracellular matrix that holds fungal cells together in the form of a lichen. Acidic polysaccharides are known to be a part of this matrix based on histological studies (e.g., Modenesi and Vanzo 1986), but acidic polysaccharides have never been experimentally assessed in lichens and are basically a black box (Spribille et al. 2020). Of the SFSs, *Tremella* is closely related to species that produce copious, capsular, GXM-like polysaccharides characterized by possessing α -1,3-mannan backbones. Several genes have been identified as related to α -1,3-mannan capsule production in *C. neoformans*, and we found putative orthologs of all of these, not only in the *Tremella* MAG but also in the *Cyphobasidium* MAG. Representatives of the same CAZyme families, though not direct *Cryptococcus* orthologs, are also found in the lecanoromycete. Interestingly, all three MAGs appear to code for genes that synthesize glucuronic acid, even though no lecanoromycete-

derived polysaccharide with glucuronic acid has been experimentally isolated. In summary, this suggests that both *Cyphobasidium* and *Tremella* produce GXM-like molecules, but that some yet-to-be-detected polysaccharides from the lecanoromycete may also carry acidic residues.

Second, both SFS MAGs code for more phosphorus scavenging enzymes than the lecanoromycete, suggesting that these fungi might play a role in lichen nutrient acquisition.

Basidiomycete mutualists in general often provide this function to their plant partners, both in arbuscular and ectomycorrhizal relationships (Smith et al. 2011; Becquer et al. 2014).

Phosphorus provision, and potential phosphorus limitation, is poorly understood in lichen systems, but notably *A. sarmentosa* has been shown to be P-limited under experimental conditions (Johansson et al. 2011).

Third and finally, our data clearly show that the lecanoromycete is the secondary metabolite cluster powerhouse of the *Alectoria* lichen. The close positive correlation of *Cyphobasidium* yeast abundance with an extracellular secondary metabolite, vulpinic acid (Spribille et al. 2016), appeared to suggest SM production either directly as a product of the SFSs or as the result of an interaction between fungi. Although we cannot address this specific SM with the data from the *Alectoria* lichen (which does not produce vulpinic acid), our data do appear to rule out the possibility that *Cyphobasidium* is producing PKS-derived SMs, such as those that dominate the *Alectoria* lichen (*Tremella* possesses one PKS cluster compared with 18 in the lecanoromycete). However, it is not clear that any of the SM clusters in the lecanoromycete can be connected with certainty to the synthesis of a known product. Crucially, our data cannot resolve the question, first advanced by Ahmadjian (1993) in a fungal–algal context, whether lichen SM precursors may be modified to form specific end products by mosaic pathways. There are precedents for

SM end products derived from an orsellinic acid precursor, as several of the *Alectoria* lichen SMs are, to be produced only in coculture of fungi and bacteria (Schroeckh et al. 2009).

Cyphobasidium was first detected in the *Alectoria* symbiosis based on samples from Alaska, BC, and Sweden (see Table S7 in Spribille et al. 2016). In the present study, we confirmed the presence in high frequency of both *Cyphobasidium* and *Tremella* in *Alectoria* thalli in different geographic localities. This is the second lichen symbiosis, after *Letharia vulpina*, in which we have found representatives of both of these genera co-occurring over a wide geographic area (Tuovinen et al. 2019). Like in *L. vulpina*, we occasionally detected only one of the two symbionts in *Alectoria*. The similarity in their secretomes raises the intriguing possibility that they may be functionally redundant, which would be consistent with our finding of one SFS but not the other in about one fifth of the thalli sampled (Fig. 2.3).

2.5.2. The Dimorphism Wildcard

Of the three fungi in the *Alectoria* lichen, the two SFSs come from species groups known to routinely occur in both a hyphal and yeast stage, both of which can manifest themselves in the lichen thallus (Spribille et al. 2016; Tuovinen et al. 2019). The lecanoromycete is known to occur in the lichen symbiosis and by virtue of its sexual reproduction by ascospores is horizontally transmitted, i.e. unaccompanied by other symbionts. It therefore must have an aposymbiotic life stage. At this point, however, nothing is known about this stage, and the fungus that occurs in the lichen is filamentous. Recently, Wang et al. (2020) confirmed dimorphism and the formation of a yeast stage, as well as the role of the PKA-cAMP pathway in regulated dimorphic switching, in the lecanoromycete *Umbilicaria muhlenbergii*. Our data show that the *Alectoria* lichen lecanoromycete likewise possesses cellular machinery for dimorphic switching. While this does not allow us to establish whether dimorphic switching actually occurs, it highlights how little is

known about the life stage between sexual sporulation and reestablishment of the symbiosis to form a new lichen.

The gap in our knowledge about the aposymbiotic life stage for lecanoromycete lichen symbionts suggests we should use caution when trying to interpret the functions some of the genes the lecanoromycete MAG codes for. The lecanoromycete MAG codes for a suite of CAZymes targeting plant polymers. Some of these may occur in the algal cell walls (e.g., cellulose and β -mannans; Honegger and Brunner 1981; Centeno et al. 2016). Cutin, by contrast, is not known from green algae (Philippe et al. 2020). A qPCR-based study showed a predicted lecanoromycete cutinase orthologue to be expressed at similar levels in both axenic culture and during coculturing of the two dominant lichen symbionts (Joneson et al. 2011). The lecanoromycete also possesses numerous features more usually associated with pathogenic fungi. It has more secreted proteases, lipases and catabolic CAZymes than either of the SFSs, and is the only one that is predicted to produce toxins. Whether these enzymes are used to process secretions of the algal symbiont or are deployed in other settings remains to be tested. Finally, the lecanoromycete codes for far more SM clusters than it has documented SMs, a situation similar to *Cladonia uncialis* (Bertrand et al. 2018). This suggests either that many SMs are synthesized in quantities below detection thresholds, or alternatively in settings other than those that have been sampled.

2.5.3. Can Genomic Data Reveal Signatures of Mycoparasitism?

When describing *Cyphobasidium* as a new genus, Millanes et al. (2016) speculated that the fungus is in fact a mycoparasite on the filamentous lecanoromycete in lichens. This they inferred from the occurrence of *Cyphobasidium* in the phylogenetic vicinity of other presumed mycoparasites in the Pucciniomycotina. The presence of genes coding for β -mannanases in the

Cyphobasidium MAG strongly suggests that it may directly interact with plant cell walls, perhaps those of the symbiotic alga, at some point in its life cycle. Extrapolations regarding trophic relationships such as mycoparasitism—and their perpetuation in the literature—are common (e.g., Oberwinkler 2017), but experimental evidence is scarce. *Tremella lethariae*, originally presumed to be a mycoparasite of the lecanoromycete *L. vulpina* (Millanes et al. 2014), has been shown to enmesh algal cells (Tuovinen et al. 2019). Direct evidence of mycoparasitism, by contrast, has yet to be found in any lichen-associated *Cyphobasidium* or *Tremella* species, but studies to date have been limited.

The use of genomic data to infer mycoparasitism is hindered by the fact that fungal–fungal interactions are far less studied than fungal–plant interactions. Like plant pathogens, mycoparasites use secreted lytic enzymes during host invasion, but studies to date have not been able to find a consistent genomic signature for this. For example, a comparative genomic study did not show any enrichment in lytic enzymes in two mycoparasitic species within the ascomycete class Dothideomycetes (Haridas et al. 2020). Although the genomes of three mycoparasitic Tremellales, *Naematella encephala*, *Tremella fuciformis*, and *Tremella mesenterica*, have been sequenced, the molecular mechanisms of *Tremella* — host interactions remain undescribed. Kues and Ruhl (2011) hypothesized that ascorbate oxidase present in genomes of several mycoparasitic fungi, including *T. mesenterica*, plays a role in suppressing fungal host defenses. We identified a putative ascorbate oxidase in the MAGs of the lecanoromycete and *Tremella*, but not *Cyphobasidium*. When comparing six species of Tremellales with different trophic strategies, including the lichen-associated *Tremella* from this study and the three verified mycoparasites mentioned above, we found no clear trend in predicted secretome size, number of CAZymes and number of proteases. Likewise, the number

of enzymes potentially active on fungal cell walls (GH16-GH18, GH128, GH152) was similar regardless of ecology, and none could be shown to act exclusively on exogenous fungal polymers. Finally, N-auxotrophy of *Tremella* inferred from our data suggests *Tremella* has a biotrophic strategy, but our data do not allow us to speculate whether it retrieves nitrogen from one of the fungal partners, from the alga, or from other sources.

2.5.4. Outlook

Our study is the first to provide complete genome assemblies for three fungal symbionts from metagenomic data. Until now, only one fungal symbiont has been assembled from whole lichen metagenomic DNA, the dominant lecanoromycete. Three innovations proved crucial. First, we employed warm water treatment of thalli to dislodge low coverage symbionts from the cortex EPS, thereby driving up coverage relative to the otherwise dominant lecanoromycete. Next, we employed recently developed algorithms to assign eukaryotic DNA to bins. Most previous lichen metagenomic studies (e.g., Greshake Tzovaras et al. 2020), relied on use of reference databases to bin their metagenomes. This allowed them to extract genomes similar to ones that already had been sequenced. Since no sequenced genome from the order Cyphobasidiales existed prior to our study, applying a reference-independent binning approach was crucial. Finally, we evaluated genome completeness based on phylogenetic relatedness. Taken together, these approaches open the door to direct assessment of multiple-eukaryote systems whilst bypassing the challenge of isolating and culturing individual members.

Our functional predictions for the three fungal genomes in the *Alectoria* lichen suggest that future experiments should focus on a possible role for yeasts in differential water retention through secretion of GXM-like polysaccharides as well as in P-scavenging, which previous studies suggest could be important in the oligotrophic conditions in which this lichen grows in

nature (Johansson et al. 2011). Comparative studies combining assessment of yeast abundance with manipulation of wetting/drying cycles or provision of isotope-labeled nutrient precursors could be one way to answer these questions. Our predictions also suggest that more attention should be paid to the diverse pathogenicity factors secreted by the dominant fungus in the symbiosis, the lecanoromycete. RNA-Seq data may reveal whether these are upregulated in initial contact with algal symbionts or whether they could play a role in the aposymbiotic lifestyle of the fungus.

2.6. Materials and Methods

2.6.1. Sample Collection, Preparation, and Sequencing

For a whole lichen metagenome, we collected a thallus of *A. sarmentosa* lichen on March 3, 2017 along the Lochsa River in Idaho County, Idaho, USA (46.56742°N, 114.63975°W; voucher ID Spribille s.n. 03.03.2017 UM-T1853). The sample was frozen at -80°C and ground in a TissueLyser II (Qiagen, Hilden, Germany). We extracted DNA using DNeasy Plant Mini Kit (Qiagen) and prepared a metagenomic library using TruSeq DNA PCR-Free Low Throughput Library Prep Kit (Illumina, San Diego, CA). The library was sequenced at the Huntsman Cancer Center at University of Utah on an Illumina HiSeq 2500 using 125-bp paired-end reads.

We generated another metagenome enriched in low-abundance organisms embedded in the matrix of the cortical layer. For that we collected a healthy-looking thallus of *A. sarmentosa* in June 2018 at the edge of Wells Gray Provincial Park, BC, Canada (51.76°N, 119.94°W; voucher ID Tagirdzhanova 0007). The lichen material was rinsed in water to remove contamination from the surface, put it in 200 ml of water and placed in a shaking incubator overnight at 60°C . We centrifuged the resulting solution for 3 min at $30 \times g$ to remove large pieces of lichen material. The remaining liquid was centrifuged for 7 min at $3,000 \times g$. We dried the resulting pellet

overnight at 60 °C and extracted DNA as described above. A total of 10 ng of DNA was used for metagenomic library preparation. We prepared the library using NEBNext Ultra II DNA Library Prep Kit (New England BioLabs, Ipswich, MA). The library was sequenced at the BC Cancer Genome Sciences Centre on an Illumina HiSeq X using 150-bp paired-end reads.

2.6.2. Metagenome Assembly and Binning

The libraries were filtered with the metaWRAP pipeline (v1.2, Uritskiy et al. 2018). Using bbmap (Bushnell 2014) within the READ_QC module, we aligned reads against hg38 to remove any human contamination. The remaining reads were then assembled into two individual metagenomes using metaSPAdes default settings (Table S1) (v3.13, Nurk et al. 2017). Individual assemblies were binned with CONCOCT within metaWRAP (Alneberg et al. 2014).

We used several tools to identify MAGs and assess their quality. First, we analyzed all bins using CheckM (v1.0.18, Parks et al. 2015), which gave taxonomic placement and quality estimation for prokaryotic MAGs. Then, we analyzed the quality of all bins using EukCC, which gave a first taxonomic assignment as well (Saary et al. 2020). To infer a taxonomic placement of all bins, we used models created by GeneMark-ES (v4.38, Lomsadze et al. 2014) for the almost complete bins of the same data set, to predict proteins in small and incomplete bins, which usually cannot be predicted with GeneMark-ES in the self-training mode. We then inferred the taxonomic position by subsampling up to 200 proteins per bin and subsequently blasting them against the UniRef90 database (UniProt release: 2019_01) using Diamond's BLASTp option (Buchfink et al. 2015). For each protein we considered the top 3 hits passing an e-value threshold of 1×10^{-20} and used a majority vote of 60% to assign the lowest common ancestor (LCA) per protein. Using the same majority vote, we assigned a LCA per bin as the sum of all sampled proteins. Additionally, we ran BUSCO (v4.0.1, Seppey et al. 2019) on all bins assigned to

eukaryotes and, additionally, FGMP (Cissé and Stajich 2019) on all fungal bins. Basic statistics of all MAGs as well as the two metagenomic assemblies were calculated using QUAST (v4.5, Gurevich et al. 2013) using default settings. Median genome coverage was calculated using bowtie2 (v2.3.4.3, Langmead and Salzberg 2012) samtools (v1.8-1, Li et al. 2009), and a custom script (see details on <https://github.com/metalichen/>).

For further analysis, we took bins with >90% genome completeness according to at least one tool and <5% contamination. In cases where we had multiple highly similar genomes assigned to the same taxonomic group, we picked the genome with the highest completeness and for further analysis used only it; in case of lecanoromycete genomes we used the one isolated from the cortex-derived metagenome.

2.6.3. Refining the Taxonomic Placement of the Genomes

We used protein predictions from the fungal MAGs to refine their taxonomic placement. We combined predicted proteomes (see the details on genome annotation below) with proteome data on 38 fungal species from published sources (Table S11). We used Orthofinder (v2.3.8, Emms and Kelly 2019) to identify single copy orthologs genes using Diamond (v0.9.29, Buchfink et al. 2015) all vs all pairwise similarity scores, and constructing a preliminary phylogeny using all shared orthologs genes using the STAG (Emms and Kelly 2018) algorithm to infer multi-copy gene trees within Orthofinder. We selected all single copy orthologs sequences resulting from Orthofinder, aligned them using MAFFT (v7.455, Katoh et al. 2002) and trimmed the low coverage sites using trimAl (v1.2rev59, Capella-Gutiérrez et al. 2009) under automatic settings. We constructed a consensus species tree concatenating all genes, using IQ-TREE (v2.0.2rc2, Nguyen et al. 2015) with a 1,000 repetitions thorough bootstrap and calculating partition evolutionary models per gene based on amino acids matrices. Then, we constructed gene trees

for each single copy ortholog gene using the partition models calculated in IQ-TREE and run in RAxML (v8.2.12, Stamatakis 2014) a maximum likelihood analysis with 1,000 thorough bootstrap under a CAT model with an LG substitution matrix per gene (Le and Gascuel 2008), using CIPRES science gateway servers (Miller et al. 2010). The resulting gene trees were combined into a species tree using the coalescence-based method ASTRAL (v5.14.5, Zhang et al. 2018) calculating a local posterior probability for induced shared quartets based on 1,000 bootstrap trees per gene.

After narrowing taxonomic placement down to the class level, we used BlastN to extract sequences of ITS (internal transcribed spacer; rDNA) for Tremellomycetes and Cystobasidiomycetes from both metagenomic assemblies. We incorporated these into published sequences of their respective class from the literature; all sequences used in this analysis and their NCBI GenBank accession numbers are presented in Table S12. The taxon sampling was done partially following Spribille et al. (2016), Millanes et al. (2011) and Liu, Wang, et al. (2015). Each set of sequences were aligned using MAFFT (v7.271, Katoh et al. 2002) with the flags --genafpair --maxiterate 10000. The alignments were trimmed using trimAl (v1.4.rev15, Capella-Gutiérrez et al. 2009) to remove all sites with $\geq 90\%$ missing data. We determined optimal nucleotide substitution model schemes using PartitionFinder (v2.1.1, Lanfear et al. 2012) with default config settings. Maximum likelihood phylogenetic analyses were performed using IQ-TREE (v1.6.12, Nguyen et al. 2015) with GTR+I+G substitution model and 50,000 rapid bootstrap replicates.

2.6.4. PCR-Based Screening

To check whether the newly identified lineages are consistently present in *A. sarmentosa*, we performed PCR screening. We collected 32 thalli of *Alectoria* in three locations (Table S7). Each

thallus was complemented with two specimens from the same tree: A lichen of a different species and a bark sample. DNA from the lichen material and pieces of bark was extracted as described above. Primers used for the screening are listed in Table S13. For screening *Cyphobasidium*, we used primers and PCR protocol described at Spribille et al. (2016). Screening *Tremella* was performed following Tuovinen et al. (2019). Amplification of *Granulicella* rpoB was done with annealing at 53 °C and 35 cycles. All PCR reactions were performed using KAPA 3G Plant PCR kit (Roche Sequencing Solutions, Pleasanton, CA). PCR products were cleaned prior to sequencing with Exonuclease I and Shrimp Alkaline Phosphatase (New England BioLabs, Ipswich, MA). Amplicons were sequenced by Psomagen Inc (Rockville, MD). We counted a lineage as present if the PCR reaction produced an assignable sequence. Taxonomy assignments of the sequences were verified either by searching them against the NCBI database (for low quality sequences) or by a phylogenetic analysis (Table S14). Produced sequences of mid and high quality were incorporated into published sequences of their respective groups (Table S12 for *Cyphobasidium* and *Tremella*, Table S15 for *Granulicella*). We produced phylogenetic trees in the way described above.

2.6.5. Genome Annotation and Analyses

Functional annotation of the three fungal genomes isolated from the cortex-derived metagenome was performed using the Funannotate pipeline (v1.5.3, github.com/nextgenusfs/funannotate, last accessed February 8, 2021). The assemblies were cleaned to remove repetitive contigs, then sorted and repeat-masked. The prepared assemblies were subjected to ab initio gene prediction using GeneMark-ES (v4.38, self-trained, Lomsadze et al. 2014) and AUGUSTUS (v3.3.2, trained using BUSCO2 gene models, Stanke et al. 2004). EvidenceModeler (v1.1.1, Haas et al.

2008) was used to create consensus gene models. Finally, the models shorter than 50 amino acids or identified as known transposons were excluded using BLASTp search.

Functional annotations were assigned to protein coding gene models using several pipelines: Output from InterProScan (v1.5.3, Jones et al. 2014) and EggNog-Mapper (v1.0.0, Huerta-Cepas et al. 2017) was parsed by funannotate and combined with annotations made by using the following databases: Pfam (v32.0, El-Gebali et al. 2019), gene2product (v1.32, <https://github.com/nextgenusfs/gene2product>, last accessed February 8, 2021), dbCAN (v7.0, Huang et al. 2018), MEROPS (v12.0, Rawlings et al. 2018), UniProtKb (downloaded Feb 2019, The UniProt Consortium 2019). We predicted gene names and product descriptions were done by parsing UniProtKb and EggNog-Mapper searches and cross-referencing results to gene2product database (v1.32). The details on how we used the funannotate pipeline for genome annotation can be found at github (<https://github.com/metalichen/>).

We analyzed the proteins predicted by funannotate using the KAAS webserver (Moriya et al. 2007). We used the antiSMASH web server (Blin et al. 2019) to detect secondary metabolite clusters. To build heatmaps of CAZy and MEROPS families across the three MAGs, we parsed the funannotate outcome using a custom R script. Subfamily-level CAZy annotations were collapsed. We used OrthoVenn webserver (Wang et al. 2015) to annotate orthologous clusters across the three fungal MAGs. To identify putative ribitol transporters, we followed (Armaleo et al. 2019). We ran BLASTp search against the predicted proteins using sequences of characterized sorbitol/mannitol/ribitol/arabitol/H⁺ symporters from *Debaryomyces hansenii* (NCBI Accession Numbers CAG86001 and CAR65543; Pereira et al. 2014) as a query.

To identify secreted proteins, we used a three-step process. First, all proteins were analyzed using SignalP (Bendtsen et al. 2004). All protein models estimated to have a secretion signal

were then analyzed with the TMHMM web server (Krogh et al. 2001). Only models with secretion signal and no transmembrane domain were retained. However, we allowed one transmembrane domain in the N-terminal 60 amino acids, since it often corresponds to the secretion signal. Finally, this set of proteins were analyzed with WoLF PSORT (Horton et al. 2007); the final list only included models with >60% of nearest neighbors belonging to secreted proteins. We defined SSP as secreted proteins <300 amino acids (Pellegrin et al. 2015); putative effectors were identified using the EffectorP webserver (v2.0, Sperschneider et al. 2018).

For four protein families that we reported missing from individual fungal MAGs, we ran an additional search to check whether they are truly missing or were missed in our analysis due to imperfect binning or genome annotation. We used metaEuk (v2, Levy Karin et al. 2020) to predict proteins across all metagenomic contigs. We then ran hmmsearch (HMMER v3.2.1, Eddy 2011) with an E-value cutoff of $10e-5$ to identify the following Pfams corresponding to the missing protein families: PF01083 for CAZY CE5, PF01670 for GH12, PF00089 for MEROPS S1, and PF01583 for adenylylsulphate kinase. We subsequently ran diamond blastp (Buchfink et al. 2015) against UniRef50 (UniProt 2020_02) with parameter -top 3 and used majority voting to identify eukaryotic hits. Among them, we selected hits associated with the studied MAGs: First identifying hits that landed on contigs assigned to these MAGs, then searching the remaining (unbinned) hits against UniRef50 and selecting those that returned fungal proteins. If our search yielded a candidate protein assignable to a MAG, we did not report this family missing.

For the comparative genomics study, we annotated fifteen additional genomes (Table S8). For each of them, we obtained nucleotide assemblies and annotated them in the same way as described above. We used the “funannotate compare” function to compare this set of genomes. “Funannotate compare” summarizes all functional annotations for the genomes; it also runs a

phylogenomic analysis based on single-copy orthologs. Randomly selected BUSCO orthologs were concatenated for each genome, aligned using MAFFT and analyzed using RAxML using PROTGAMMAAUTO substitution model and 100 rapid bootstrap replicates.

2.6.6. CAZyme Analysis

We calculated the distribution of different CAZy families in the three fungal MAGs using dbCAN annotations produced by funannotate. For this purpose, all annotations on the sub-family level were collapsed. Then, we isolated all CAZymes labeled as secreted proteins and analyzed them in the same way.

We selected families of interest and analyzed them in depth using SACCHARIS pipeline (Jones et al. 2018). Characterized GH5 full length sequences from these families were downloaded from the CAZy website and aligned with the CAZymes identified in the MAGs. Sequences were trimmed to the catalytic domains using dbCAN (Huang et al. 2018) and aligned with MUSCLE (Edgar 2004). The phylogenies were reconstructed using FastTree2 (Price et al. 2010) and visualized using iTOL (Letunic and Bork 2019).

2.6.7. Supplementary material and data availability

Supplementary tables and figures are published at <https://doi.org/10.1093/gbe/evab129>. Raw metagenomic data, metagenomic assemblies, and annotated MAGs have been submitted to the European Nucleotide Archive (PRJEB40332). PCR-produced sequences are deposited: high-quality sequences in NCBI (Table S7). Custom scripts and other data used in the analyses are available in a Dryad repository at <https://doi.org/10.5061/dryad.c2fqz617h>.

References

- Abdel-Hameed, M., Bertrand, R. L., Piercey-Normore, M. D., Sorensen, J. L. (2016). Putative identification of the usnic acid biosynthetic gene cluster by *de novo* whole-genome sequencing of a lichen-forming fungus. *Fungal Biol.* 120(3), 306–316.
- Adrio, J. L. (2017). Oleaginous yeasts: promising platforms for the production of oleochemicals and biofuels. *Biotechnol Bioeng.* 114(9), 1915–1920.
- Ahmadjian, V. (1993). *The lichen symbiosis*. New York: John Wiley & Sons.
- Alneberg, J., et al. (2014). Binning metagenomic contigs by coverage and composition. *Nat Methods.* 11(11), 1144–1146.
- Armaleo, D., et al. (2019). The lichen symbiosis re-viewed through the genomes of *Cladonia grayi* and its algal partner *Asterochloris glomerata*. *BMC Genomics* 20(1), 605.
- Becquer, A., Trap, J., Irshad, U., Ali, M. A., Claude, P. (2014). From soil to plant, the journey of P through trophic relationships and ectomycorrhizal association. *Front Plant Sci.* 5, 548.
- Bendtsen, J. D., Nielsen, H., von Heijne, G., Brunak, S. (2004). Improved prediction of signal peptides: signalP 3.0. *J Mol Biol.* 340(4), 783–795.
- Beopoulos, A., et al. (2009). *Yarrowia lipolytica* as a model for bio-oil production. *Prog Lipid Res.* 48(6), 375–387.
- Bertrand, R. L., Abdel-Hameed, M., Sorensen, J. L. (2018). Lichen biosynthetic gene clusters. Part I. Genome sequencing reveals a rich biosynthetic potential. *J Nat Prod.* 81(4), 723–731.
- Blin, K., et al. (2019). AntiSMASH 5.0: updates to the secondary metabolite genome mining pipeline. *Nucleic Acids Res.* 47(W1), W81–W87.

- Borges-Walmsley, M. I., Walmsley, A. R. (2000). cAMP signalling in pathogenic fungi: control of dimorphic switching and pathogenicity. *Trends Microbiol.* 8(3), 133–141.
- Bowers, R. M., et al. (2017). Minimum information about a single amplified genome (MISAG) and a metagenome-assembled genome (MIMAG) of bacteria and archaea. *Nat Biotechnol.* 35(8), 725–731.
- Brodo, I., Hawksworth, D. L. (1977). *Alectoria* and allied genera in North America. *Opera Bot.* 42, 1–164.
- Buchfink, B., Xie, C., Huson, D. H. (2015). Fast and sensitive protein alignment using DIAMOND. *Nat Methods.* 12(1), 59–60.
- Burton, R. A., Gidley, M. J., Fincher, G. B. (2010). Heterogeneity in the chemistry, structure and function of plant cell walls. *Nat Chem Biol.* 6(10), 724–732.
- Bushnell, B. (2014). BBMap: a fast, accurate, splice-aware aligner. Berkeley (CA): Ernest Orlando Lawrence Berkeley National Laboratory.
- Capella-Gutiérrez, S., Silla-Martínez, J. M., Gabaldón, T. (2009). trimAl: a tool for automated alignment trimming in large-scale phylogenetic analyses. *Bioinformatics* 25(15), 1972–1973.
- Centeno, D. C., Hell, A. F., Braga, M. R., del Campo, E. M., Casano, L. M. (2016). Contrasting strategies used by lichen microalgae to cope with desiccation-rehydration stress revealed by metabolite profiling and cell wall analysis. *Environ Microbiol.* 18(5), 1546–1560.
- Černajová, I., Škaloud, P. (2019). The first survey of Cystobasidiomycete yeasts in the lichen genus *Cladonia*; with the description of *Lichenozyma pisutiana* gen. nov., sp. nov. *Fungal Biol.* 123(9), 625–637.

- Chang, H. X., Yendrek, C. R., Caetano-Anolles, G., Hartman, G. L. (2016). Genomic characterization of plant cell wall degrading enzymes and in silico analysis of xylanases and polygalacturonases of *Fusarium virguliforme*. *BMC Microbiol.* 16(1), 147.
- Chen, E. C. H., et al. (2018). High intraspecific genome diversity in the model arbuscular mycorrhizal symbiont *Rhizophagus irregularis*. *New Phytol.* 220(4), 1161–1171.
- Cissé, O. H., Stajich, J. E. (2019). FGMP: assessing fungal genome completeness. *BMC Bioinformatics* 20(1), 184.
- de Baets, S., Vandamme, E. J. (2001). Extracellular *Tremella* polysaccharides: structure, properties and applications. *Biotechnol Lett.* 23(17), 1361–1366.
- Delmont, T. O., et al. (2018). Nitrogen-fixing populations of Planctomycetes and Proteobacteria are abundant in surface ocean metagenomes. *Nat Microbiol.* 3(7), 804–813.
- Doering, T. L. (2009). How sweet it is! Cell wall biogenesis and polysaccharide capsule formation in *Cryptococcus neoformans*. *Annu Rev Microbiol.* 63, 223–247.
- Dubovenko, A. G., et al. (2010). Trypsin-like proteins of the fungi as possible markers of pathogenicity. *Fungal Biol.* 114(2–3), 151–159.
- Eddy, S. R. (2011). Accelerated profile HMM searches. *PLoS Comput Biol.* 7(10), e1002195.
- Edgar, R. C. (2004). MUSCLE: multiple sequence alignment with high accuracy and high throughput. *Nucleic Acids Res.* 32(5), 1792–1797.
- El-Gebali, S., et al. (2019). The Pfam protein families database in 2019. *Nucleic Acids Res.* 47(D1), D427–D432.

- Emms, D. M., Kelly, S. (2018). STAG: species tree inference from all genes. *bioRxiv*. Available from: 10.1101/267914.
- Emms, D. M., Kelly, S. (2019). OrthoFinder: phylogenetic orthology inference for comparative genomics. *Genome Biol.* 20(1), 238.
- Fan, H., et al. (2014). Functional analysis of a subtilisin-like serine protease gene from biocontrol fungus *Trichoderma harzianum*. *J Microbiol.* 52(2), 129–138.
- Geshi, N., Harholt, J., Sakuragi, Y., Jensen, J. K., Scheller, H. V. (2018). Glycosyltransferases of the GT47 family. In: *Annual plant reviews online*. p. 265–283.
- Greshake Tzovaras, B., et al. (2020). What is in *Umbilicaria pustulata*? A metagenomic approach to reconstruct the holo-genome of a lichen. *Genome Biol Evol.* 12(4), 309–324.
- Grijpstra, J. (2008). Capsule biogenesis in *Cryptococcus neoformans*. Utrecht, The Netherlands: Utrecht University.
- Gurevich, A., Saveliev, V., Vyahhi, N., Tesler, G. (2013). QUASt: quality assessment tool for genome assemblies. *Bioinformatics* 29(8), 1072–1075.
- Haas, B. J., et al. (2008). Automated eukaryotic gene structure annotation using EVidenceModeler and the Program to Assemble Spliced Alignments. *Genome Biol.* 9(1), R7.
- Haridas, S., et al. (2020). 101 Dothideomycetes genomes: a test case for predicting lifestyles and emergence of pathogens. *Stud Mycol.* 96, 141–153.
- Henry, C., et al. (2016). Biosynthesis of cell wall mannan in the conidium and the mycelium of *Aspergillus fumigatus*. *Cell Microbiol.* 18(12), 1881–1891.

Honegger, R., Bartnicki-Garcia, S. (1991). Cell wall structure and composition of cultured mycobionts from the lichens *Cladonia macrophylla*, *Cladonia caespiticia*, and *Physcia stellaris* (Lecanorales, Ascomycetes). *Mycol Res.* 95(8), 905–914.

Honegger, R., Brunner, U. (1981). Sporopollenin in the cell walls of *Coccomyxa* and *Myrmecia* phycobionts of various lichens: an ultrastructural and chemical investigation. *Can J Bot.* 59(12), 2713–2734.

Horton, P., et al. (2007). WoLF PSORT: protein localization predictor. *Nucleic Acids Res.* 35(Web Server issue), W585–W587.

Huang, L., et al. (2018). DbCAN-seq: a database of carbohydrate-active enzyme (CAZyme) sequence and annotation. *Nucleic Acids Res.* 46(D1), D516–D521.

Huerta-Cepas, J., et al. (2017). Fast genome-wide functional annotation through orthology assignment by eggNOG-mapper. *Mol Biol Evol.* 34(8), 2115–2122.

Hurtado, C. A. R., Rachubinski, R. A. (1999). Mhy1 encodes a c2h2-type zinc finger protein that promotes dimorphic transition in the yeast *Yarrowia lipolytica*. *J Bacteriol.* 181(10), 3051–3057.

Jeong, M. H., Park, S. Y., Kim, J. A., Cheong, Y. H., Hur, J. S. (2015). RDS1 involved in yeast-to-mycelium transition in lichen-forming fungus *Umbilicaria muehlenbergii*. *Korean Mycol Soc News.* 27(2), 93.

Johansson, O., Olofsson, J., Giesler, R., Palmqvist, K. (2011). Lichen responses to nitrogen and phosphorus additions can be explained by the different symbiont responses. *New Phytol.* 191(3), 795–805.

- Jones, D. R., et al. (2018). SACCHARIS: an automated pipeline to streamline discovery of carbohydrate active enzyme activities within polyspecific families and *de novo* sequence datasets. *Biotechnol Biofuels*. 11, 27.
- Jones, P., et al. (2014). InterProScan 5: genome-scale protein function classification. *Bioinformatics* 30(9), 1236–1240.
- Joneson, S., Armaleo, D., Lutzoni, F. (2011). Fungal and algal gene expression in early developmental stages of lichen-symbiosis. *Mycologia*, 103(2), 291–306.
- Kadosh, D., Johnson, A. D. (2001). Rfg1, a protein related to the *Saccharomyces cerevisiae* hypoxic regulator Rox1, controls filamentous growth and virulence in *Candida albicans*. *Mol Cell Biol*. 21(7), 2496–2505.
- Karimi, E., et al. (2018). Metagenomic binning reveals versatile nutrient cycling and distinct adaptive features in alphaproteobacterial symbionts of marine sponges. *FEMS Microbiol Ecol*. 94(6), fyy074.
- Katoh, K., Misawa, K., Kuma, K. I., Miyata, T. (2002). MAFFT: a novel method for rapid multiple sequence alignment based on fast Fourier transform. *Nucleic Acids Res*. 30(14), 3059–3066.
- Kombrink, A., Thomma, B. P. H. J. (2013). LysM effectors: secreted proteins supporting fungal life. *PLoS Pathog*. 9(12), e1003769.
- Kono, M., Kon, Y., Ohmura, Y., Satta, Y., Terai, Y. (2020). In vitro resynthesis of lichenization reveals the genetic background of symbiosis-specific fungal–algal interaction in *Usnea hakonensis*. *BMC Genomics* 21(1), 671.

- Krogh, A., Larsson, B., von Heijne, G., Sonnhammer, E. L. L. (2001). Predicting transmembrane protein topology with a hidden Markov model: application to complete genomes. *J Mol Biol.* 305(3), 567–580.
- Kues, U., Ruhl, M. (2011). Multiple multi-copper oxidase gene families in basidiomycetes—what for? *Curr Genomics.* 12(2), 72–94.
- Lanfear, R., Calcott, B., Ho, S. Y. W., Guindon, S. (2012). PartitionFinder: combined selection of partitioning schemes and substitution models for phylogenetic analyses. *Mol Biol Evol.* 29(6), 1695–1701.
- Langmead, B., Salzberg, S. L. (2012). Fast gapped-read alignment with Bowtie 2. *Nat Methods.* 9(4), 357–359.
- Le, S. Q., Gascuel, O. (2008). An improved general amino acid replacement matrix. *Mol Biol Evol.* 25(7), 1307–1320.
- Leal, J. A., Prieto, A., Bernabé, M., Hawksworth, D. L. (2010). An assessment of fungal wall heteromannans as a phylogenetically informative character in ascomycetes. *FEMS Microbiol Rev.* 34(6), 986–1014.
- Leandro, M. J., Fonseca, C., Gonçalves, P. (2009). Hexose and pentose transport in ascomycetous yeasts: an overview. *FEMS Yeast Res.* 9(4), 511–525.
- Lee, I. R., Chow, E. W., Morrow, C. A., Djordjevic, J. T., Fraser, J. A. (2011). Nitrogen metabolite repression of metabolism and virulence in the human fungal pathogen *Cryptococcus neoformans*. *Genetics* 188(2), 309–323.

- Lendemer, J. C., et al. (2019). A taxonomically broad metagenomic survey of 339 species spanning 57 families suggests cystobasidiomycete yeasts are not ubiquitous across all lichens. *Am J Bot.* 106(8), 1090–1095.
- Lenova, L. I., Blum, O. B. (1983). K voprosu o tret'em komponente lishaynikov (On the question of the third component of lichens). *Bot Zhurn.* 68, 21–28.
- Lesage, G., et al. (2004). Analysis of β -1,3-glucan assembly in *Saccharomyces cerevisiae* using a synthetic interaction network and altered sensitivity to caspofungin. *Genetics* 167(1), 35–49.
- Lesage, G., et al. (2005). An interactional network of genes involved in chitin synthesis in *Saccharomyces cerevisiae*. *BMC Genet.* 6(1), 8.
- Letunic, I., Bork, P. (2019). Interactive Tree of Life (iTOL) v4: recent updates and new developments. *Nucleic Acids Res.* 47(W1), W256–W259.
- Levy Karin, E., Mirdita, M., Söding, J. (2020). MetaEuk—sensitive, high-throughput gene discovery, and annotation for large-scale eukaryotic metagenomics. *Microbiome* 8(1):1–15.
- Li, H., et al. (2009). The Sequence Alignment/Map format and SAMtools. *Bioinformatics* 25(16), 2078–2079.
- Liu, L., Zhang, Z., et al. (2015). Bioinformatical analysis of the sequences, structures and functions of fungal polyketide synthase product template domains. *Sci Rep.* 5, 10463.
- Liu, X.-Z., Wang, Q.-M., et al. (2015). Phylogeny of tremellomycetous yeasts and related dimorphic and filamentous basidiomycetes reconstructed from multiple gene sequence analyses. *Stud Mycol.* 81, 1–26.
- Lomsadze, A., Burns, P. D., Borodovsky, M. (2014). Integration of mapped RNA-Seq reads into automatic training of eukaryotic gene finding algorithm. *Nucleic Acids Res.* 42(15), e119.

- Mark, K., et al. (2020). Contrasting co-occurrence patterns of photobiont and cystobasidiomycete yeast associated with common epiphytic lichen species. *New Phytol.* 227(5), 1362–1375.
- Martinou, A., Koutsioulis, D., Bouriotis, V. (2003). Cloning and expression of a chitin deacetylase gene (CDA2) from *Saccharomyces cerevisiae* in *Escherichia coli*: purification and characterization of the cobalt-dependent recombinant enzyme. *Enzyme Microb Tech.* 32(6), 757–763.
- Matsuura, Y., et al. (2018). Recurrent symbiont recruitment from fungal parasites in cicadas. *Proc Natl Acad Sci USA.* 115(26), E5970–E5979.
- Millanes, A. M., Diederich, P., Ekman, S., Wedin, M. (2011). Phylogeny and character evolution in the jelly fungi (Tremellomycetes, Basidiomycota, Fungi). *Mol Phylogenet Evol.* 61(1), 12–28.
- Millanes, A. M., Diederich, P., Wedin, M. (2016). *Cyphobasidium* gen. nov., a new lichen-inhabiting lineage in the Cystobasidiomycetes (Pucciniomycotina, Basidiomycota, Fungi). *Fungal Biol.* 120(11), 1468–1477.
- Millanes, A. M., Truong, C., Westberg, M., Diederich, P., Wedin, M. (2014). Host switching promotes diversity in host-specialized mycoparasitic fungi: uncoupled evolution in the *Biatoropsis-Usnea* system. *Evolution* 68(6), 1576–1593.
- Miller, M. A., Pfeiffer, W., Schwartz, T. (2010). Creating the CIPRES science gateway for inference of large phylogenetic trees. In: *2010 Gateway Computing Environments Workshop, GCE 2010.* p. 1–8.
- Modenesi, P., Vanzo, C. (1986). The cortical surfaces in *Parmelia saxatilis* and *P. caperata*: a histochemical approach. *Lichenologist* 18(4), 329–338.

Moriya, Y., Itoh, M., Okuda, S., Yoshizawa, A. C., Kanehisa, M. (2007). KAAS: an automatic genome annotation and pathway reconstruction server. *Nucleic Acids Res.* 35(Web Server issue), W182–W185.

Murad, A. M. A., et al. (2001). NRG1 represses yeast–hypha morphogenesis and hypha-specific gene expression in *Candida albicans*. *EMBO J.* 20(17), 4742–4752.

Nakamura, A. M., Nascimento, A. S., Polikarpov, I. (2017). Structural diversity of carbohydrate esterases. *Biotechnol Res Innov.* 1(1), 35–51.

Nguyen, L. T., Schmidt, H. A., von Haeseler, A., Minh, B. Q. (2015). IQ-TREE: a fast and effective stochastic algorithm for estimating maximum-likelihood phylogenies. *Mol Biol Evol.* 32(1), 268–274.

Nurk, S., Meleshko, D., Korobeynikov, A., Pevzner, P. A. (2017). MetaSPAdes: a new versatile metagenomic assembler. *Genome Res.* 27(5), 824–834.

Oberwinkler, F. (2017). Yeasts in Pucciniomycotina. *Mycol Progress.* 16(9):831–856.

Park, S. Y., et al. (2013). *Agrobacterium tumefaciens*-mediated transformation of the lichen fungus, *Umbilicaria muehlenbergii*. *PLoS One* 8(12), e83896.

Parks, D. H., Imelfort, M., Skennerton, C. T., Hugenholtz, P., Tyson, G. W. (2015). CheckM: assessing the quality of microbial genomes recovered from isolates, single cells, and metagenomes. *Genome Res.* 25(7), 1043–1055.

Pellegrin, C., Morin, E., Martin, F. M., Veneault-Fourrey, C. (2015). Comparative analysis of secretomes from ectomycorrhizal fungi with an emphasis on small-secreted proteins. *Front Microbiol.* 6, 1278.

- Pereira, I., Madeira, A., Prista, C., Loureiro-Dias, M. C., Leandro, M. J. (2014). Characterization of new polyol/H⁺ symporters in *Debaryomyces hansenii*. *PLoS One* 9(2), e88180.
- Philippe, G., et al. (2020). Cutin and suberin: assembly and origins of specialized lipidic cell wall scaffolds. *Curr Opin Plant Biol.* 55, 11–20.
- Price, M. N., Dehal, P. S., Arkin, A. P. (2010). FastTree 2—Approximately maximum-likelihood trees for large alignments. *PLoS One* 5(3), e9490.
- Rawlings, N. D., et al. (2018). The MEROPS database of proteolytic enzymes, their substrates and inhibitors in 2017 and a comparison with peptidases in the PANTHER database. *Nucleic Acids Res.* 46(D1), D624–D632.
- Rigden, D. J. (2008). The histidine phosphatase superfamily: structure and function. *Biochem J.* 409(2), 333–348.
- Saary, P., Mitchell, A. L., Finn, R. D. (2020). Estimating the quality of eukaryotic genomes recovered from metagenomic analysis with EukCC. *Genome Biol.* 21(1), 1–21.
- Sanz-Martín, J. M., et al. (2016). A highly conserved metalloprotease effector enhances virulence in the maize anthracnose fungus *Colletotrichum graminicola*. *Mol Plant Pathol.* 17(7), 1048–1062.
- Schroeckh, V., et al. (2009). Intimate bacterial-fungal interaction triggers biosynthesis of archetypal polyketides in *Aspergillus nidulans*. *Proc Natl Acad Sci USA.* 106(34), 14558–14563.
- Seppy, M., Manni, M., Zdobnov, E. M. (2019). BUSCO: assessing genome assembly and annotation completeness. In: *Gene prediction*. New York: Humana. p. 227–245.
- Sitepu, I. R., et al. (2014). Oleaginous yeasts for biodiesel: current and future trends in biology and production. *Biotechnol Adv.* 32(7), 1336–1360.

- Smith, S. E., Jakobsen, I., Grønlund, M., Smith, F. A. (2011). Roles of arbuscular mycorrhizas in plant phosphorus nutrition: interactions between pathways of phosphorus uptake in arbuscular mycorrhizal roots have important implications for understanding and manipulating plant phosphorus acquisition. *Plant Physiol.* 156(3), 1050–1057.
- Sperschneider, J., Dodds, P. N., Gardiner, D. M., Singh, K. B., Taylor, J. M. (2018). Improved prediction of fungal effector proteins from secretomes with EffectorP 2.0. *Mol Plant Pathol.* 19(9), 2094–2110.
- Spribille, T., et al. (2020). 3D biofilms: in search of the polysaccharides holding together lichen symbioses. *FEMS Microbiol Lett.* 367(5), fnaa023.
- Spribille, T., et al. (2016). Basidiomycete yeasts in the cortex of ascomycete macrolichens. *Science* 353(6298), 488–492.
- Stamatakis, A. (2014). RAxML version 8: a tool for phylogenetic analysis and post-analysis of large phylogenies. *Bioinformatics* 30(9), 1312–1313.
- Stanke, M., Steinkamp, R., Waack, S., Morgenstern, B. (2004). AUGUSTUS: a web server for gene finding in eukaryotes. *Nucleic Acids Res.* 32(Web Server issue), W309–W312.
- Sudbery, P. E. (2011). Growth of *Candida albicans* hyphae. *Nat Rev Microbiol.* 9(10), 737–748.
- Takashima, M., Hamamoto, M., Nakase, T. (2000). Taxonomic significance of fucose in the class urediniomycetes: distribution of fucose in cell wall and phylogeny of urediniomycetous yeasts. *Syst Appl Microbiol.* 23(1), 63–70.
- The UniProt Consortium. (2019). UniProt: a worldwide hub of protein knowledge. The UniProt Consortium. *Nucleic Acids Res.* 47(D1), D506–D515.

- Tuovinen, V., Millanes, A. M., Freire-Rallo, S., Rosling, A., Wedin, M. (2021). *Tremella macrobasidiata* and *Tremella variae* have abundant and widespread yeast stages in *Lecanora* lichens. *Environ Microbiol.* doi: 10.1111/1462-2920.15455.
- Tuovinen, V., et al. (2019). Two basidiomycete fungi in the cortex of wolf lichens. *Curr Biol.* 29(3), 476–483.
- Uritskiy, G. V., DiRuggiero, J., Taylor, J. (2018). MetaWRAP—a flexible pipeline for genome-resolved metagenomic data analysis. *Microbiome* 6(1), 158.
- Wang, Y., Coleman-Derr, D., Chen, G., Gu, Y. Q. (2015). OrthoVenn: a web server for genome wide comparison and annotation of orthologous clusters across multiple species. *Nucleic Acids Res.* 43(W1), W78–W84.
- Wang, Y., Wei, X., Bian, Z., Wei, J., Xu, J.-R. (2020). Coregulation of dimorphism and symbiosis by cyclic AMP signaling in the lichenized fungus *Umbilicaria muhlenbergii*. *Proc Natl Acad Sci USA.* 117(38), 23847–23858.
- West, P. T., Probst, A. J., Grigoriev, I. V., Thomas, B. C., Banfield, J. F. (2018). Genome-reconstruction for eukaryotes from complex natural microbial communities. *Genome Res.* 28(4), 569–580.
- Wolfe, S. A., Nekludova, L., Pabo, C. O. (2000). DNA recognition by Cys2His2 zinc finger proteins. *Annu Rev Biophys Biomol Struct.* 29, 183–212.
- Zaragoza, O., et al. (2009). The capsule of the fungal pathogen *Cryptococcus neoformans*. *Adv Appl Microbiol.* 68, 133–216.
- Zhang, C., Rabiee, M., Sayyari, E., Mirarab, S. (2018). ASTRAL-III: polynomial time species tree reconstruction from partially resolved gene trees. *BMC Bioinformatics* 19(Suppl 6), 153.

Zuccaro, A., et al. (2011). Endophytic life strategies decoded by genome and transcriptome analyses of the mutualistic root symbiont *Piriformospora indica*. *PLoS Pathog.* 7(10), e1002290.

Table 2.1. Draft Genome Statistics for the Bulk-Lichen and Cortex-Slurry Metagenomes Following Bin Merging.

Metagenome	Taxonomic Assignment*	Lineage Assigned by BUSCO4	Completeness**	Contamination	Total Length, Mb	N50, kb	Largest Contig, kb	Number of Scaffolds	Median Coverage
Bulk-lichen	<i>Alectoria</i> , Ascomycota	Ascomycota	EukCC: 98.84% FGMP: 98.7% BUSCO: 95.5%	EukCC: 1.16% BUSCO: 0.7%	53.4	86.2	529.3	1136	188.8
Cortex-slurry	<i>Alectoria</i> , Ascomycota	Ascomycota	EukCC: 98.58% FGMP: 98.8% BUSCO: 95%	EukCC: 0.33% BUSCO: 0.1%	53.4	73.3	397.5	1578	40.8
	<i>Cyphobasidium</i> , Basidiomycota	Basidiomycota	EukCC:97.67% FGMP: 94.4% BUSCO: 83.9%	EukCC: 0% BUSCO: 0.3%	17.6	58.5	245.6	565	40.9
	<i>Tremella</i> , Basidiomycota	Tremellomycetes	EukCC: 90.74% FGMP: 88.9% BUSCO: 83.4%	EukCC: 0.87% BUSCO: 0.2%	17.2	23.1	107.8	1090	11.2
	<i>Granulicella</i> , Acidobacteria	Acidobacteria	CheckM: 98.71% BUSCO: 96%	CheckM: 0.86% BUSCO: 0.5%	4.1	140.1	454.6	84	514.9
	<i>Granulicella</i> , Acidobacteria	Acidobacteria	CheckM: 96.88% BUSCO 97.2%	CheckM: 0.85% BUSCO: 0.2%	3.9	101.8	221.4	118	46.5

NOTE.—Here, we list only MAGs with completeness >90% according to at least one tool used and contamination <5%.

*To assign taxonomic placement of bacterial genomes we used CheckM. Taxonomy of eukaryotes was inferred using phylogenomic and phylogenetic analyses. **BUSCO completeness defined as 100% minus missing BUSCOs. Only genomes with completeness > 90% are listed.

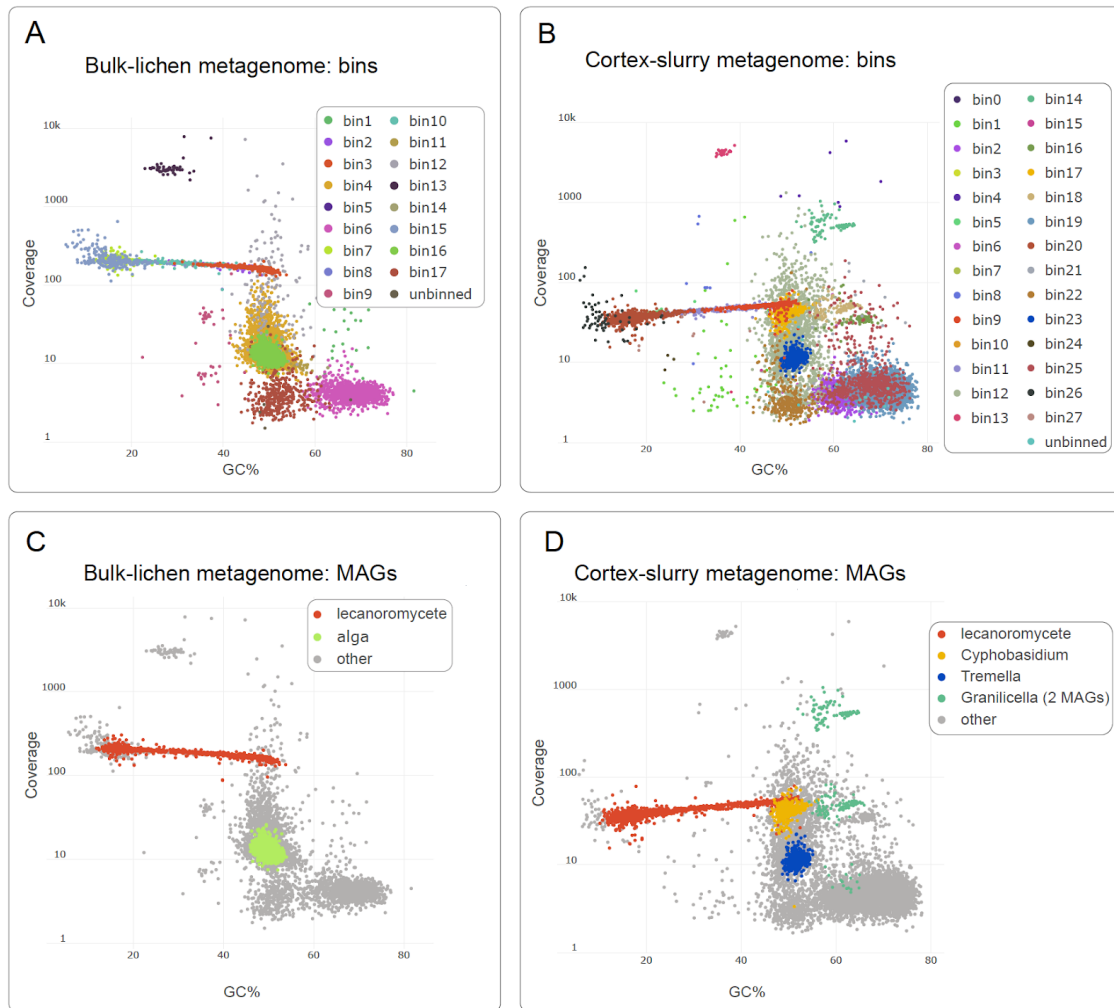


Fig. 2.1. The assignment of contigs to bins and genomes in the two *Alectoria* lichen metagenomes.

(A) Bulk-lichen metagenome, colours assigned based on the initial binning. (B) Cortex-slurry metagenome, colours assigned based on the initial binning. (C) Bulk-lichen metagenome, colours represent MAG assignments. (D) cortex-slurry metagenome, colours represent MAG assignments. According to preliminary taxonomic assignment, bin 3 from the bulk-lichen metagenome, and bin 9 from the cortex-slurry metagenome were assigned to Ascomycota. Each of them was a part of a linear-shaped cloud extending from 10% to 55% of GC-content. In each metagenome separately, we merged bins constituting the linear cloud, which was additionally verified by the taxonomic placement of the bins. The bulk-lichen metagenome contained MAGs of the two core partners of the symbiosis, the lecanoromycete and the alga. The cortex-slurry metagenome, in addition to the lecanoromycete genome, contained MAGs of two SFSs and two bacterial MAGs.

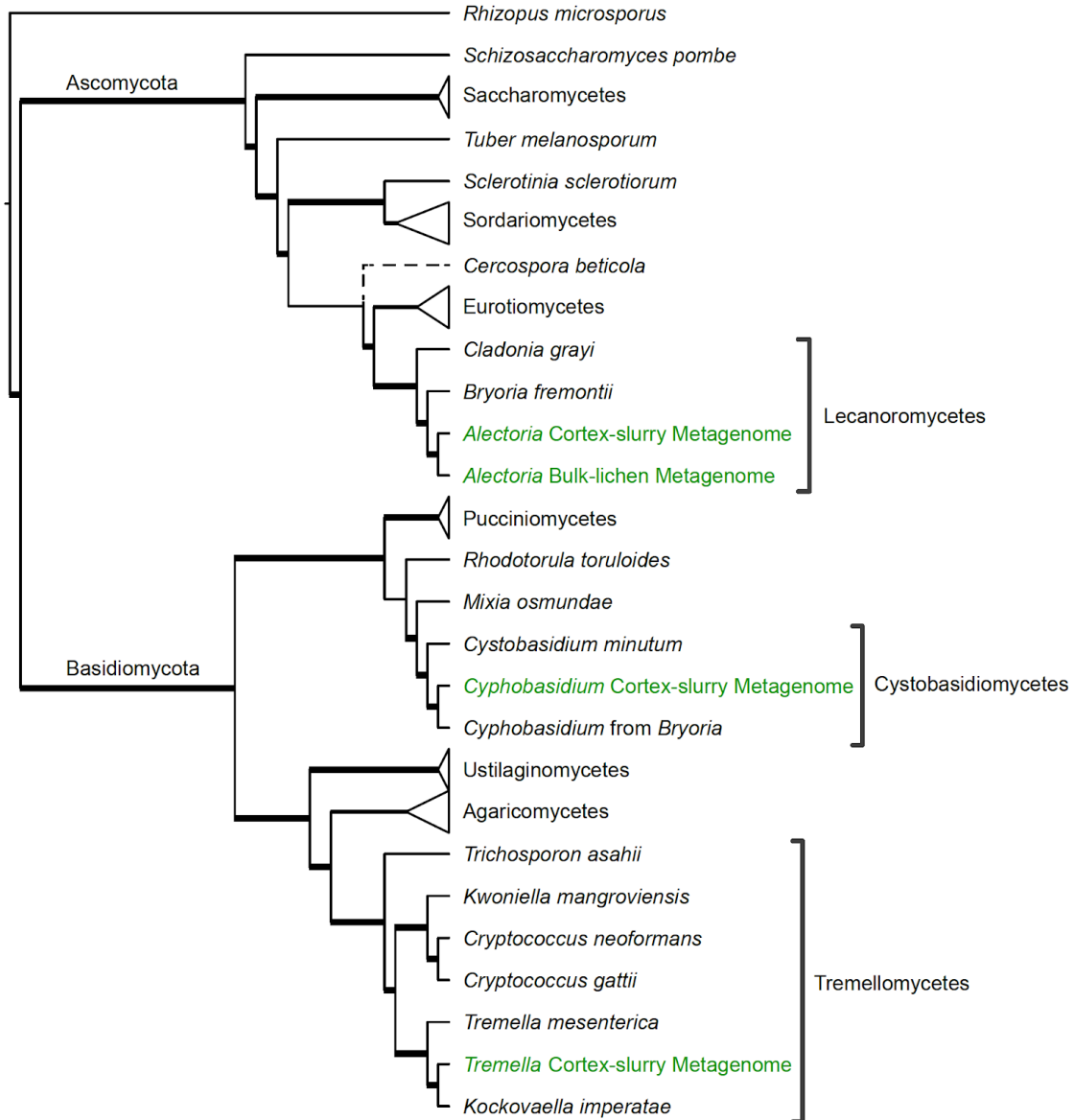


Fig. 2.2. Maximum likelihood phylogenomic tree based on 42 fungal proteomes and 71 single-copy orthologous loci.

Data derived from the studied metagenomes are indicated in green. Bold lines indicate ASTRAL bootstrapping >90 (species tree) based on 1000 bootstrap replicates per gene, and IQTREE ultrafast bootstrap >95 (concatenated tree) based on 1000 replicates. The dashed line indicates a conflict between the species tree and the concatenated tree.

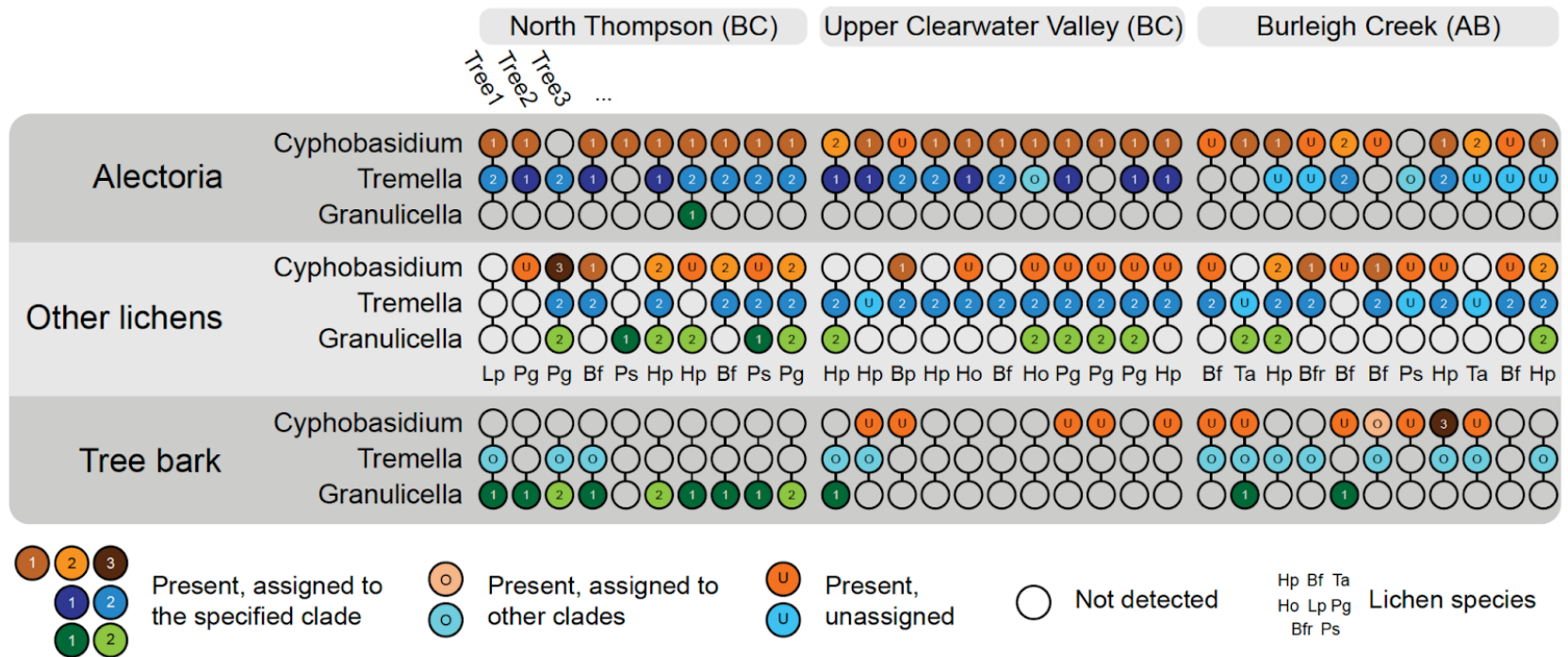


Fig. 2.3. Frequency of association of the three low-abundance partners identified in the cortex-derived metagenome based on PCR-screening of *Alectoria* lichen thalli paired with a random non-*Alectoria* lichen and tree bark from the same branch on 32 trees from three localities in BC and AB, Canada.

Each vertical column represents one sample tree. Coloured circles represent presence; numbers 1–3 correspond to the clade the sequence was recovered from (Figs. S4–S6), “O” are sequences recovered in other parts of the tree, “A” are sequences unassigned due to poor quality (identity of these was sequences verified by searching them against NCBI). Letter codes stand for species of associated macrolichens used for assays: Bfr, *Bryoria fremontii*; Bf, *Bryoria fuscescens*; Ho, *Hypogymnia occidentalis*; Hp, *Hypogymnia physodes*; Lp, *Lobaria pulmonaria*; Ps, *Parmelia sulcata*; Pg, *Platismatia glauca*; Ta, *Tuckermannopsis americana*.

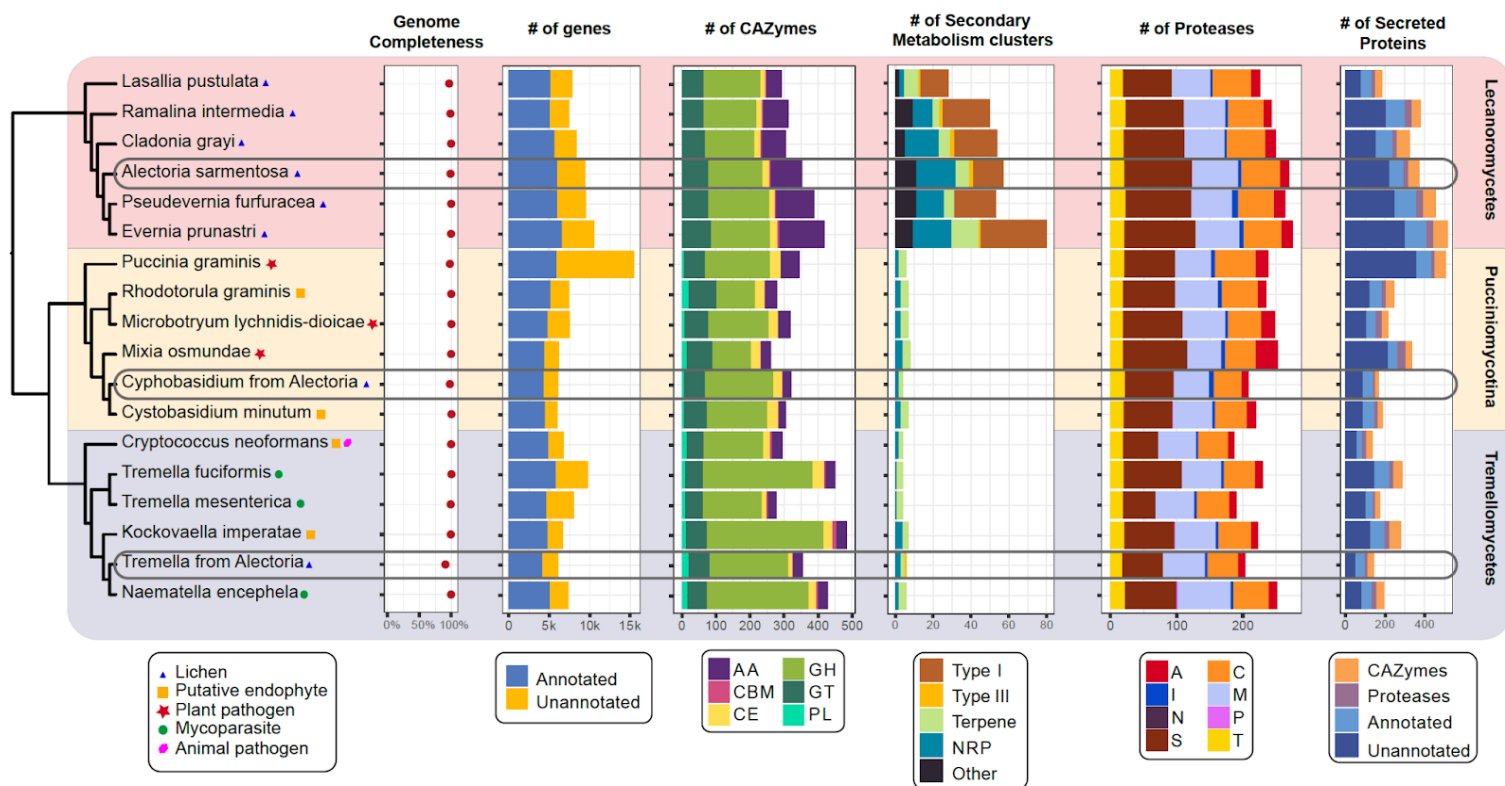


Fig. 2.4. Comparative genomic analysis of the three fungi from *Alectoria* lichen with closely related genomes.

Maximum likelihood phylogeny based on 500 loci was juxtaposed with the genome-level comparisons of number of genes, carbohydrate-active enzymes (CAZymes), secondary metabolism gene clusters (SMGC), proteases, and secreted proteins across the twelve genomes. Classes of CAZymes included auxillary activity enzymes (AA), carbohydrate-binding modules (CBM), carbohydrate esterases (CE), glycoside hydrolases (GH), glycosyl transferases (GT), and polysaccharide lyases (PL). SMGCs included various polyketide synthases (PKS), nonribosomal peptide-synthetases (NRPS), terpene synthases and other. Protease classes included aspartic peptidases (A), cysteine peptidases (C), metallopeptidases (M), asparagine peptidases (N), mixed peptidases (P), serine peptidases (S), threonine peptidases (T), and protease inhibitors (I). Genome completeness was calculated using EukCC. We counted proteins as unannotated if they had no UniProt, Pfam, dbcan, or MEROPS annotation.

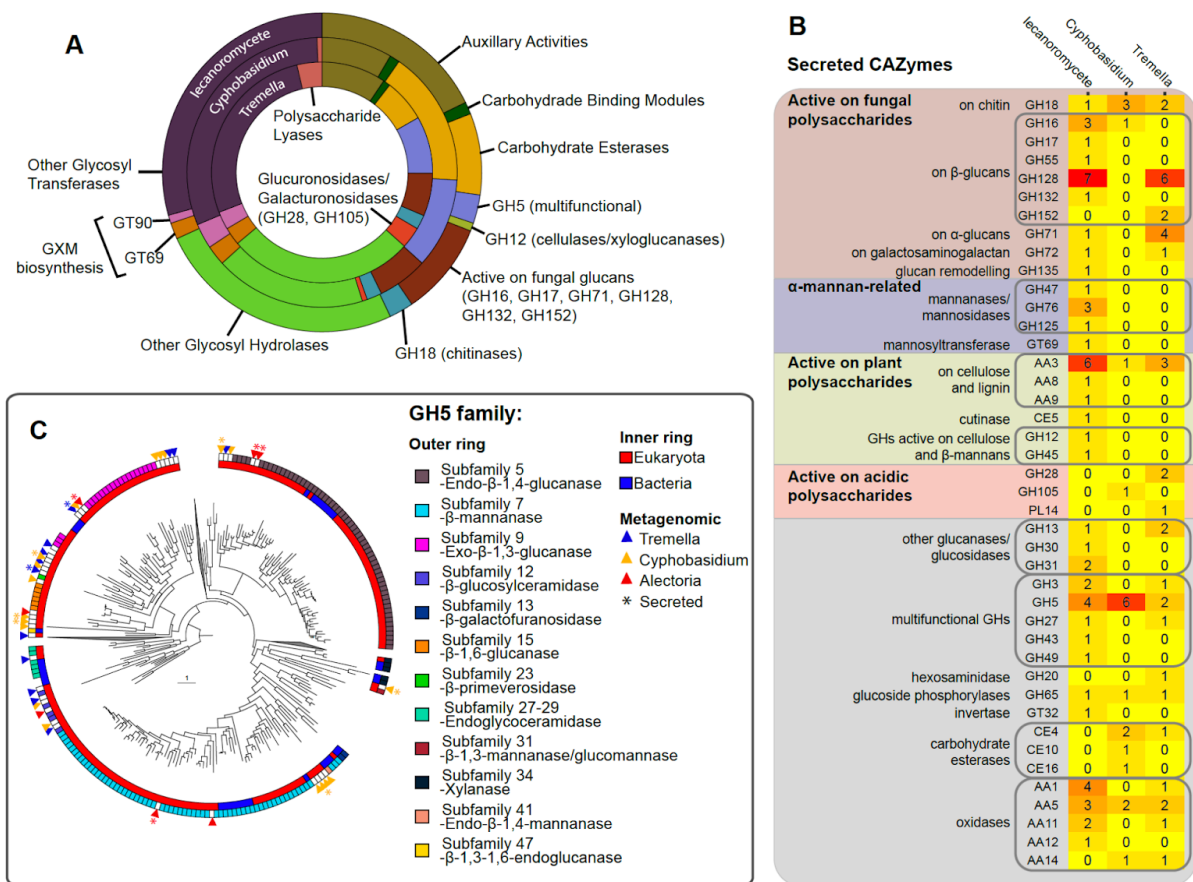


Fig. 2.5. Carbohydrate-active enzymes (CAZymes) in the three fungal MAGs.

(A) Relative abundance of major groups of CAZymes in the three MAGs, highlighting specific families of glycoside hydrolases and glycosyl transferases discussed in the text. (B) Heatmap of CAZyme families predicted to be secreted by the three fungi, grouped by major types of activity. (C) Results of the SACCHARIS analysis of GH5 enzymes from the studied MAGs, showing the position of GH5 enzymes identified in the studied MAGs (indicated with triangles) in relation to characterized GH5s. Secreted proteins are indicated with an asterisk. Colour rings are assigned based on the primary subfamily enzymatic activity and origin (bacterial vs. eukaryotic).

Chapter 3. Lichen fungi do not depend on the alga for ATP production

A version of this chapter has been published as Tagirdzhanova, G., McCutcheon, J. P. & Spribille, T. (2021) Lichen fungi do not depend on the alga for ATP production: A comment on Pogoda et al. (2018). *Molecular Ecology*, 30(17), 4155-4159.

3.1. Abstract

Lichen fungi live in a symbiotic association with unicellular phototrophs and have no known aposymbiotic stage. A recent study postulated that some of them have lost mitochondrial oxidative phosphorylation and rely on their algal partners for ATP. This claim originated from an apparent lack of *ATP9*, a gene encoding one subunit of ATP synthase, from a few mitochondrial genomes. Here we show that while these fungi indeed have lost the mitochondrial *ATP9*, each retain a nuclear copy of this gene. Our analysis reaffirms that lichen fungi produce their own ATP.

3.2. Introduction

In obligate symbioses, co-evolution of the partners often drives gene loss that results in complementarity of the symbionts' metabolic capacities (e.g., Bublitz et al. 2019). Lichens are a diverse group of fungal-algal symbioses composed of at least one phototrophic partner (a green alga or a cyanobacterium) and at least one fungus. The fungus is currently assumed to be obligatorily associated with the phototroph. However, despite early suggestions for complementarity between fungal and phototroph gene products (Ahmadjian 1993), evidence for this has been lacking. In 2018, Pogoda and colleagues were the first to report ostensible gene loss and complementarity in the lichen symbiosis. Based on analysis of mitochondrial genomes of several lichen-forming lecanoromycete fungi, Pogoda et al. (2018) reported that *ATP9*, a gene

encoding F₁F₀ ATP synthase subunit C, one of the key proteins involved in oxidative phosphorylation, was missing from several fungal mitochondrial genomes (see also Funk et al. 2018; Stewart et al. 2018; Pogoda et al. 2019). For some of these species, the authors were able to find a copy of this gene in the nuclear genome (a gene transfer phenomenon known from a variety of ascomycetes, see Déquard-Chablat et al. 2011). For four lichen symbioses—*Alectoria fallacina*, *Gomphillus americanus*, *Heterodermia speciosa*, and *Imshaugia aleurites*—they did not detect any copy of the fungal *ATP9* gene. The authors concluded that in these symbioses, the fungus may rely on the alga for ATP production. This result has been since cited as evidence of obligate dependence of lichen fungi on their algal partners (e.g., Funk et al. 2018; Puri et al. 2021).

Several lines of evidence make this scenario improbable:

1. The complete loss of oxidative phosphorylation would inevitably be reflected in massive change in the mitochondrial genome (e.g., Heinz et al. 2012). The fact that all but one of the analyzed mitochondrial loci were found in all the genomes suggests that the function of mitochondria remains intact.
2. Fungal sexual reproduction via ascospores is intact in all four species; *Gomphillus americanus* reproduces only sexually. No vertical transmission of symbionts is associated with this route. The ascospore has to be autonomous in order to germinate and find a compatible alga.
3. Close relatives of some of these species have been isolated in axenic cultures (e.g., *Heterodermia pseudospeciosa* and *Alectoria ochroleuca*; Crittenden et al. 1995; Yoshimura et al. 2002). They, therefore, are autonomous in ATP production.

4. All known instances of symbionts importing host ATP are from intracellular endosymbioses (e.g., Haferkamp et al. 2006). In lichens, the transfer would require sophisticated new mechanisms, given that ATP would need to move through the cell walls and membranes of both of the partners involved in the exchange.

We therefore hypothesized that the *ATP9* gene was present in the genomes but overlooked during the analysis. By replicating the analysis of Pogoda et al. (2018) on the species of interest, and then applying a series of stress tests, we were able to detect a putative homologue *ATP9* in all four fungi.

3.3. Methods

3.3.1. Sample preparation and sequencing

We generated metagenomic libraries for four lichen specimens: *Alectoria fallacina*, *Gomphillus americanus*, *Heterodermia speciosa*, and *Imshaugia aleurites* (Table S1). The samples were frozen at -80°C and ground in a TissueLyser II (Qiagen). We extracted DNA using QIAamp DNA Investigator Kit (Qiagen) for *Gomphillus* and DNeasy Plant Mini Kit (Qiagen) for the rest of the samples. The metagenomic libraries were prepared using Nextera Flex DNA kit (Illumina) and sequenced at the BC Cancer Genome Sciences Centre on an Illumina HiSeq X using 150 bp paired-end reads.

3.3.2. Metagenomic assembly and genome annotation

The metagenomic data were filtered and assembled with the metaWRAP pipeline v1.2 (Uritskiy et al. 2018). We used the READ_QC module to remove any human contamination, and then assembled the remaining reads into metagenomes using metaSPAdes default settings (v3.13, Nurk et al. 2017). We binned individual assemblies using CONCOCT within metaWRAP

(Alneberg et al. 2014). To identify the lecanoromycete genome assemblies among the bins, we analyzed each bin with BUSCO (v4.0.1, Seppey et al. 2019).

Some lecanoromycete genomes are heterogeneous in their GC content, which can result in these genomes being split between multiple bins (Tagirdzhanova et al. 2021). To obtain full genomes of the lecanoromycetes, we merged multiple bins as described in Tagirdzhanova et al. (2021). Briefly, we made GC-content vs coverage scatter plots for each metagenome and located the bin identified as an ascomycete genome by BUSCO. In all metagenomes except that of *Gomphillus*, these bins were part of a linear-shaped cloud (Fig. 3.1). In each metagenome individually, we merged bins forming this cloud into one MAG and confirmed with BUSCO that the merging improved completeness of the genome while maintaining low contamination.

We annotated the MAGs and six lecanoromycete genomes from GenBank (Table S2) using the Funannotate pipeline (v1.5.3, github.com/nextgenusfs/funannotate). We removed repetitive contigs from the assemblies, then sorted the assemblies and masked the repeats. *Ab initio* gene prediction was run using GeneMark-ES (v4.38, self-trained, Lomsadze et al. 2014), AUGUSTUS (v3.3.2, Stanke et al. 2004), SNAP (v 2006-07-28, Korf 2004), and GlimmerHMM (v3.0.4, Majoros et al. 2006), trained using BUSCO2 gene models. We used EVIDENCEModeler (v1.1.1, Haas et al. 2008) to create consensus gene models, and removed models shorter than 50 amino acids or identified as transposons. The details on how we used funannotate are at [github \(https://github.com/metalichen/Lichen-fungi-do-not-depend-on-the-alga-for-ATP-production\)](https://github.com/metalichen/Lichen-fungi-do-not-depend-on-the-alga-for-ATP-production).

3.3.3. Replicating Pogoda et al. (2018)

We searched the metagenomic assemblies using command line tBLASTn with default settings (v2.4.0, Camacho et al. 2009) and *ATP9*, *ATP8*, and *ATP6* genes from the mitochondrial genome

of *Peltigera dolichorrhiza* as a query (NCBI Protein YP_009316289, YP_009316290, YP_009316291).

3.3.4. Protein Family Dataset Assembly

We searched a recently published annotated genome of *Alectoria sarmentosa* (ENA GCA_904859925) for the genes assigned to pfam accession PF00137 and InterProScan accession IPR000454. We used the identified sequence as a query to locate putative lecanoromycete *ATP9* in the protein coding predictions produced by the genome annotation. We aligned all *de novo* produced *ATP9* sequences against published sequences (Table S2) and manually curated the annotation. In the case of three gene models (*Alectoria fallacina*, *Evernia prunastri*, and *Ramalina intermedia*; Table S3), we moved the intron boundaries to better match published *ATP9* sequences.

We extracted the putative protein sequences, and combined them with publicly available sequences of F₁F₀ ATP synthase subunit c from a variety of fungi and bacteria (Table S2). The sampling of the nuclear *ATP9* was done following Déquard-Chablat et al. (2011). As an outgroup we used N-ATPase following Koumandou & Kossida (2014). We aligned the sequences using MAFFT v7.271 (Kato et al. 2002) with the flags --genafpair --maxiterate 10000 and excluded positions with more than 90% of data missing using trimal v1.2rev59 (Capella-Gutiérrez et al. 2009). The phylogeny was reconstructed with IQTree v1.6.12 (Nguyen et al. 2015) using LG+F+G4 substitution model and 50000 rapid bootstrap replicates.

3.3.5. dN/dS analysis

To calculate the ratio of non-synonymous to synonymous substitutions (dN/dS) we followed Aylward (2018). We aligned the protein sequences of nuclear *ATP9* from lecanoromycetes using

MAFFT as described above. We used this alignment together with the nucleotide sequences to create codon-based alignment with PAL2NAL (Suyama et al. 2006). To calculate the dN/dS ratios, we used the codeml function in the PAML package (Yang 2007).

3.4. Results

3.4.1. Pogoda et al. (2018) results replicated

We were able to replicate the results of Pogoda et al. (2018) on our data. When using mitochondrial loci from the lecanoromycete of the *Peltigera dolichorrhiza* lichen as a tblastn query, we located *ATP6* and *ATP8*, but not *ATP9*. In all four metagenomes, *ATP6* and *ATP8* resided together in a single high-coverage contig (Fig. 3.1). The search for the gene in question, *ATP9*, failed to produce a blast hit above the threshold used by Pogoda et al. 2018 (bit score > 100).

3.4.2. Putative ATP9 in the nuclear genomes

To test the hypothesis that the four species which Pogoda et al. reported as lacking *ATP9* in fact retain the gene, we began with the recently published lecanoromycete genome of *Alectoria sarmentosa* (Tagirdzhanova et al. 2021), a close relative of *A. fallacina*, one of the four fungi reportedly lacking *ATP9*. We identified one putative *ATP9* homologue, ASARMPREDX12_000654, in the *A. sarmentosa* lecanoromycete nuclear genome. This was the only gene from this genome assigned to Interproscan accession IPR000454 (ATP synthase, F₀ complex, subunit C), and one of four assigned to pfam accession PF00137 (ATP synthase subunit C). When blasted against the NCBI Protein, it aligned with other fungal *ATP9* (Table S4).

Next, we generated metagenomes from newly acquired samples of all four lichen symbioses in which Pogoda et al. (2018) claimed fungal *ATP9* had been lost, and from them assembled and binned near-complete lecanoromycete genomes (metagenome-assembled genomes, MAGs). Using ASARMPREDX12_000654 as a blast query, we found putative *ATP9* homologs in all MAGs. Each of these *ATP9* homologs showed up in the blast search we ran replicating Pogoda et al. (2018; see the previous section). However, their bit scores ranged from 35 to 48 and therefore were below the threshold set by Pogoda et al. (2018). We then checked the original metagenomic assemblies used in Pogoda et al. (2018) for the presence of these genes. Using the putative *ATP9* genes as a blast query we found similar genomic regions in all four genomes. For *Alectoria fallacina* and *Gomphillus americanus* the putative *ATP9* genes were identical in our assemblies and the assemblies from Pogoda et al. (2018); in *Heterodermia speciosa* and *Imshaugia aleurites* the sequences were > 98% identical with bit score > 1000.

Analysis of coverage suggests that the putative *ATP9* copy was located in the nuclear genome. In all four cases, contig coverage was similar to other contigs assigned to their respective MAGs and much less than that of the mitochondrial contig (Fig. 3.1). Of the six additional lecanoromycete genomes we surveyed, five contained putative nuclear *ATP9* (Table S2). In one of them, *Ramalina intermedia*, the nuclear *ATP9* homolog existed alongside the already reported *mtATP9* (NCBI Protein YP_009687549.1). Only in *Cladonia macilenta* were we unable to detect nuclear *ATP9*, but a fungal *mtATP9* was present.

3.4.3. Two nuclear *ATP9* homologs present in different Lecanoromycetes

We constructed a phylogeny of lecanoromycete *ATP9* genes identified in this study together with other fungal and bacterial *ATP9* genes. In the phylogeny, the putative lecanoromycete nuclear *ATP9* genes grouped together with known nuclear *ATP9* from other fungi (Fig. 3.2). The nuclear

ATP9 were split between two clades corresponding to *ATP9-5* and *ATP9-7* homologs described in Déquard-Chablat et al. (2011). All but one lecanoromycete nuclear *ATP9* were assigned to the *ATP9-5* clade; these fungi were from the Lecanoromycetes subclass Lecanoromycetidae. The only member of subclass Ostropomycetidae, *Gomphillus americanus*, grouped with *ATP9-7*. The ascomycete nuclear *ATP9* clade was nested within the fungal *mtATP9*; its sister clade was formed by *mtATP9* from Pezizomycotina. This differs from the tree produced by Déquard-Chablat et al. (2011), as in their analysis the split between *ATP9-5* and *ATP9-7* is deeper and the two clades branch off in different places of the fungal *mtATP9* clade.

3.4.4. Nuclear *ATP9* contain introns and are under purifying selection.

All four putative *ATP9* contained at least one intron. In the three members of Lecanoromycetes subclass Lecanoromycetidae—*Alectoria fallacina*, *Heterodermia speciosa*, and *Imshaugia aleurites*—*ATP9* contained one intron, always in the same position (Table S3). The *Gomphillus americanus ATP9*, by contrast, contained two introns. The introns had either canonical GT-AG or one of the more common fungal non-canonical splicing sites (Table S3; Frey & Pucker 2020). The dN/dS ratios between the nuclear *ATP9* from Lecanoromycetes ranged from 0.007 to 0.249 indicating that the gene is under purifying selection and is not a non-functional mitochondrial to nuclear genome transfer (see Richly & Leister 2004).

3.5. Discussion

Pogoda et al. (2018) hypothesized that some lichen fungi rely on other members of the symbiosis for ATP production based on the apparent lack of the *ATP9* gene in four Lecanoromycetes. We were able to find a putative *ATP9* homolog in all four genomes, both in new data produced for this study and in metagenomic data from the original publication. Our reanalysis reaffirms that,

as expected, the fungi postulated to lack *ATP9* retain a nuclear copy of the gene, as in many other fungi. The fact that the putative *ATP9* were under purifying selection suggests that these genes are functional.

Our analysis suggests the nuclear *ATP9* originates in a transfer from the mitochondria to the nucleus, supporting the conclusion made by Déquard-Chablat et al. (2011). We included bacterial *ATP9* counterparts in the phylogeny to test for an alternative hypothesis that the nuclear homologs are acquired not from mitochondria but from bacteria via horizontal gene transfer. This hypothesis was not supported: nuclear *ATP9* clade was nested within the *mtATP9* clade, which in turn was nested within Alphaproteobacterial clade.

Both known nuclear *ATP9* homologs, *ATP9-5* and *ATP9-7*, were present in the lecanoromycete genomes. Déquard-Chablat et al. (2011) believed these genes to come from two independent transfers. They were previously reported in different combinations from several other classes of Pezizomycotina: Eurotiomycetes, Sordariomycetes, and Dothideomycetes (Déquard-Chablat et al. 2011). Adding Lecanoromycetes to the list further supports the hypothesis that the acquisition of *ATP9-5* and *ATP9-7* happened early in the evolution of Pezizomycotina and was followed by gene loss in some lineages.

With the combined evidence from this study and from Pogoda et al. (2018) we can begin to chart the evolutionary history of the *ATP9* in Lecanoromycetes. Most notably in the context of this study, several groups of Lecanoromycetes have lost *mtATP9* and retained only a nuclear copy. We agree with Pogoda et al. (2018) in their assessment that the loss of *mtATP9* happened at least three times independently in the evolution of Lecanoromycetes (see Fig. 1A in their study).

Gene loss affected nuclear *ATP9* homologs as well. None of the ten surveyed species retained both *ATP9-5* and *ATP9-7*: *Cladonia macilenta* had neither (while retaining *mtATP9*), the other

species had either one or the other. Members of Lecanoromycetidae, other than *Cladonia*, retained *ATP9-5*, while the only member of Ostropomycetidae retained *ATP9-7*. Further research will map the nuclear *ATP9* across the lecanoromycete fungi and check how the new data points alter our understanding of the evolutionary history of this gene.

Our reanalysis of the Pogoda et al. (2018) paper underlines that the apparent lack of any one gene does not automatically translate into the loss of biological function, especially when the rest of the pathway is maintained. While *ATP9* indeed appears missing from mitochondrial genomes of some Lecanoromycetes, this result by itself was not sufficient to back the claim of lichen fungi having lost oxidative phosphorylation.

3.6. Supplementary material and data availability

Supplementary tables are published at <https://doi.org/10.1111/mec.16010>. Raw metagenomic data, metagenomic assemblies, and genome annotations: European Nucleotide Archive (PRJEB42325). Full description of the analysis, custom scripts, and data files have been made available at the Dryad repository at <https://doi.org/10.5061/dryad.xgxd254gd>.

References

- Ahmadjian, V. (1993). *The lichen symbiosis*. New York, NY: John Wiley & Sons.
- Alneberg, J., Bjarnason, B. S., De Bruijn, I., Schirmer, M., Quick, J., Ijaz, U. Z., ... & Quince, C. (2014). Binning metagenomic contigs by coverage and composition. *Nature Methods*, *11*(11), 1144–1146.
- Aylward, F.O. (2018). Introduction to calculating dN/dS ratios with codeml. *protocols.io* doi: <https://dx.doi.org/10.17504/protocols.io.qhwdt7e>

Bublitz, D.C., Chadwick, G.L., Magyar, J.S., Sandoz, K.M., Brooks, D.M., Mesnage, S., ...
McCutcheon, J.P. (2019). Peptidoglycan production by an insect-bacterial mosaic. *Cell*, *179*(3),
703–712.

Camacho, C., Coulouris, G., Avagyan, V., Ma, N., Papadopoulos, J., Bealer, K., & Madden, T.
L. (2009). BLAST+: architecture and applications. *BMC Bioinformatics*, *10*(1), 421.

Capella-Gutiérrez, S., Silla-Martínez, J. M., & Gabaldón, T. (2009). trimAl: a tool for automated
alignment trimming in large-scale phylogenetic analyses. *Bioinformatics*, *25*(15), 1972–1973.

Crittenden, P. D., David, J. C., Hawksworth, D. L., & Campbell, F. S. (1995). Attempted
isolation and success in the culturing of a broad spectrum of lichen-forming and lichenicolous
fungi. *New Phytologist*, *130*(2), 267–297.

Déquard-Chablat, M., Sellem, C. H., Golik, P., Bidard, F., Martos, A., Bietenhader, M., ... &
Contamine, V. (2011). Two nuclear life cycle–regulated genes encode interchangeable subunits c
of mitochondrial ATP synthase in *Podospora anserina*. *Molecular Biology and Evolution*, *28*(7),
2063-2075.

Frey, K., & Pucker, B. (2020). Animal, Fungi, and Plant Genome Sequences Harbor Different
Non-Canonical Splice Sites. *Cells*, *9*(2), 458.

Funk, E. R., Adams, A. N., Spotten, S. M., Van Hove, R. A., Whittington, K. T., Keepers, K. G.,
... & Kane, N. C. (2018). The complete mitochondrial genomes of five lichenized fungi in the
genus *Usnea* (Ascomycota: Parmeliaceae). *Mitochondrial DNA Part B*, *3*(1), 305–308.

Haas, B. J., Salzberg, S. L., Zhu, W., Pertea, M., Allen, J. E., Orvis, J., ... & Wortman, J. R.
(2008). Automated eukaryotic gene structure annotation using EVIDENCEModeler and the
Program to Assemble Spliced Alignments. *Genome Biology*, *9*(1), R7.

- Haferkamp, I., Schmitz-Esser, S., Wagner, M., Neigel, N., Horn, M., & Neuhaus, H. E. (2006). Tapping the nucleotide pool of the host: novel nucleotide carrier proteins of *Protochlamydia amoebophila*. *Molecular Microbiology*, *60*(6), 1534–1545.
- Heinz, E., Williams, T. A., Nakjang, S., Noël, C. J., Swan, D. C., Goldberg, A. V., ... & Bernhardt, J. (2012). The genome of the obligate intracellular parasite *Trachipleistophora hominis*: new insights into microsporidian genome dynamics and reductive evolution. *PLoS Pathog*, *8*(10), e1002979.
- Katoh, K., Misawa, K., Kuma, K. I., & Miyata, T. (2002). MAFFT: a novel method for rapid multiple sequence alignment based on fast Fourier transform. *Nucleic Acids Research*, *30*(14), 3059–3066.
- Korf, I. (2004). Gene finding in novel genomes. *BMC Bioinformatics*, *5*(1), 59.
- Koumandou, V. L., & Kossida, S. (2014). Evolution of the F₀F₁ ATP synthase complex in light of the patchy distribution of different bioenergetic pathways across prokaryotes. *PLoS Comput Biol*, *10*(9), e1003821.
- Lomsadze, A., Burns, P. D., & Borodovsky, M. (2014). Integration of mapped RNA-Seq reads into automatic training of eukaryotic gene finding algorithm. *Nucleic Acids Research*, *42*(15), e119–e119.
- Majoros, W. H., Pertea, M., & Salzberg, S. L. (2004). TigrScan and GlimmerHMM: two open source ab initio eukaryotic gene-finders. *Bioinformatics*, *20*(16), 2878–2879.
- Nguyen, L. T., Schmidt, H. A., Von Haeseler, A., & Minh, B. Q. (2015). IQ-TREE: a fast and effective stochastic algorithm for estimating maximum-likelihood phylogenies. *Molecular Biology and Evolution*, *32*(1), 268–274.

- Nurk, S., Meleshko, D., Korobeynikov, A., & Pevzner, P. A. (2017). metaSPAdes: a new versatile metagenomic assembler. *Genome Research*, 27(5), 824–834.
- Pogoda, C. S., Keepers, K. G., Lendemer, J. C., Kane, N. C., & Tripp, E. A. (2018). Reductions in complexity of mitochondrial genomes in lichen-forming fungi shed light on genome architecture of obligate symbioses. *Molecular Ecology*, 27(5), 1155–1169.
- Pogoda, C. S., Keepers, K. G., Nadiadi, A. Y., Bailey, D. W., Lendemer, J. C., Tripp, E. A., & Kane, N. C. (2019). Genome streamlining via complete loss of introns has occurred multiple times in lichenized fungal mitochondria. *Ecology and Evolution*, 9(7), 4245–4263.
- Puri, K. M., Butardo, V., & Sumer, H. (2021). Evaluation of natural endosymbiosis for progress towards artificial endosymbiosis. *Symbiosis*, 84, 1–17
- Richly, E., & Leister, D. (2004). NUMTs in sequenced eukaryotic genomes. *Molecular biology and evolution*, 21(6), 1081–1084.
- Sepey, M., Manni, M., & Zdobnov, E. M. (2019). BUSCO: assessing genome assembly and annotation completeness. In M. Kollmar (Ed.) *Gene Prediction* (pp. 227–4245). New York, NY: Humana.
- Stanke, M., Steinkamp, R., Waack, S., & Morgenstern, B. (2004). AUGUSTUS: a web server for gene finding in eukaryotes. *Nucleic acids research*, 32(suppl_2), W309–W312.
- Stewart, C. R. A., Lendemer, J. C., Keepers, K. G., Pogoda, C. S., Kane, N. C., McCain, C. M., & Tripp, E. A. (2018). *Lecanora markjohnstonii* (Lecanoraceae, lichenized Ascomycetes), a new sorediate crustose lichen from the southeastern United States. *The Bryologist*, 121(4), 498–512.

Suyama, M., Torrents, D., & Bork, P. (2006). PAL2NAL: robust conversion of protein sequence alignments into the corresponding codon alignments. *Nucleic Acids Research*, *34*(suppl_2), W609–W612.

Tagirdzhanova, G., Saary, P., Tingley, J. P., Díaz-Escandón, D., Abbott, D. W., Finn, R. D., & Spribille, T. (2021). Predicted input of uncultured fungal symbionts to a lichen symbiosis from metagenome-assembled genomes. *Genome Biology and Evolution*, *13*(4), evab047.

Uritskiy, G. V., DiRuggiero, J., & Taylor, J. (2018). MetaWRAP—a flexible pipeline for genome-resolved metagenomic data analysis. *Microbiome*, *6*(1), 1–13.

Yang, Z. (2007). PAML 4: phylogenetic analysis by maximum likelihood. *Molecular Biology and Evolution*, *24*(8), 1586–1591.

Yoshimura, I., Yamamoto, Y., Nakano, T., & Finnie, J. (2002). Isolation and culture of lichen photobionts and mycobionts. In I. C. Kranner, R. P. Beckett & A. K. Varma (Eds.), *Protocols in lichenology* (pp. 3–33). Berlin, Heidelberg: Springer.

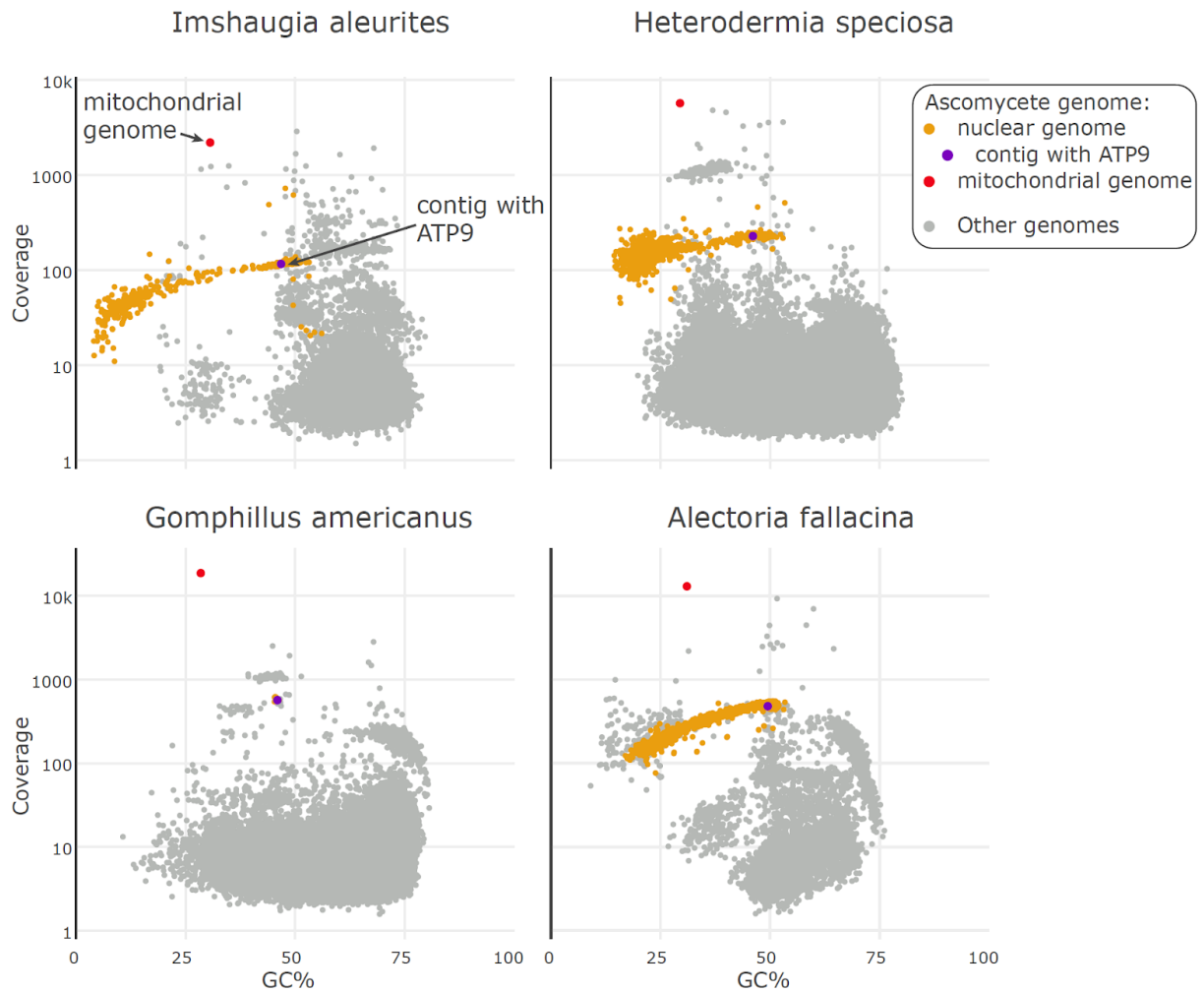


Fig. 3.1. GC-coverage plots for the four metagenomes produced in this study.

Dots representing contigs are positioned according to their GC content and coverage. Orange dots are contigs assigned to the lecanoromycete MAGs, purple dots are the contigs that contain the putative ATP9 homolog. Red dots are putative mitochondrial genomes.

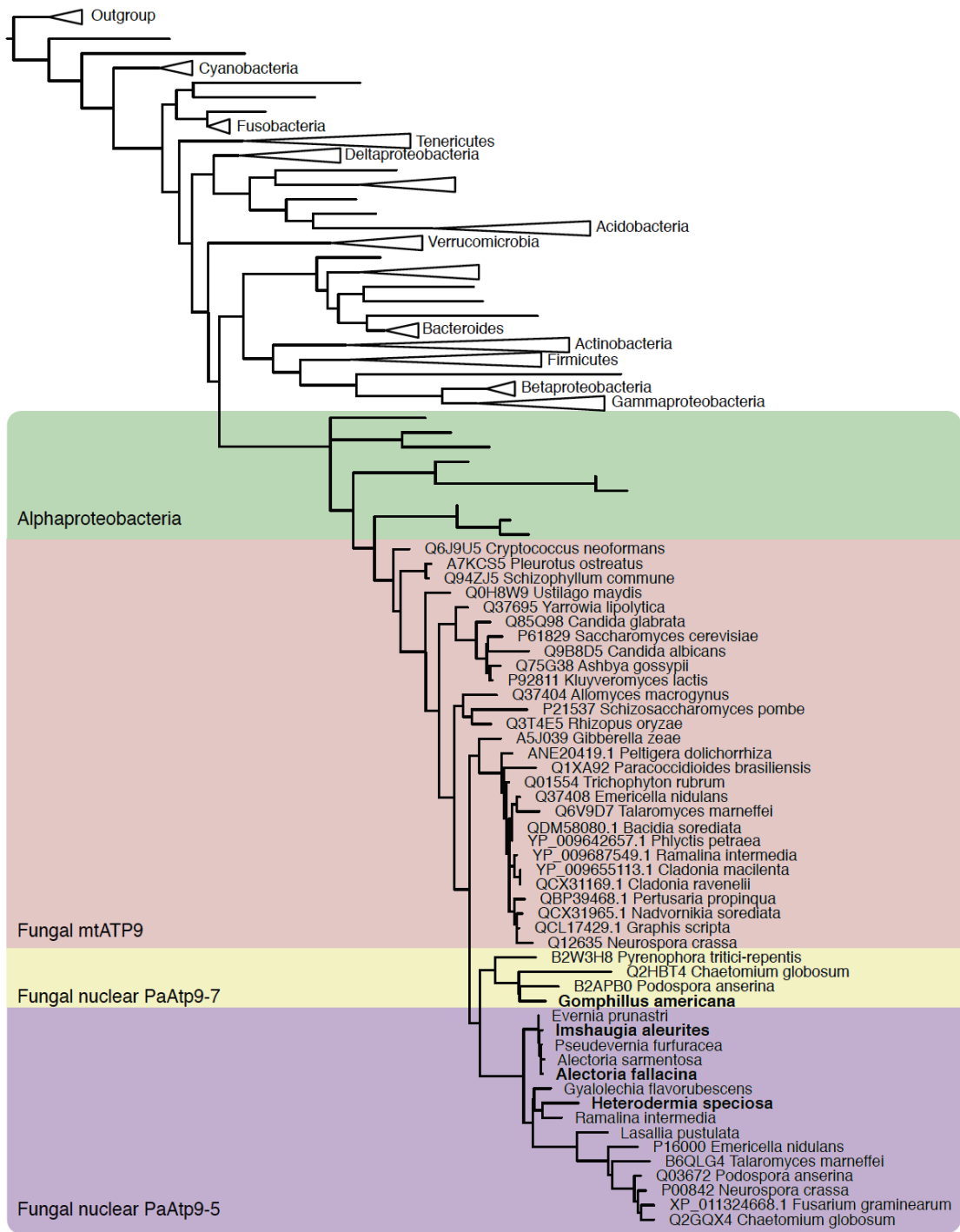


Fig. 3.2. Phylogenetic tree of F1F0 ATP synthase subunit C across fungi and bacteria.
ATP9 from the studied genomes are in bold.

Chapter 4. Lichen bacterial communities revealed by metagenomics

A version of this chapter is intended for publication as: Tagirdzhanova, G., Cameron, E., Saary, P., Garber, A., Stein, L., Finn, R. D., & Spribille, T. Lichen bacterial communities revealed by metagenomics.

4.1. Abstract

In addition to the two main eukaryotic partners, lichen symbioses often contain bacteria and additional fungal symbionts, but their composition is studied in a small fraction of lichens. Here we present the first systematic survey of composition of lichen symbiosis based on metagenomic data. We show that bacterial lineages present in lichens are unexpectedly structured. The majority of bacteria we found come from just four bacterial families: Acetobacteraceae, Beijerinckiaceae and Sphingomonadaceae (Alphaproteobacteria) and Acidobacteriaceae (Acidobacteria). The most frequently occurring clade, *Lichenihabitans*, along with other Beijerinckiaceae and some Acetobacteraceae, have the machinery for anoxygenic photosynthesis. Based on the genome annotations, we propose that these bacteria supply the eukaryotic partners with cofactors, in exchange for nitrogen and carbon. Contrary to a previously made hypothesis, neither *Lichenihabitans* nor other common bacterial lineages have the machinery for nitrogen fixation.

4.2. Introduction

Lichens were revealed to be composite organisms in 1869 (Schwendener 1869), in an unexpected twist that remained controversial for many decades as many biologists maintained that no such co-living of different organisms is possible (Honegger 2000). Later, it became clear that in addition to the two main partners — a hyphal fungus and a phototrophic microorganism

— lichens contain a suite of other organisms, chiefly bacteria and yeasts, sometimes referred to as “lichen microbiota” (Cengia Sambo 1926, Grimm et al. 2021).

The studies of lichen bacteria began by culturing them (Cengia Sambo 1926, Henkel & Yuzhakova 1936, Iskina 1938), and to this day culturing studies provide useful insight into the physiology of lichen bacteria (e.g., Noh et al. 2019, Pankratov et al. 2020). However, culturing studies tend to favor some phylogenetic groups and completely exclude others, and therefore cannot give the full picture (Overmann et al. 2017). PCR followed by sequencing offered an effective way to profile bacterial communities without need to culture them. Studies based on specific primers (e.g., Hodkinson & Lutzoni 2009) allowed screening for certain bacterial lineages, but only on a lineage-by-lineage basis. In contrast, high-throughput sequencing and generic primers allowed researchers to profile entire communities. However, metabarcoding also has limitations. First, it is prone to primer bias and therefore can miss some lineages (Klindworth et al. 2013). Second, the information it provides is purely taxonomic. Anything beyond that (physiology, metabolism, ecology, etc.) can only be inferred indirectly, if at all, as in bacteria taxonomy does not always correlate with function (Louca et al. 2016).

Both of the aforementioned challenges — culture bias and primer bias — have largely been sidelined by the advent of shotgun omics-based studies. Approaches such as metagenomics, metatranscriptomics, and metaproteomics, can provide unbiased information on both the taxonomic structure of a community and its functional profiles (Taş et al. 2021). These advantages come, quite literally, with a price. For metagenomics to produce reliable results, researchers need to produce large amounts of data. The quantity of sequencing data — sequencing depth, measured in base pairs (bp) — is one of the considerations, since metagenomes sequenced too shallowly might fail to capture the diversity of the microbial

community (Zaheer et al. 2018). Thus, describing a microbial community via shotgun metagenomics is estimated to be 1000 times more expensive than metabarcoding, and large-scale metagenomics studies can accordingly be prohibitively expensive (Gołębiewski & Tretyn 2020). Perhaps owing to all the challenges outlined above, information about lichen bacteria remains patchy: while some lichen symbioses are studied in depth, most are not. Bacteria of *Lobaria pulmonaria*, a model lichen symbiosis, have been studied by a variety of methods, from metabarcoding (Aschenbrenner et al. 2017) and fluorescent *in situ* hybridization (FISH; Cardinale et al. 2012, Erlacher et al. 2015) to metaproteomics (Schneider et al. 2011, Grube et al. 2015) and everything in between (Cernava et al. 2017). However, *L. pulmonaria* is only one example from almost 20,000 lichen symbioses (Spribille et al. 2022). Lichen symbioses have evolved multiple times and are extremely diverse: different lichens might have either eukaryotic algae or cyanobacteria as photosynthetic partners, or, as in the case of *L. pulmonaria*, both. Similarly, the main fungal partner of a lichen can come from six fungal classes in two phyla (Spribille et al. 2022). For the majority of types of lichen symbioses, we have no data on bacteria present in them.

Here we aim to fill this gap. In recent years, lichen biologists have generated hundreds of metagenomes from lichens (e.g., Lendemer et al. 2019). Mostly, these data were generated to study fungal partners (e.g., McDonald et al. 2013, Grewe et al. 2020, Resl et al. 2022, Keepers 2021). Only a few of these metagenomes have been screened for bacteria (e.g. Greshake Tzovaras et al. 2020, Tagirdzhanova et al. 2021, Cornet et al. 2021). We used both publicly available and newly generated data to conduct the first systematic survey of the composition of lichen symbiosis based on metagenomic data. Using the recovered genomes of lichen bacteria,

we attempted to understand how lichen bacteria fit into the flow of goods and services that define the lichen symbiosis.

4.3. Methods

4.3.1. Dataset construction

We analyzed a total of 437 lichen metagenomes (Table 4.1). Most of the data were obtained from NCBI, and 25 metagenomes were generated *de novo* (Table 4.1). The publicly available data used in this project came from 14 publications and various geographic locations in North and South America, Europe, Australia, and Antarctica (Table 4.1).

To generate new metagenomes, we collected lichen samples, froze them at -80°C and pulverized them using a TissueLyser II (Qiagen). We extracted DNA from the samples with DNAEasy Plant Mini Kit (Qiagen) and prepared metagenomic libraries. The libraries were sequenced on different Illumina HiSeq platforms to paired-end reads. The details on the procedure, including voucher information, library prep, and sequencing are given in Table 4.2. In the later steps of the analysis, we excluded the metagenomes that we suspected were made from misidentified samples (see below).

4.3.2. Initial steps of metagenomic analysis

4.3.2a. Obtaining Metagenome-Assembled Genomes (MAGs)

We started by assembling each metagenome individually and extracting MAGs from them. The metagenomic libraries were filtered using fastp (Chen et al., 2018) to remove adapters and low-quality bases, and the READ_QC module of the metaWRAP pipeline (v.1.2, Uritskiy et al. 2018) to remove human contamination. The filtered data were assembled with metaSPAdes (Nurk et al. 2017). Individual assemblies were binned using CONCOCT (Alneberg et al. 2014) and

metaBAT2 (Kang et al. 2015). To refine prokaryotic MAGs, we used the *binrefine* module of the metaWRAP pipeline. Bins that passed the QS50 threshold were used for further analysis: we evaluated them using CheckM (v1.1.3, Parks et al. 2015) and dereplicated them using dRep (v3, Olm et al. 2017) at 95% ANI (average nucleotide identity) and 30% AF (alignment fraction) thresholds in order to obtain species-level representatives.

Eukaryotic MAGs were identified and refined with EukCC (v2, Saary et al. 2020). Bins with a quality score of at least 50 were dereplicated with dRep at two levels: first, on the level of the individual binned metagenome (with the 99% ANI threshold); and second on the level of the whole dataset, where bins from all metagenomes were dereplicated at 95% ANI and 40% AF to create species-representative MAGs. For each MAG, we calculated the EukCC and BUSCO5 (Seppey et al. 2019) quality scores. For the purpose of analyzing the relationship between sequencing depth and recovery of MAGs of the main symbiotic partners, we used the pre-dereplication set of MAGs.

4.3.2b. MAG taxonomic assignments

We classified prokaryotic MAGs using GTDB-Tk (v1.5.0, Chaumeil et al. 2020), a tool based on the Genome Taxonomy DataBase (GTDB). In one case, we found an inconsistency between GTDB and the literature. Namely, *Lichenibacterium* and *Lichenihabitans* are two genera from Rhizobiales published within months of each other (Noh et al. 2019, Pankratov et al. 2020). In GTDB, which provides taxonomic-rank normalization, *Lichenibacterium* is included in *Lichenihabitans*. We followed GTDB because it appears likely that Noh et al. (2019) and Pankratov et al. (2020) independently described the same lineage.

We generated a phylogenomic tree for all prokaryotic MAGs that passed the QS50 threshold. For this tree, we used the marker gene alignment produced by GTDB-Tk (concatenated alignment of

120 loci). We generated the tree with IQ-TREE (Nguyen et al. 2015) using the model finder (selected model: LG+F+R10) and 1000 bootstraps.

To obtain preliminary taxonomy annotations for eukaryotic MAGs, we used BAT (CAT v5.2.3, database version: 20210107, von Meijenfeldt et al. 2019), which predicts taxonomy based on searching predicted genes against the NCBI database. These taxonomic assignments were refined using phylogenomics. A set of 50 EukCC marker genes were aligned using famsa (Deorowicz et al. 2016) and concatenated. The tree was generated as described above, using the VT+F+R10 substitution model.

In each metagenome, we identified the MAG of the main fungal partner. To do that, we manually inspected all fungal MAGs, and checked that their placement on the phylogenomic tree is consistent with the taxonomic assignment provided in the NCBI metadata; otherwise we excluded metagenomes as potentially derived from misidentified samples. A total of 14 metagenomes were thus excluded (Table 4.3). For metagenomes where multiple fungal MAGs were present, we selected one as the main fungal MAG based on their position on the tree and the depth of coverage (defined as the number of reads “covering” each base of the assembled contig), since the genome of the main, most abundant, fungal partner is expected to have greater depth of coverage than a genome from a fungal contaminant. Metagenomes for which no clear-cut decision could be made were excluded from further analysis (Table 4.3).

4.3.3. Occurrence analysis

4.3.3a. MAG-based occurrences

To map MAG occurrence across the metagenomes, we aligned reads from all metagenomes against all MAGs using BWA (Li & Durbin 2009). All MAGs that were at least 50% covered in

a given metagenome were counted as present. Using these data, we constructed an occurrence matrix of MAGs in metagenomes. To estimate the depth of coverage of MAGs, we used the number of reads aligned to the MAG, multiplied by the read length and divided by the total length of the contigs assigned to the MAG. We estimated MAG abundances by computing their depth of coverage relative to that of the MAG of the main fungal partner. Only metagenomes that yielded a MAG of the main fungal partner were used for the occurrence analysis.

4.3.3b. Statistical analysis of bacterial occurrences

We clustered both metagenomes and bacterial lineages based on the MAG occurrence matrix. For that, we constructed correlation matrices for metagenomes and for bacterial genera based on Pearson coefficients. We used the R library `simplifyEnrichment` to compare different clustering methods: `hdbscan`, `apcluster`, `MCL`, `walktrap`, `kmeans`, `binary_cut`, and `dynamicTreeCut`. The resulting clustering was visualized using the `ComplexHeatmaps` library. In addition to clustering, we used Canonical Correspondence Analysis (CCA) with the occurrence matrix as response data, and three features of each metagenome (sequencing depth and taxonomic positions of the main fungal and the photosynthetic partners, respectively) as predictors. In this analysis, we included only bacterial groups occurring in at least five metagenomes and metagenomes with sequencing depth above 2 Gbp. We picked the 2 Gbp threshold since this amount of data was required to capture both main partners (see results 4.3.3), and therefore we decided it was adequate to capture the metagenome complexity.

4.3.3c. rDNA screening

In the course of the occurrence analysis, it became clear that MAG presence/absence did not always reflect the occurrence of an organism within a sample, as some genomes might be missed due to insufficient sequencing depth. To provide another metric of the actual occurrence of

specific organisms of interest within our lichen metagenomes, we searched metagenomic assemblies and raw, unassembled metagenomic data for SSU rDNA. This process consisted of two steps: the detection of 16S and 18S sequences, and their taxonomic assignment. 16S and 18S sequences were used for two reasons: first, they are the marker loci most frequently used for taxonomic profiling, and second, because they tend to be present in multiple copies in a genome (Gruber-Vodicka et al. 2020) and therefore have better chances of being recovered in a shallow metagenome. For the first step, we used Metaxa2 (Bengtsson-Palme et al. 2015), an HMM-based searching algorithm. For eukaryotic lineages, taxonomic placement was done through Metaxa2 as well. For bacteria, we used 16S sequences extracted by Metaxa2, to which we assigned taxonomic positions with IDTAXA (Murali et al. 2018), which allowed us to use taxonomy consistent with GTDB.

4.3.4. Functional analysis

4.3.4a. Multivariate analysis of functional annotations

We annotated all bacterial MAGs using PROKKA (Seemann 2014). Predicted protein models were functionally annotated against KEGG Orthologue Database (Kanehisa et al. 2002) using KofamScan (Aramaki et al. 2020). We selected high-quality MAGs (CheckM completeness score > 90%) and used their KEGG annotations to reconstruct KEGG modules with a script from Zoccarato et al. (2022). To compensate for potential false absences (e.g. caused by genes being split between contigs due to imperfect metagenome assembly), we allowed one missing gene per module.

To determine whether bacterial MAGs can be clustered into functional groups, we constructed a matrix of presence/absence of all identified KEGG modules across all studied MAGs. Using this matrix, we clustered the MAGs in the same way as described above for the occurrence analysis.

We used the following clustering methods: hdbscan, apcluster, MCL, walktrap, kmeans, binary_cut, dynamicTreeCut, leading_eigen, fast_greedy. To estimate the taxonomic coherence of different clustering outcomes, we followed Zoccarato et al. (2022).

4.3.4b. In-depth functional annotation

From bacterial MAGs we selected the MAGs of the most frequent lineages and annotated them in depth. To select the MAGs, we first ranked all bacterial genera based on the number of occurrences. For the MAGs that did not have a genus level assignment, we used family-level annotations. Next, we selected the MAGs assigned to the top 13 genera, and among them retained only MAGs with a completeness score above 95% and contamination score below 10%, as estimated by CheckM. For the resulting set of MAGs, we obtained functional annotations of groups of genes that we suspected might be relevant to the lichen lifestyle of these bacteria. We used the following tools: run_dbcan (standalone tool of dbcan2, v3.0.2, https://github.com/linnabrown/run_dbcan) for annotations of Carbohydrate-Active EnZymes (CAZymes), FeGenie (Garber et al. 2020) for the genes related to iron metabolism, and the antiSMASH webserver (Blin et al. 2021) for biosynthetic gene clusters. In addition, we used blastp (evaluate $<1e-5$, Altschul et al. 1990) to search predicted protein models for homologs of several proteins. To check whether the studied bacteria can fix nitrogen, we searched for nitrogenase reductase subunit *NifH* (as a query we used a *NifH* sequence from NCBI, ABZ89802.1). For *NifH*, we ran an additional tblastn search against the metagenomic assemblies and checked the taxonomy of the hits using reciprocal blast search against the NCBI database. To check whether the studied bacteria can use the energy of light, we searched for rhodopsin (KMO17446.1), and beta-carotene oxygenase (GJE49492.1, is involved in producing the chromophore).

4.3.4c. Loss of function in Rhizobiales MAGs

Rhizobiales MAGs from our dataset lacked several functions typical for bacteria from this order. To put these MAGs into the evolutionary context, we assembled a data set that included 518 previously published genomes across the whole order (taxon sampling following Volpiano et al. 2021; Table 4.4) and a genome of *Rhodobacter* (GCF_009908265.2), which served as an outgroup. Using GTDB-Tk, we identified and aligned 120 marker genes. From this alignment, we generated a phylogenomic tree using IQ-TREE (v2.1.2, Nguyen et al. 2015).

To screen the genomes for the presence of genes related to nitrogen fixation, methanotrophy, and methylotrophy, we ran a tblastn search against the nucleotide assemblies using as query sequences from NCBI (Table 4.5). For the genomes from GenBank, we confirmed that the tblastn results were consistent with the protein annotations available at NCBI.

4.3.5. Data handling and visualization

Custom scripts used for data analysis and visualization were written in R (v4.1.0, R Core Team 2013), using the following libraries: dplyr (v1.0.8, Wickham et al. 2018), tidyr (v1.2.0, Wickham & Girlich 2022), scales (v1.1.1, Wickham & Seidel 2020) for data handling; ggplot2 (v3.3.5, Wickham 2016), ComplexHeatmap (v2.11.1, Gu et al. 2016), ape (v5.0, Paradis & Schliep 2019), phangorn (v2.8.1, Schliep 2011), phytools (v1.0-3, Revell 2012), circlize (v0.4.14, Gu et al. 2014), igraph (v1.3.0, Csardi & Nepusz 2006), qgraph (v1.9.2, Epskamp et al. 2012), treeio (v1.16.2, Wang et al. 2020a), DECIPHER (v2.14.0, Wright 2016) for data visualization; vegan (v2.5-7, Oksanen et al. 2020), simplifyEnrichment (Gu & Hübschmann 2021); apcluster (v1.4.9, Bodenhofer et al. 2011) for the statistical analysis of occurrence matrices and genome functional profiles. For visualizing phylogenetic trees, we also used iTOL (Letunic & Bork 2007).

4.4. Results

4.4.1. Metagenomes and MAGs: overview

Of the 437 lichen metagenomes we analyzed, 387 came from lichens with fungal partners from the class Lecanoromycetes (Ascomycota). Only 50 came from other ascomycete groups (i.e. with fungal partners from the classes Arthoniomycetes, Dothideomycetes, Eurotiomycetes, or Lichinomycetes). Almost all deeply sequenced metagenomes (> 5 Gbp) were from Lecanoromycetes (Fig. 4.1).

Reference-free binning of the metagenomes yielded exactly 1000 MAGs: 674 bacterial, 294 fungal, and 32 algal (Fig. 4.2).

4.4.1a. Highly structured bacterial communities revealed by the bacterial MAG composition

All prokaryotic MAGs extracted from the lichen metagenomes belonged to Eubacteria. While 15 bacterial phyla were represented in total, the majority (65%) of MAGs came from just two: Proteobacteria and Acidobacteria (Fig. 4.2). Moreover, over half of all bacterial MAGs (51%) came from just four families: Acetobacteraceae (Acetobacterales, Alphaproteobacteria), Beijerinckiaceae (Rhizobiales, Alphaproteobacteria), Acidobacteriaceae (Acidobacteriales, Acidobacteria), and Sphingomonadaceae (Sphingomonadales, Alphaproteobacteria).

The same four dominant families accounted for an even larger portion (62%) of all bacterial occurrences. The distinction between the number of MAGs and the number of occurrences was adopted since a MAG can be present in more than one metagenome. In fact, 46% of bacterial MAGs were detected more than once. While most MAGs were detected in one or two metagenomes, some MAGs were widespread. *Lichenihabitans* (Beijerinckiaceae) had 16 MAGs

in our dataset and 139 occurrences, which was the highest number by far. One of the *Lichenihabitans* MAGs was detected in 52 metagenomes, which included samples from different collectors, lichen groups, and geographies.

4.4.1b. Eukaryotic MAGs

Most eukaryotic MAGs belonged to the main lichen symbionts. MAGs of the main fungal partner made up the largest portion of fungal MAGs (85%), with most MAGs coming from lecanoromycete fungi. Other fungal MAGs included ascomycete fungi mainly from the classes Dothideomycetes and Eurotiomycetes, and the two basidiomycete fungi known to be stably associated with lichens: *Cyphobasidium* (Cystobasidiomycetes, Pucciniomycotina; Spribille et al. 2016) and *Tremella* (Tremellomycetes, Agaricomycotina; Tuovinen et al. 2019).

A portion of metagenomes in this study potentially came from misidentified or mislabeled samples. In several cases (Table 4.3), our phylogenomic analysis contradicted the metadata associated with the sample. For instance, the only fungal MAG from a metagenome labeled as *Rinodina brauniana* (Caliciales, SRR14722303) was nested within the *Lecanora* (Lecanorales) clade and given that these two lichen groups are somewhat similar, we suspected that the metagenome was produced from a misidentified specimen. All 14 such metagenomes were removed from further analysis. All algal MAGs belonged to Trebouxiophyceae algae.

4.4.2. Patterns of bacterial occurrence

4.4.2a. Structure of co-occurrence networks differ in lichen bacteria

Network analysis revealed that the structure of co-occurrence at the MAG level differed greatly between bacterial groups. Acetobacteraceae and Beijerinckiaceae exhibited centroid network structures relative to the “core” fungal symbiont similar to that of algal and cyanobacterial

photobionts (Fig. 4.3). For instance, although we recovered 16 *Lichenihabitans* MAGs, two dominant MAGs accounted for over half of the total occurrences. Acidobacteriaceae, by contrast, had a decentralized network, with few individual MAGs associated with more than three fungal symbiont MAGs.

4.4.2b. Bacteria overrepresented in certain lichen groups

To establish whether the composition of bacterial communities correlated with the main fungal partner, we analyzed bacterial occurrences on the level of lichen groups. For that, we divided our dataset into 20 groups based on the phylogeny of the main fungal partner. Lichens involving lecanoromycete fungi were split on the order level (Acarosporales, Baeomycetales, Caliciales, Gyalectales, Lecanorales, Lecideales, Leprocaulales, Ostropomycetidae *incertae sedis*, Peltigerales, Pertusariales, Rhizocarpaceae, Sarrameanales, Schaereriales, Teloschistales, Umbilicariales); the remaining groups were on the class level (Arthoniomycetes, Dothideomycetes, Eurotiomycetes, Lichinomycetes). We excluded from this analysis metagenomes that did not yield a MAG of the main fungal partner (27 metagenomes) or any bacterial MAGs (80 metagenomes).

For each lichen group, we created a list of the most common bacteria. The majority of the large groups shared the most common bacteria; this included lichens involving fungi from the orders Baeomycetales, Caliciales, Lecanorales, Pertusariales, and Teloschistales. Other groups exhibited a divergent bacterial composition. First, lichens involving fungal symbionts from the Peltigerales (hereafter ‘peltigerean fungi’) possessed Nostocaceae among the dominant bacteria, which was expected since cyanobacteria are the known primary or secondary photosynthetic partner in most lichens in this group (so-called “cyanolichens”). Less expected was the finding that Sphingomonadaceae were the second most common group in peltigerean

lichens, while being less frequent in other groups. Second, Burkholderiaceae were more common in both peltigeralean lichens and lichens with Umbilicariales as main fungal symbiont than in other lichen groups. In addition, lichens with Umbilicariales fungi contained almost no Beijerinckiaceae MAGs. Third, some lichen groups represented by a small number of metagenomes and/or shallowly sequenced metagenomes (e.g. involving fungi of the classes Arthoniomycetes or Lichinomycetes) exhibited high frequencies of bacteria otherwise rare in our dataset. However, this pattern might be an artifact caused by small sample sizes.

4.4.2c. Bacterial occurrence patterns do not result in strong multivariate clustering

Results from the previous section led us to think that some lichen groups might differ in their bacterial symbionts. To test for that, we used multivariate statistical methods. We started by clustering metagenomes and bacteria based on the occurrence matrix. We wanted to know whether lichen metagenomes can be divided into clusters based on their bacterial communities and whether these clusters correspond to the groups we created based on the main fungal partner. After comparing seven clustering methods, we picked two: *apcluster* and *kmeans*. These algorithms appeared to give the optimal number of clusters (Fig. 4.4–4.5), both for clustering bacteria and metagenomes. Confirming the pattern we described above, both methods separated peltigeralean lichens from others to a degree: half of them were recovered in a single cluster that included only a few non-peltigeralean lichens. Clustering of bacteria based on their occurrence profiles also grouped together bacteria common in peltigeralean lichens, including *Nostoc* (Nostocaceae), *Sphingomonas* (Sphingomonadaceae), *Enterovigra* (Beijerinckiaceae), and *Methylobacterium* (Beijerinckiaceae). However, in other cases the two methods gave inconsistent results, which led us to conclude that lichen metagenomes do not show strong clustering based on their bacterial communities.

Next, we explored how sequencing depth affects recovered bacterial diversity. We attempted to exclude this factor already during the clustering analysis, where we only included metagenomes with more than 2 Gbp of data. However, we suspected that sequencing depth might influence the results nonetheless: on average Peltigerales lichens in our dataset were more deeply sequenced and had a higher number of MAGs than the rest of the metagenomes, which might explain why they were clustered together. To account for this, we analyzed the same occurrence matrix with CCA, where sequencing depth was used as one of the predictors. The results suggest that sequencing depth indeed plays an important role in determining the “visible” bacterial diversity in the metagenomes (Fig. 4.6).

Overall, CCA confirmed the patterns from the clustering analysis and the lists of the most frequent bacteria from section 4.3.2b. First, a majority of lichen groups were similar to each other and showed no clear grouping. Second, several lichen groups were recovered as outliers; these mostly included groups with a small number of metagenomes assigned to them, or with shallowly sequenced metagenomes (e.g., Lichinomycetes or Verrucariales).

4.4.2d. Photosynthetic partner as a predictor of bacterial community

In comparing lichen groups to each other, one difficulty lies in establishing whether the fungal partner or the photosynthetic partner affects the bacterial community. In principle, we could extract the effect of the photosynthetic partner by showing some similarities between lichens that share the same photosynthetic partner but differ in the main fungal partners. In practice, however, the identity of the photosynthetic partner and the main fungal partner were not independent variables. For instance, among the metagenomes included in this analysis, two sets — of lichens involving Peltigerales fungi and of cyanolichens — overlapped almost entirely.

This difficulty could be overcome, to an extent, with peltigeralean lichens — lichens involving Peltigerales fungi. Our dataset included such lichens with either of two sets of photosynthetic partners: a) cyanobacteria alone (21 metagenomes included in this analysis), or b) trebouxoid algae and cyanobacteria (4 metagenomes) (Table 4.1). Both types included deeply sequenced metagenomes, which allowed us to compare lichens with and without *Trebouxia*, with all other things being more or less equal.

Both types of peltigeralean lichens had high frequency of Sphingomonadaceae, Beijerinckiaceae, and Acetobacteraceae. However, on the genus level the two sets differed: *Lichenihabitans* was the most common bacterial genus in the lichens that included trebouxoid algae but rarely occurred in cyanolichens. CCA of peltigeralean lichens showed sequencing depth and photobiont type as two factors shaping the bacterial community “visible” to us (Fig. 4.7).

4.4.3. Symbiont detection beyond MAGs

4.4.3a. Link between sequencing depth and number of recovered MAGs

The number of MAGs per metagenome increased with increasing sequencing depth and did not appear to plateau (Fig. 4.8). The highest number of MAGs was 50 in the *Lobaria pulmonaria* metagenome (ERR4179390), which was also the second most deeply sequenced, with almost 35 Gbp of data. The number of MAGs did not appear to depend on the architecture type of the lichen (crust vs. macrolichen).

High number of MAGs in metagenomes was primarily driven by the presence of bacteria. In some cases, multiple fungal MAGs were present. Some metagenomes, in addition to the MAG of the main fungal partner of the source lichen, contained a low-coverage MAG of another lichen fungus. For example, a metagenome of *Platismatia glauca* (X3) contained two lecanoromycete

MAGs: one was nearly identical to other *Platismatia* MAGs from this study and had high coverage (221×); and another was low-coverage (4×) and nearly identical to the only fungal MAG from the *Hypogymnia physodes* (X14) metagenome.

4.4.3b. Recovery of the key symbiont MAGs depends on the sequencing depth

Sequencing depth appeared to be the main factor determining whether a metagenome would yield MAGs of the two main symbionts, the main fungal symbiont and the photobiont. The minimal sequencing depth that allowed recovery of the main fungal symbiont MAG was about 550 Mbp, and at least 2 Gbp were required to obtain both the main fungal symbiont and photobiont MAGs (Fig. 4.9). At the same time, several metagenomes with sequencing depths well above these thresholds failed to yield a MAG for one or both main partners. This might be explained by higher complexity of those metagenomes or the presence of multiple strains, which would drive down the coverage depth for each genome.

4.4.3c. Marker gene-based screening confirms high prevalence of the dominant bacterial clades

To test for false absences caused by e.g. insufficient sequencing depth, we performed additional screening based on presence/absence of SSU rDNA genes. Both in metagenomic assemblies and raw, unassembled reads, the top four bacterial families were the same as in the MAGs: Acetobacteraceae, Acidobacteriaceae, Beijerinckiaceae, and Sphingomonadaceae. Screening of raw reads revealed that the four dominant bacterial families are present universally with their occurrence exceeding 90% (Fig. 4.10). On the level of assembly screening, Acetobacteraceae were detected in 92% of metagenomes, more than trebouxiophycean algae, which were found in 83% of metagenomes.

In addition to profiling bacteria, we screened for several eukaryotic lineages known to be stably involved in lichen symbioses (cystobasidiomycete and tremellomycete fungi and trebouxiphycean algae). For all lineages, MAG-level screening yielded fewer positives than rDNA-based screening; rDNA screening of metagenomic assemblies, in turn, resulted in a lower rate of detection than screening of raw unassembled reads (Fig. 4.10).

4.4.4. Symbiont abundance approximated by genome coverage

4.4.4a. Bacteria often outnumber the main symbionts

The abundance of the most frequent bacterial lineages, as estimated by the relative depth of coverage, was often higher than that of the algal symbionts, but only a fraction of that of the main fungal partner (Fig. 4.11). An exception to the latter rule were cyanobacteria: *Nostoc* was typically twice as abundant as the main fungal partner. High abundance of *Nostoc*, as compared to other bacteria, was not surprising: in lichens, it often plays the role of the main photosynthetic partner. Another exception was a lineage of Sphingomonadales (UBA1936): it occurred in three lichens formed by Peltigerales mycobionts, and in each its coverage depth was near a 1:1 ratio to the main fungal partner.

Despite the fact that individual bacteria are less abundant than the main fungal symbiont, the total coverage depth of bacterial MAGs (excluding cyanobacteria) per metagenome exceeded the coverage depth of the main fungal partner MAG in 19% of metagenomes.

4.4.5. Functional genomics of lichen bacteria

To study the biology and functions of bacteria in lichens, we selected all bacterial MAGs that passed the 90% completeness threshold and annotated them.

4.4.5a. Functional clustering of bacteria

First, we explored the link between functional profiles of bacteria and their taxonomy. In bacteria, taxonomy and function do not correlate perfectly, and therefore some patterns can be lost in a taxonomy-based profiling. Could it be that multiple taxonomic groups, each too rare to attract our attention on its own, together form a single functional group that plays an important role in lichens? To test for this possibility, we attempted to classify MAGs of lichen bacteria into functional clusters based on their KEGG profiles. The three clustering methods that produced clustering with a reasonable number of clusters were: apcluster, hdbscan, and kmeans (Fig. 4.12). The clusters produced by hdbscan closely followed the taxonomy, and each cluster, with two exceptions, mapped to one bacterial phylum (Fig. 4.13). Apcluster and kmeans disagreed with taxonomy more often (Fig. 4.13). However, in cases where the clustering was not consistent with taxonomy, apcluster and kmeans also did not agree with each other. For example, in both methods Proteobacteria were split between six clusters, but the boundaries of the clusters differed. We concluded that lichen bacteria cannot be separated into functional clusters beyond their taxonomic profiles.

4.4.5b. Aerobic anoxygenic phototrophs among the dominant lichen bacteria

We selected 63 bacterial MAGs for in-depth annotation. To select the MAGs, we ranked bacterial genera based on the occurrence numbers, then selected 13 genera, which together accounted for over half of all bacterial occurrences. These genera came from six families: Acetobacteraceae, Beijerinckiaceae, Acidobacteriaceae, Sphingomonadaceae, Nostocaceae (Nostocales, Cyanobacteria), and UBA10450 (Chthoniobacterales, Verrucomicrobia). Finally, we only retained the MAGs that passed the completeness and contamination thresholds.

The majority of the analyzed MAGs from the two most frequent clades, Acetobacteraceae and Beijerinckiaceae, corresponded to the description of aerobic anoxygenic phototrophs (see Yurkov & Csotonyi 2009). As such, they possessed: 1) a complete set of anoxygenic photosystem II proteins (KEGG modules M00597 M00165; *pufABCML-puhA*), 2) a bacteriochlorophyll synthesis pathway (*AcsF*, *ChlBNL*, *BchCFGPXYZ*), and 3) carotenoid biosynthetic gene clusters, as identified by antiSMASH and KEGG (Fig. 4.14). Divinyl chlorophyllide a 8-vinyl-reductase (*DVR*), a part of the bacteriochlorophyll synthesis pathway, was mostly lacking in the MAGs, but we still counted the pathway as complete, since its function (converting divinyl chlorophyllide into monovinyl chlorophyllide) can be performed by chlorophyllide oxidoreductases (Harada et al. 2014).

With few exceptions in Acetobacteraceae, the putative aerobic anoxygenic phototrophs lacked any complete carbon fixation pathway (Fig. 4.14). Only three MAGs had a complete Calvin-Benson cycle, and the majority lacked *RuBisCO*, the key enzyme required for fixing carbon. In addition, none of the putative aerobic anoxygenic phototrophs had alternative carbon fixation pathways (see Assié et al. 2020): reductive citrate cycle (M00173), 3-hydroxypropionate bi-cycle (M00376), hydroxypropionate-hydroxybutyrate cycle (M00375), dicarboxylate-hydroxybutyrate cycle (M00374), Wood-Ljungdahl pathway (M00377), or the phosphate acetyltransferase-acetate kinase pathway (M00579).

In addition to genes of the anoxygenic photosystem II, several MAGs had genes homologous to bacteriorhodopsin, another protein used by bacteria to harness the energy of light (Jaffe et al. 2022). These MAGs occurred sporadically in all analyzed bacterial clades, except cyanobacteria. Beta-carotene oxygenase *Blh*, required for the production of the rhodopsin chromophore (Jaffe et

al. 2022), was also found in several MAGs, though seemingly its presence did not correlate with that of bacteriorhodopsin.

4.4.5c. Nitrogen fixation is present only in cyanobacteria

To test the hypothesis that non-cyanobacterial bacteria in lichens fix nitrogen, we searched the selected MAGs for *NifH*, the key gene required for fixing nitrogen. Contrary to the hypothesis, *Nostoc* MAGs were the only MAGs in our dataset that possessed *NifH*. We failed to find a copy of this gene in any of the Rhizobiales MAGs. To account for the possibility that *NifH* genes were present in a plasmid and therefore failed to be included in the core MAGs, we searched metagenomic assemblies, but all hits but one were cyanobacterial. The only exception was a *NifH* hit, classified as Rhizobiales, which was present in one metagenome in low coverage, and not assigned to any MAG.

The Rhizobiales MAGs from our dataset lacked *NifH* genes, despite being closely related to genomes with this gene (Fig. 4.15). For instance, in the clade that included *Lichenihabitans* and RH-AL1, nearly every non-lichen bacterium (21 out of 23) possessed *NifH*, but none of the lichen-derived bacteria did.

4.4.5d. Methylotrophy in lichen bacteria

Multiple bacterial MAGs exhibited signs of methylotrophy, the ability to utilize methanol. Methanol dehydrogenases (*XoxF* or *MxaF*) were detected in 45% of lichen-derived Rhizobiales, including some *Lichenihabitans* and RH-AL1 (Fig. 4.15). In Acetobacteraceae, we found putative *XoxF* in nine MAGs from five genera (out of six genera selected for the in-depth analysis) (Fig. 4.14).

Lichenihabitans and RH-AL1 are closely related to methanotrophs, bacteria utilizing methane (Fig. 4.15). Still, neither them, nor other studied MAGs, contained any methane monooxygenase required for methanotrophy.

4.4.5e. Lichen bacteria are not iron-limited

To test the hypothesis that lichen bacteria scavenge iron for the eukaryotic symbionts, we profiled genes related to iron metabolism. Contrary to our expectations, clusters potentially involved in siderophore biosynthesis were rare in all studied bacterial groups, except cyanobacteria. Instead, the majority of MAGs had iron ion transporters, which signals that they are not limited in iron. Every MAG also had genes classified by FeGenie as related to siderophore transport, although the tool developers note that these genes are not exclusively connected to siderophore uptake and cannot be viewed as evidence of siderophore uptake (Garber et al. 2020).

4.4.5f. The most frequent bacterial lineages have cofactor biosynthesis pathways

The majority of MAGs in Acetobacteraceae and Beijerinckiaceae included pathways for biosynthesis of cobalamin (vitamin B12; KEGG Module M00122). Riboflavin (vitamin B2; KEGG Module M00125) was present almost universally (Fig. 4.14). Even though our KEGG annotations showed the riboflavin pathway as incomplete due to the lack of 5-amino-6-(5-phospho-D-ribitylamino)uracil phosphatase, we counted them as complete, since its function can be performed by a broad spectrum of hydrolases (García-Angulo 2017).

Other vitamin pathways varied in their completeness. Complete biotin (vitamin B7) biosynthesis pathways (KEGG modules M00123, M00577, and M00950) were present in only some genera (Fig. 4.14). The thiamine biosynthesis pathway was present in some MAGs only partially, but

the thiamine salvage pathway was more common (KEGG Module M00899 or *thiMDE*, see Karunakaran et al. 2006).

4.4.5g. Acidobacteriaceae have a larger pool of carbohydrate degradative enzymes

We compared the CAZyme profiles of the selected MAGs, and revealed that Acidobacteriaceae MAGs had 50% more glycoside hydrolases (GH) per genome than the selected MAGs had on average. Acidobacteriaceae was the only family where GHs were the dominant CAZy class (i.e. had the highest number of predicted genes) (Fig. 4.16). Contributing to this were several mannosidase families that were widespread in Acidobacteriaceae and almost lacking in other bacterial families in the annotation subset, including GH92 (mannosidase), GH125 (exo-alpha-1,6-mannosidase), GH38 (alpha-mannosidase), and GH76 (alpha-1,6-mannosidase/alpha-glucosidase). Also overrepresented in Acidobacteriaceae were enzymes potentially acting on fungal polysaccharides, such as GH18 (chitinase), GH55 (beta-1,3-glucanase), and GH51 (endoglucanase, endoxylanase, cellobiohydrolase).

4.4.5h. Predicting flow of goods based on transporters

To predict what types of substances lichen bacteria import from the outside, we annotated transporter systems. Most studied MAGs contained at least one transporter system for sugars or sugar alcohols (Fig. 4.14). Based on the identified transporter systems, Acetobacteraceae and *Lichenihabitans* (Beijerinckiaceae) had multiple potential carbon sources they can absorb: monosaccharides (ribose/D-xylose transporter *RbcABC*, D-xylose *XylFGH*, multiple sugars *ChvE-GguAB*, more rarely fructose *FrcABC* and L-arabinose *AraFGH*) and sugar alcohols (glycerol *GlpPQSTV*, sorbitol/mannitol *SmoEFGK*, xylitol *XltABC*, erythritol *EryEFG*, glucitol/sorbitol *SrlABE*) (Fig. 4.14). Other studied families had fewer transporter systems, although Acidobacteriaceae had a glycerol transporter *GLPF*, which was lacking in other MAGs.

Unexpectedly, we could not find any sugar or sugar alcohol transporter in the RH-AL1 MAGs, even though this genus was closely related to *Lichenihabitans*, which had a large arsenal of transporters.

We identified ammonium as a potential source of nitrogen. Nearly all studied MAGs contained the ammonium transporter *amtB* (Fig. 4.14). Urea and amino acids might be additional sources of nitrogen. In three families (Acetobacteraceae, Beijerinckiaceae and Nostocaceae), the majority of the studied MAGs had urea transporters *urtABCDE* and urease *UreABC*. In addition, several MAGs had amino acid transport systems (branched-chain amino acids *LivKHMGF*, general L-amino acids *AapJMPQ*, glutamate/aspartate *GltIJKL*). We predicted several lineages from Acetobacteraceae, Beijerinckiaceae and Sphingomonadaceae to produce capsule polysaccharides: several MAGs from these groups contained *kpsMTE* transporters, which export capsule polysaccharides.

4.5. Discussion

Almost exactly 100 years ago, biologists became aware of bacteria associated with lichens. Cengia Sambo (1926) reported them first, and soon after Henkel and colleagues suggested that some of these bacteria might play a role in the symbiosis by fixing nitrogen and supplying it to other symbionts (Henkel & Yuzhakova 1936, Iskina 1938). Studies were taken up again in the age of PCR and shotgun sequencing. From profiling lichen bacteria using these methods, biologists learned that: a) bacteria are indeed ubiquitous in lichens, b) bacterial communities are dominated by Alphaproteobacteria, and c) the composition of bacterial communities and the abundance of its members vary between different lichens and collection sites (Bates et al. 2011, Hodkinson et al. 2012, Grube et al. 2015, Grimm et al. 2021). It was also suggested that bacteria

play a role in the functioning of the symbiosis, by e.g. producing vitamins or antibiotics (Grube et al. 2015).

Our study expands the survey of bacteria in lichens by orders of magnitude. While most previous studies focused on one or a handful of ‘model’ symbioses, we surveyed lichens from nearly all major lichen groups. We studied all symbionts simultaneously, using metagenomic data that have no taxonomic bias. We show that specific bacterial lineages occur with greater frequency in lichen metagenomes than any photosynthetic symbiont, and with far greater frequency than basidiomycete yeasts recently reported to occur as stably associated symbionts in some lichen groups (Spribille et al. 2016, Tuovinen et al. 2019).

Starting this study, we expected bacteria in lichen metagenomes to be a more or less random “soup” of Alphaproteobacteria. This expectation stemmed from previous studies that reported lichen bacterial communities to be distinct from those of their microhabitats, but still connected to them, and to vary depending on environmental factors (Cardinale et al. 2012, Aschenbrenner et al. 2017). Unexpectedly, we found that bacterial communities in lichens are highly structured and dominated by only a few bacterial lineages. Bacterial lineages most frequent in the global lichen sample were Acetobacteraceae, Beijerinckiaceae, Acidobacteriaceae, and Sphingomonadaceae. All four families belong to the orders and classes that were previously recognized as dominant in the “model” lichens (Bates et al. 2011, Hodkinson et al. 2012, Grube et al. 2015), but were never known to be present in lichens across the board. We suspect that Acetobacteraceae — the most frequently occurring bacterial family — did not receive much attention before because of the primer bias: Cernava et al. (2017) show that Acetobacteraceae abundance derived from metabarcoding was much lower compared to the unbiased metagenomic data.

When we looked at the bacterial communities on a more granular taxonomic level — genus and species-level lineages — we again saw unexpected structure. While *Lichenihabitans* was already known to occur in about 25 different lichens (Hodkinson & Lutzoni 2009, Bates et al. 2011, Hodkinson et al. 2012, Noh et al. 2019, Pankratov et al. 2020), now it emerged as a highly widespread bacterium in lichens and a potential stable member of lichen symbioses. One, most common, species-level lineage within *Lichenihabitans* was present in one seventh of the studied metagenomes, derived from multiple different lichen groups, data sets, investigators, and geographies.

If *Lichenihabitans* is indeed ubiquitous in lichens, why wasn't it discovered as such previously? Previous studies have suggested that *Lichenihabitans* (as LAR1) is common and might play a role in the symbiosis (Hodkinson & Lutzoni 2009, Bates et al. 2011, Hodkinson et al. 2012). However, the true extent of its occurrence in lichens was not known. Often, studies reported taxonomic composition of lichen bacteria only on the family level or above (e.g., Grube et al. 2015, Cernava et al. 2017), which could mask finer-level patterns. At the same time, even studies that did finer taxonomic analysis could miss *Lichenihabitans*. The bacterium was formally described only three years ago (Noh et al. 2019), and before that was not included in reference databases. Consequently, it could not be detected by the standard protocols of taxonomic profiling, unless searched for specifically (as was done by Hodkinson et al. 2012 and Aschenbrenner et al. 2017). We suspect that some of the “unclassified Rhizobiales” reported from lichens by e.g. Erlacher et al. (2015) were, in fact, *Lichenihabitans*.

4.5.1. Should we treat bacteria as lichen symbionts?

Grube and Berg (2009) introduced the term ‘bacteriobionts’ for bacterial assemblages in lichens. They and their co-authors have argued that bacteria should be treated as an element of the

symbiosis (Grube & Berg 2009, Aschenbrenner et al. 2016, Grimm et al. 2021). Two lines of evidence emerged from our study that support their framing. First, the dominant bacterial lineages — and especially *Lichenhabitans* — are shared by a large portion of lichens in our dataset. Second, our estimates suggest that these bacteria have high cellular abundance and usually outnumber the green alga, one of the main symbionts. Bacterial lineages that occur so often and in high numbers are not likely to be random contaminants from the environment. In fact, the alternative hypothesis — that bacterial communities in lichens are a mere extension of surrounding microbiota — has already been rejected for the model lichen species (Aschenbrenner et al. 2017, Leiva et al. 2021).

The conclusion that lichen bacteria are symbionts is also supported by ultrastructural studies on lichens. Studies based on FISH demonstrate that bacteria usually colonize the lichen cortex, a biofilm-like layer that primarily consists of hyphae of the main fungal partner and an extracellular matrix (Cardinale et al. 2008, Cardinale et al. 2012, Erlacher et al. 2015). This layer shapes lichen architectures and facilitates water exchange (Spribille et al. 2020), which raises questions about the potential impact of lichen bacteria on these processes (Goodenough & Roth 2021). One study went as far as to report bacteria living inside fungal hyphae (Erlacher et al. 2015), although this claim has not been replicated elsewhere. Bacteria are structurally integrated into the symbiosis, which reinforces the view of them as symbiotic partners.

Taken together, these lines of evidence suggest that lichen bacteria are symbiotic — meaning that they engage in a relationship with the rest of the lichen symbionts. To what extent bacteria benefit their eukaryotic partners and whether they are required for the symbiosis to function is a separate question, which we attempt to answer below.

4.5.2. How do bacterial communities assemble?

To understand how bacterial communities assemble in lichens, we need to start with clarifying their transmission mode: vertical or horizontal. In lichen biology, transmission modes are usually brought up in the context of the two main partners, the main fungus and the photosynthetic partner (Spribille et al. 2022). Between these two partners, both horizontal and vertical transmission are possible, although the two strategies rarely co-occur in one symbiosis. Vertical transmission comes in the form of vegetative propagules, which contain cells of multiple symbionts, a “package deal” leading to co-transmission. Alternatively, lichens can undergo “resynthesis”: for every generation, a spore of the main fungus germinates and contacts the cells of the other partners, acquiring them horizontally. How exactly it happens remains unknown, as this process has never been observed in nature.

A big portion of microbial symbioses use a combination of vertical and horizontal transmission (Ebert 2013), and Leiva et al. (2021) suggested that lichen bacteria too have a mixed strategy. This hypothesis is consistent with the occurrence patterns we identified for the most common bacterial lineages, especially *Lichenihabitans*. In favor of horizontal transmission speaks the low specificity of the bacteria, which contrasts them with the basidiomycete yeasts, other organisms recently discovered in lichens (Spribille et al. 2016). We suspect that the low specificity arises from lichens acquiring *Lichenihabitans* from other lichen symbioses nearby. In addition, *Lichenihabitans* occurs in microbiomes of tree bark and moss (Aschenbrenner et al. 2017), where it can be selected and acquired by a developing lichen. On the other hand, vertical transmission is possible too, as Aschenbrenner et al. (2014) demonstrated bacteria in the vegetative propagules of the *Lobaria* lichen. We suspect that vertical transmission of bacteria should be common in other lichens as well, since the propagules often include fragments of the

cortex — the layer that harbors most bacteria in lichens. If bacteria indeed are transmitted as a part of lichen propagules, that would explain why in our dataset certain species-level lineages occur in lichens from different continents.

What features of a lichen symbiosis influence the bacterial community? Previous studies on model lichen symbioses have identified several factors that influence the composition of lichen bacteria: the phylogeny of the main fungus, the photosynthetic partner, and the geography (Hodkinson et al. 2012). Some of the patterns identified in the literature were supported by our results. For instance, Hodkinson et al. (2012) concluded that Sphingomonadaceae were more common in cyanolichens than in lichens with green algae, based on a metabarcoding study of 24 lichen symbioses — and the same pattern emerged from our dataset. Similarly, both West et al. (2018) and we reported higher frequency of Chloroflexi in Lichinomycetes lichens. However, the impact of each individual factor is obscured by their interdependence: the identity of the fungal partner correlates with the identity of the photobiont; both are linked with the ecology. For instance, we cannot confidently interpret the difference in bacterial communities between Lichinomycetes, Umbilicariales, and the rest of the dataset: in addition to having distinct fungal partners, Lichinomycetes and Umbilicariales lichens may also be ecologically divergent from the majority of lichens in our data set. More research is needed to clarify the impact of each factor.

Going into this study, we expected bacterial communities to exhibit some correlation with lichen architecture type. Depending on their architecture, lichens have different degrees of separation from their ecological substratum (Honegger 1993). ‘Macrolichens’ usually rise above the substrate and develop a cortex, which isolates an internal hydrophobic layer of fungal hyphae from the surrounding environment. In contrast, crusts adhere closely to the substratum or are even immersed in it, often with little stratification. On account of their intimate attachment to

substrata we expected crusts to contain a larger variety of bacteria, but this hypothesis was not supported by our data.

4.5.3. Can we tell how symbionts interact?

If lichen bacteria are indeed a stable part of lichen symbiosis, they are integrated into the flow of goods and services that defines the lichen symbiosis. Researchers started speculating about the role of lichen bacteria almost as soon as they were discovered (Henkel & Yuzhakova 1936). Currently, most evidence we have comes from the omics-based studies of the *Lobaria* lichen (most recent summary in Grimm et al. 2021). Here, we attempted to create a more full picture that is based not on one but on many lichen symbioses. Our estimates of functional capabilities are more conservative and specific than those of the previous studies (Grube et al. 2015, Cernava et al. 2017, 2019): instead of assigning bacterial genes to broad functional categories, we report reconstruction of specific biosynthetic pathways and protein complexes. Our approach is prone to false-absences caused by the incompleteness of our functional assignments, but it is less prone to false-positive results.

4.5.3a. Carbon

Lichen bacteria have always been assumed to be heterotrophic, with the exception of cyanobacteria. This assumption largely holds up in our study, although we suspect that more exceptions exist: we identified three Acetobacteraceae lineages that appear to have machinery for anoxygenic photosynthesis and carbon fixation. Still, the majority of lichen bacteria likely acquire carbon from the eukaryotic symbionts. To identify the potential carbon sources, we looked into transporter genes we predicted in the bacterial genomes. Based on the transporters, we suspect that bacteria mainly use the algal-produced polyols and sugars, which they absorb from the matrix.

Whether lichen bacteria can use single-carbon compounds as an additional carbon source was not clear from the literature. On one hand, Eymann et al. (2017) reported proteins involved in C1 metabolism from the *Lobaria* lichen metaproteome. They attributed these proteins to the lichen-associated Rhizobiales, which are closely related to methanotrophs and methylotrophs. On the other hand, culture-based studies showed that *Lichenhabitans* cannot utilize any C1 compounds (Noh et al. 2019, Pankratov et al. 2020). Our genomic analysis shows that the most common bacteria cannot use methane, but multiple lineages can utilize methanol. The inconsistency in the literature can be explained through the inconsistency of the presence of methylotrophy. The lineages that we identified as methylotrophic were scattered throughout Beijerinckiaceae and Acetobacteraceae. Among *Lichenhabitans* genomes two thirds lacked methanol dehydrogenases, including the published genomes isolated from cultures (Noh et al. 2019, Pankratov et al. 2020).

If a portion of lichen bacteria are facultative methylotrophs, where do they get the methanol? The possible sources can be split into two categories: either methanol is a product of metabolism of other symbionts, or it comes directly from the outside. We cannot rule out either. On one hand, lichens often occupy microhabitats where methanol should be available. In terrestrial ecosystems, methanol primarily originates from decaying plant biomass (Wohlfahrt et al. 2015). Lichens often live in close contact with tree bark, wood, or soil, where decomposition is happening. Possibly, lichens even contribute to the decomposition, since lichen fungi retain cellular machinery for degrading plant biomass (Resl et al. 2022). Methanol emitted in the process could, in theory, be used by the lichen bacteria. If this is the case, methylotrophic lichen bacteria are a minor contributor to the “carbon budget” of the symbiosis. Alternatively, the

methanol can come from the decomposition of lichen matter. Eymann et al. (2017) hypothesized that methanol is produced during the degradation of phenolic secondary metabolites.

4.5.3b. Nitrogen

For a long time, it has been known that cyanobacteria in lichens fix nitrogen and supply it to other symbionts (Millbank & Kershaw 1970), and for a long time it was hypothesized that other bacteria might too. The hypothesis was partially based on the prevalence of Rhizobiales in lichens and their taxonomic proximity to nitrogen fixers (Wang et al. 2020b). The evidence remained inconclusive: on one hand culture-based studies reported nitrogen fixers from lichens (Liba et al. 2006), and *NifH*, one of the key enzymes in nitrogen fixation, was detected by PCR in a few lichen symbioses (Hodkinson & Lutzoni 2009, Almendras et al. 2018) and in some bacteria isolated from lichens (Jiang et al. 2017). On the other hand, studies on specific Rhizobiales showed them lacking both *NifH* and the ability to fix nitrogen (Pankratov et al. 2020), and proteomics studies failed to detect any non-cyanobacterial proteins involved in nitrogen fixation (Eymann et al. 2017).

Our results speak against nitrogen fixation in lichen bacteria other than cyanobacteria. We cannot exclude that “rare biosphere” bacteria in lichens fix nitrogen and evade detection due to low abundance, but none of the dominant bacteria have the machinery consistent with known mechanisms of nitrogen fixation, including Beijerinckiaceae. We suspect that bacteria rely on eukaryotes for nitrogen, not the reverse. Based on the transporter annotations, potential nitrogen sources used by the bacteria are ammonium and amino acids, which is consistent with the physiological profile of *Lichenihabitans* in culture (Pankratov et al. 2020).

Pankratov et al. (2022) already have shown urea hydrolysis in *Lichenihabitans*. They hypothesized that the bacteria use it as a way to release ammonium and bicarbonate. The former

makes nitrogen more accessible for all symbionts, while the latter can be used by the alga for carbon fixation. We detected the machinery for urea hydrolysis and transport in the majority of lichen Acetobacteraceae and Beijerinckiaceae genomes.

4.5.3c. Vitamins and cofactors

Bacterial symbionts often supply their eukaryotic partners with vitamins and cofactors (McCutcheon et al. 2009, Husnik et al. 2021). Although less commonly than animals, fungi and algae also have been shown to depend on bacteria for vitamins (Croft et al. 2005, Jiang et al. 2018). Blanch et al. (2001) first hypothesized that lichen bacteria contribute to the symbiosis by producing cofactors. Their hypothesis was based on their observation of lichen fungi in culture, and later it was supported by meta-omics studies that reported bacterial genes associated with cofactor metabolism (Grube et al. 2015, Eymann et al. 2017). We show that lichen bacteria, and especially Acetobacteraceae and Beijerinckiaceae, have pathways for biosynthesis of cobalamin, required by many green algae (Helliwell et al. 2011) and, although less consistently, for thiamine and biotin, required by the main fungal partner (shown for several species; Hale 1958, Richardson & Smith 1968).

4.5.3d. Recycling

Recycling biomass from old, senescent parts of the lichen body is often listed a potential role bacteria play in lichens (Grimm et al. 2021). We suspect that the role of “grazers” is played by Acidobacteriaceae. We show that Acidobacteriaceae differ from other frequent lineages by a higher number of degradative CAZymes, including enzymes that potentially target polysaccharides most abundant in lichens. The role of grazers is consistent with the pattern of occurrence of this group. While other studied bacterial families had super-common lineages that occurred in many lichens, Acidobacteriaceae have more species-level lineages, none of which

was particularly common or showed preference to any specific lichen group. This hypothesis also matches what is known about non-lichen Acidobacteria. Members of Acidobacteria isolated from acidic soil or peat bogs can break down various polysaccharides, including lichenan. Co-culture experiments suggested that soil Acidobacteria feed off extracellular polysaccharides produced by other microbes, including Proteobacteria (Pankratov et al. 2008, Kielak et al. 2016). Such syntrophy remains to be demonstrated in lichens.

4.5.3e. Building the extracellular matrix

The lichen extracellular matrix is usually attributed to the main fungal partner. However, bacteria and yeasts inhabiting the matrix can potentially also play a role in producing it (Spribille et al. 2020). Among the studied bacteria, Acidobacteriaceae are the most likely to contribute to the matrix. In culturing studies, Acidobacteriaceae often produce copious amounts of extracellular polysaccharides (Kielak et al. 2017). The composition of these polysaccharides (mannose, glucose, xylose, and glucuronic acid) matches the profiles of polysaccharides isolated from lichens (Spribille et al. 2020). In addition to Acidobacteriaceae, we predicted several Beijerinckiaceae, Acetobacteraceae, and Sphingomonadaceae to produce capsule polysaccharides or exopolysaccharides.

4.5.4. Aerobic Anoxygenic Phototrophs (AAPs)

AAPs are a functional group of bacteria capable of anoxygenic photosynthesis under aerobic conditions, which mostly includes Alphaproteobacteria (Yurkov & Beatty 1998). Originally discovered in aquatic environments, they were later identified as a key player in soil crusts (Tang et al. 2021b). The taxonomic groups of AAPs in soil crusts are similar to the most common lichen bacteria and include Acetobacteraceae and Sphingomonadaceae (Tang et al. 2021b).

Although Pankratov et al. (2022) recently reported an anoxygenic photosystem in one *Lichenihabitans* genome, the place AAPs occupy in lichens has never been discussed. Based on our genomic analysis, we conclude that a big portion of the most common lichen bacteria — Acetobacteraceae and Beijerinckiaceae — are, in fact, AAPs. These bacteria appear capable of photoheterotrophic growth, and a small number of them are capable of fixing carbon as well. The ability to photosynthesize is probably horizontally acquired, since even lineages within one genus can differ. We therefore suspect that photosynthesis is an additional source of energy for the lichen bacteria and is not essential for their survival. Still, the existence of AAPs in lichens challenges the term “photobiont”, which until now has been applied only to the green algal and cyanobacterial symbionts.

4.5.5. Challenges of taxonomic profiling and opportunities provided by a large dataset

Using metagenomes to study symbiosis composition has two limitations: one is related to false negatives and the other to false positives. False negatives are linked to sequencing depth. In shallowly sequenced metagenomes, we can only detect lineages that have high enough relative abundance. In these cases, less abundant bacteria would fly under the radar. However, less abundant does not mean less important: the so-called rare biosphere bacteria sometimes play a crucial role in shaping their microbial communities (Jousset et al. 2017).

On the other hand, false positives can stem from the environmental contaminants that are not removed from the sample before the DNA extraction. The most powerful approach for lineage detection was screening raw reads, and in several metagenomes, this way we detected genome fragments of animals and conifer trees, which are safe to call contaminants. In a previous study (Tagirdzhanova et al. 2021), we used second-level screening to identify potential contaminants: we screened multiple samples of the target lichen symbiosis collected in various locations, and

only the organisms present consistently were selected for further study. This way we established that an Acidobacteriaceae, *Granulicella*, is not consistently present in the *Alectoria* lichens, even though it was detected in many studied samples of other lichens. In this study, the majority of lichen symbioses are represented by just one sample. However, a large dataset with metagenomes coming from various locations in itself provides a large sample size. While the composition of any individual lichen symbiosis should be verified through an additional screening, the broader patterns we detected on the level of our entire dataset will likely stand.

4.5.6. Conclusions

The results we present here call for rethinking the place of bacteria in lichen symbiosis. Going into this project, we expected bacteria in our dataset to be primarily from Proteobacteria (echoing Cardinale et al. 2012, Grimm et al. 2021), and to vary significantly between different metagenomes. Instead, we found a small number of lineages that were present across all studied lichen groups. Using this big dataset gave us the ability to unearth this pattern that was inevitably overlooked during previous studies that focused on few selected lichens. By analyzing the genomes of most common lichen bacteria, we made predictions regarding the metabolic potential of the dominant lichen bacteria and the role they play in the symbiosis. Our results support some of the previously voiced hypotheses: we expect bacteria to participate in the synthesis of cofactors, recycling biomass, and producing the extracellular matrix. We found no evidence of bacteria (other than cyanobacteria) fixing nitrogen. At the same time, we suspect that the way lichen bacteria contribute to the carbon “budget” of the symbiosis is not as simple as was believed before, and future research needs to account for potential methylotrophy and photoheterotrophy of the lichen bacteria.

Here we attempted to paint a broad picture, which now requires more detailed work. More research is needed to follow up on the dominant bacterial lineages, to clarify their occurrence patterns and to test the hypotheses on their functional roles. Some of this work can be aided by the genomes of lichen symbionts that we will make publicly available.

References

- Almendras, K., García, J., Carú, M., & Orlando, J. (2018). Nitrogen-fixing bacteria associated with *Peltigera cyanolichens* and *Cladonia chlorolichens*. *Molecules*, *23*(12), 3077.
- Alneberg, J., Bjarnason, B. S., De Bruijn, I., Schirmer, M., Quick, J., Ijaz, U. Z., ... & Quince, C. (2014). Binning metagenomic contigs by coverage and composition. *Nature Methods*, *11*(11), 1144–1146.
- Altschul, S. F., Gish, W., Miller, W., Myers, E. W., & Lipman, D. J. (1990). Basic local alignment search tool. *Journal of Molecular Biology*, *215*(3), 403–410.
- Aramaki, T., Blanc-Mathieu, R., Endo, H., Ohkubo, K., Kanehisa, M., Goto, S., & Ogata, H. (2020). KofamKOALA: KEGG ortholog assignment based on profile HMM and adaptive score threshold. *Bioinformatics*, *36*(7), 2251–2252.
- Aschenbrenner, I. A., Cardinale, M., Berg, G., & Grube, M. (2014). Microbial cargo: do bacteria on symbiotic propagules reinforce the microbiome of lichens?. *Environmental Microbiology*, *16*(12), 3743–3752.
- Aschenbrenner, I. A., Cernava, T., Berg, G., & Grube, M. (2016). Understanding microbial multi-species symbioses. *Frontiers in Microbiology*, *7*, 180.

- Aschenbrenner, I. A., Cernava, T., Erlacher, A., Berg, G., & Grube, M. (2017). Differential sharing and distinct co-occurrence networks among spatially close bacterial microbiota of bark, mosses and lichens. *Molecular Ecology*, *26*(10), 2826–2838.
- Assié, A., Leisch, N., Meier, D. V., Gruber-Vodicka, H., Tegetmeyer, H. E., Meyerdierks, A., ... & Petersen, J. M. (2020). Horizontal acquisition of a patchwork Calvin cycle by symbiotic and free-living Campylobacterota (formerly Epsilonproteobacteria). *The ISME journal*, *14*(1), 104–122.
- Bates, S. T., Cropsey, G. W., Caporaso, J. G., Knight, R., & Fierer, N. (2011). Bacterial communities associated with the lichen symbiosis. *Applied and Environmental Microbiology*, *77*(4), 1309–1314.
- Bengtsson-Palme, J., Hartmann, M., Eriksson, K. M., Pal, C., Thorell, K., Larsson, D. G. J., & Nilsson, R. H. (2015). METAXA2: improved identification and taxonomic classification of small and large subunit rRNA in metagenomic data. *Molecular Ecology Resources*, *15*(6), 1403–1414.
- Blanch, M., Blanco, Y., Fontaniella, B., Legaz, M. E., & Vicente, C. (2001). Production of phenolics by immobilized cells of the lichen *Pseudevernia furfuracea*: the role of epiphytic bacteria. *International Microbiology*, *4*(2), 89–92.
- Blin, K., Shaw, S., Kloosterman, A. M., Charlop-Powers, Z., van Wezel, G. P., Medema, M. H., & Tilmann, W. (2021). antismash 6.0. *Nucleic Acids Research*.
- Bodenhofer, U., Kothmeier, A., & Hochreiter, S. (2011). APCluster: an R package for affinity propagation clustering. *Bioinformatics*, *27*(17), 2463–2464.

Cardinale, M., Grube, M., Castro Jr, J. V., Müller, H., & Berg, G. (2012). Bacterial taxa associated with the lung lichen *Lobaria pulmonaria* are differentially shaped by geography and habitat. *FEMS Microbiology Letters*, *329*(2), 111–115.

Cardinale, M., Vieira de Castro Jr, J., Müller, H., Berg, G., & Grube, M. (2008). In situ analysis of the bacterial community associated with the reindeer lichen *Cladonia arbuscula* reveals predominance of Alphaproteobacteria. *FEMS Microbiology Ecology*, *66*(1), 63–71.

Cengia Sambo, M. (1926). Ancora della polysimbiosi nei licheni ad alghe cianoficee. 1. Batteri simbiotici. *Atti della Società Italiana di Scienze Naturali e del Museo Civico di Storia Naturale in Milano*, *64*, 191–195.

Cernava, T., Aschenbrenner, I. A., Soh, J., Sensen, C. W., Grube, M., & Berg, G. (2019). Plasticity of a holobiont: desiccation induces fasting-like metabolism within the lichen microbiota. *The ISME journal*, *13*(2), 547–556.

Cernava, T., Erlacher, A., Aschenbrenner, I. A., Krug, L., Lassek, C., Riedel, K., ... & Berg, G. (2017). Deciphering functional diversification within the lichen microbiota by meta-omics. *Microbiome*, *5*(1), 1–13.

Chaumeil, P. A., Mussig, A. J., Hugenholtz, P., & Parks, D. H. (2020). GTDB-Tk: a toolkit to classify genomes with the Genome Taxonomy Database. *Bioinformatics*, *36*(6), 1925–1927.

Chen, S., Zhou, Y., Chen, Y., & Gu, J. (2018). fastp: an ultra-fast all-in-one FASTQ preprocessor. *Bioinformatics*, *34*(17), i884–i890.

Cornet, L., Magain, N., Baurain, D., & Lutzoni, F. (2021). Exploring syntenic conservation across genomes for phylogenetic studies of organisms subjected to horizontal gene transfers: A

case study with Cyanobacteria and cyanolichens. *Molecular Phylogenetics and Evolution*, 162, 107100.

Croft, M. T., Lawrence, A. D., Raux-Deery, E., Warren, M. J., & Smith, A. G. (2005). Algae acquire vitamin B12 through a symbiotic relationship with bacteria. *Nature*, 438(7064), 90–93.

Csardi, G., & Nepusz, T. (2006). The igraph software package for complex network research. *InterJournal, complex systems*, 1695(5), 1–9.

Deorowicz, S., Debudaj-Grabysz, A., & Gudyś, A. (2016). FAMSA: Fast and accurate multiple sequence alignment of huge protein families. *Scientific Reports*, 6(1), 1–13.

Ebert, D. (2013). The epidemiology and evolution of symbionts with mixed-mode transmission. *Annual Review of Ecology, Evolution, and Systematics*, 44, 623–643.

Epskamp, S., Cramer, A. O., Waldorp, L. J., Schmittmann, V. D., & Borsboom, D. (2012). qgraph: Network visualizations of relationships in psychometric data. *Journal of Statistical Software*, 48, 1–18.

Erlacher, A., Cernava, T., Cardinale, M., Soh, J., Sensen, C. W., Grube, M., & Berg, G. (2015). Rhizobiales as functional and endosymbiotic members in the lichen symbiosis of *Lobaria pulmonaria* L. *Frontiers in Microbiology*, 6, 53.

Eymann, C., Lassek, C., Wegner, U., Bernhardt, J., Fritsch, O. A., Fuchs, S., ... & Riedel, K. (2017). Symbiotic interplay of fungi, algae, and bacteria within the lung lichen *Lobaria pulmonaria* L. Hoffm. as assessed by state-of-the-art metaproteomics. *Journal of Proteome Research*, 16(6), 2160–2173.

- Garber, A. I., Neelson, K. H., Okamoto, A., McAllister, S. M., Chan, C. S., Barco, R. A., & Merino, N. (2020). FeGenie: a comprehensive tool for the identification of iron genes and iron gene neighborhoods in genome and metagenome assemblies. *Frontiers in Microbiology*, 37.
- García-Angulo, V. A. (2017). Overlapping riboflavin supply pathways in bacteria. *Critical Reviews in Microbiology*, 43(2), 196–209.
- Gołębiewski, M., & Tretyn, A. (2020). Generating amplicon reads for microbial community assessment with next-generation sequencing. *Journal of applied microbiology*, 128(2), 330–354.
- Goodenough, U., & Roth, R. (2021). Lichen 5. Medullary and bacterial biofilm layers. *Algal Research*, 58, 102333.
- Greshake Tzovaras, B., Segers, F. H., Bicker, A., Dal Grande, F., Otte, J., Anvar, S. Y., ... & Ebersberger, I. (2020). What is in *Umbilicaria pustulata*? A metagenomic approach to reconstruct the holo-genome of a lichen. *Genome Biology and Evolution*, 12(4), 309–324.
- Grewe, F., Ametrano, C., Widhelm, T. J., Leavitt, S., Distefano, I., Polyiam, W., ... & Lumbsch, H. T. (2020). Using target enrichment sequencing to study the higher-level phylogeny of the largest lichen-forming fungi family: Parmeliaceae (Ascomycota). *IMA Fungus*, 11(1), 1–11.
- Grimm, M., Grube, M., Schiefelbein, U., Zühlke, D., Bernhardt, J., & Riedel, K. (2021). The lichens' microbiota, still a mystery?. *Frontiers in Microbiology*, 12, 714.
- Grube, M., & Berg, G. (2009). Microbial consortia of bacteria and fungi with focus on the lichen symbiosis. *Fungal Biology Reviews*, 23(3), 72–85.
- Grube, M., Cernava, T., Soh, J., Fuchs, S., Aschenbrenner, I., Lassek, C., ... & Berg, G. (2015). Exploring functional contexts of symbiotic sustain within lichen-associated bacteria by comparative omics. *The ISME journal*, 9(2), 412–424.

- Gruber-Vodicka, H. R., Seah, B. K., & Pruesse, E. (2020). phyloFlash: rapid small-subunit rRNA profiling and targeted assembly from metagenomes. *Msystems*, 5(5), e00920–20.
- Gu, Z., & Hübschmann, D. (2021). simplifyEnrichment: an R/Bioconductor package for clustering and visualizing functional enrichment results. *bioRxiv*, doi.org/10.1101/2020.10.27.312116.
- Gu, Z., Eils, R., & Schlesner, M. (2016). Complex heatmaps reveal patterns and correlations in multidimensional genomic data. *Bioinformatics*, 32(18), 2847–2849.
- Gu, Z., Gu, L., Eils, R., Schlesner, M., & Brors, B. (2014). Circlize implements and enhances circular visualization in R. *Bioinformatics*, 30(19), 2811–2812.
- Hale Jr, M. E. (1958). Vitamin requirements of three lichen fungi. *Bulletin of the Torrey Botanical Club*, 182–187.
- Harada, J., Mizoguchi, T., Tsukatani, Y., Yokono, M., Tanaka, A., & Tamiaki, H. (2014). Chlorophyllide a oxidoreductase works as one of the divinyl reductases specifically involved in bacteriochlorophyll a biosynthesis. *Journal of Biological Chemistry*, 289(18), 12716–12726.
- Helliwell, K. E., Wheeler, G. L., Leptos, K. C., Goldstein, R. E., & Smith, A. G. (2011). Insights into the evolution of vitamin B12 auxotrophy from sequenced algal genomes. *Molecular Biology and Evolution*, 28(10), 2921–2933.
- Henkel, P. A., Yuzhakova, L. A. (1936). Azotfiksiruyuschie bakterii v lishaynikah [nitrogen-fixing bacteria in lichens]. *Izv Biol Inst Permsk Gos Univ*, 10, 9–10.
- Hodkinson, B. P., & Lutzoni, F. (2009). A microbiotic survey of lichen-associated bacteria reveals a new lineage from the Rhizobiales. *Symbiosis*, 49(3), 163–180.

Hodkinson, B. P., Gottel, N. R., Schadt, C. W., & Lutzoni, F. (2012). Photoautotrophic symbiont and geography are major factors affecting highly structured and diverse bacterial communities in the lichen microbiome. *Environmental Microbiology*, *14*(1), 147–161.

Honegger, R. (1993). Developmental biology of lichens. *New Phytologist*, *125*(4), 659–677.

Honegger, R. (2000). Simon Schwendener (1829–1919) and the dual hypothesis of lichens. *The Bryologist*, *103*(2), 307–313.

Husnik, F., Tashyreva, D., Boscaro, V., George, E. E., Lukeš, J., & Keeling, P. J. (2021). Bacterial and archaeal symbioses with protists. *Current Biology*, *31*(13), R862–R877.

Iskina, R. E. (1938). K voprosu ob azotfiksiruyushchikh bakteriyakh v lishaynikakh (On the question of nitrogen-fixing bacteria in lichens). *Izvestiya Permskogo Nauchno-Issledovatel'skogo Instituta*, *11*, 133–140.

Jaffe, A. L., Konno, M., Kawasaki, Y., Kataoka, C., Béjà, O., Kandori, H., ... & Banfield, J. F. (2022). Saccharibacteria harness light energy using Type-1 rhodopsins that may rely on retinal sourced from microbial hosts. *The ISME Journal*, 1–4.

Jiang, D. F., Wang, H. Y., Si, H. L., Zhao, L., Liu, C. P., & Zhang, H. (2017). Isolation and culture of lichen bacteriobionts. *The Lichenologist*, *49*(2), 175–181.

Jiang, X., Zerfaß, C., Feng, S., Eichmann, R., Asally, M., Schäfer, P., & Soyer, O. S. (2018). Impact of spatial organization on a novel auxotrophic interaction among soil microbes. *The ISME journal*, *12*(6), 1443–1456.

Jousset, A., Bienhold, C., Chatzinotas, A., Gallien, L., Gobet, A., Kurm, V., ... & Hol, W. H. (2017). Where less may be more: how the rare biosphere pulls ecosystems strings. *The ISME journal*, *11*(4), 853–862.

- Kanehisa, M., Goto, S., Kawashima, S., & Nakaya, A. (2002). The KEGG databases at GenomeNet. *Nucleic Acids Research*, *30*(1), 42–46.
- Kang, D. D., Li, F., Kirton, E., Thomas, A., Egan, R., An, H., & Wang, Z. (2019). MetaBAT 2: an adaptive binning algorithm for robust and efficient genome reconstruction from metagenome assemblies. *PeerJ*, *7*, e7359.
- Karunakaran, R., Ebert, K., Harvey, S., Leonard, M. E., Ramachandran, V., & Poole, P. S. (2006). Thiamine is synthesized by a salvage pathway in *Rhizobium leguminosarum* bv. viciae strain 3841. *Journal of Bacteriology*, *188*(18), 6661–6668.
- Keepers, K. G. (2021). *Harnessing Genomic and Bioinformatic Tools to Inform Conservation Decisions of Species that Are Vulnerable to Human-Driven Impacts of Climate Change* (Doctoral dissertation, University of Colorado at Boulder).
- Kielak, A. M., Barreto, C. C., Kowalchuk, G. A., Van Veen, J. A., & Kuramae, E. E. (2016). The ecology of Acidobacteria: moving beyond genes and genomes. *Frontiers in Microbiology*, *7*, 744.
- Kielak, A. M., Castellane, T. C., Campanharo, J. C., Colnago, L. A., Costa, O. Y., Corradi da Silva, M. L., ... & Kuramae, E. E. (2017). Characterization of novel Acidobacteria exopolysaccharides with potential industrial and ecological applications. *Scientific Reports*, *7*(1), 1–11.
- Klindworth, A., Pruesse, E., Schweer, T., Peplies, J., Quast, C., Horn, M., & Glöckner, F. O. (2013). Evaluation of general 16S ribosomal RNA gene PCR primers for classical and next-generation sequencing-based diversity studies. *Nucleic Acids Research*, *41*(1), e1.

- Leiva, D., Fernández-Mendoza, F., Acevedo, J., Carú, M., Grube, M., & Orlando, J. (2021). The bacterial community of the foliose macro-lichen *Peltigera frigida* is more than a mere extension of the microbiota of the subjacent substrate. *Microbial Ecology*, *81*(4), 965–976.
- Lendemer, J. C., Keepers, K. G., Tripp, E. A., Pogoda, C. S., McCain, C. M., & Kane, N. C. (2019). A taxonomically broad metagenomic survey of 339 species spanning 57 families suggests cystobasidiomycete yeasts are not ubiquitous across all lichens. *American Journal of Botany*, *106*(8), 1090–1095.
- Letunic, I., & Bork, P. (2007). Interactive Tree Of Life (iTOL): an online tool for phylogenetic tree display and annotation. *Bioinformatics*, *23*(1), 127–128.
- Li, H., & Durbin, R. (2009). Fast and accurate short read alignment with Burrows–Wheeler transform. *Bioinformatics*, *25*(14), 1754–1760.
- Liba, C. M., Ferrara, F. I. D. S., Manfio, G. P., Fantinatti-Garboggini, F., Albuquerque, R. C., Pavan, C., ... & Barbosa, H. R. (2006). Nitrogen-fixing chemo-organotrophic bacteria isolated from cyanobacteria-deprived lichens and their ability to solubilize phosphate and to release amino acids and phytohormones. *Journal of Applied Microbiology*, *101*(5), 1076–1086.
- Louca, S., Parfrey, L. W., & Doebeli, M. (2016). Decoupling function and taxonomy in the global ocean microbiome. *Science*, *353*(6305), 1272–1277.
- McCutcheon, J. P., McDonald, B. R., & Moran, N. A. (2009). Convergent evolution of metabolic roles in bacterial co-symbionts of insects. *Proceedings of the National Academy of Sciences*, *106*(36), 15394–15399.

- McDonald, T. R., Mueller, O., Dietrich, F. S., & Lutzoni, F. (2013). High-throughput genome sequencing of lichenizing fungi to assess gene loss in the ammonium transporter/ammonia permease gene family. *BMC Genomics*, *14*(1), 1–14.
- Millbank, J. W., & Kershaw, K. A. (1970). Nitrogen metabolism in lichens: III. Nitrogen fixation by internal cephalodia in *Lobaria pulmonaria*. *New Phytologist*, *69*(2), 595–597.
- Murali, A., Bhargava, A., & Wright, E. S. (2018). IDTAXA: a novel approach for accurate taxonomic classification of microbiome sequences. *Microbiome*, *6*(1), 1–14.
- Nguyen, L. T., Schmidt, H. A., Von Haeseler, A., & Minh, B. Q. (2015). IQ-TREE: a fast and effective stochastic algorithm for estimating maximum-likelihood phylogenies. *Molecular Biology and Evolution*, *32*(1), 268–274.
- Noh, H. J., Baek, K., Hwang, C. Y., Shin, S. C., Hong, S. G., & Lee, Y. M. (2019). *Lichenihabitans psoromatis* gen. nov., sp. nov., a member of a novel lineage (Lichenihabitantaceae fam. nov.) within the order of Rhizobiales isolated from Antarctic lichen. *International Journal of Systematic and Evolutionary Microbiology*, *69*(12), 3837–3842.
- Nurk, S., Meleshko, D., Korobeynikov, A., & Pevzner, P. A. (2017). metaSPAdes: a new versatile metagenomic assembler. *Genome Research*, *27*(5), 824–834.
- Oksanen, J., Blanchet, F. G., Friendly, M., Kindt, R., Legendre, P., McGlinn, D., Minchin, P. R., O'Hara, R. B., Simpson, G. L., Solymos, P., Stevens, M. H. H., Szoecs E., Wagner, H. (2020). vegan: Community Ecology Package. R package version 2.5-7. <https://CRAN.R-project.org/package=vegan>

- Olm, M. R., Brown, C. T., Brooks, B., & Banfield, J. F. (2017). dRep: a tool for fast and accurate genomic comparisons that enables improved genome recovery from metagenomes through de-replication. *The ISME journal*, *11*(12), 2864–2868.
- Overmann, J., Abt, B., & Sikorski, J. (2017). Present and future of culturing bacteria. *Annual Review of Microbiology*, *71*, 711–730.
- Pankratov, T. A., Grouzdev, D. S., Patutina, E. O., Kolganova, T. V., Suzina, N. E., & Berestovskaya, J. J. (2020). *Lichenibacterium ramalinae* gen. nov, sp. nov., *Lichenibacterium minor* sp. nov., the first endophytic, beta-carotene producing bacterial representatives from lichen thalli and the proposal of the new family Lichenibacteriaceae within the order Rhizobiales. *Antonie van Leeuwenhoek*, *113*(4), 477–489.
- Pankratov, T. A., Nikitin, P. A., & Patutina, E. O. (2022). Genome Analysis of Two Lichen Bacteriobionts, *Lichenibacterium ramalinae* and *Lichenibacterium minor*: Toxin–Antitoxin Systems and Secretion Proteins. *Microbiology*, *91*(2), 160–172.
- Pankratov, T. A., Serkebaeva, Y. M., Kulichevskaya, I. S., Liesack, W., & Dedysh, S. N. (2008). Substrate-induced growth and isolation of Acidobacteria from acidic *Sphagnum* peat. *The ISME Journal*, *2*(5), 551–560.
- Paradis, E., & Schliep, K. (2019). ape 5.0: an environment for modern phylogenetics and evolutionary analyses in R. *Bioinformatics*, *35*(3), 526–528.
- Parks, D. H., Imelfort, M., Skennerton, C. T., Hugenholtz, P., & Tyson, G. W. (2015). CheckM: assessing the quality of microbial genomes recovered from isolates, single cells, and metagenomes. *Genome Research*, *25*(7), 1043–1055.
- R Core Team (2013). R: A language and environment for statistical computing.

- Resl, P., Bujold, A. R., Tagirdzhanova, G., Meidl, P., Freire Rallo, S., Kono, M., ... & Spribille, T. (2022). Large differences in carbohydrate degradation and transport potential among lichen fungal symbionts. *Nature Communications*, *13*(1), 1–13.
- Revell, L. J. (2012). phytools: An R package for phylogenetic comparative biology (and other things). *Methods Ecol. Evol.*, *3*, 217–223.
- Richardson, D. H. S., & Smith, D. C. (1968). Lichen physiology: X. The isolated algal and fungal symbionts of *Xanthoria aureola*. *New Phytologist*, *67*(1), 69–77.
- Saary, P., Mitchell, A. L., & Finn, R. D. (2020). Estimating the quality of eukaryotic genomes recovered from metagenomic analysis with EukCC. *Genome Biology*, *21*(1), 1–21.
- Schliep, K. P. (2011). phangorn: phylogenetic analysis in R. *Bioinformatics*, *27*(4), 592–593.
- Schneider, T., Schmid, E., de Castro Jr, J. V., Cardinale, M., Eberl, L., Grube, M., ... & Riedel, K. (2011). Structure and function of the symbiosis partners of the lung lichen (*Lobaria pulmonaria* L. Hoffm.) analyzed by metaproteomics. *Proteomics*, *11*(13), 2752–2756.
- Schwendener, S. (1869). *Die algentypen der Flechtengonidien*. C. Schultze.
- Seemann, T. (2014). Prokka: rapid prokaryotic genome annotation. *Bioinformatics*, *30*(14), 2068–2069.
- Seppey, M., Manni, M., & Zdobnov, E. M. (2019). BUSCO: assessing genome assembly and annotation completeness. In *Gene prediction* (pp. 227-245). Humana, New York, NY.
- Spribille, T., Resl, P., Stanton, D. E., & Tagirdzhanova, G. (2022). Evolutionary biology of lichen symbioses. *New Phytologist*, *234*(5), 1566–1582.

- Spribille, T., Tagirdzhanova, G., Goyette, S., Tuovinen, V., Case, R., & Zandberg, W. F. (2020). 3D biofilms: in search of the polysaccharides holding together lichen symbioses. *FEMS Microbiology Letters*, *367*(5), fnaa023.
- Spribille, T., Tuovinen, V., Resl, P., Vanderpool, D., Wolinski, H., Aime, M. C., ... & McCutcheon, J. P. (2016). Basidiomycete yeasts in the cortex of ascomycete macrolichens. *Science*, *353*(6298), 488–492.
- Tagirdzhanova, G., Saary, P., Tingley, J. P., Díaz-Escandón, D., Abbott, D. W., Finn, R. D., & Spribille, T. (2021). Predicted input of uncultured fungal symbionts to a lichen symbiosis from metagenome-assembled genomes. *Genome Biology and Evolution*, *13*(4), evab047.
- Tang, K., Liu, Y., Zeng, Y., Feng, F., Jin, K., & Yuan, B. (2021a). An Aerobic Anoxygenic Phototrophic Bacterium Fixes CO₂ via the Calvin-Benson-Bassham Cycle. *bioRxiv*.
- Tang, K., Yuan, B., Jia, L., Pan, X., Feng, F., & Jin, K. (2021b). Spatial and temporal distribution of aerobic anoxygenic phototrophic bacteria: key functional groups in biological soil crusts. *Environmental Microbiology*, *23*(7), 3554–3567.
- Taş, N., de Jong, A. E., Li, Y., Trubl, G., Xue, Y., & Dove, N. C. (2021). Metagenomic tools in microbial ecology research. *Current Opinion in Biotechnology*, *67*, 184–191.
- Tuovinen, V., Ekman, S., Thor, G., Vanderpool, D., Spribille, T., & Johannesson, H. (2019). Two basidiomycete fungi in the cortex of wolf lichens. *Current Biology*, *29*(3), 476–483.
- Uritskiy, G. V., DiRuggiero, J., & Taylor, J. (2018). MetaWRAP—a flexible pipeline for genome-resolved metagenomic data analysis. *Microbiome*, *6*(1), 1–13.
- Volpiano, C. G., Sant’Anna, F. H., Ambrosini, A., de São José, J. F. B., Beneduzi, A., Whitman, W. B., ... & Passaglia, L. M. P. (2021). Genomic metrics applied to Rhizobiales

(Hyphomicrobiales): species reclassification, identification of unauthentic genomes and false type strains. *Frontiers in Microbiology*, 12, 614957.

von Meijenfeldt, F. A., Arkhipova, K., Cambuy, D. D., Coutinho, F. H., & Dutilh, B. E. (2019). Robust taxonomic classification of uncharted microbial sequences and bins with CAT and BAT. *Genome Biology*, 20(1), 1–14.

Wang, L. G., Lam, T. T. Y., Xu, S., Dai, Z., Zhou, L., Feng, T., ... & Yu, G. (2020a). Treeio: an R package for phylogenetic tree input and output with richly annotated and associated data. *Molecular Biology and Evolution*, 37(2), 599–603.

Wang, S., Meade, A., Lam, H. M., & Luo, H. (2020b). Evolutionary timeline and genomic plasticity underlying the lifestyle diversity in Rhizobiales. *Msystems*, 5(4), e00438–20.

West, N. J., Parrot, D., Fayet, C., Grube, M., Tomasi, S., & Suzuki, M. T. (2018). Marine cyanolichens from different littoral zones are associated with distinct bacterial communities. *PeerJ*, 6, e5208.

Wickham, H. (2016) ggplot2: Elegant Graphics for Data Analysis. Springer-Verlag New York.

Wickham, H. & Girlich, M. (2022). tidy: Tidy Messy Data. R package version 1.2.0.

<https://CRAN.R-project.org/package=tidy>

Wickham, H. & Seidel, D. (2020). scales: Scale Functions for Visualization. R package version 1.1.1. <https://CRAN.R-project.org/package=scales>

Wickham, H., François, R., Henry, L., & Müller, K. (2018). Dplyr: A grammar of data manipulation (R package v1.0.8). <https://CRAN.R-project.org/package=dplyr>

Wohlfahrt, G., Amelynck, C., Ammann, C., Arneth, A., Bamberger, I., Goldstein, A. H., ... & Schoon, N. (2015). An ecosystem-scale perspective of the net land methanol flux: synthesis of

micrometeorological flux measurements. *Atmospheric Chemistry and Physics*, 15(13), 7413–7427.

Wright, E. S. (2016). Using DECIPHER v2. 0 to analyze big biological sequence data in R. *R J.*, 8(1), 352.

Yurkov, V. V., & Beatty, J. T. (1998). Aerobic anoxygenic phototrophic bacteria. *Microbiology and Molecular Biology Reviews*, 62(3), 695–724.

Yurkov, V., & Csotonyi, J. T. (2009). New light on aerobic anoxygenic phototrophs. In *The purple phototrophic bacteria* (pp. 31–55). Springer, Dordrecht.

Zaheer, R., Noyes, N., Polo, R. O., Cook, S. R., Marinier, E., Van Domselaar, G., ... & McAllister, T. A. (2018). Impact of sequencing depth on the characterization of the microbiome and resistome. *Scientific Reports*, 8(1), 1–11.

Zoccarato, L., Sher, D., Miki, T., Segrè, D., & Grossart, H. P. (2022). A comparative whole-genome approach identifies bacterial traits for marine microbial interactions. *Communications Biology*, 5(1), 1–13.

Table 4.1. Metagenomic data used in the analysis.

Lichen	Reference	Produced by	Metagenome ID	Fungal partner order
<i>Acarospora aff. strigata</i>	Resl et al. 2022. Nature Communications, 13, 2634	Spribille Lab, University of Alberta	T1882	Acarosporales
<i>Hypocenomyce scalaris</i>	Resl et al. 2022. Nature Communications, 13, 2634	Spribille Lab, University of Alberta	T1881	Umbilicariales
<i>Bachmanniomyces S44760</i>	Resl et al. 2022. Nature Communications, 13, 2634	Spribille Lab, University of Alberta	T1894	Ostropomycetidae ins. ced.
<i>Lignoscripta atroalba</i>	Resl et al. 2022. Nature Communications, 13, 2634	Spribille Lab, University of Alberta	T1887	Baeomycetales
<i>Loxospora cismonica</i>	Resl et al. 2022. Nature Communications, 13, 2634	Spribille Lab, University of Alberta	X13	Sarrameanales
<i>Mycoblastus sanguinarius</i>	Resl et al. 2022. Nature Communications, 13, 2634	Spribille Lab, University of Alberta	T1914	Lecanorales
<i>Ptychographa xylographoides</i>	Resl et al. 2022. Nature Communications, 13, 2634	Spribille Lab, University of Alberta	T1868	Baeomycetales
<i>Puttea exsequens</i>	Resl et al. 2022. Nature Communications, 13, 2634	Spribille Lab, University of Alberta	T1888	Lecanorales
<i>Schaereria dolodes</i>	Resl et al. 2022. Nature Communications, 13, 2634	Spribille Lab, University of Alberta	X15	Schaereriales
<i>Thelotrema lepadinum</i>	Resl et al. 2022. Nature Communications, 13, 2634	Spribille Lab, University of Alberta	T1916	Gyalectales
<i>Toensbergia leucococca</i>	Resl et al. 2022. Nature Communications, 13, 2634	Spribille Lab, University of Alberta	T1904	Rhizocarpales
<i>Varicellaria rhodocarpa</i>	Resl et al. 2022. Nature Communications, 13, 2634	Spribille Lab, University of Alberta	T1912	Pertusariales
<i>Xylographa carneopallida</i>	Resl et al. 2022. Nature Communications, 13, 2634	Spribille Lab, University of Alberta	T1889	Baeomycetales
<i>Xylographa vitiligo</i>	Resl et al. 2022. Nature Communications, 13, 2634	Spribille Lab, University of Alberta	T1867	Baeomycetales

<i>Gomphillus americanus</i>	Tagirdzhanova et al. 2021. Molecular ecology, 30(17), 4155-4159	Spribille Lab, University of Alberta	GTX0158	Gyalectales
<i>Alectoria fallacina</i>	Tagirdzhanova et al. 2021. Molecular ecology, 30(17), 4155-4159	Spribille Lab, University of Alberta	GTX0161	Lecanorales
<i>Heterodermia speciosa</i>	Tagirdzhanova et al. 2021. Molecular ecology, 30(17), 4155-4159	Spribille Lab, University of Alberta	GTX0163	Caliciales
<i>Imshaugia aleurites</i>	Tagirdzhanova et al. 2021. Molecular ecology, 30(17), 4155-4159	Spribille Lab, University of Alberta	TS1974	Lecanorales
<i>Xanthoparmelia neocumberlandia</i>	Smith et al. 2020. Symbiosis, 82(1), 133-147	Brigham Young University	SRR12240174	Lecanorales
<i>Xanthoparmelia aff.chlorochroa</i>	Smith et al. 2020. Symbiosis, 82(1), 133-147	Brigham Young University	SRR12240180	Lecanorales
<i>Physciella chloantha</i>	Smith et al. 2020. Symbiosis, 82(1), 133-147	Brigham Young University	SRR12240182	Caliciales
<i>Mobergia calculiformis</i>	Smith et al. 2020. Symbiosis, 82(1), 133-147	Brigham Young University	SRR12240185	Caliciales
<i>Physcia biziana</i>	Smith et al. 2020. Symbiosis, 82(1), 133-147	Brigham Young University	SRR12240183	Caliciales
<i>Peltigera malacea</i>	Cornet et al. 2021. Molecular Phylogenetics and Evolution, 162, 107100	Sequenced in University of Iowa, Submitted by University of Liege	SRR11456913	Peltigerales
<i>Peltigera extenuata</i>	Cornet et al. 2021. Molecular Phylogenetics and Evolution, 162, 107100	Sequenced in University of Iowa, Submitted by University of Liege	SRR11456914	Peltigerales
<i>Peltigera aphthosa</i>	Cornet et al. 2021. Molecular Phylogenetics and Evolution, 162, 107100	Sequenced in University of Iowa, Submitted by University of Liege	SRR11456915	Peltigerales
<i>Peltigera phyllidiosa</i>	Cornet et al. 2021. Molecular Phylogenetics and Evolution, 162, 107100	Sequenced in Duke University, Submitted by University of Liege	SRR11456917	Peltigerales
<i>Solorina crocea</i>	Cornet et al. 2021. Molecular Phylogenetics and Evolution, 162, 107100	Sequenced in Duke University, Submitted by University of Liege	SRR11456919	Peltigerales

<i>Peltigera evansiana</i>	Cornet et al. 2021. Molecular Phylogenetics and Evolution, 162, 107100	Sequenced in University of Iowa, Submitted by University of Liege	SRR11456921	Peltigerales
<i>Letharia lupina</i>	Tuovinen et al. 2019. Current Biology, 29(3), 476-483	Uppsala University	SRR7232214	Lecanorales
<i>Letharia columbiana</i>	Tuovinen et al. 2019. Current Biology, 29(3), 476-483	Uppsala University	SRR7232213	Lecanorales
<i>Letharia rugosa</i>	Tuovinen et al. 2019. Current Biology, 29(3), 476-483	Uppsala University	SRR7232212	Lecanorales
<i>Letharia vulpina</i>	Tuovinen et al. 2019. Current Biology, 29(3), 476-483	Uppsala University	SRR7232211	Lecanorales
<i>Evernia prunastri</i>	Meiser et al. 2017. Scientific Reports, 7, 14881	Senckenberg Biodiversity and Climate Research Centre	SRR5808930	Lecanorales
<i>Pseudevernia furfuracea</i>	Meiser et al. 2017. Scientific Reports, 7, 14881	Senckenberg Biodiversity and Climate Research Centre	SRR5808932	Lecanorales
<i>Arthonia susa</i>	Lendemmer et al. 2019. American Journal of Botany, 106(8), 1090-1095	University of Colorado, Boulder	SRR13685140	Arthoniales
<i>Opegrapha vulgata</i>	Lendemmer et al. 2019. American Journal of Botany, 106(8), 1090-1095	University of Colorado, Boulder	SRR13685142	Arthoniales
<i>Lecanora cinereofusca</i>	Lendemmer et al. 2019. American Journal of Botany, 106(8), 1090-1095	University of Colorado, Boulder	SRR13685153	Lecanorales
<i>Gomphillus americanus</i>	Lendemmer et al. 2019. American Journal of Botany, 106(8), 1090-1095	University of Colorado, Boulder	SRR13685154	Gyalectales
<i>Phyllopsora corallina</i>	Lendemmer et al. 2019. American Journal of Botany, 106(8), 1090-1095	University of Colorado, Boulder	SRR13685157	Lecanorales
<i>Phlyctis boliviensis</i>	Lendemmer et al. 2019. American Journal of Botany, 106(8), 1090-1095	University of Colorado, Boulder	SRR13685158	Gyalectales
<i>Icmadophila ericetorum</i>	Lendemmer et al. 2019. American Journal of Botany, 106(8), 1090-1095	University of Colorado, Boulder	SRR13685159	Pertusariales
<i>Heterodermia casarettiana</i>	Lendemmer et al. 2019. American Journal of Botany, 106(8), 1090-1095	University of Colorado, Boulder	SRR13685161	Caliciales
<i>Usnea subfusca</i>	Lendemmer et al. 2019. American Journal of Botany, 106(8), 1090-1095	University of Colorado, Boulder	SRR13685162	Lecanorales

<i>Menegazzia subsimilis</i>	Lendemer et al. 2019. American Journal of Botany, 106(8), 1090-1095	University of Colorado, Boulder	SRR13685163	Lecanorales
<i>Usnea ceratina</i>	Lendemer et al. 2019. American Journal of Botany, 106(8), 1090-1095	University of Colorado, Boulder	SRR13685164	Lecanorales
<i>Usnea cornuta</i>	Lendemer et al. 2019. American Journal of Botany, 106(8), 1090-1095	University of Colorado, Boulder	SRR13685165	Lecanorales
<i>Enchylium coccophorum</i>	Lendemer et al. 2019. American Journal of Botany, 106(8), 1090-1095	University of Colorado, Boulder	SRR14721921	Peltigerales
<i>Heterodermia albicans</i>	Lendemer et al. 2019. American Journal of Botany, 106(8), 1090-1095	University of Colorado, Boulder	SRR14721922	Caliciales
<i>Acanthothecis fontana</i>	Lendemer et al. 2019. American Journal of Botany, 106(8), 1090-1095	University of Colorado, Boulder	SRR14721923	Gyalectales
<i>Placidium arboreum</i>	Lendemer et al. 2019. American Journal of Botany, 106(8), 1090-1095	University of Colorado, Boulder	SRR14721924	Verrucariales
<i>Heterodermia speciosa</i>	Lendemer et al. 2019. American Journal of Botany, 106(8), 1090-1095	University of Colorado, Boulder	SRR14721925	Caliciales
<i>Buellia mamillana</i>	Lendemer et al. 2019. American Journal of Botany, 106(8), 1090-1095	University of Colorado, Boulder	SRR14721926	Caliciales
<i>Crespoa crozalsiana</i>	Lendemer et al. 2019. American Journal of Botany, 106(8), 1090-1095	University of Colorado, Boulder	SRR14721927	Lecanorales
<i>Leptogium hirsutum</i>	Lendemer et al. 2019. American Journal of Botany, 106(8), 1090-1095	University of Colorado, Boulder	SRR14721928	Peltigerales
<i>Buellia stillingiana</i>	Lendemer et al. 2019. American Journal of Botany, 106(8), 1090-1095	University of Colorado, Boulder	SRR14721929	Caliciales
<i>Leptogium corticola</i>	Lendemer et al. 2019. American Journal of Botany, 106(8), 1090-1095	University of Colorado, Boulder	SRR14721930	Peltigerales
<i>Phaeophyscia rubropulchra</i>	Lendemer et al. 2019. American Journal of Botany, 106(8), 1090-1095	University of Colorado, Boulder	SRR14721931	Caliciales
<i>Thelotrema subtile</i>	Lendemer et al. 2019. American Journal of Botany, 106(8), 1090-1095	University of Colorado, Boulder	SRR14721932	Gyalectales
<i>Bathelium carolinianum</i>	Lendemer et al. 2019. American Journal of Botany, 106(8), 1090-1095	University of Colorado, Boulder	SRR14721933	Strigulales

<i>Sporodophoron americanum</i>	Lendemer et al. 2019. American Journal of Botany, 106(8), 1090-1095	University of Colorado, Boulder	SRR14721934	Arthoniales
<i>Parmotrema submarginale</i>	Lendemer et al. 2019. American Journal of Botany, 106(8), 1090-1095	University of Colorado, Boulder	SRR14721935	Lecanorales
<i>Cladonia peziziformis</i>	Lendemer et al. 2019. American Journal of Botany, 106(8), 1090-1095	University of Colorado, Boulder	SRR14721936	Lecanorales
<i>Dermatocarpon luridum</i>	Lendemer et al. 2019. American Journal of Botany, 106(8), 1090-1095	University of Colorado, Boulder	SRR14721937	Verrucariales
<i>Anaptychia palmatula</i>	Lendemer et al. 2019. American Journal of Botany, 106(8), 1090-1095	University of Colorado, Boulder	SRR14721938	Caliciales
<i>Cladonia polycarpoides</i>	Lendemer et al. 2019. American Journal of Botany, 106(8), 1090-1095	University of Colorado, Boulder	SRR14721939	Lecanorales
<i>Porpidia subsimplex</i>	Lendemer et al. 2019. American Journal of Botany, 106(8), 1090-1095	University of Colorado, Boulder	SRR14721941	Lecideales
<i>Bulbothrix scortella</i>	Lendemer et al. 2019. American Journal of Botany, 106(8), 1090-1095	University of Colorado, Boulder	SRR14721942	Lecanorales
<i>Parmotrema neotropicum</i>	Lendemer et al. 2019. American Journal of Botany, 106(8), 1090-1095	University of Colorado, Boulder	SRR14721943	Lecanorales
<i>Pyrrhospora varians</i>	Lendemer et al. 2019. American Journal of Botany, 106(8), 1090-1095	University of Colorado, Boulder	SRR14721944	Lecanorales
<i>Trapelia placodioides</i>	Lendemer et al. 2019. American Journal of Botany, 106(8), 1090-1095	University of Colorado, Boulder	SRR14721945	Baeomycetales
<i>Thelotrema defectum</i>	Lendemer et al. 2019. American Journal of Botany, 106(8), 1090-1095	University of Colorado, Boulder	SRR14721946	Gyalectales
<i>Usnea mutabilis</i>	Lendemer et al. 2019. American Journal of Botany, 106(8), 1090-1095	University of Colorado, Boulder	SRR14721947	Lecanorales
<i>Porpidia albocaerulescens</i>	Lendemer et al. 2019. American Journal of Botany, 106(8), 1090-1095	University of Colorado, Boulder	SRR14721948	Lecideales
<i>Buellia spuria</i>	Lendemer et al. 2019. American Journal of Botany, 106(8), 1090-1095	University of Colorado, Boulder	SRR14721949	Caliciales
<i>Pseudosagedia chlorotica</i>	Lendemer et al. 2019. American Journal of Botany, 106(8), 1090-1095	University of Colorado, Boulder	SRR14721950	Gyalectales

<i>Cladonia ochrochlora</i>	Lendemer et al. 2019. American Journal of Botany, 106(8), 1090-1095	University of Colorado, Boulder	SRR14721952	Lecanorales
<i>Pannaria tavaresii</i>	Lendemer et al. 2019. American Journal of Botany, 106(8), 1090-1095	University of Colorado, Boulder	SRR14721953	Peltigerales
<i>Collema furfuraceum</i>	Lendemer et al. 2019. American Journal of Botany, 106(8), 1090-1095	University of Colorado, Boulder	SRR14721954	Peltigerales
<i>Halecania pepegospora</i>	Lendemer et al. 2019. American Journal of Botany, 106(8), 1090-1095	University of Colorado, Boulder	SRR14721955	Leprocaulales
<i>Parmotrema ultralucens</i>	Lendemer et al. 2019. American Journal of Botany, 106(8), 1090-1095	University of Colorado, Boulder	SRR14721956	Lecanorales
<i>Ephebe solida</i>	Lendemer et al. 2019. American Journal of Botany, 106(8), 1090-1095	University of Colorado, Boulder	SRR14721957	Lichinales
<i>Dibaeis absoluta</i>	Lendemer et al. 2019. American Journal of Botany, 106(8), 1090-1095	University of Colorado, Boulder	SRR14721958	Pertusariales
<i>Ionaspis lacustris</i>	Lendemer et al. 2019. American Journal of Botany, 106(8), 1090-1095	University of Colorado, Boulder	SRR14721959	Baeomycetales
<i>Phyllopsora corallina</i>	Lendemer et al. 2019. American Journal of Botany, 106(8), 1090-1095	University of Colorado, Boulder	SRR14721960	Lecanorales
<i>Dermatocarpon muhlenbergii</i>	Lendemer et al. 2019. American Journal of Botany, 106(8), 1090-1095	University of Colorado, Boulder	SRR14721961	Verrucariales
<i>Ramalina petrina</i>	Lendemer et al. 2019. American Journal of Botany, 106(8), 1090-1095	University of Colorado, Boulder	SRR14721962	Lecanorales
<i>Phyllopsora parvifolia</i>	Lendemer et al. 2019. American Journal of Botany, 106(8), 1090-1095	University of Colorado, Boulder	SRR14721964	Lecanorales
<i>Cladonia petrophila</i>	Lendemer et al. 2019. American Journal of Botany, 106(8), 1090-1095	University of Colorado, Boulder	SRR14721965	Lecanorales
<i>Opegrapha moroziana</i>	Lendemer et al. 2019. American Journal of Botany, 106(8), 1090-1095	University of Colorado, Boulder	SRR14721966	Arthoniales
<i>Phaeophyscia adiastrata</i>	Lendemer et al. 2019. American Journal of Botany, 106(8), 1090-1095	University of Colorado, Boulder	SRR14721967	Caliciales
<i>Botryolepraria lesdainii</i>	Lendemer et al. 2019. American Journal of Botany, 106(8), 1090-1095	University of Colorado, Boulder	SRR14721968	Verrucariales

<i>Chrysothrix onokoensis</i>	Lendemer et al. 2019. American Journal of Botany, 106(8), 1090-1095	University of Colorado, Boulder	SRR14721969	Arthoniales
<i>Leucodecton sp.</i>	Lendemer et al. 2019. American Journal of Botany, 106(8), 1090-1095	University of Colorado, Boulder	SRR14721970	Gyalectales
<i>Tripp_6156_NY-2796959</i>	Lendemer et al. 2019. American Journal of Botany, 106(8), 1090-1095	University of Colorado, Boulder	SRR14721971	Gyalectales
<i>Porina heterospora</i>	Lendemer et al. 2019. American Journal of Botany, 106(8), 1090-1095	University of Colorado, Boulder	SRR14721972	Peltigerales
<i>Sticta carolinensis</i>	Lendemer et al. 2019. American Journal of Botany, 106(8), 1090-1095	University of Colorado, Boulder	SRR14721973	Gyalectales
<i>Fissurina insidiosa</i>	Lendemer et al. 2019. American Journal of Botany, 106(8), 1090-1095	University of Colorado, Boulder	SRR14721974	Lecanorales
<i>Hypotrachyna catawbiensis</i>	Lendemer et al. 2019. American Journal of Botany, 106(8), 1090-1095	University of Colorado, Boulder	SRR14721975	Peltigerales
<i>Leptogium cyanescens</i>	Lendemer et al. 2019. American Journal of Botany, 106(8), 1090-1095	University of Colorado, Boulder	SRR14721976	Gyalectales
<i>Porina scabrida</i>	Lendemer et al. 2019. American Journal of Botany, 106(8), 1090-1095	University of Colorado, Boulder	SRR14721977	Gyalectales
<i>Pseudosagedia cestrensis</i>	Lendemer et al. 2019. American Journal of Botany, 106(8), 1090-1095	University of Colorado, Boulder	SRR14721978	Arthoniales
<i>Arthonia rubella</i>	Lendemer et al. 2019. American Journal of Botany, 106(8), 1090-1095	University of Colorado, Boulder	SRR14721979	Lecanorales
<i>Parmotrema tinctorum</i>	Lendemer et al. 2019. American Journal of Botany, 106(8), 1090-1095	University of Colorado, Boulder	SRR14721980	Pertusariales
<i>Aspicilia laevata</i>	Lendemer et al. 2019. American Journal of Botany, 106(8), 1090-1095	University of Colorado, Boulder	SRR14721981	Caliciales
<i>Pyxine albovirens</i>	Lendemer et al. 2019. American Journal of Botany, 106(8), 1090-1095	University of Colorado, Boulder	SRR14721982	NA
<i>funga sp.</i>	Lendemer et al. 2019. American Journal of Botany, 106(8), 1090-1095	University of Colorado, Boulder	SRR14721983	Gyalectales
<i>Lendemer_49042_NY-3033146</i>	Lendemer et al. 2019. American Journal of Botany, 106(8), 1090-1095	University of Colorado, Boulder	SRR14721984	Pertusariales
<i>Gyalecta farlowii</i>	Lendemer et al. 2019. American Journal of Botany, 106(8), 1090-1095	University of Colorado, Boulder		
<i>Pertusaria plittiana</i>	Lendemer et al. 2019. American Journal of Botany, 106(8), 1090-1095	University of Colorado, Boulder		

<i>Imshaugia aleurites</i>	Lendemer et al. 2019. American Journal of Botany, 106(8), 1090-1095	University of Colorado, Boulder	SRR14721985	Lecanorales
<i>Dirinaria frostii</i>	Lendemer et al. 2019. American Journal of Botany, 106(8), 1090-1095	University of Colorado, Boulder	SRR14721986	Caliciales
<i>Lecanora subimmergens</i>	Lendemer et al. 2019. American Journal of Botany, 106(8), 1090-1095	University of Colorado, Boulder	SRR14721987	Lecanorales
<i>Chrysothrix xanthina</i>	Lendemer et al. 2019. American Journal of Botany, 106(8), 1090-1095	University of Colorado, Boulder	SRR14721988	Arthoniales
<i>Heterodermia granulifera</i>	Lendemer et al. 2019. American Journal of Botany, 106(8), 1090-1095	University of Colorado, Boulder	SRR14721989	Caliciales
<i>Pyxine soorediata</i>	Lendemer et al. 2019. American Journal of Botany, 106(8), 1090-1095	University of Colorado, Boulder	SRR14721990	Caliciales
<i>Rinodina dolichospora</i>	Lendemer et al. 2019. American Journal of Botany, 106(8), 1090-1095	University of Colorado, Boulder	SRR14721991	Caliciales
<i>Flavoparmelia baltimorensis fungal sp.</i>	Lendemer et al. 2019. American Journal of Botany, 106(8), 1090-1095	University of Colorado, Boulder	SRR14721992	Lecanorales
<i>Lendemer_48835_NY-3720155</i>	Lendemer et al. 2019. American Journal of Botany, 106(8), 1090-1095	University of Colorado, Boulder	SRR14721993	NA
<i>Bacidia sp.</i>				
<i>Lendemer_48883_NY-3033306</i>	Lendemer et al. 2019. American Journal of Botany, 106(8), 1090-1095	University of Colorado, Boulder	SRR14721994	Lecanorales
<i>Lepra amara</i>	Lendemer et al. 2019. American Journal of Botany, 106(8), 1090-1095	University of Colorado, Boulder	SRR14721995	Pertusariales
<i>Hypogymnia vittata</i>	Lendemer et al. 2019. American Journal of Botany, 106(8), 1090-1095	University of Colorado, Boulder	SRR14721996	Lecanorales
<i>Parmotrema simulans</i>	Lendemer et al. 2019. American Journal of Botany, 106(8), 1090-1095	University of Colorado, Boulder	SRR14721997	Lecanorales
<i>Lepraria normandinoidea</i>	Lendemer et al. 2019. American Journal of Botany, 106(8), 1090-1095	University of Colorado, Boulder	SRR14721998	Lecanorales
<i>Ochrolechia trochophora</i>	Lendemer et al. 2019. American Journal of Botany, 106(8), 1090-1095	University of Colorado, Boulder	SRR14721999	Pertusariales

<i>Parmotrema mellissii</i>	Lendemer et al. 2019. American Journal of Botany, 106(8), 1090-1095	University of Colorado, Boulder	SRR14722000	Lecanorales
<i>Bacidia soorediata</i>	Lendemer et al. 2019. American Journal of Botany, 106(8), 1090-1095	University of Colorado, Boulder	SRR14722001	Lecanorales
<i>Hypotrachyna lividescens</i>	Lendemer et al. 2019. American Journal of Botany, 106(8), 1090-1095	University of Colorado, Boulder	SRR14722002	Lecanorales
<i>Ramalina culbersoniorum</i>	Lendemer et al. 2019. American Journal of Botany, 106(8), 1090-1095	University of Colorado, Boulder	SRR14722003	Lecanorales
<i>Cetrelia chicitae</i>	Lendemer et al. 2019. American Journal of Botany, 106(8), 1090-1095	University of Colorado, Boulder	SRR14722004	Lecanorales
<i>Heterodermia neglecta</i>	Lendemer et al. 2019. American Journal of Botany, 106(8), 1090-1095	University of Colorado, Boulder	SRR14722005	Caliciales
<i>Cetrelia olivetorum</i>	Lendemer et al. 2019. American Journal of Botany, 106(8), 1090-1095	University of Colorado, Boulder	SRR14722006	Lecanorales
<i>Platismatia glauca</i>	Lendemer et al. 2019. American Journal of Botany, 106(8), 1090-1095	University of Colorado, Boulder	SRR14722007	Lecanorales
<i>Sticta fragilinata</i>	Lendemer et al. 2019. American Journal of Botany, 106(8), 1090-1095	University of Colorado, Boulder	SRR14722008	Peltigerales
<i>Cladonia apodocarpa</i>	Lendemer et al. 2019. American Journal of Botany, 106(8), 1090-1095	University of Colorado, Boulder	SRR14722009	Lecanorales
<i>Pertusaria propinqua</i>	Lendemer et al. 2019. American Journal of Botany, 106(8), 1090-1095	University of Colorado, Boulder	SRR14722010	Pertusariales
<i>Biatora longispora</i>	Lendemer et al. 2019. American Journal of Botany, 106(8), 1090-1095	University of Colorado, Boulder	SRR14722011	Lecanorales
<i>Stictis urceolatum</i>	Lendemer et al. 2019. American Journal of Botany, 106(8), 1090-1095	University of Colorado, Boulder	SRR14722012	Ostropales
<i>Biatora pontica</i>	Lendemer et al. 2019. American Journal of Botany, 106(8), 1090-1095	University of Colorado, Boulder	SRR14722013	Lecanorales
<i>Hypotrachyna minarum</i>	Lendemer et al. 2019. American Journal of Botany, 106(8), 1090-1095	University of Colorado, Boulder	SRR14722014	Lecanorales
<i>Leptogium corticola</i>	Lendemer et al. 2019. American Journal of Botany, 106(8), 1090-1095	University of Colorado, Boulder	SRR14722015	Peltigerales

<i>Umbilicaria mammulata</i>	Lendemer et al. 2019. American Journal of Botany, 106(8), 1090-1095	University of Colorado, Boulder	SRR14722016	Umbilicariales
<i>Heterodermia squamulosa</i>	Lendemer et al. 2019. American Journal of Botany, 106(8), 1090-1095	University of Colorado, Boulder	SRR14722017	Caliciales
<i>Lepraria oxybapha</i>	Lendemer et al. 2019. American Journal of Botany, 106(8), 1090-1095	University of Colorado, Boulder	SRR14722018	Lecanorales
<i>Dendriscocaulon intricatulum</i>	Lendemer et al. 2019. American Journal of Botany, 106(8), 1090-1095	University of Colorado, Boulder	SRR14722019	Peltigerales
<i>Parmotrema crinitum</i>	Lendemer et al. 2019. American Journal of Botany, 106(8), 1090-1095	University of Colorado, Boulder	SRR14722020	Lecanorales
<i>Parmotrema perlatum</i>	Lendemer et al. 2019. American Journal of Botany, 106(8), 1090-1095	University of Colorado, Boulder	SRR14722021	Lecanorales
<i>Usnea subgracilis</i>	Lendemer et al. 2019. American Journal of Botany, 106(8), 1090-1095	University of Colorado, Boulder	SRR14722022	Lecanorales
<i>Usnea ceratina</i>	Lendemer et al. 2019. American Journal of Botany, 106(8), 1090-1095	University of Colorado, Boulder	SRR14722023	Lecanorales
<i>Dermiscellum oulocheilum</i>	Lendemer et al. 2019. American Journal of Botany, 106(8), 1090-1095	University of Colorado, Boulder	SRR14722024	Caliciales
<i>Enchylimum conglomeratum</i>	Lendemer et al. 2019. American Journal of Botany, 106(8), 1090-1095	University of Colorado, Boulder	SRR14722025	Peltigerales
<i>Tuckermannopsis ciliaris</i>	Lendemer et al. 2019. American Journal of Botany, 106(8), 1090-1095	University of Colorado, Boulder	SRR14722026	Lecanorales
<i>Parmotrema reticulatum</i>	Lendemer et al. 2019. American Journal of Botany, 106(8), 1090-1095	University of Colorado, Boulder	SRR14722028	Lecanorales
<i>Arthonia kermesina</i>	Lendemer et al. 2019. American Journal of Botany, 106(8), 1090-1095	University of Colorado, Boulder	SRR14722029	Arthoniales
<i>Parmelia squarrosa</i>	Lendemer et al. 2019. American Journal of Botany, 106(8), 1090-1095	University of Colorado, Boulder	SRR14722030	Lecanorales
<i>Ramalina americana</i>	Lendemer et al. 2019. American Journal of Botany, 106(8), 1090-1095	University of Colorado, Boulder	SRR14722031	Lecanorales
<i>Platismatia tuckermanii</i>	Lendemer et al. 2019. American Journal of Botany, 106(8), 1090-1095	University of Colorado, Boulder	SRR14722032	Lecanorales

<i>Lecanora pseudistera</i>	Lendemer et al. 2019. American Journal of Botany, 106(8), 1090-1095	University of Colorado, Boulder	SRR14722033	Lecanorales
<i>Lepraria caesiella</i>	Lendemer et al. 2019. American Journal of Botany, 106(8), 1090-1095	University of Colorado, Boulder	SRR14722034	Lecanorales
<i>Melanohalea halei</i>	Lendemer et al. 2019. American Journal of Botany, 106(8), 1090-1095	University of Colorado, Boulder	SRR14722035	Lecanorales
<i>Phaeophyscia hispidula</i>	Lendemer et al. 2019. American Journal of Botany, 106(8), 1090-1095	University of Colorado, Boulder	SRR14722036	Caliciales
<i>Phlyctis speirea</i>	Lendemer et al. 2019. American Journal of Botany, 106(8), 1090-1095	University of Colorado, Boulder	SRR14722037	Gyalectales
<i>Flavopunctelia flaventior</i>	Lendemer et al. 2019. American Journal of Botany, 106(8), 1090-1095	University of Colorado, Boulder	SRR14722038	Lecanorales
<i>Trapeliopsis flexuosa</i>	Lendemer et al. 2019. American Journal of Botany, 106(8), 1090-1095	University of Colorado, Boulder	SRR14722039	Baeomycetales
<i>Arthonia kermesina</i>	Lendemer et al. 2019. American Journal of Botany, 106(8), 1090-1095	University of Colorado, Boulder	SRR14722040	Arthoniales
<i>Stereocaulon dactylophyllum</i>	Lendemer et al. 2019. American Journal of Botany, 106(8), 1090-1095	University of Colorado, Boulder	SRR14722041	Lecanorales
<i>Scoliciosporum umbrinum</i>	Lendemer et al. 2019. American Journal of Botany, 106(8), 1090-1095	University of Colorado, Boulder	SRR14722042	Lecanorales
<i>Rinodina tephraeaspis</i>	Lendemer et al. 2019. American Journal of Botany, 106(8), 1090-1095	University of Colorado, Boulder	SRR14722043	Caliciales
<i>Rinodina chrysiidiata</i>	Lendemer et al. 2019. American Journal of Botany, 106(8), 1090-1095	University of Colorado, Boulder	SRR14722044	Caliciales
<i>Rinodina ascociscana</i>	Lendemer et al. 2019. American Journal of Botany, 106(8), 1090-1095	University of Colorado, Boulder	SRR14722045	Caliciales
<i>Rhizocarpon geographicum</i>	Lendemer et al. 2019. American Journal of Botany, 106(8), 1090-1095	University of Colorado, Boulder	SRR14722046	Rhizocarpales
<i>Heterodermia leucomelaena</i>	Lendemer et al. 2019. American Journal of Botany, 106(8), 1090-1095	University of Colorado, Boulder	SRR14722047	Caliciales
<i>Pyrenula subelliptica</i>	Lendemer et al. 2019. American Journal of Botany, 106(8), 1090-1095	University of Colorado, Boulder	SRR14722048	Pyrenulales

<i>Porpidia macrocarpa</i>	Lendemer et al. 2019. American Journal of Botany, 106(8), 1090-1095	University of Colorado, Boulder	SRR14722049	Lecideales
<i>Porpidia crustulata</i>	Lendemer et al. 2019. American Journal of Botany, 106(8), 1090-1095	University of Colorado, Boulder	SRR14722050	Lecideales
<i>Xylographa trunciseda</i>	Lendemer et al. 2019. American Journal of Botany, 106(8), 1090-1095	University of Colorado, Boulder	SRR14722051	Baeomycetales
<i>Physconia leucoleiptes</i>	Lendemer et al. 2019. American Journal of Botany, 106(8), 1090-1095	University of Colorado, Boulder	SRR14722052	Caliciales
<i>Phlyctis boliviensis</i>	Lendemer et al. 2019. American Journal of Botany, 106(8), 1090-1095	University of Colorado, Boulder	SRR14722053	Gyalectales
<i>Phaeophyscia rubropulchra</i>	Lendemer et al. 2019. American Journal of Botany, 106(8), 1090-1095	University of Colorado, Boulder	SRR14722054	Caliciales
<i>Pertusaria rubefacta</i>	Lendemer et al. 2019. American Journal of Botany, 106(8), 1090-1095	University of Colorado, Boulder	SRR14722055	Pertusariales
<i>Pertusaria plittiana</i>	Lendemer et al. 2019. American Journal of Botany, 106(8), 1090-1095	University of Colorado, Boulder	SRR14722056	Pertusariales
<i>Cladonia squamosa</i>	Lendemer et al. 2019. American Journal of Botany, 106(8), 1090-1095	University of Colorado, Boulder	SRR14722057	Lecanorales
<i>Umbilicaria mammulata</i>	Lendemer et al. 2019. American Journal of Botany, 106(8), 1090-1095	University of Colorado, Boulder	SRR14722058	Umbilicariales
<i>Tuckermannopsis ciliaris</i>	Lendemer et al. 2019. American Journal of Botany, 106(8), 1090-1095	University of Colorado, Boulder	SRR14722059	Lecanorales
<i>Nigrovothelium tropicum</i>	Lendemer et al. 2019. American Journal of Botany, 106(8), 1090-1095	University of Colorado, Boulder	SRR14722060	Trypetheliales
<i>Pyrenula pseudobufonia</i>	Lendemer et al. 2019. American Journal of Botany, 106(8), 1090-1095	University of Colorado, Boulder	SRR14722061	Pyrenulales
<i>Fuscopannaria leucosticta</i>	Lendemer et al. 2019. American Journal of Botany, 106(8), 1090-1095	University of Colorado, Boulder	SRR14722062	Peltigerales
<i>Parmelia squarrosa</i>	Lendemer et al. 2019. American Journal of Botany, 106(8), 1090-1095	University of Colorado, Boulder	SRR14722063	Lecanorales
<i>Porpidia contraponenda</i>	Lendemer et al. 2019. American Journal of Botany, 106(8), 1090-1095	University of Colorado, Boulder	SRR14722064	Lecideales

<i>Polysporina simplex</i>	Lendemer et al. 2019. American Journal of Botany, 106(8), 1090-1095	University of Colorado, Boulder	SRR14722065	Acarosporales
<i>Pilophorus fibula</i>	Lendemer et al. 2019. American Journal of Botany, 106(8), 1090-1095	University of Colorado, Boulder	SRR14722066	Lecanorales
<i>Pertusaria epixantha</i>	Lendemer et al. 2019. American Journal of Botany, 106(8), 1090-1095	University of Colorado, Boulder	SRR14722067	Pertusariales
<i>Parmotrema neotropicum</i>	Lendemer et al. 2019. American Journal of Botany, 106(8), 1090-1095	University of Colorado, Boulder	SRR14722068	Lecanorales
<i>Parmotrema subsidiosum</i>	Lendemer et al. 2019. American Journal of Botany, 106(8), 1090-1095	University of Colorado, Boulder	SRR14722069	Lecanorales
<i>Botryolepraria lesdainii</i>	Lendemer et al. 2019. American Journal of Botany, 106(8), 1090-1095	University of Colorado, Boulder	SRR14722070	Verrucariales
<i>Arthonia cupressina</i>	Lendemer et al. 2019. American Journal of Botany, 106(8), 1090-1095	University of Colorado, Boulder	SRR14722071	Arthoniales
<i>Brigantiaea leucoxantha</i>	Lendemer et al. 2019. American Journal of Botany, 106(8), 1090-1095	University of Colorado, Boulder	SRR14722072	Teloschistales
<i>Parmotrema mellissii</i>	Lendemer et al. 2019. American Journal of Botany, 106(8), 1090-1095	University of Colorado, Boulder	SRR14722073	Lecanorales
<i>Arthothelium spectabile</i>	Lendemer et al. 2019. American Journal of Botany, 106(8), 1090-1095	University of Colorado, Boulder	SRR14722074	Arthoniales
<i>Parmotrema margaritatum</i>	Lendemer et al. 2019. American Journal of Botany, 106(8), 1090-1095	University of Colorado, Boulder	SRR14722075	Lecanorales
<i>Peltigera phyllidiosa</i>	Lendemer et al. 2019. American Journal of Botany, 106(8), 1090-1095	University of Colorado, Boulder	SRR14722076	Peltigerales
<i>Parmotrema reticulatum</i>	Lendemer et al. 2019. American Journal of Botany, 106(8), 1090-1095	University of Colorado, Boulder	SRR14722077	Lecanorales
<i>Lecanora oreinoides</i>	Lendemer et al. 2019. American Journal of Botany, 106(8), 1090-1095	University of Colorado, Boulder	SRR14722078	Lecanorales
<i>Pyrrhospora varians</i>	Lendemer et al. 2019. American Journal of Botany, 106(8), 1090-1095	University of Colorado, Boulder	SRR14722079	Lecanorales
<i>Cladonia didyma</i>	Lendemer et al. 2019. American Journal of Botany, 106(8), 1090-1095	University of Colorado, Boulder	SRR14722080	Lecanorales

<i>Heterodermia appalachiensis</i>	Lendemer et al. 2019. American Journal of Botany, 106(8), 1090-1095	University of Colorado, Boulder	SRR14722081	Caliciales
<i>Cladonia mateocyatha</i>	Lendemer et al. 2019. American Journal of Botany, 106(8), 1090-1095	University of Colorado, Boulder	SRR14722082	Lecanorales
<i>Buellia spuria</i>	Lendemer et al. 2019. American Journal of Botany, 106(8), 1090-1095	University of Colorado, Boulder	SRR14722083	Caliciales
<i>Cladonia squamosa</i>	Lendemer et al. 2019. American Journal of Botany, 106(8), 1090-1095	University of Colorado, Boulder	SRR14722084	Lecanorales
<i>Pseudosagedia raphidosperma fungal sp.</i>	Lendemer et al. 2019. American Journal of Botany, 106(8), 1090-1095	University of Colorado, Boulder	SRR14722085	Gyalectales
<i>Tripp_6058_COLO-L-0051364</i>	Lendemer et al. 2019. American Journal of Botany, 106(8), 1090-1095	University of Colorado, Boulder	SRR14722086	NA
<i>Cladonia stipitata</i>	Lendemer et al. 2019. American Journal of Botany, 106(8), 1090-1095	University of Colorado, Boulder	SRR14722087	Lecanorales
<i>Cladonia uncialis</i>	Lendemer et al. 2019. American Journal of Botany, 106(8), 1090-1095	University of Colorado, Boulder	SRR14722088	Lecanorales
<i>Diploschistes scruposus</i>	Lendemer et al. 2019. American Journal of Botany, 106(8), 1090-1095	University of Colorado, Boulder	SRR14722089	Gyalectales
<i>Acarospora sp.</i>	Lendemer et al. 2019. American Journal of Botany, 106(8), 1090-1095	University of Colorado, Boulder	SRR14722090	Acarosporales
<i>Tripp_6053_NY-2858381</i>	Lendemer et al. 2019. American Journal of Botany, 106(8), 1090-1095	University of Colorado, Boulder	SRR14722091	Verrucariales
<i>Placidium arboreum</i>	Lendemer et al. 2019. American Journal of Botany, 106(8), 1090-1095	University of Colorado, Boulder	SRR14722092	Arthoniales
<i>Chrysothrix susquehannensis</i>	Lendemer et al. 2019. American Journal of Botany, 106(8), 1090-1095	University of Colorado, Boulder	SRR14722093	Gyalectales
<i>Porina scabrada</i>	Lendemer et al. 2019. American Journal of Botany, 106(8), 1090-1095	University of Colorado, Boulder	SRR14722094	Lecanorales
<i>Usnea strigosa</i>	Lendemer et al. 2019. American Journal of Botany, 106(8), 1090-1095	University of Colorado, Boulder	SRR14722095	Umbilicariales
<i>Umbilicaria papulosa</i>	Lendemer et al. 2019. American Journal of Botany, 106(8), 1090-1095	University of Colorado, Boulder	SRR14722096	Gyalectales
<i>Graphis scripta</i>	Lendemer et al. 2019. American Journal of Botany, 106(8), 1090-1095	University of Colorado, Boulder	SRR14722096	Gyalectales

<i>Physcia americana</i>	Lendemer et al. 2019. American Journal of Botany, 106(8), 1090-1095	University of Colorado, Boulder	SRR14722097	Caliciales
<i>Acarospora sinopica</i>	Lendemer et al. 2019. American Journal of Botany, 106(8), 1090-1095	University of Colorado, Boulder	SRR14722098	Acarosporales
<i>Cladonia pyxidata</i>	Lendemer et al. 2019. American Journal of Botany, 106(8), 1090-1095	University of Colorado, Boulder	SRR14722099	Lecanorales
<i>Anisomeridium sp.</i>				
<i>Tripp_6040_COLO-L-0051344</i>	Lendemer et al. 2019. American Journal of Botany, 106(8), 1090-1095	University of Colorado, Boulder	SRR14722100	Monoblastiales
<i>Cladonia strepsilis</i>	Lendemer et al. 2019. American Journal of Botany, 106(8), 1090-1095	University of Colorado, Boulder	SRR14722101	Lecanorales
<i>Solitaria chrysophthalma</i>	Lendemer et al. 2019. American Journal of Botany, 106(8), 1090-1095	University of Colorado, Boulder	SRR14722102	Teloschistales
<i>Cladonia coccifera</i>	Lendemer et al. 2019. American Journal of Botany, 106(8), 1090-1095	University of Colorado, Boulder	SRR14722103	Lecanorales
<i>Parmotrema hypotropum</i>	Lendemer et al. 2019. American Journal of Botany, 106(8), 1090-1095	University of Colorado, Boulder	SRR14722104	Lecanorales
<i>Buellia spuria</i>	Lendemer et al. 2019. American Journal of Botany, 106(8), 1090-1095	University of Colorado, Boulder	SRR14722105	Caliciales
<i>Flavoparmelia baltimorensis</i>	Lendemer et al. 2019. American Journal of Botany, 106(8), 1090-1095	University of Colorado, Boulder	SRR14722106	Lecanorales
<i>Alyxoria varia</i>	Lendemer et al. 2019. American Journal of Botany, 106(8), 1090-1095	University of Colorado, Boulder	SRR14722107	Arthoniales
<i>Parmotrema subsumptum</i>	Lendemer et al. 2019. American Journal of Botany, 106(8), 1090-1095	University of Colorado, Boulder	SRR14722108	Lecanorales
<i>Pertusaria andersoniae</i>	Lendemer et al. 2019. American Journal of Botany, 106(8), 1090-1095	University of Colorado, Boulder	SRR14722109	Pertusariales
<i>Physconia subpallida</i>	Lendemer et al. 2019. American Journal of Botany, 106(8), 1090-1095	University of Colorado, Boulder	SRR14722110	Caliciales
<i>Cystocoleus ebeneus</i>	Lendemer et al. 2019. American Journal of Botany, 106(8), 1090-1095	University of Colorado, Boulder	SRR14722111	Capnodiales

<i>Sticta sp.</i>	Lendemmer et al. 2019. American Journal of Botany, 106(8), 1090-1095	University of Colorado, Boulder	SRR14722112	Peltigerales
<i>Lendemmer_47364_NY-2795562</i>	Lendemmer et al. 2019. American Journal of Botany, 106(8), 1090-1095	University of Colorado, Boulder	SRR14722113	Peltigerales
<i>Nephroma helveticum</i>	Lendemmer et al. 2019. American Journal of Botany, 106(8), 1090-1095	University of Colorado, Boulder	SRR14722114	Lecanorales
<i>Cladonia stipitata</i>	Lendemmer et al. 2019. American Journal of Botany, 106(8), 1090-1095	University of Colorado, Boulder	SRR14722115	Lecanorales
<i>Usnea halei</i>	Lendemmer et al. 2019. American Journal of Botany, 106(8), 1090-1095	University of Colorado, Boulder	SRR14722116	Lecanorales
<i>Usnea subscabrosa</i>	Lendemmer et al. 2019. American Journal of Botany, 106(8), 1090-1095	University of Colorado, Boulder	SRR14722117	Lecanorales
<i>Cladonia mateocyatha</i>	Lendemmer et al. 2019. American Journal of Botany, 106(8), 1090-1095	University of Colorado, Boulder	SRR14722118	Lecanorales
<i>Bryoria tenuis</i>	Lendemmer et al. 2019. American Journal of Botany, 106(8), 1090-1095	University of Colorado, Boulder	SRR14722119	Lecanorales
<i>Cladonia grayi</i>	Lendemmer et al. 2019. American Journal of Botany, 106(8), 1090-1095	University of Colorado, Boulder	SRR14722120	Lecanorales
<i>Usnea merrillii</i>	Lendemmer et al. 2019. American Journal of Botany, 106(8), 1090-1095	University of Colorado, Boulder	SRR14722121	Lecanorales
<i>Cladonia macilenta</i>	Lendemmer et al. 2019. American Journal of Botany, 106(8), 1090-1095	University of Colorado, Boulder	SRR14722122	Pertusariales
<i>Ochrolechia yasudae</i>	Lendemmer et al. 2019. American Journal of Botany, 106(8), 1090-1095	University of Colorado, Boulder	SRR14722123	Lecanorales
<i>Brianaria bauschiana</i>	Lendemmer et al. 2019. American Journal of Botany, 106(8), 1090-1095	University of Colorado, Boulder	SRR14722124	Lecanorales
<i>Melanelia culbersonii</i>	Lendemmer et al. 2019. American Journal of Botany, 106(8), 1090-1095	University of Colorado, Boulder	SRR14722125	Baeomycetales
<i>Ionaspis alba</i>	Lendemmer et al. 2019. American Journal of Botany, 106(8), 1090-1095	University of Colorado, Boulder	SRR14722126	Lecanorales
<i>Biatora chrysantha</i>	Lendemmer et al. 2019. American Journal of Botany, 106(8), 1090-1095	University of Colorado, Boulder	SRR14722127	Lecanorales
<i>Xanthoparmelia mexicana</i>	Lendemmer et al. 2019. American Journal of Botany, 106(8), 1090-1095	University of Colorado, Boulder	SRR14722127	Lecanorales

<i>Lecidella sp.</i>	Lendemer et al. 2019. American Journal of Botany, 106(8), 1090-1095	University of Colorado, Boulder	SRR14722128	Lecanorales
<i>Lendemer_46226_NY-2606722</i>	Lendemer et al. 2019. American Journal of Botany, 106(8), 1090-1095	University of Colorado, Boulder	SRR14722129	Lecanorales
<i>Pseudevernia cladonia</i>	Lendemer et al. 2019. American Journal of Botany, 106(8), 1090-1095	University of Colorado, Boulder	SRR14722130	Lecanorales
<i>Parmotrema hypotropum</i>	Lendemer et al. 2019. American Journal of Botany, 106(8), 1090-1095	University of Colorado, Boulder	SRR14722131	Lecanorales
<i>Parmotrema gardneri</i>	Lendemer et al. 2019. American Journal of Botany, 106(8), 1090-1095	University of Colorado, Boulder	SRR14722132	Lecanorales
<i>Anzia colpodes</i>	Lendemer et al. 2019. American Journal of Botany, 106(8), 1090-1095	University of Colorado, Boulder	SRR14722133	Caliciales
<i>Heterodermia hypoleuca</i>	Lendemer et al. 2019. American Journal of Botany, 106(8), 1090-1095	University of Colorado, Boulder	SRR14722134	Ostropales
<i>Absconditella delutula</i>	Lendemer et al. 2019. American Journal of Botany, 106(8), 1090-1095	University of Colorado, Boulder	SRR14722135	Mycocaliciales
<i>Mycocalicium subtile</i>	Lendemer et al. 2019. American Journal of Botany, 106(8), 1090-1095	University of Colorado, Boulder	SRR14722136	Pertusariales
<i>Pertusaria ostiolata</i>	Lendemer et al. 2019. American Journal of Botany, 106(8), 1090-1095	University of Colorado, Boulder	SRR14722137	Peltigerales
<i>Leptogium hirsutum</i>	Lendemer et al. 2019. American Journal of Botany, 106(8), 1090-1095	University of Colorado, Boulder	SRR14722138	Caliciales
<i>Heterodermia speciosa</i>	Lendemer et al. 2019. American Journal of Botany, 106(8), 1090-1095	University of Colorado, Boulder	SRR14722139	Lecanorales
<i>Parmotrema cetratum</i>	Lendemer et al. 2019. American Journal of Botany, 106(8), 1090-1095	University of Colorado, Boulder	SRR14722140	Lecanorales
<i>Platismatia tuckermanii</i>	Lendemer et al. 2019. American Journal of Botany, 106(8), 1090-1095	University of Colorado, Boulder	SRR14722141	Caliciales
<i>Phaeophyscia squarrosa</i>	Lendemer et al. 2019. American Journal of Botany, 106(8), 1090-1095	University of Colorado, Boulder	SRR14722142	Monoblastiales
<i>Acrocordia megalospora</i>	Lendemer et al. 2019. American Journal of Botany, 106(8), 1090-1095	University of Colorado, Boulder	SRR14722143	Arthoniales
<i>Zwackhia viridis</i>	Lendemer et al. 2019. American Journal of Botany, 106(8), 1090-1095	University of Colorado, Boulder	SRR14722143	Arthoniales

<i>Heterodermia appalachiensis</i>	Lendemer et al. 2019. American Journal of Botany, 106(8), 1090-1095	University of Colorado, Boulder	SRR14722144	Caliciales
<i>Leptogium chloromelum</i>	Lendemer et al. 2019. American Journal of Botany, 106(8), 1090-1095	University of Colorado, Boulder	SRR14722145	Peltigerales
<i>Phaeocalicium polyporaenum</i>	Lendemer et al. 2019. American Journal of Botany, 106(8), 1090-1095	University of Colorado, Boulder	SRR14722146	Mycocaliciales
<i>Byssoloma subdiscordans</i>	Lendemer et al. 2019. American Journal of Botany, 106(8), 1090-1095	University of Colorado, Boulder	SRR14722147	Lecanorales
<i>Peltigera neopolydactyla</i> <i>Peltigera sp.</i>	Lendemer et al. 2019. American Journal of Botany, 106(8), 1090-1095	University of Colorado, Boulder	SRR14722148	Peltigerales
<i>Lendemer_46965_NY-2794668</i>	Lendemer et al. 2019. American Journal of Botany, 106(8), 1090-1095	University of Colorado, Boulder	SRR14722149	Peltigerales
<i>Cladonia arbuscula</i>	Lendemer et al. 2019. American Journal of Botany, 106(8), 1090-1095	University of Colorado, Boulder	SRR14722150	Lecanorales
<i>Usnocetraria oakesiana</i>	Lendemer et al. 2019. American Journal of Botany, 106(8), 1090-1095	University of Colorado, Boulder	SRR14722151	Lecanorales
<i>Micarea neostipitata</i>	Lendemer et al. 2019. American Journal of Botany, 106(8), 1090-1095	University of Colorado, Boulder	SRR14722152	Lecanorales
<i>Sarea resiniae</i>	Lendemer et al. 2019. American Journal of Botany, 106(8), 1090-1095	University of Colorado, Boulder	SRR14722153	NA
<i>Lecanora strobilina</i>	Lendemer et al. 2019. American Journal of Botany, 106(8), 1090-1095	University of Colorado, Boulder	SRR14722154	Lecanorales
<i>Umbilicaria pennsylvanica</i>	Lendemer et al. 2019. American Journal of Botany, 106(8), 1090-1095	University of Colorado, Boulder	SRR14722155	Umbilicariales
<i>Melanelia stygia</i> <i>Lecidea sp.</i>	Lendemer et al. 2019. American Journal of Botany, 106(8), 1090-1095	University of Colorado, Boulder	SRR14722156	Lecanorales
<i>Lendemer_46382_NY-2795264</i>	Lendemer et al. 2019. American Journal of Botany, 106(8), 1090-1095	University of Colorado, Boulder	SRR14722157	Lecideales
<i>Lecanora albella</i>	Lendemer et al. 2019. American Journal of Botany, 106(8), 1090-1095	University of Colorado, Boulder	SRR14722158	Lecanorales

<i>Ochrolechia arborea</i>	Lendemer et al. 2019. American Journal of Botany, 106(8), 1090-1095	University of Colorado, Boulder	SRR14722159	Pertusariales
<i>Herteliana schuyleriana</i>	Lendemer et al. 2019. American Journal of Botany, 106(8), 1090-1095	University of Colorado, Boulder	SRR14722160	Lecanorales
<i>Leptogium austroamericanum</i>	Lendemer et al. 2019. American Journal of Botany, 106(8), 1090-1095	University of Colorado, Boulder	SRR14722161	Peltigerales
<i>Hypogymnia incurvoides</i>	Lendemer et al. 2019. American Journal of Botany, 106(8), 1090-1095	University of Colorado, Boulder	SRR14722162	Lecanorales
<i>Tephromela atra</i>	Lendemer et al. 2019. American Journal of Botany, 106(8), 1090-1095	University of Colorado, Boulder	SRR14722163	Lecanorales
<i>Lecidea tessellata</i>	Lendemer et al. 2019. American Journal of Botany, 106(8), 1090-1095	University of Colorado, Boulder	SRR14722164	Lecideales
<i>Rhizocarpon subgeminatum</i>	Lendemer et al. 2019. American Journal of Botany, 106(8), 1090-1095	University of Colorado, Boulder	SRR14722165	Rhizocarpales
<i>Parmotrema xanthinum</i>	Lendemer et al. 2019. American Journal of Botany, 106(8), 1090-1095	University of Colorado, Boulder	SRR14722166	Lecanorales
<i>Dimelaena oreina</i>	Lendemer et al. 2019. American Journal of Botany, 106(8), 1090-1095	University of Colorado, Boulder	SRR14722167	Caliciales
<i>Parmotrema stuppeum</i>	Lendemer et al. 2019. American Journal of Botany, 106(8), 1090-1095	University of Colorado, Boulder	SRR14722168	Lecanorales
<i>Punctelia appalachiensis</i>	Lendemer et al. 2019. American Journal of Botany, 106(8), 1090-1095	University of Colorado, Boulder	SRR14722169	Lecanorales
<i>Cladonia rangiferina</i>	Lendemer et al. 2019. American Journal of Botany, 106(8), 1090-1095	University of Colorado, Boulder	SRR14722170	Lecanorales
<i>Cladonia uncialis</i>	Lendemer et al. 2019. American Journal of Botany, 106(8), 1090-1095	University of Colorado, Boulder	SRR14722171	Lecanorales
<i>Chrysothrix xanthina</i>	Lendemer et al. 2019. American Journal of Botany, 106(8), 1090-1095	University of Colorado, Boulder	SRR14722172	Arthoniales
<i>Melanohalea halei</i>	Lendemer et al. 2019. American Journal of Botany, 106(8), 1090-1095	University of Colorado, Boulder	SRR14722173	Lecanorales
<i>Parmotrema diffractaicum</i>	Lendemer et al. 2019. American Journal of Botany, 106(8), 1090-1095	University of Colorado, Boulder	SRR14722174	Lecanorales

<i>Nephroma helveticum</i>	Lendemer et al. 2019. American Journal of Botany, 106(8), 1090-1095	University of Colorado, Boulder	SRR14722175	Peltigerales
<i>Xanthocarpia feracissima</i>	Lendemer et al. 2019. American Journal of Botany, 106(8), 1090-1095	University of Colorado, Boulder	SRR14722176	Teloschistales
<i>Biatora appalachensis</i>	Lendemer et al. 2019. American Journal of Botany, 106(8), 1090-1095	University of Colorado, Boulder	SRR14722177	Lecanorales
<i>Schismatomma glaucescens</i>	Lendemer et al. 2019. American Journal of Botany, 106(8), 1090-1095	University of Colorado, Boulder	SRR14722178	Arthoniales
<i>Porina heterospora</i> <i>fungus sp.</i>	Lendemer et al. 2019. American Journal of Botany, 106(8), 1090-1095	University of Colorado, Boulder	SRR14722179	Gyalectales
<i>Lendemer_46730_NY-2794914</i>	Lendemer et al. 2019. American Journal of Botany, 106(8), 1090-1095	University of Colorado, Boulder	SRR14722180	NA
<i>Gomphillus calycioides</i>	Lendemer et al. 2019. American Journal of Botany, 106(8), 1090-1095	University of Colorado, Boulder	SRR14722181	Gyalectales
<i>Chaenotheca balsamconensis</i>	Lendemer et al. 2019. American Journal of Botany, 106(8), 1090-1095	University of Colorado, Boulder	SRR14722182	Coniocybales
<i>Chaenotheca furfuracea</i>	Lendemer et al. 2019. American Journal of Botany, 106(8), 1090-1095	University of Colorado, Boulder	SRR14722183	Coniocybales
<i>Lecanora hybocarpa</i> <i>Mycobilimbia sp.</i>	Lendemer et al. 2019. American Journal of Botany, 106(8), 1090-1095	University of Colorado, Boulder	SRR14722184	Lecanorales
<i>Lendemer_46123_NY-2606825</i>	Lendemer et al. 2019. American Journal of Botany, 106(8), 1090-1095	University of Colorado, Boulder	SRR14722185	Lecideales
<i>Lepra pustulata</i>	Lendemer et al. 2019. American Journal of Botany, 106(8), 1090-1095	University of Colorado, Boulder	SRR14722186	Pertusariales
<i>Lepraria xanthonica</i>	Lendemer et al. 2019. American Journal of Botany, 106(8), 1090-1095	University of Colorado, Boulder	SRR14722187	Lecanorales
<i>Xylographa vitiligo</i>	Lendemer et al. 2019. American Journal of Botany, 106(8), 1090-1095	University of Colorado, Boulder	SRR14722188	Baeomycetales
<i>Bacidia schweinitzii</i>	Lendemer et al. 2019. American Journal of Botany, 106(8), 1090-1095	University of Colorado, Boulder	SRR14722195	Lecanorales

<i>Leptogium corticola</i>	Lendemer et al. 2019. American Journal of Botany, 106(8), 1090-1095	University of Colorado, Boulder	SRR14722197	Peltigerales
<i>Arthonia vinosa</i>	Lendemer et al. 2019. American Journal of Botany, 106(8), 1090-1095	University of Colorado, Boulder	SRR14722200	Arthoniales
<i>Lecidea nylanderii</i>	Lendemer et al. 2019. American Journal of Botany, 106(8), 1090-1095	University of Colorado, Boulder	SRR14722201	Lecanorales
<i>Hypocenomyce scalaris</i>	Lendemer et al. 2019. American Journal of Botany, 106(8), 1090-1095	University of Colorado, Boulder	SRR14722202	Umbilicariales
<i>Ricasolia quercizans</i>	Lendemer et al. 2019. American Journal of Botany, 106(8), 1090-1095	University of Colorado, Boulder	SRR14722208	Peltigerales
<i>Rinodina buckii</i>	Lendemer et al. 2019. American Journal of Botany, 106(8), 1090-1095	University of Colorado, Boulder	SRR14722209	Caliciales
<i>Caloplaca camptidia</i>	Lendemer et al. 2019. American Journal of Botany, 106(8), 1090-1095	University of Colorado, Boulder	SRR14722210	Teloschistales
<i>Pseudosagedia isidiata</i>	Lendemer et al. 2019. American Journal of Botany, 106(8), 1090-1095	University of Colorado, Boulder	SRR14722213	Gyalectales
<i>Buellia vernicoma</i>	Lendemer et al. 2019. American Journal of Botany, 106(8), 1090-1095	University of Colorado, Boulder	SRR14722215	Caliciales
<i>Hypotrachyna sp. JCL-2020a</i>	Lendemer et al. 2019. American Journal of Botany, 106(8), 1090-1095	University of Colorado, Boulder	SRR14722219	Lecanorales
<i>Lecania croatica</i>	Lendemer et al. 2019. American Journal of Botany, 106(8), 1090-1095	University of Colorado, Boulder	SRR14722220	Lecanorales
<i>Megalospora porphyritis</i>	Lendemer et al. 2019. American Journal of Botany, 106(8), 1090-1095	University of Colorado, Boulder	SRR14722221	Teloschistales
<i>Arthonia quintaria</i>	Lendemer et al. 2019. American Journal of Botany, 106(8), 1090-1095	University of Colorado, Boulder	SRR14722222	Arthoniales
<i>Lopadium disciforme</i>	Lendemer et al. 2019. American Journal of Botany, 106(8), 1090-1095	University of Colorado, Boulder	SRR14722225	Lecideales
<i>Lecidea roseotincta</i>	Lendemer et al. 2019. American Journal of Botany, 106(8), 1090-1095	University of Colorado, Boulder	SRR14722229	Lecideales
<i>Coccocarpia palmicola</i>	Lendemer et al. 2019. American Journal of Botany, 106(8), 1090-1095	University of Colorado, Boulder	SRR14722230	Peltigerales

<i>Lecanora masana</i>	Lendemer et al. 2019. American Journal of Botany, 106(8), 1090-1095	University of Colorado, Boulder	SRR14722231	Lecanorales
<i>Lecanora rugosella</i>	Lendemer et al. 2019. American Journal of Botany, 106(8), 1090-1095	University of Colorado, Boulder	SRR14722232	Lecanorales
<i>Arthothelium ruanum</i>	Lendemer et al. 2019. American Journal of Botany, 106(8), 1090-1095	University of Colorado, Boulder	SRR14722233	Arthoniales
<i>Trapelia coarctata</i>	Lendemer et al. 2019. American Journal of Botany, 106(8), 1090-1095	University of Colorado, Boulder	SRR14722251	Baeomycetales
<i>Lepraria leprolomopsis</i>	Lendemer et al. 2019. American Journal of Botany, 106(8), 1090-1095	University of Colorado, Boulder	SRR14722272	Lecanorales
<i>Leprocaulon nicholsiae</i>	Lendemer et al. 2019. American Journal of Botany, 106(8), 1090-1095	University of Colorado, Boulder	SRR14722274	Leprocaulales
<i>Micareopsis irriguata</i>	Lendemer et al. 2019. American Journal of Botany, 106(8), 1090-1095	University of Colorado, Boulder	SRR14722275	Lecanorales
<i>Cystocoleus ebeneus</i>	Lendemer et al. 2019. American Journal of Botany, 106(8), 1090-1095	University of Colorado, Boulder	SRR14722276	Capnodiales
<i>Cladonia furcata</i>	Lendemer et al. 2019. American Journal of Botany, 106(8), 1090-1095	University of Colorado, Boulder	SRR14722277	Lecanorales
<i>Buellia spuria</i>	Lendemer et al. 2019. American Journal of Botany, 106(8), 1090-1095	University of Colorado, Boulder	SRR14722278	Caliciales
<i>Byssoloma meadii</i>	Lendemer et al. 2019. American Journal of Botany, 106(8), 1090-1095	University of Colorado, Boulder	SRR14722279	Lecanorales
<i>Dictyomeridium proponens</i>	Lendemer et al. 2019. American Journal of Botany, 106(8), 1090-1095	University of Colorado, Boulder	SRR14722280	Trypetheliales
<i>Viridothelium virens</i>	Lendemer et al. 2019. American Journal of Botany, 106(8), 1090-1095	University of Colorado, Boulder	SRR14722281	Trypetheliales
<i>Peltigera neckeri</i>	Lendemer et al. 2019. American Journal of Botany, 106(8), 1090-1095	University of Colorado, Boulder	SRR14722282	Peltigerales
<i>Cresponea flava</i>	Lendemer et al. 2019. American Journal of Botany, 106(8), 1090-1095	University of Colorado, Boulder	SRR14722283	Arthoniales
<i>Scytinium dactylinum</i>	Lendemer et al. 2019. American Journal of Botany, 106(8), 1090-1095	University of Colorado, Boulder	SRR14722285	Peltigerales

<i>Micarea peliocarpa</i>	Lendemer et al. 2019. American Journal of Botany, 106(8), 1090-1095	University of Colorado, Boulder	SRR14722286	Lecanorales
<i>Flakea papillata</i>	Lendemer et al. 2019. American Journal of Botany, 106(8), 1090-1095	University of Colorado, Boulder	SRR14722287	Verrucariales
<i>Dibaeis sorediata</i>	Lendemer et al. 2019. American Journal of Botany, 106(8), 1090-1095	University of Colorado, Boulder	SRR14722288	Pertusariales
<i>Parmotrema rampoddense</i>	Lendemer et al. 2019. American Journal of Botany, 106(8), 1090-1095	University of Colorado, Boulder	SRR14722289	Lecanorales
<i>Cladonia robbinsii</i>	Lendemer et al. 2019. American Journal of Botany, 106(8), 1090-1095	University of Colorado, Boulder	SRR14722290	Lecanorales
<i>Tuckermannopsis ciliaris</i>	Lendemer et al. 2019. American Journal of Botany, 106(8), 1090-1095	University of Colorado, Boulder	SRR14722291	Lecanorales
<i>Cladonia rangiferina</i>	Lendemer et al. 2019. American Journal of Botany, 106(8), 1090-1095	University of Colorado, Boulder	SRR14722292	Lecanorales
<i>Cladonia subtenuis</i>	Lendemer et al. 2019. American Journal of Botany, 106(8), 1090-1095	University of Colorado, Boulder	SRR14722293	Lecanorales
<i>Cladonia caroliniana</i>	Lendemer et al. 2019. American Journal of Botany, 106(8), 1090-1095	University of Colorado, Boulder	SRR14722294	Lecanorales
<i>Cladonia ravenelii</i>	Lendemer et al. 2019. American Journal of Botany, 106(8), 1090-1095	University of Colorado, Boulder	SRR14722296	Lecanorales
<i>Gyalideopsis bartramiorum</i>	Lendemer et al. 2019. American Journal of Botany, 106(8), 1090-1095	University of Colorado, Boulder	SRR14722297	Gyalectales
<i>Cladonia subtenuis</i>	Lendemer et al. 2019. American Journal of Botany, 106(8), 1090-1095	University of Colorado, Boulder	SRR14722298	Lecanorales
<i>Cladonia squamosa</i>	Lendemer et al. 2019. American Journal of Botany, 106(8), 1090-1095	University of Colorado, Boulder	SRR14722299	Lecanorales
<i>Punctelia caseana</i>	Lendemer et al. 2019. American Journal of Botany, 106(8), 1090-1095	University of Colorado, Boulder	SRR14722300	Lecanorales
<i>Cladonia leporina</i>	Lendemer et al. 2019. American Journal of Botany, 106(8), 1090-1095	University of Colorado, Boulder	SRR14722301	Lecanorales
<i>Hypotrachyna osseoalba</i>	Lendemer et al. 2019. American Journal of Botany, 106(8), 1090-1095	University of Colorado, Boulder	SRR14722302	Lecanorales

<i>Rinodina brauniana</i>	Lendemer et al. 2019. American Journal of Botany, 106(8), 1090-1095	University of Colorado, Boulder	SRR14722303	Caliciales
<i>Micareopsis irriguata</i>	Lendemer et al. 2019. American Journal of Botany, 106(8), 1090-1095	University of Colorado, Boulder	SRR14722304	Lecanorales
<i>Heterodermia langdoniana</i>	Lendemer et al. 2019. American Journal of Botany, 106(8), 1090-1095	University of Colorado, Boulder	SRR14722305	Caliciales
<i>Placynthium petersii</i>	Lendemer et al. 2019. American Journal of Botany, 106(8), 1090-1095	University of Colorado, Boulder	SRR14722307	Peltigerales
<i>Willeya diffractella</i>	Lendemer et al. 2019. American Journal of Botany, 106(8), 1090-1095	University of Colorado, Boulder	SRR14722308	Verrucariales
<i>Lecanora markjohnstonii</i>	Lendemer et al. 2019. American Journal of Botany, 106(8), 1090-1095	University of Colorado, Boulder	SRR14722309	Lecanorales
<i>Parmotrema austrosinense</i>	Lendemer et al. 2019. American Journal of Botany, 106(8), 1090-1095	University of Colorado, Boulder	SRR14722310	Lecanorales
<i>Phlyctis boliviensis</i>	Lendemer et al. 2019. American Journal of Botany, 106(8), 1090-1095	University of Colorado, Boulder	SRR14722311	Gyalectales
<i>Protoblastenia rupestris</i>	Lendemer et al. 2019. American Journal of Botany, 106(8), 1090-1095	University of Colorado, Boulder	SRR14722312	Lecanorales
<i>Phlyctis petraea</i>	Lendemer et al. 2019. American Journal of Botany, 106(8), 1090-1095	University of Colorado, Boulder	SRR14722313	Gyalectales
<i>Peltigera phyllidiosa</i>	Lendemer et al. 2019. American Journal of Botany, 106(8), 1090-1095	University of Colorado, Boulder	SRR14722314	Peltigerales
<i>Scytinium lichenoides</i>	Lendemer et al. 2019. American Journal of Botany, 106(8), 1090-1095	University of Colorado, Boulder	SRR14722315	Peltigerales
<i>Heterodermia echinata</i>	Lendemer et al. 2019. American Journal of Botany, 106(8), 1090-1095	University of Colorado, Boulder	SRR14722316	Caliciales
<i>Kephartia crystalligera</i>	Lendemer et al. 2019. American Journal of Botany, 106(8), 1090-1095	University of Colorado, Boulder	SRR14722318	Lecideales
<i>Cladonia furcata</i>	Lendemer et al. 2019. American Journal of Botany, 106(8), 1090-1095	University of Colorado, Boulder	SRR14722319	Lecanorales
<i>Peltigera praetextata</i>	Lendemer et al. 2019. American Journal of Botany, 106(8), 1090-1095	University of Colorado, Boulder	SRR14722320	Peltigerales

<i>Bagliettoa baldensis</i>	Lendemer et al. 2019. American Journal of Botany, 106(8), 1090-1095	University of Colorado, Boulder	SRR14722321	Verrucariales
<i>Trentepohlia sp.</i>	Lendemer et al. 2019. American Journal of Botany, 106(8), 1090-1095	University of Colorado, Boulder	SRR14722322	NA
<i>Tripp_6417_NY-2796640</i>	Lendemer et al. 2019. American Journal of Botany, 106(8), 1090-1095	University of Colorado, Boulder	SRR14722322	NA
<i>Nadvornikia soredata</i>	Lendemer et al. 2019. American Journal of Botany, 106(8), 1090-1095	University of Colorado, Boulder	SRR14722323	Gyalectales
<i>Lepraria disjuncta</i>	Lendemer et al. 2019. American Journal of Botany, 106(8), 1090-1095	University of Colorado, Boulder	SRR14722324	Lecanorales
<i>Parmotrema internexum</i>	Lendemer et al. 2019. American Journal of Botany, 106(8), 1090-1095	University of Colorado, Boulder	SRR14722325	Lecanorales
<i>Parmotrema arnoldii</i>	Lendemer et al. 2019. American Journal of Botany, 106(8), 1090-1095	University of Colorado, Boulder	SRR14722326	Lecanorales
<i>Catillaria lenticularis</i>	Lendemer et al. 2019. American Journal of Botany, 106(8), 1090-1095	University of Colorado, Boulder	SRR14722327	Lecanorales
<i>Parmotrema cetratum</i>	Lendemer et al. 2019. American Journal of Botany, 106(8), 1090-1095	University of Colorado, Boulder	SRR14722329	Lecanorales
<i>Pertusaria obruta</i>	Lendemer et al. 2019. American Journal of Botany, 106(8), 1090-1095	University of Colorado, Boulder	SRR14722330	Pertusariales
<i>Peltigera dolichorhiza</i>	Cornet et al. 2021. Molecular Phylogenetics and Evolution, 162, 107100	Sequenced in University of Iowa, Submitted by University of Liege	SRR11456918	Peltigerales
<i>Peltigera hydrothyria</i>	Cornet et al. 2021. Molecular Phylogenetics and Evolution, 162, 107100	Sequenced in University of Iowa, Submitted by University of Liege	SRR11456922	Peltigerales
<i>Peltigera hydrothyria</i>	Cornet et al. 2021. Molecular Phylogenetics and Evolution, 162, 107100	Sequenced in University of Iowa, Submitted by University of Liege	SRR11456923	Peltigerales
<i>Xanthoparmelia neocumberlandia</i>	Smith et al. 2020. Symbiosis, 82(1), 133-147	Brigham Young University	SRR12240175	Lecanorales
<i>Xanthoparmelia maricopensis</i>	Smith et al. 2020. Symbiosis, 82(1), 133-147	Brigham Young University	SRR12240177	Lecanorales
<i>Xanthoparmelia aff plittii</i>	Smith et al. 2020. Symbiosis, 82(1), 133-147	Brigham Young University	SRR12240178	Lecanorales

<i>Xanthoparmelia aff mexicana</i>	Smith et al. 2020. Symbiosis, 82(1), 133-147	Brigham Young University	SRR12240179	Lecanorales
<i>Rinodina sp</i>	Smith et al. 2020. Symbiosis, 82(1), 133-147	Brigham Young University	SRR12240181	Caliciales
<i>Oxnerella safavidiorum</i>	Smith et al. 2020. Symbiosis, 82(1), 133-147	Brigham Young University	SRR12240184	Caliciales
<i>Xanthoparmelia aff chlorochroa</i>	Smith et al. 2020. Symbiosis, 82(1), 133-147	Brigham Young University	SRR12240187	Lecanorales
<i>Xanthoparmelia aff chlorochroa</i>	Smith et al. 2020. Symbiosis, 82(1), 133-147	Brigham Young University Spribille Lab, University of Alberta	SRR12240188	Lecanorales
<i>Protousnea poeppigii</i>	This study	Spribille Lab, University of Alberta	X1	Lecanorales
<i>Usnea cavernosa</i>	This study	Spribille Lab, University of Alberta	X2	Lecanorales
<i>Platismatia glauca</i>	This study	Spribille Lab, University of Alberta	X3	Lecanorales
<i>Pecteniam plumbea</i>	This study	Spribille Lab, University of Alberta	X4	Peltigerales
<i>Pecteniam cyanoloma</i>	This study	Spribille Lab, University of Alberta	X5	Peltigerales
<i>Protousnea magellanica</i>	This study	Spribille Lab, University of Alberta	X7	Lecanorales
<i>Ramalina thrausta</i>	This study	Spribille Lab, University of Alberta	X8	Lecanorales
<i>Evernia divaricata</i>	This study	Spribille Lab, University of Alberta	X9	Lecanorales
<i>Sulcaria badia</i>	This study	Spribille Lab, University of Alberta	X10	Lecanorales
<i>Ramalina menziesii</i>	This study	Spribille Lab, University of Alberta	X11	Lecanorales
<i>Alectoria sarmentosa</i>	Tagirdzhanova et al. 2021. Genome biology and evolution, 13(4), evab047	Spribille Lab, University of Alberta	X12	Lecanorales

<i>Hypogymnia physodes</i>	This study	Spribille Lab, University of Alberta	X14	Lecanorales
<i>Umbilicaria americana</i>	This study	Spribille Lab, University of Alberta	X16	Umbilicariales
<i>Pseudophebe minuscula</i>	This study	Spribille Lab, University of Alberta	VT22	Lecanorales
<i>Bryoria fremontii</i>	This study	Spribille Lab, University of Alberta	VT31	Lecanorales
<i>Platismatia glauca</i>	This study	Spribille Lab, University of Alberta	VT1	Lecanorales
<i>Gypsoplaca macrophylla</i>	This study	Spribille Lab, University of Alberta	VT34	Lecanorales
<i>Punctelia caseana</i>	This study	Spribille Lab, University of Alberta	VT16	Lecanorales
<i>Kaernefeltia merillii</i>	This study	Spribille Lab, University of Alberta	VT12	Lecanorales
<i>Vulpicida juniperina</i>	This study	Spribille Lab, University of Alberta	VT2	Lecanorales
<i>Allantoparmelia sp</i>	This study	Spribille Lab, University of Alberta	VT33	Lecanorales
<i>Flavocetraria cucullata</i>	This study	Spribille Lab, University of Alberta	VT15	Lecanorales
<i>Cornicularia normoerica</i>	This study	Spribille Lab, University of Alberta	VT38	Lecanorales
<i>Evernia mesomorpha</i>	This study	Spribille Lab, University of Alberta	VT26	Lecanorales
<i>Alectoria ochroleuca</i>	This study	Spribille Lab, University of Alberta	VT19	Lecanorales
<i>Xanthoparmelia aff chlorochroa</i>	Grewe et al 2020. IMA fungus, 11, 27	Field Museum of Natural History	SRR13167197	Lecanorales
<i>Xanthoparmelia verrucella</i>	Grewe et al 2020. IMA fungus, 11, 27	Field Museum of Natural History	SRR13126859	Lecanorales

<i>Xanthoparmelia tasmanica</i>	Grewe et al 2020. IMA fungus, 11, 27	Field Museum of Natural History	SRR13126828	Lecanorales
<i>Xanthoparmelia stenophylla</i>	Grewe et al 2020. IMA fungus, 11, 27	Field Museum of Natural History	SRR13126796	Lecanorales
<i>Xanthoparmelia barbatica</i>	Grewe et al 2020. IMA fungus, 11, 27	Field Museum of Natural History	SRR13126647	Lecanorales
<i>Xanthoparmelia arapilensis</i>	Grewe et al 2020. IMA fungus, 11, 27	Field Museum of Natural History	SRR13125985	Lecanorales
<i>Usnea aurantiacoatra</i>	Grewe et al 2020. IMA fungus, 11, 27	Field Museum of Natural History	SRR13125762	Lecanorales
<i>Everniopsis trulla</i>	Grewe et al 2020. IMA fungus, 11, 27	Field Museum of Natural History	SRR13125477	Lecanorales
<i>Lobaria pulmonaria</i>	Wicaksono et al 2020. Microbiology Resource Announcements, 9(38), e00622-20	GRAZ UNIVERSITY OF TECHNOLOGY	ERR4179390	Peltigerales
<i>Peltigera polydactylon</i>	Wicaksono et al 2020. Microbiology Resource Announcements, 9(38), e00622-20	GRAZ UNIVERSITY OF TECHNOLOGY	ERR4179391	Peltigerales
<i>Cladonia furcata</i>	Wicaksono et al 2020. Microbiology Resource Announcements, 9(38), e00622-20	GRAZ UNIVERSITY OF TECHNOLOGY	ERR4179389	Lecanorales
<i>Lasallia pustulata</i>	Greshake et al 2016. Molecular Ecology Resources, 16(2), 511-523	Goethe University	SRR2387885	Umbilicariales
<i>Physcia stellaris</i>	McDonald et al 2013. Bmc Genomics, 14, 225	Duke University	SRR1532736	Caliciales
<i>Peltula cylindrica</i>	McDonald et al 2013. Bmc Genomics, 14, 225	Duke University	SRR1531569	Lichinales
<i>Leptogium austroamericanum</i>	McDonald et al 2013. Bmc Genomics, 14, 225	Duke University	SRR1531545	Peltigerales
<i>Dibaeis baeomyces</i>	McDonald et al 2013. Bmc Genomics, 14, 225	Duke University	SRR1531517	Pertusariales

Table 4.2. Details on the metagenomes generated de novo for this study.

Lichen	Metagenome ID	Isolate Number	Country	Library prep kit	Sequencing platform
<i>Protousnea poeppigii</i>	X1	T1828-1830 (pooled)	Argentina	TruSeq DNA Library Prep Kit	HiSeq 2500
<i>Usnea cavernosa</i>	X2	T1842-1845 (pooled)	Canada	TruSeq DNA Library Prep Kit	HiSeq 2500
<i>Platismatia glauca</i>	X3	Genome extraction 1-8 (TS, Missoula)	USA	TruSeq DNA Library Prep Kit	HiSeq 2500
<i>Pecteniam plumbea</i>	X4	T1813	Norway	TruSeq DNA Library Prep Kit	HiSeq 2500
<i>Pecteniam cyanoloma</i>	X5	T1812	Norway	TruSeq DNA Library Prep Kit	HiSeq 2500
<i>Protousnea magellanica</i>	X7	T1831-1833 (pooled)	Argentina	TruSeq DNA Library Prep Kit	HiSeq 2500
<i>Ramalina thrausta</i>	X8	Rthr3 (Missoula)	Canada	TruSeq DNA Library Prep Kit	HiSeq 2500
<i>Evernia divaricata</i>	X9	T1838-1839 (pooled)	Canada	TruSeq DNA Library Prep Kit	HiSeq 2500
<i>Sulcaria badia</i>	X10	T1826-1827 (pooled)	USA	TruSeq DNA Library Prep Kit	HiSeq 2500
<i>Ramalina menziesii</i>	X11	T1816	USA	TruSeq DNA Library Prep Kit	HiSeq 2500
<i>Hypogymnia physodes</i>	X14	T1820	USA	TruSeq DNA Library Prep Kit	HiSeq 2500
<i>Umbilicaria americana</i>	X16	T1834-1835	USA	TruSeq DNA Library Prep Kit	HiSeq 2500
<i>Platismatia glauca</i>	VT1	LID1	Canada	NEBNext Ultra II	HiSeq X
<i>Kaernefeltia merrillii</i>	VT12	LID12	Canada	NEBNext Ultra II	HiSeq X
<i>Flavocetraria cucullata</i>	VT15	LID15	Canada	NEBNext Ultra II	HiSeq X
<i>Punctelia caseana</i>	VT16	LID16	Canada	NEBNext Ultra II	HiSeq X
<i>Alectoria ochroleuca</i>	VT19	LID19	Canada	NEBNext Ultra II	HiSeq X
<i>Vulpicida juniperina</i>	VT2	LID2	Canada	NEBNext Ultra II	HiSeq X
<i>Pseudophebe minuscula</i>	VT22	LID22	Canada	NEBNext Ultra II	HiSeq X
<i>Evernia mesomorpha</i>	VT26	LID26	Canada	NEBNext Ultra II	HiSeq X
<i>Bryoria fremontii</i>	VT31	LID31	Canada	NEBNext Ultra II	HiSeq X
<i>Allantoparmelia sp</i>	VT33	LID33	Canada	NEBNext Ultra II	HiSeq X
<i>Gypsoplaca macrophylla</i>	VT34	LID34	Canada	NEBNext Ultra II	HiSeq X
<i>Cornicularia normoerica</i>	VT38	LID38	Austria	NEBNext Ultra II	HiSeq X

Table 4.3. Metagenomes derived from potentially misidentified samples.

Metagenomes in this list had inconsistencies between their metadata and the taxonomy of the main fungal partner as estimated from the phylogenomic tree. These metagenomes were excluded from the occurrence analysis.

Metagenome ID	Species as listed in the metadata	Reason for exclusion
SRR14722032	<i>Platismatia tuckermanii</i>	grouped with <i>Ochrolechia/Pertusaria/Lepra</i>
SRR14722092	<i>Chrysothrix susquehannensis</i>	grouped with <i>Trapeliopsis/Gomphillus</i>
SRR14722327	<i>Catillaria lenticularis</i>	grouped with <i>Leprocaulon</i>
SRR14722303	<i>Rinodina brauniana</i>	grouped with <i>Lecanora</i>
SRR14722033	<i>Lecanora pseudistera</i>	grouped with Parmeliaceae
SRR14722324	<i>Lepraria disjuncta</i>	groupes with <i>Leprocaulon</i>
SRR14722131	<i>Parmotrema gardneri</i>	grouped with <i>Thelotrema</i>
SRR14722208	<i>Ricasolia quercizans</i>	grouped with Parmeliaceae
SRR14722229	<i>Lecidea roseotincta</i>	grouped with <i>Lecanora</i>
SRR14722034	<i>Lepraria caesiella</i>	grouped with Parmeliaceae
SRR14722085	<i>Pseudosagedia rhapsidosperma</i>	grouped with Theloschistales
SRR14722185	<i>Mycobilimbia sp. Lendemmer_46123_NY-2606825</i>	groups with <i>Byssoloma</i>
SRR14722222	<i>Arthonia quintaria</i>	grouped with Eurotiomycetes
SRR14722160	<i>Herteliana schuylariana</i>	groups with <i>Lepraria</i>

Table 4.4. Reference genomes from NCBI used for the Rhizobiales phylogenomic tree.

Taxon sampling followed Volpiano et al. 2021

NCBI ID	Species
GCF_000007125.1	<i>Brucella melitensis</i> bv. 1 str. 16M
GCF_000007505.1	<i>Brucella suis</i> 1330
GCF_000009625.1	<i>Mesorhizobium japonicum</i> MAFF 303099
GCF_000010525.1	<i>Azorhizobium caulinodans</i> ORS 571
GCF_000011365.1	<i>Bradyrhizobium diazoefficiens</i> USDA 110
GCF_000012725.1	<i>Nitrobacter winogradskyi</i> Nb-255
GCF_000013885.1	<i>Nitrobacter hamburgensis</i> XI4
GCF_000015445.1	<i>Bartonella bacilliformis</i> KC583
GCF_000016845.1	<i>Brucella ovis</i> ATCC 25840
GCF_000017405.1	<i>Ochrobactrum anthropi</i> ATCC 49188
GCF_000017565.1	<i>Parvibaculum lavamentivorans</i> DS-1
GCF_000017645.1	<i>Xanthobacter autotrophicus</i> Py2
GCF_000018525.1	<i>Brucella canis</i> ATCC 23365
GCF_000019725.1	<i>Methylobacterium radiotolerans</i> JCM 2831
GCF_000019845.1	<i>Beijerinckia indica</i> subsp. <i>indica</i> ATCC 9039
GCF_000019945.1	<i>Methylobacterium populi</i> BJ001
GCF_000021365.1	<i>Oligotropha carboxidovorans</i> OM5
GCF_000021745.1	<i>Methylocella silvestris</i> BL2
GCF_000021845.1	<i>Methylobacterium extorquens</i> CM4
GCF_000022085.1	<i>Methylobacterium nodulans</i> ORS 2060
GCF_000022745.1	<i>Brucella microti</i> CCM 4915
GCF_000046705.1	<i>Bartonella henselae</i> str. <i>Houston-1</i>
GCF_000083545.1	<i>Methylobacterium extorquens</i> AM1
GCF_000092025.1	<i>Agrobacterium fabrum</i> str. C58
GCF_000092045.1	<i>Rhizobium etli</i> CFN 42
GCF_000092925.1	<i>Starkeya novella</i> DSM 506
GCF_000143145.1	<i>Hyphomicrobium denitrificans</i> ATCC 51888
GCF_000153465.1	<i>Aurantimonas manganoxydans</i> SI85-9A1
GCF_000153705.1	<i>Fulvimarina pelagi</i> HTCC2506
GCF_000154705.2	<i>Hoeflea phototrophica</i> DFL-43
GCF_000158715.1	<i>Brucella neotomae</i> 5K33
GCF_000160295.1	<i>Brucella melitensis</i> bv. 1 str. 16M
GCF_000166055.1	<i>Rhodomicrobium vannielii</i> ATCC 17100
GCF_000176035.2	<i>Mesorhizobium opportunistum</i> WSM2075
GCF_000178815.2	<i>Methylosinus trichosporium</i> OB3b
GCF_000182645.1	<i>Ochrobactrum intermedium</i> LMG 3301
GCF_000182725.1	<i>Brucella inopinata</i> BO1

GCF_000196435.1 *Bartonella tribocorum* CIP 105476
GCF_000218565.1 *Oligotropha carboxidovorans* OM5
GCF_000223195.1 *Brucella suis* 1330
GCF_000230555.1 *Pelagibacterium halotolerans* B2
GCF_000230995.2 *Mesorhizobium australicum* WSM2073
GCF_000236565.1 *Mesorhizobium alhagi* CCNWXJ12-2
GCF_000250795.1 *Brucella melitensis* bv. 1 str. 16M
GCF_000261485.1 *Ensifer sojae* CCBAU 05684
GCF_000262405.1 *Microvirga lotononidis*
GCF_000273375.1 *Bartonella birtlesii* IBS 325
GCF_000278155.1 *Bartonella doshiae* NCTC 12862 = ATCC 700133
GCF_000278215.1 *Bartonella rattimassiliensis* 15908
GCF_000278235.1 *Bartonella vinsonii* subsp. *arupensis* OK-94-513
GCF_000278315.1 *Bartonella elizabethae* F9251 = ATCC 49927
GCF_000280015.1 *Bartonella alsatica* IBS 382
GCF_000283235.1 *Methylocystis parvus* OBBP
GCF_000284375.1 *Bradyrhizobium japonicum* USDA 6
GCF_000298315.2 *Rhizobium grahamii* CCGE 502
GCF_000300335.1 *Nitratireductor pacificus* pht-3B
GCF_000300515.1 *Nitratireductor indicus* C115
GCF_000308295.2 *Afipia birgiae* 34632
GCF_000312525.1 *Bartonella florencae*
GCF_000312545.1 *Bartonella senegalensis* OS02
GCF_000312565.1 *Bartonella rattaaustraliani* AUST/NH4
GCF_000312605.1 *Bartonella rattimassiliensis* 15908
GCF_000314675.2 *Afipia broomeae* ATCC 49717
GCF_000314735.2 *Afipia felis* ATCC 53690
GCF_000325745.1 *Liberibacter crescens* BT-1
GCF_000330885.1 *Rhizobium tropici* CIAT 899
GCF_000336555.1 *Afipia clevelandensis* ATCC 49720
GCF_000341355.1 *Bartonella australis* Aust/NH1
GCF_000344805.1 *Bradyrhizobium oligotrophicum* S58
GCF_000350085.1 *Mesorhizobium metallidurans* STM 2683
GCF_000359745.1 *Rhizobium freirei* PRF 81
GCF_000369945.1 *Brucella abortus* 544
GCF_000372845.1 *Methylocystis rosea* SV97
GCF_000373025.1 *Rhizobium gallicum* bv. *gallicum* R602sp
GCF_000374145.1 *Neomegalonema perideroedes* DSM 15528
GCF_000374525.1 *Amorphus coralli* DSM 19760
GCF_000376125.1 *Martelella mediterranea* DSM 17316
GCF_000379145.1 *Bradyrhizobium elkanii* USDA 76

GCF_000379605.1 *Rhizobium giardinii* bv. *giardinii* H152
GCF_000380505.1 *Kaistia granuli* DSM 23481
Aureimonas ureilytica DSM 18598 = NBRC
106430
GCF_000382705.1 *Hyphomicrobium zavarzinii* ATCC 27496
GCF_000383415.1 *Bartonella bovis* 91-4
GCF_000384965.1 *Methyloferula stellata* AR4
GCF_000385335.1 *Rhizobium mongolense* USDA 1844
GCF_000419765.1 *Aurantimonas coralicida* DSM 14790
GCF_000421645.1 *Agrobacterium radiobacter* DSM 30147
GCF_000421945.1 *Pleomorphomonas oryzae* DSM 16300
GCF_000422965.1 *Kaistia adipata* DSM 17808
GCF_000423225.1 *Maritalea myrionectae* DSM 19524
GCF_000423365.1 *Pleomorphomonas koreensis* DSM 23070
GCF_000425185.1 *Rhizobium leucaenae* USDA 9039
GCF_000426285.1 *Methylocapsa acidiphila* B2
GCF_000427445.1 *Sinorhizobium arboris* LMG 14919
GCF_000427465.1 *Salinarimonas rosea* DSM 21201
GCF_000429045.1 *Cucumibacter marinus* DSM 18995
GCF_000429865.1 *Mesorhizobium erdmanii* USDA 3471
GCF_000472705.1 *Bradyrhizobium japonicum* USDA 6
GCF_000472985.1 *Azorhizobium doebereineriae* UFLA1-100
GCF_000473085.1 *Lutibaculum baratangense* AMV1
GCF_000496075.1 *Hyphomicrobium nitrativorans* NL23
GCF_000503895.1 *Bartonella grahamii* ATCC 700132
GCF_000518085.1 *Bartonella vinsonii* subsp. *berkhoffii* ATCC 51672
GCF_000518105.1 *Bartonella elizabethae* F9251 = ATCC 49927
GCF_000518165.1 *Bartonella clarridgeiae* ATCC 51734
GCF_000518185.1 *Agrobacterium larrymoorei* AF3.10 = ATCC
51759
GCF_000518585.1 *Microvirga flocculans* ATCC BAA-817
GCF_000518665.1 *Rhizobium selenitireducens* ATCC BAA-1503
GCF_000518785.1 *Bartonella doshiae* NCTC 12862 = ATCC 700133
GCF_000526895.1 *Rhizobium favelukesii*
GCF_000577275.2 *Nitratisreductor aquibiodomus* NL21 = JCM
21793
GCF_000615975.1 *Rhizobium undicola* ORS 992 = ATCC 700741
GCF_000621665.1 *Rhodomicrobium udaipurensense* JA643
GCF_000636015.1 *Brucella ceti* B1/94
GCF_000662035.2 *Terasakiella pusilla* DSM 6293
GCF_000688235.1 *Afifella pfennigii* DSM 17143
GCF_000688515.1

GCF_000696095.1	<i>Agrobacterium rhizogenes</i> NBRC 13257
GCF_000697965.2	<i>Ensifer adhaerens</i>
GCF_000705355.1	<i>Rhizobium marinum</i>
GCF_000706625.1	<i>Bartonella koehlerae</i> C-29
GCF_000706645.1	<i>Bartonella rochalimae</i> ATCC BAA-1498
GCF_000712255.1	<i>Brucella neotomae</i> 5K33
GCF_000722615.1	<i>Pseudorhizobium pelagicum</i>
	<i>Neorhizobium galegae</i> bv. <i>orientalis</i> str. HAMB1 540
GCF_000731315.1	<i>Rhizobium vignae</i>
GCF_000732195.1	<i>Tepidicaulis marinus</i>
GCF_000739695.1	<i>Agrobacterium rubi</i> TR3 = NBRC 13261
GCF_000739935.1	<i>Brucella canis</i>
GCF_000740335.1	<i>Brucella melitensis</i> bv. 1 str. 16M
GCF_000740415.1	<i>Brucella suis</i> 1330
GCF_000742005.1	<i>Brucella neotomae</i> 5K33
GCF_000742255.1	<i>Devosia riboflavina</i>
GCF_000743575.1	<i>Beijerinckia mobilis</i>
GCF_000745425.1	<i>Methylocapsa aurea</i>
GCF_000746085.1	<i>Methylobacterium oryzae</i> CBMB20
GCF_000757795.1	<i>Methyloceanibacter caenitepidi</i>
GCF_000828475.1	<i>Rhizobium nepotum</i> 39/7
GCF_000949865.1	<i>Martellella endophytica</i>
GCF_000960975.1	<i>Devosia geojensis</i>
GCF_000969415.1	<i>Devosia chinhatensis</i>
GCF_000969445.1	<i>Devosia limi</i> DSM 17137
GCF_000970435.1	<i>Devosia soli</i>
GCF_000970455.1	<i>Devosia insulae</i> DS-56
GCF_000970465.2	<i>Devosia psychrophila</i>
GCF_000971275.1	<i>Devosia epidermidihirudinis</i>
GCF_000971295.1	<i>Microvirga massiliensis</i>
GCF_001006805.1	<i>Microvirga vignae</i>
GCF_001017175.1	<i>Methylobacterium platani</i> JCM 14648
GCF_001043885.1	<i>Methylobacterium indicum</i>
GCF_001043895.1	<i>Methylobacterium aquaticum</i>
GCF_001043915.1	<i>Methylobacterium tarhaniae</i>
GCF_001043955.1	<i>Methylobacterium variabile</i>
GCF_001043975.1	<i>Nitratireductor soli</i>
GCF_001050155.1	<i>Microvirga massiliensis</i>
GCF_001050495.1	<i>Rhizobium ecuadorensis</i>
GCF_001187535.1	<i>Bradyrhizobium embrapense</i>
GCF_001189235.2	

GCF_001189245.1	<i>Bradyrhizobium pachyrhizi</i>
GCF_001189845.1	<i>Bradyrhizobium tropiciagri</i>
GCF_001238275.1	<i>Bradyrhizobium viridifuturi</i>
GCF_001281405.1	<i>Bartonella ancashensis</i>
GCF_001305515.1	<i>Prosthecomicrobium hirschii</i>
GCF_001402875.1	<i>Blastochloris viridis</i>
GCF_001418005.1	<i>Chelatococcus sambhunathii</i>
GCF_001440035.1	<i>Bradyrhizobium manausense</i>
GCF_001440395.1	<i>Bradyrhizobium jicamae</i>
GCF_001440405.1	<i>Bradyrhizobium valentinum</i>
GCF_001440415.1	<i>Bradyrhizobium retamae</i>
GCF_001440475.1	<i>Bradyrhizobium lablabi</i>
GCF_001461695.1	<i>Sinorhizobium fredii</i> USDA 205
GCF_001463825.1	<i>Aurantimonas coralicida</i>
GCF_001463845.1	<i>Fulvimarina pelagi</i>
GCF_001463865.1	<i>Aurantimonas manganoxydans</i> SI85-9A1
GCF_001463885.1	<i>Aureimonas altamirensis</i>
GCF_001463905.1	<i>Aureimonas frigidaquae</i>
	<i>Aureimonas ureilytica</i> DSM 18598 = NBRC 106430
GCF_001463945.1	<i>Chelatococcus sambhunathii</i>
GCF_001517345.1	<i>Bartonella henselae</i> str. Houston-1
GCF_001525625.2	<i>Agrobacterium tumefaciens</i>
GCF_001541305.1	<i>Agrobacterium tumefaciens</i> str. B6
GCF_001541315.1	<i>Agrobacterium vitis</i>
GCF_001541345.2	<i>Rhizobium altiplani</i>
GCF_001542405.1	<i>Bradyrhizobium macuxiense</i>
GCF_001542415.1	<i>Blastochloris viridis</i>
GCF_001548155.2	<i>Paramesorhizobium deserti</i>
GCF_001558695.1	<i>Bartonella bacilliformis</i>
GCF_001559035.2	<i>Aminobacter aminovorans</i>
GCF_001605015.1	<i>Bradyrhizobium stylosanthis</i>
GCF_001641335.1	<i>Bradyrhizobium centrolobii</i>
GCF_001641635.1	<i>Bradyrhizobium neotropicale</i>
GCF_001641695.1	<i>Bradyrhizobium diazoefficiens</i> USDA 110
GCF_001642675.1	<i>Devosia elaeis</i>
GCF_001650025.1	<i>Sinorhizobium americanum</i>
GCF_001651855.1	<i>Ensifer glycinis</i>
GCF_001651865.1	<i>Sinorhizobium saheli</i>
GCF_001651875.1	<i>Methylobacterium platani</i>
GCF_001653715.1	<i>Pararhizobium polonicum</i>
GCF_001687365.1	

GCF_001693385.1	<i>Bradyrhizobium icense</i>
GCF_001693515.2	<i>Bradyrhizobium paxllaeri</i>
GCF_001703635.1	<i>Hoeflea olei</i>
GCF_001708935.1	<i>Methyloligella halotolerans</i>
GCF_001720135.1	<i>Methylobrevis pamukkalensis</i>
GCF_001723275.1	<i>Ensifer alkalisoli</i>
GCF_001723285.1	<i>Methyloceanibacter methanicus</i>
GCF_001723295.1	<i>Methyloceanibacter marginalis</i>
GCF_001723305.1	<i>Methyloceanibacter superfactus</i>
GCF_001723355.1	<i>Methyloceanibacter stevinii</i>
GCF_001741865.1	<i>Bosea vaviloviae</i>
GCF_001885585.1	<i>Pararhizobium antarcticum</i>
GCF_001889605.1	<i>Mesorhizobium oceanicum</i>
GCF_001927285.1	<i>Mongoliimonas terrestris</i>
GCF_001931685.1	<i>Rhizobium arenae</i>
GCF_001936175.1	<i>Methylobacterium phyllosphaerae</i>
GCF_001938945.1	<i>Rhizobium rhizosphaerae</i>
GCF_001938985.1	<i>Rhizobium taibaishanense</i>
GCF_001939045.1	<i>Rhizobium oryzae</i>
GCF_001952075.1	<i>Bartonella apis</i>
GCF_001953055.1	<i>Salaquimonas pukyongi</i>
GCF_001982635.1	<i>Bradyrhizobium mercantei</i>
GCF_002000045.1	<i>Rhizobium flavum</i>
GCF_002008165.1	<i>Rhizobium laguerreae</i>
GCF_002008215.1	<i>Agrobacterium tumefaciens</i>
GCF_002008225.1	<i>Agrobacterium salinitolerans</i>
GCF_002008275.1	<i>Rhizobium pusense</i>
GCF_002008365.1	<i>Rhizobium leguminosarum</i> bv. <i>viciae</i> USDA 2370
GCF_002022685.1	<i>Bartonella schoenbuchensis</i> R1
GCF_002043005.1	<i>Martelella mediterranea</i> DSM 17316
GCF_002068095.1	<i>Bradyrhizobium sacchari</i>
GCF_002075885.1	<i>Pseudaminobacter manganicus</i>
GCF_002119765.1	<i>Pseudorhodoplanes sinuspersici</i>
GCF_002204185.1	<i>Rhizobium esperanzae</i>
GCF_002238045.1	<i>Notoacmeibacter marinus</i>
GCF_002252445.1	<i>Ochrobactrum thiophenivorans</i>
GCF_002252475.1	<i>Ochrobactrum rhizosphaerae</i>
GCF_002252505.1	<i>Ochrobactrum grignonense</i>
GCF_002252525.1	<i>Ochrobactrum pseudogrignonense</i>
GCF_002252535.1	<i>Ochrobactrum lupini</i>
GCF_002266435.2	<i>Bradyrhizobium amphicarpaceae</i>

GCF_002266465.2	<i>Bradyrhizobium symbiodeficiens</i>
GCF_002270415.1	<i>Mesorhizobium sophorae</i>
GCF_002278035.1	<i>Ochrobactrum quorumnocens</i>
GCF_002278135.2	<i>Bradyrhizobium ottawaense</i>
GCF_002284535.1	<i>Mesorhizobium wenxiniae</i>
GCF_002284575.1	<i>Mesorhizobium temperatum</i>
GCF_002288525.1	<i>Ensifer sojae</i> CCBAU 05684
GCF_002355335.1	<i>Variibacter gotjawalensis</i>
GCF_002529485.1	<i>Mesorhizobium sanjuanii</i>
GCF_002531855.1	<i>Rhizobium hidalgonense</i>
GCF_002727065.1	<i>Zhengella mangrovi</i>
GCF_002741015.1	<i>Microvirga ossetica</i>
GCF_002750855.1	<i>Pararhizobium haloflavum</i>
GCF_002752655.1	<i>Methylosinus trichosporium</i> OB3b
GCF_002759055.1	<i>Methylobacterium frigidaeris</i>
GCF_002764115.1	<i>Phyllobacterium zundukense</i>
GCF_002770725.1	<i>Pleomorphomonas carboxyditropha</i>
GCF_002795245.1	<i>Bradyrhizobium forestalis</i>
GCF_002844595.1	<i>Pleomorphomonas diazotrophica</i>
GCF_002866925.1	<i>Cohaesibacter celericrescens</i>
GCF_002879535.1	<i>Mesorhizobium intechi</i>
GCF_002893625.1	<i>Mangrovicella endophytica</i>
GCF_002896715.1	<i>Agrobacterium bohemicum</i>
GCF_002914525.1	<i>Rhizobium hidalgonense</i>
GCF_002915175.1	<i>Agrobacterium rosae</i>
GCF_002930635.1	<i>Kaistia algarum</i>
GCF_002937075.1	<i>Rhodoblastus sphagnicola</i>
GCF_002937135.1	<i>Rhodoblastus acidophilus</i>
GCF_002968575.1	<i>Neorhizobium huautlense</i>
GCF_002968635.1	<i>Neorhizobium alkalisoli</i>
GCF_002980495.1	<i>Phyllobacterium phragmitis</i>
GCF_002980555.1	<i>Phyllobacterium myrsinacearum</i>
GCF_003010935.1	<i>Phyllobacterium endophyticum</i>
GCF_003010955.1	<i>Phyllobacterium brassicacearum</i>
GCF_003010965.1	<i>Phyllobacterium sophorae</i>
GCF_003012705.1	<i>Mesorhizobium soli</i>
GCF_003012745.1	<i>Mesorhizobium ephedrae</i>
GCF_003024595.1	<i>Mesorhizobium plurifarum</i>
GCF_003024615.1	<i>Mesorhizobium loti</i>
GCF_003034915.1	<i>Mesorhizobium helmanticense</i>
GCF_003046475.1	<i>Mycoplana dimorpha</i>

GCF_003049685.1	<i>Ochrobactrum pituitosum</i>
GCF_003053845.1	<i>Breoghania corrubedonensis</i>
GCF_003056345.1	<i>Devosia submarina</i>
GCF_003056405.1	<i>Devosia indica</i>
GCF_003058325.1	<i>Methylobacterium currus</i>
GCF_003058385.1	<i>Rhizobium leguminosarum</i> bv. <i>viciae</i> USDA 2370
GCF_003096615.1	<i>Methylobacterium organophilum</i>
GCF_003113265.1	<i>Methylosinus sporium</i>
GCF_003122325.1	<i>Rhizobium album</i>
GCF_003148475.1	<i>Pseudaminobacter salicylatoxidans</i>
GCF_003148495.1	<i>Mesorhizobium loti</i>
GCF_003149475.2	<i>Oceaniradius stylonematis</i>
GCF_003173715.1	<i>Methylobacterium durans</i>
GCF_003173755.1	<i>Methylobacterium terrae</i>
GCF_003182235.1	<i>Phyllobacterium myrsinacearum</i>
GCF_003182275.1	<i>Hoeflea marina</i>
GCF_003201475.1	<i>Chelatococcus asaccharovorans</i>
GCF_003205195.1	<i>Rhizobium wuzhouense</i>
GCF_003217235.1	<i>Phyllobacterium leguminum</i>
GCF_003217325.1	<i>Rhodopseudomonas faecalis</i>
GCF_003234965.1	<i>Aestuariivirga litoralis</i>
GCF_003240565.1	<i>Rhizobium tumorigenes</i>
GCF_003240585.1	<i>Rhizobium tubonense</i>
GCF_003258765.1	<i>Rhodoblastus acidophilus</i>
GCF_003258805.1	<i>Rhodoplanes elegans</i>
GCF_003258835.1	<i>Rhodobium orientis</i>
GCF_003258855.1	<i>Rhodoplanes piscinae</i>
GCF_003258865.1	<i>Rhodoplanes roseus</i>
GCF_003258905.1	<i>Afifella marina</i> DSM 2698
GCF_003259955.1	<i>Falsochromobacterium ovis</i>
GCF_003289945.1	<i>Mesorhizobium hawassense</i>
GCF_003314995.1	<i>Pseudochrobacterium asaccharolyticum</i>
GCF_003315135.1	<i>Roseiarcus fermentans</i>
GCF_003324485.1	<i>Cohaesibacter intestini</i>
GCF_003332305.1	<i>Microvirga aerophila</i>
GCF_003335045.1	<i>Phyllobacterium salinisoli</i>
GCF_003337575.1	<i>Phyllobacterium bourgognense</i>
GCF_003337715.1	<i>Ciceribacter lividus</i>
GCF_003347665.1	<i>Microvirga calopogonii</i>
GCF_003350535.1	<i>Microvirga subterranea</i>
GCF_003367395.1	<i>Pseudolabrys taiwanensis</i>

GCF_003385925.1	<i>Rhodopseudomonas pentothentaxigens</i>
GCF_003387225.1	<i>Methylovirgula ligni</i>
GCF_003403015.1	<i>Fulvimarina endophytica</i>
GCF_003403035.1	<i>Mesorhizobium denitrificans</i>
GCF_003547145.1	<i>Rhodopseudomonas palustris</i>
GCF_003550175.1	<i>Dichotomicrobium thermohalophilum</i>
GCF_003574465.1	<i>Methylobacterium crusticola</i>
GCF_003574655.1	<i>Cohaesibacter haloalkalitolerans</i>
GCF_003583935.1	<i>Aureimonas flava</i>
GCF_003601975.1	<i>Mesorhizobium waimense</i>
GCF_003601985.1	<i>Mesorhizobium jarvisii</i>
GCF_003610435.1	<i>Pseudorhodoplanes sinuspersici</i>
GCF_003627755.1	<i>Rhizobium jaguaris</i>
GCF_003664555.1	<i>Ochrobactrum soli</i>
GCF_003667445.1	<i>Xanthobacter tagetidis</i>
GCF_003668555.1	<i>Notoacmeibacter ruber</i>
GCF_003722355.1	<i>Methylocystis hirsuta</i>
GCF_003863365.1	<i>Mesorhizobium tamadayense</i>
GCF_003934165.1	<i>Pseudaminobacter arsenicus</i>
GCF_003938655.1	<i>Rhizobium pisi</i>
GCF_003939025.1	<i>Rhizobium sophoriradicis</i>
GCF_003952725.1	<i>Georhizobium profundi</i>
GCF_003966715.1	<i>Blastochloris tepida</i>
GCF_003970795.1	<i>Mesorhizobium carbonis</i>
GCF_003985125.1	<i>Rhizobium phaseoli</i>
GCF_003985135.1	<i>Rhizobium fabae</i>
GCF_003985145.1	<i>Rhizobium anhuiense</i>
GCF_003985155.1	<i>Rhizobium vallis</i>
GCF_003992625.1	<i>Pelagibacterium lentulum</i>
GCF_003992665.1	<i>Pelagibacterium montanilacus</i>
GCF_003993795.1	<i>Aquabacter cavernae</i>
GCF_003994485.1	<i>Arsenicitalea aurantiaca</i>
GCF_004023665.1	<i>Afifella aestuarii</i>
GCF_004103825.1	<i>Hansschlegelia zihuaiaie</i>
GCF_004114425.1	<i>Bradyrhizobium vignae</i>
GCF_004114535.1	<i>Bradyrhizobium nanningense</i>
GCF_004114915.1	<i>Bradyrhizobium guangxiense</i>
GCF_004114935.1	<i>Bradyrhizobium zhanjiangense</i>
GCF_004114955.1	<i>Bradyrhizobium guangzhouense</i>
GCF_004114975.1	<i>Bradyrhizobium guangdongense</i>
GCF_004135935.1	<i>Methylovirgula ligni</i>

GCF_004137085.1	<i>Lichenibacterium ramalinae</i>
GCF_004137685.1	<i>Lichenibacterium minor</i>
GCF_004216635.1	<i>Variibacter gotjawalensis</i>
GCF_004216655.1	<i>Phyllobacterium myrsinacearum</i>
GCF_004217385.1	<i>Phyllobacterium myrsinacearum</i>
GCF_004323635.1	<i>Lichenihabitans psoromatis</i>
GCF_004328075.1	<i>Siculibacillus lacustris</i>
GCF_004331955.1	<i>Roseitalea porphyridii</i>
GCF_004339465.1	<i>Ancylobacter aquaticus</i>
GCF_004341645.1	<i>Aminobacter aminovorans</i>
GCF_004341885.1	<i>Shinella granuli</i>
GCF_004342915.1	<i>Camelimonas lactis</i>
GCF_004346185.1	<i>Aquabacter spiritensis</i>
GCF_004346195.1	<i>Tepidamorphus gemmatus</i>
GCF_004348265.1	<i>Methylobacterium segetis</i>
GCF_004354915.1	<i>Pseudohoeflea suaedae</i>
GCF_004358025.1	<i>Rhizobium deserti</i>
GCF_004362745.1	<i>Oharaeibacter diazotrophicus</i>
GCF_004363175.1	<i>Maritalea mobilis</i>
GCF_004363725.1	<i>Aquamicrobium defluvii</i>
GCF_004363955.1	<i>Enterovirga rhinocerotis</i>
GCF_004365425.1	<i>Rhizobium azibense</i>
GCF_004458765.1	<i>Microvirga pakistanensis</i>
GCF_004519335.1	<i>Jiella endophytica</i>
GCF_004801285.1	<i>Mesorhizobium composti</i>
GCF_004802635.2	<i>Methylocystis heyeri</i>
GCF_004912135.1	<i>Rhizobium rosettiformans W3</i>
GCF_004912165.1	<i>Rhizobium ipomoeae</i>
GCF_005145045.1	<i>Agrobacterium larrymoorei</i>
GCF_005871085.1	<i>Xanthobacter autotrophicus</i>
GCF_005924265.1	<i>Martelella lutilitoris</i>
GCF_005938105.1	<i>Ochrobactrum haematophilum</i>
GCF_006335145.1	<i>Rhizobium smilacinae</i>
GCF_006376675.1	<i>Ochrobactrum pecoris</i>
GCF_006443685.1	<i>Rhizobium glycinendophyticum</i>
GCF_006476605.1	<i>Ochrobactrum gallinifaecis</i>
GCF_006539605.1	<i>Sinorhizobium fredii</i>
GCF_006539645.1	<i>Bradyrhizobium japonicum</i>
GCF_006539665.1	<i>Bradyrhizobium elkanii</i>
GCF_007002985.1	<i>Agrobacterium rhizogenes</i>
GCF_007474605.1	<i>Rhodoligotrophos appendicifer</i>

GCF_007827505.1	<i>Rhizobium mongolense</i> USDA 1844
GCF_007827695.1	<i>Sinorhizobium medicae</i>
GCF_007830205.1	<i>Bradyrhizobium daqingense</i>
GCF_007830635.1	<i>Bradyrhizobium huanghuaihaiense</i>
GCF_007859655.1	<i>Devosia ginsengisoli</i>
GCF_007991055.1	<i>Methylobacterium radiotolerans</i>
GCF_007991675.1	<i>Microvirga aerophila</i>
GCF_007992095.1	<i>Rhizobium naphthalenivorans</i>
GCF_007992175.1	<i>Methylobacterium haplocladii</i>
GCF_007992195.1	<i>Methylobacterium oxalidis</i>
GCF_007992215.1	<i>Methylobacterium gnaphalii</i>
GCF_008000755.1	<i>Youhaiella tibetensis</i>
GCF_008123425.1	<i>Bradyrhizobium rifense</i>
GCF_008123515.1	<i>Bradyrhizobium cytisi</i>
GCF_008180215.1	<i>Phyllobacterium endophyticum</i>
GCF_008630065.1	<i>Blastochloris sulfoviridis</i>
GCF_008641065.1	<i>Rhabdaerophilum calidifontis</i>
GCF_008757455.1	<i>Microvirga brassicacearum</i>
GCF_008801385.1	<i>Agrobacterium tumefaciens</i>
GCF_008801705.1	<i>Ochrobactrum pituitosum</i>
GCF_008801715.1	<i>Pseudochrobactrum saccharolyticum</i>
GCF_008802405.1	<i>Aureimonas leprariae</i>
GCF_008806385.1	<i>Methylobacterium soli</i>
GCF_008932115.1	<i>Bradyrhizobium betae</i>
GCF_008932245.1	<i>Ensifer alkalisoli</i>
GCF_008932295.1	<i>Ochrobactrum tritici</i>
GCF_009498475.1	<i>Agrobacterium tumefaciens</i>
GCF_009599935.1	<i>Sinorhizobium medicae</i>
GCF_009601385.1	<i>Sinorhizobium meliloti</i>
GCF_009601405.1	<i>Sinorhizobium fredii</i>
GCF_009720755.1	<i>Rhodoplanes serenus</i>
GCF_009811675.1	<i>Methylosinus sporium</i>
GCF_009826855.1	<i>Shinella zoogloeoides</i>
GCF_009827055.1	<i>Shinella kummerowiae</i>
GCF_009830105.1	<i>Microvirga makkahensis</i>
GCF_009910475.1	<i>Pyruvatibacter mobilis</i>
GCF_010500835.1	<i>Aurantimonas aggregata</i>
GCF_010669125.1	<i>Ancylobacter pratisalsi</i>
GCF_011045115.1	<i>Mesorhizobium zhangyense</i>
GCF_011045125.1	<i>Mesorhizobium camelthorni</i>
GCF_011045155.1	<i>Rhizobium daejeonense</i>

GCF_011317445.1	<i>Chelativorans multitrophicus</i>
GCF_011317485.1	<i>Oharaeibacter diazotrophicus</i>
GCF_011317505.1	<i>Chelativorans oligotrophicus</i>
GCF_011761465.1	<i>Variibacter gotjawalensis</i>
GCF_013004495.1	<i>Rhizobium</i> sp. SEMIA 4085
GCF_900045375.1	<i>Agrobacterium tumefaciens</i> str. B6
GCF_900094545.1	<i>Rhizobium miluonense</i>
GCF_900094555.1	<i>Rhizobium hainanense</i>
GCF_900094565.1	<i>Rhizobium lusitanum</i>
GCF_900094575.1	<i>Bradyrhizobium yuanmingense</i>
GCF_900094585.1	<i>Rhizobium multihospitium</i>
GCF_900094605.1	<i>Bradyrhizobium shewense</i>
GCF_900094625.1	<i>Rhizobium aethiopicum</i>
GCF_900099775.1	<i>Rhizobium loessense</i>
GCF_900099905.1	<i>Mesorhizobium muleiense</i>
GCF_900100155.1	<i>Ancylobacter rudongensis</i>
GCF_900100455.1	<i>Roseospirillum parvum</i>
GCF_900100665.1	<i>Pelagibacterium luteolum</i>
GCF_900102105.1	<i>Rhizobium pusense</i>
GCF_900102135.1	<i>Microvirga guangxiensis</i>
GCF_900102525.1	<i>Bosea robiniae</i>
GCF_900102695.1	<i>Afifella marina</i> DSM 2698
GCF_900103325.1	<i>Mesorhizobium qingshengii</i>
GCF_900103445.1	<i>Methylobacterium phyllostachyos</i>
GCF_900104305.1	<i>Filomicrobium insigne</i>
GCF_900104485.1	<i>Bauldia litoralis</i>
GCF_900108245.1	<i>Bosea lathyri</i>
GCF_900108425.1	<i>Rhizobium tibeticum</i>
GCF_900109605.1	<i>Rhizobium oryzae</i>
GCF_900110205.1	<i>Rhizobium tibeticum</i>
GCF_900110435.1	<i>Rhodopseudomonas pseudopalustris</i>
GCF_900112505.1	<i>Devosia psychrophila</i>
GCF_900113465.1	<i>Methylobacterium phyllosphaerae</i>
GCF_900113485.1	<i>Methylobacterium gossipiicola</i>
GCF_900113935.1	<i>Aquamicrobium aerolatum</i> DSM 21857
GCF_900114255.1	<i>Mesorhizobium albiziae</i>
GCF_900114285.1	<i>Methylocapsa palsarum</i>
GCF_900114375.1	<i>Methylorubrum salsuginis</i>
GCF_900114535.1	<i>Methylobacterium pseudosasicola</i>
GCF_900114935.1	<i>Pleomorphomonas diazotrophica</i>
GCF_900115225.1	<i>Cohaesibacter marisflavi</i>

GCF_900116175.1	<i>Hyphomicrobium facile</i>
GCF_900116545.1	<i>Devosia crocina</i>
GCF_900116675.1	<i>Bradyrhizobium arachidis</i>
GCF_900119845.1	<i>Devosia enhydra</i>
GCF_900128975.1	<i>Devosia limi</i> DSM 17137
GCF_900129325.1	<i>Kaistia soli</i> DSM 19436
GCF_900141975.1	<i>Aureimonas altamirensis</i> DSM 21988
GCF_900148505.1	<i>Pseudoxanthobacter soli</i> DSM 19599
GCF_900167365.1	<i>Consotaella salsifontis</i>
GCF_900168195.1	<i>Bosea thiooxidans</i>
GCF_900176465.1	<i>Fulvimarina manganooxydans</i>
GCF_900177655.1	<i>Devosia lucknowensis</i>
GCF_900185775.1	<i>Bartonella mastomydis</i>
GCF_900187365.1	<i>Rhodoblastus acidophilus</i>
GCF_900215605.1	<i>Cohaesibacter gelatinilyticus</i>
GCF_900218015.1	<i>Rhodopseudomonas pentothentatexigens</i>
GCF_900220975.1	<i>Rhizobium subbaraonis</i>
GCF_900220985.1	<i>Hoeflea halophila</i>
GCF_900231165.1	<i>Hartmannibacter diazotrophicus</i>
GCF_900234795.1	<i>Methylorubrum extorquens</i>
GCF_900445155.1	<i>Afipia felis</i>
GCF_900445235.1	<i>Aminobacter aminovorans</i>
GCF_900445535.1	<i>Bartonella doshiae</i>
GCF_900445635.1	<i>Bartonella grahamii</i>
GCF_900446005.1	<i>Brucella abortus</i>
GCF_900446125.1	<i>Brucella neotomae</i>
GCF_900446135.1	<i>Brucella ovis</i>
GCF_900454225.1	<i>Ochrobactrum intermedium</i>
GCF_900454235.1	<i>Ochrobactrum anthropi</i>
GCF_900460605.1	<i>Brucella suis</i>
GCF_902141855.1	<i>Methylobacterium dankookense</i>
GCF_902150025.1	<i>Bartonella massiliensis</i>
GCF_902153235.1	<i>Rhizobium halotolerans</i>
GCF_902153245.1	<i>Rhizobium endolithicum</i>
GCF_902162175.1	<i>Bartonella sahelensis</i>
GCF_009908265.2	<i>Rhodobacter amnigenus</i> (outgroup)

Table 4.5. Sequences used as a tblastn query for the screening of Rhizobiales genomes.

Gene	Description	Function	NCBI ID
NifH	nitrogenase	Nitrogen fixation	ABZ89802.1
PmoC	particulate methane monooxygenase	Methanotrophy	WP_016921575.1
MmoX	soluble methane monooxygenase	Methanotrophy	ABD13903.1
XxoF	methanol dehydrogenase	Methylotrophy	VVC56072.1
MxaF	methanol dehydrogenase	Methylotrophy	CAD91828.2

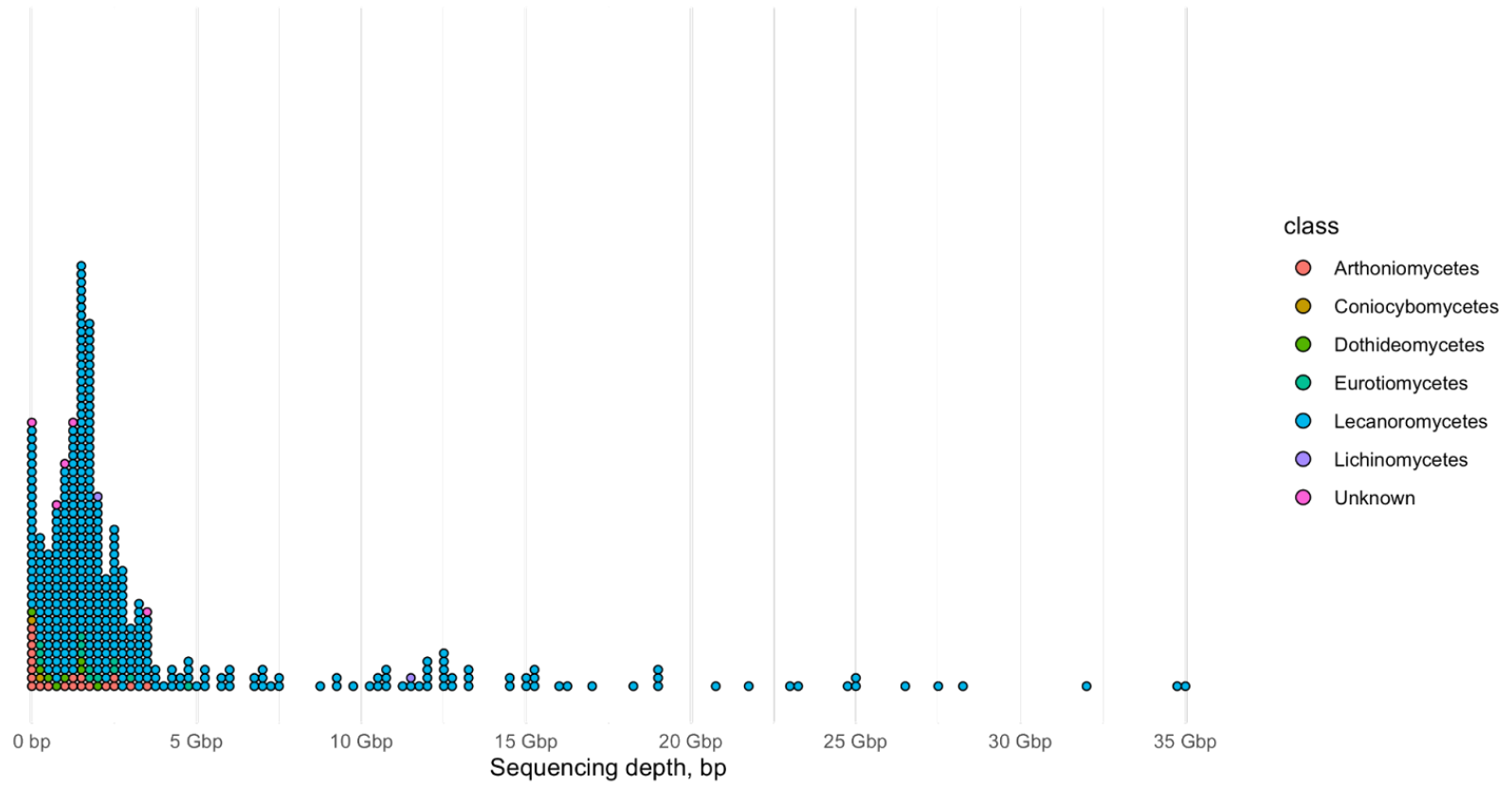


Fig. 4.1. Lichen metagenomes arranged by sequencing depth.

Dots, representing metagenomes, are coloured according to the class of the main fungal partner.

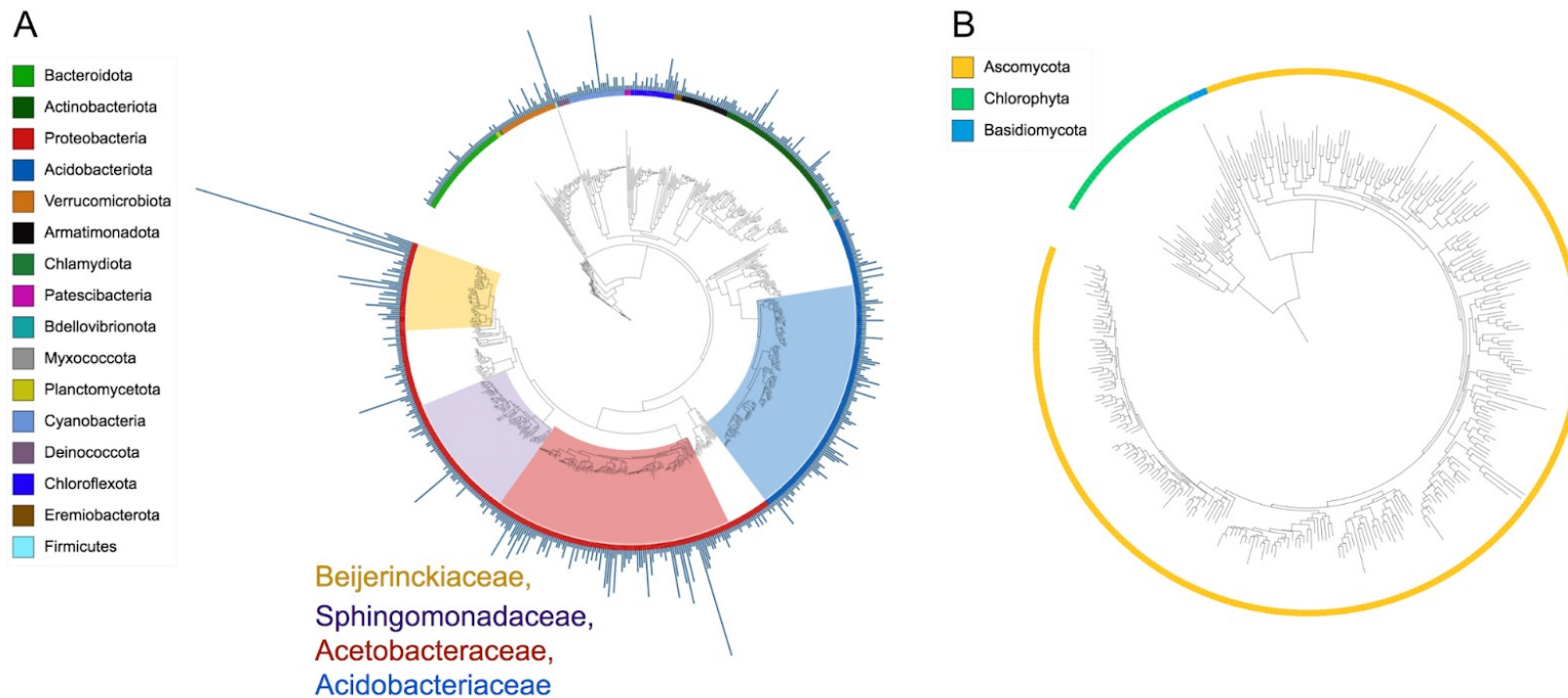


Fig. 4.2. Maximum likelihood phylogenetic trees of the MAGs.

Both trees are calculated using IQ-TREE and are based on alignments of marker genes (for prokaryotes: 120 marker genes from GTDB-Tk, for eukaryotes: 50 marker genes from EukCC). The annotation tracks show the clade the MAG was assigned to. The trees in Newick format are available in FigShare (<https://doi.org/10.6084/m9.figshare.20097167.v1>). A. Tree of the prokaryotic MAGs. The four most frequent bacterial families are highlighted. The bars show the number of metagenomes that contained the MAG. B. Tree of the eukaryotic MAGs.

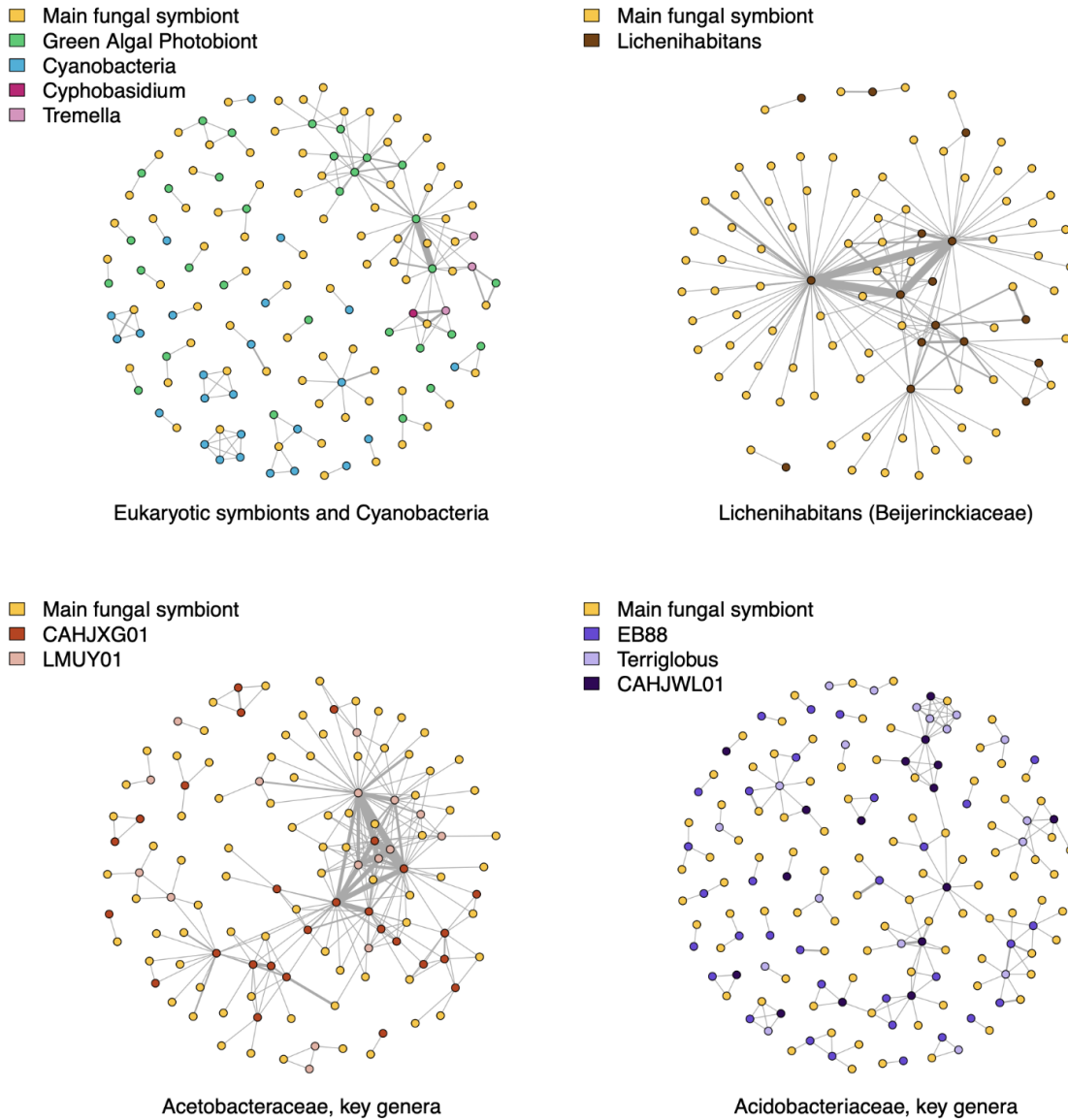


Fig. 4.3. Co-occurrence networks of lichen symbionts based on presence-absence of MAGs in each metagenome.

Each node is a MAG, and edges represent the co-occurrence of MAGs within one metagenome; the thicker is the edge, the more often two MAGs co-occur. Nodes are coloured based on the taxonomy and function of the symbiont; in each network, yellow nodes represent MAGs of the main fungal symbiont.

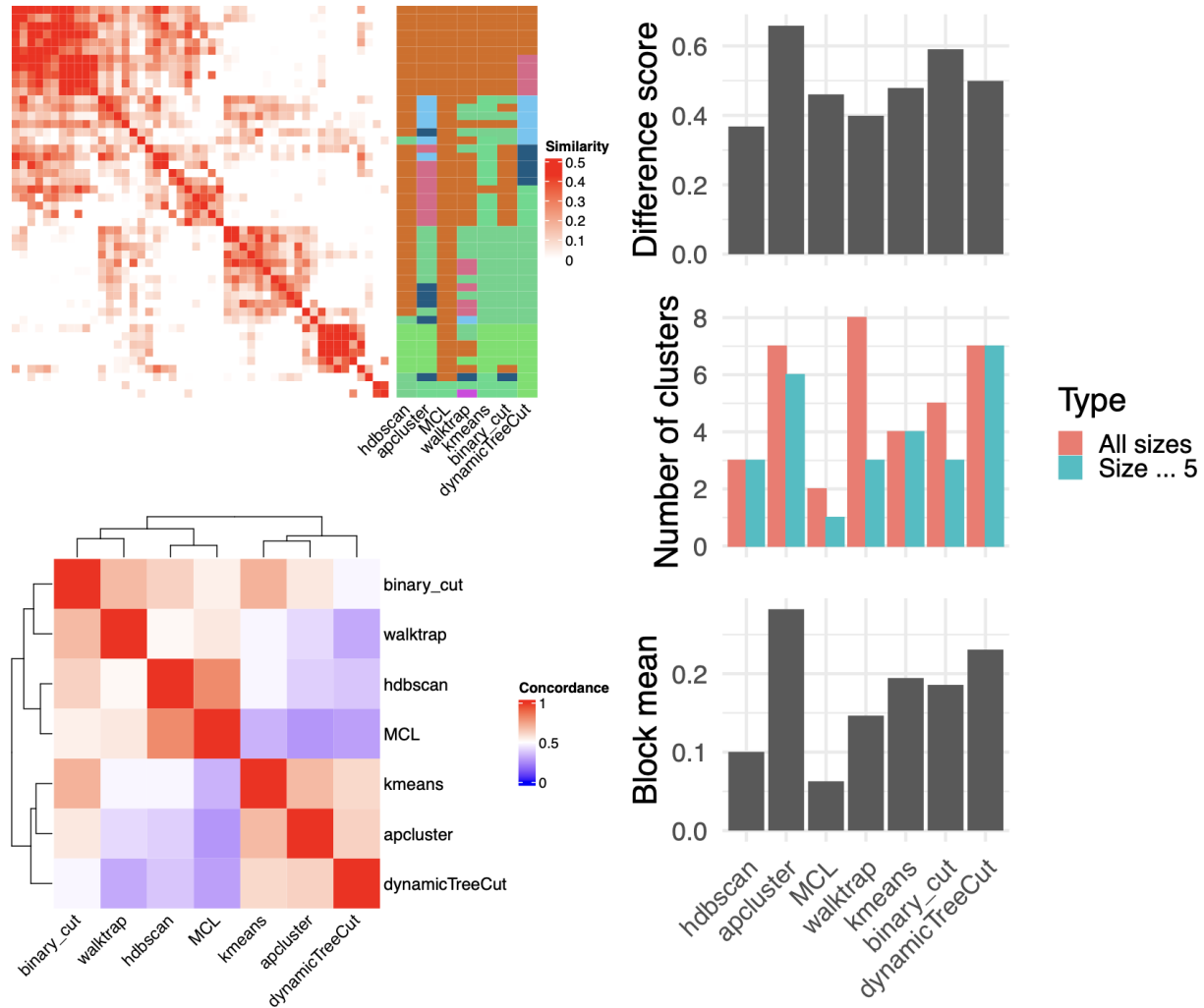


Fig. 4.4. Comparing different clustering methods for grouping bacterial genera based on their occurrence profiles in lichen metagenomes.

The left panel shows: the heatmap of the similarity matrix with different classifications shown as bars (top) and the heatmap of pairwise concordance between the clustering methods (bottom). The right panel shows barplots for each clustering method: Difference score (top, measure of difference between the similarity metric between objects in one cluster and objects in different clusters), Number of clusters (middle), and Block mean (bottom, mean similarity values of the diagonal blocks in the similarity matrix). All the methods were applied to the similarity matrix, which was based on Pearson coefficients. The comparison was done using the SimplifyEnrichment R library.

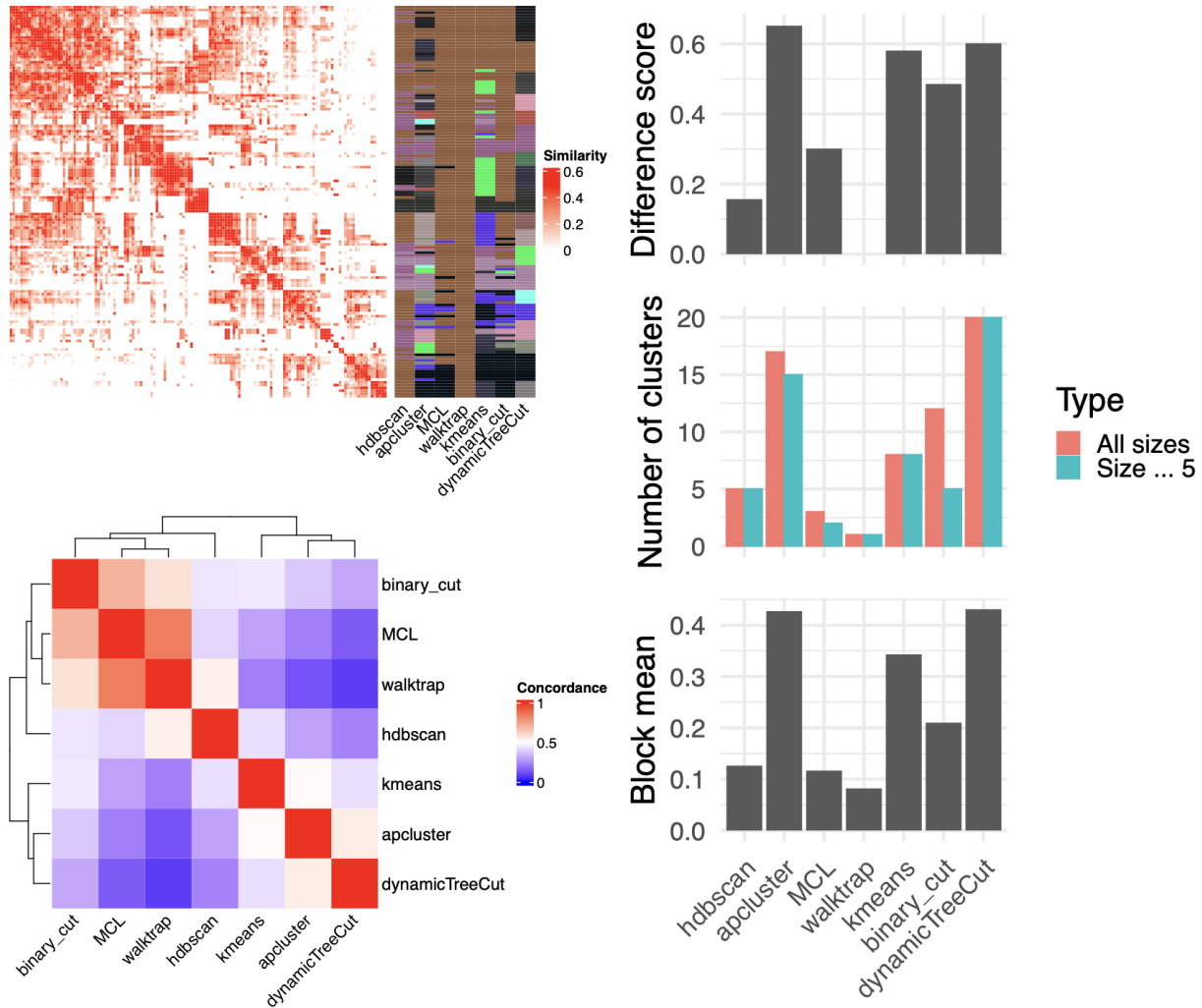


Fig. 4.5. Comparing different clustering methods for grouping metagenomes based on their bacterial communities.

The left panel shows: the heatmap of the similarity matrix with different classifications shown as bars (top) and the heatmap of pairwise concordance between the clustering methods (bottom). The right panel shows barplots for each clustering method: Difference score (top, measure of difference between the similarity metric between objects in one cluster and objects in different clusters), Number of clusters (middle), and Block mean (bottom, mean similarity values of the diagonal blocks in the similarity matrix). All the methods were applied to the similarity matrix, which was based on Pearson coefficients. The comparison was done using the SimplifyEnrichment R library.

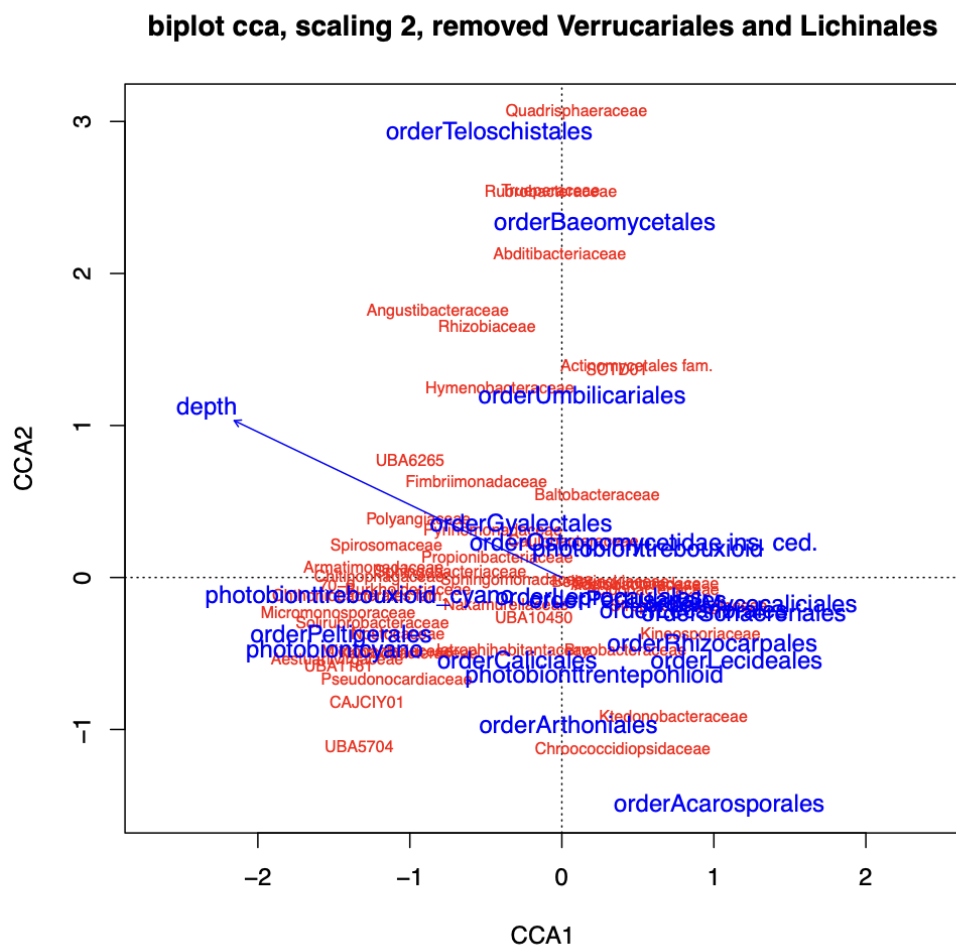


Fig. 4.6. Ordination plot of lichen bacterial communities.

The plot is generated by Canonical Correspondence Analysis; the occurrence matrix was constructed based on presence-absence of MAGs assigned to different bacterial genera. As predictors we included: the identity of the main fungal and the photosynthetic partners, and sequencing depth. Only metagenomes with more than 2 Gbp were included in this analysis, and only bacterial genera that occurred in at least five analyzed metagenomes. This ordination excludes two outliers: lichens involving fungi from Lichinomycetes and Eurotiomycetes.

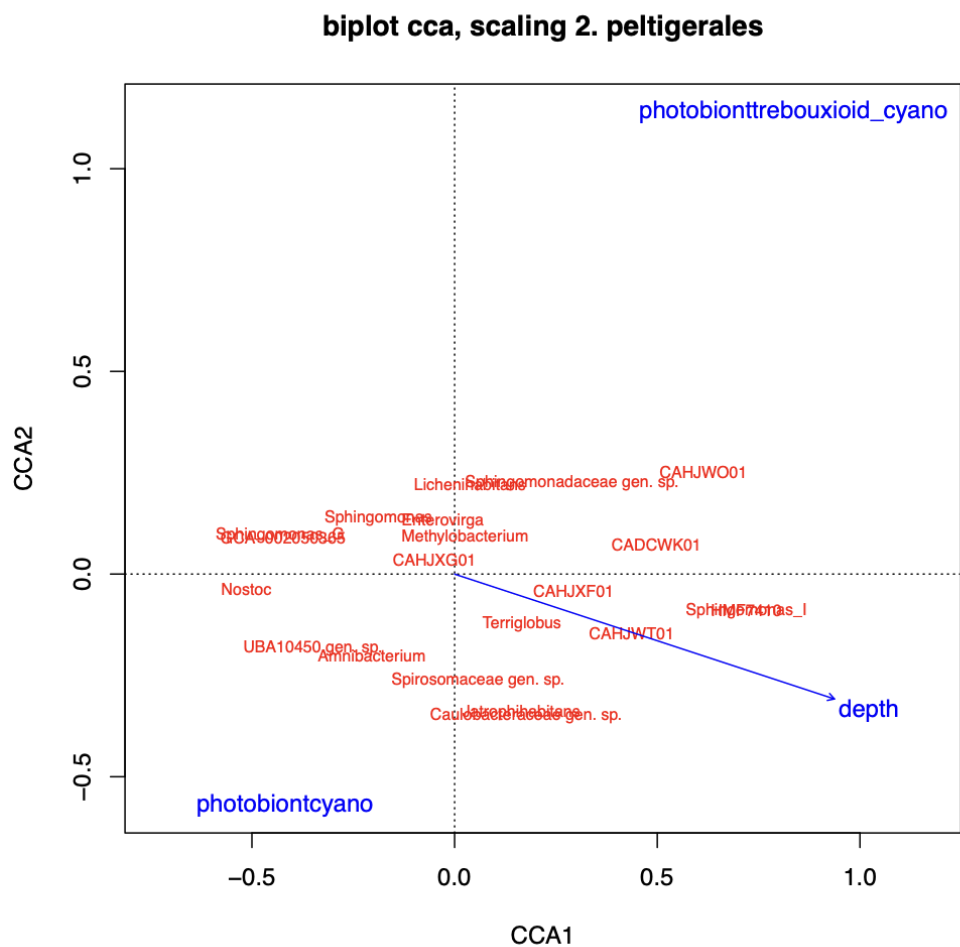


Fig. 4.7. CCA ordination plot of bacterial communities in peltigeralean lichens.

As predictors we included: the identity of the main fungal and the photosynthetic partners, and sequencing depth. Only metagenomes with more than 2 Gbp were included in this analysis, and only bacterial genera that occurred in at least two analyzed metagenomes.

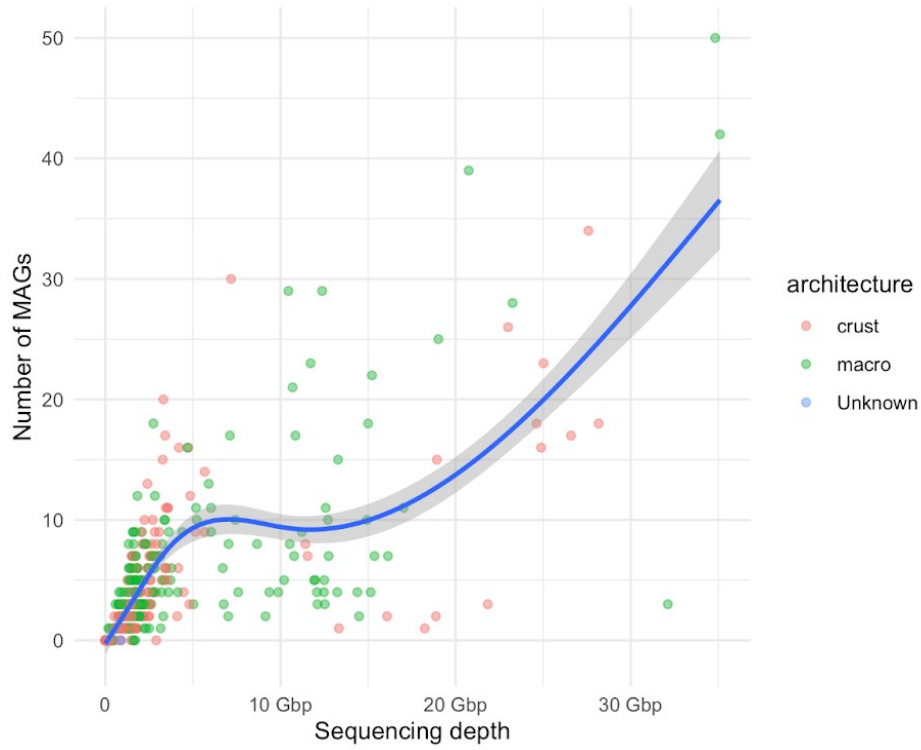


Fig. 4.8. Number of recovered MAGs as a function of sequencing depth (bp).

Each dot represents a metagenome coloured based on the lichen architecture type. The curve indicates a GAM smoothing.

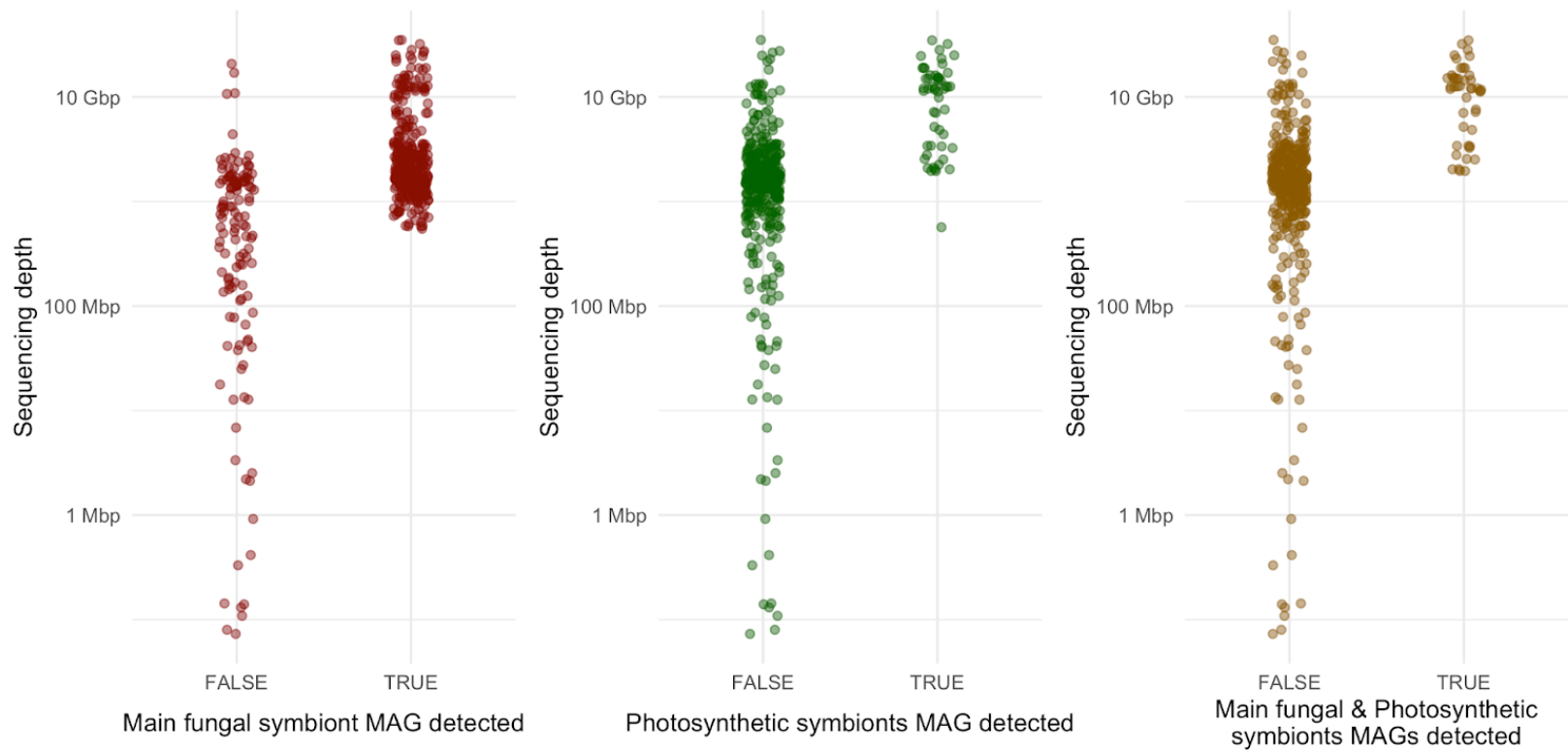


Fig. 4.9. Recovery of MAGs of the main two symbionts as a function of sequencing depth.

These graphs are based on the pre-dereplication set of MAGs, each dot represents a metagenome position based on whether it contained a MAG assigned to the main fungal symbiont and/or the photobiont.

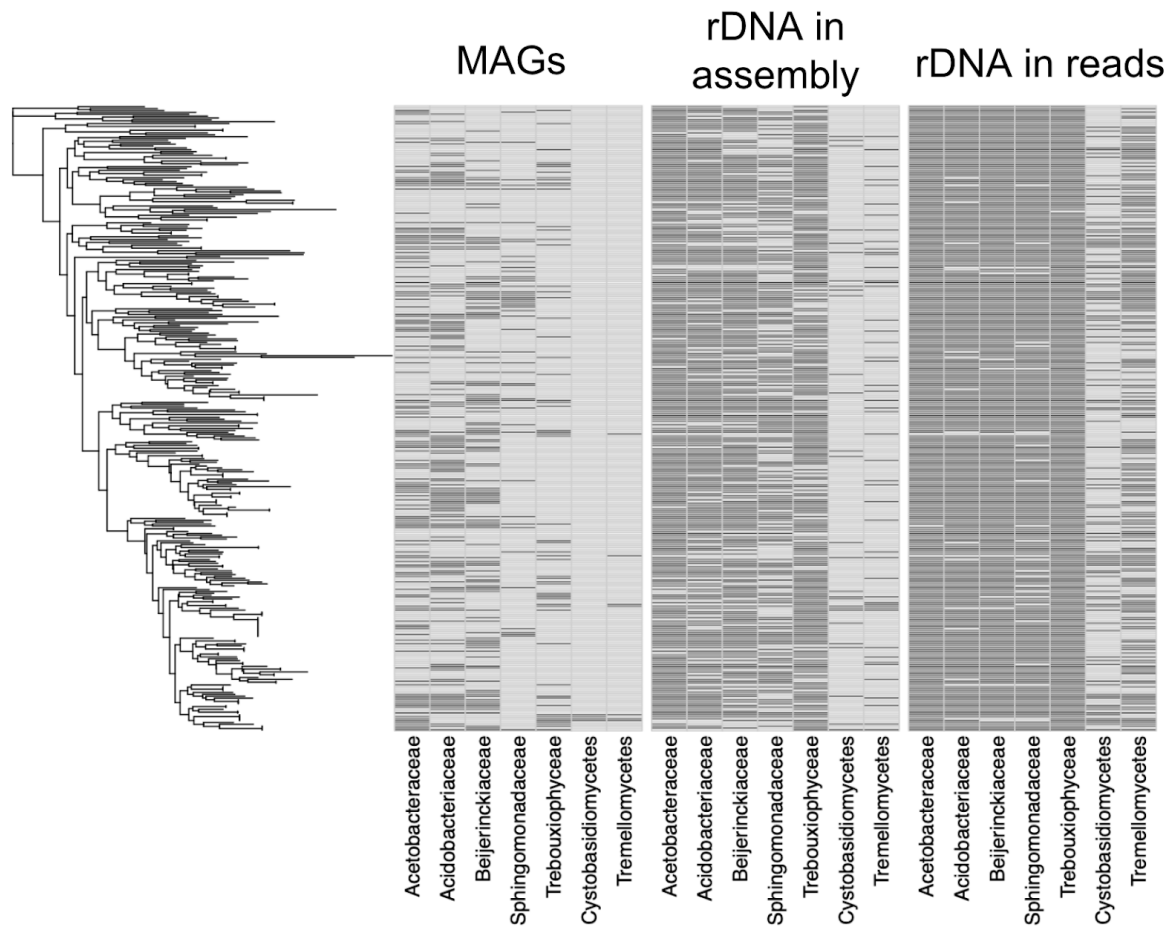


Fig. 4.10. Detection of the key groups of symbionts in lichen metagenomes based on three methods of screening: presence of MAGs, presence of rDNA (16S for prokaryotes and 18S for eukaryotes) in the metagenomic assemblies, and presence of rDNA in the raw, unassembled reads.

The tree on the left shows phylogeny of the main fungal symbionts, presence is indicated by the dark stripes. Here are shown data on the four most frequent bacterial families and on the three eukaryotic lineages known to be stably associated with lichens.

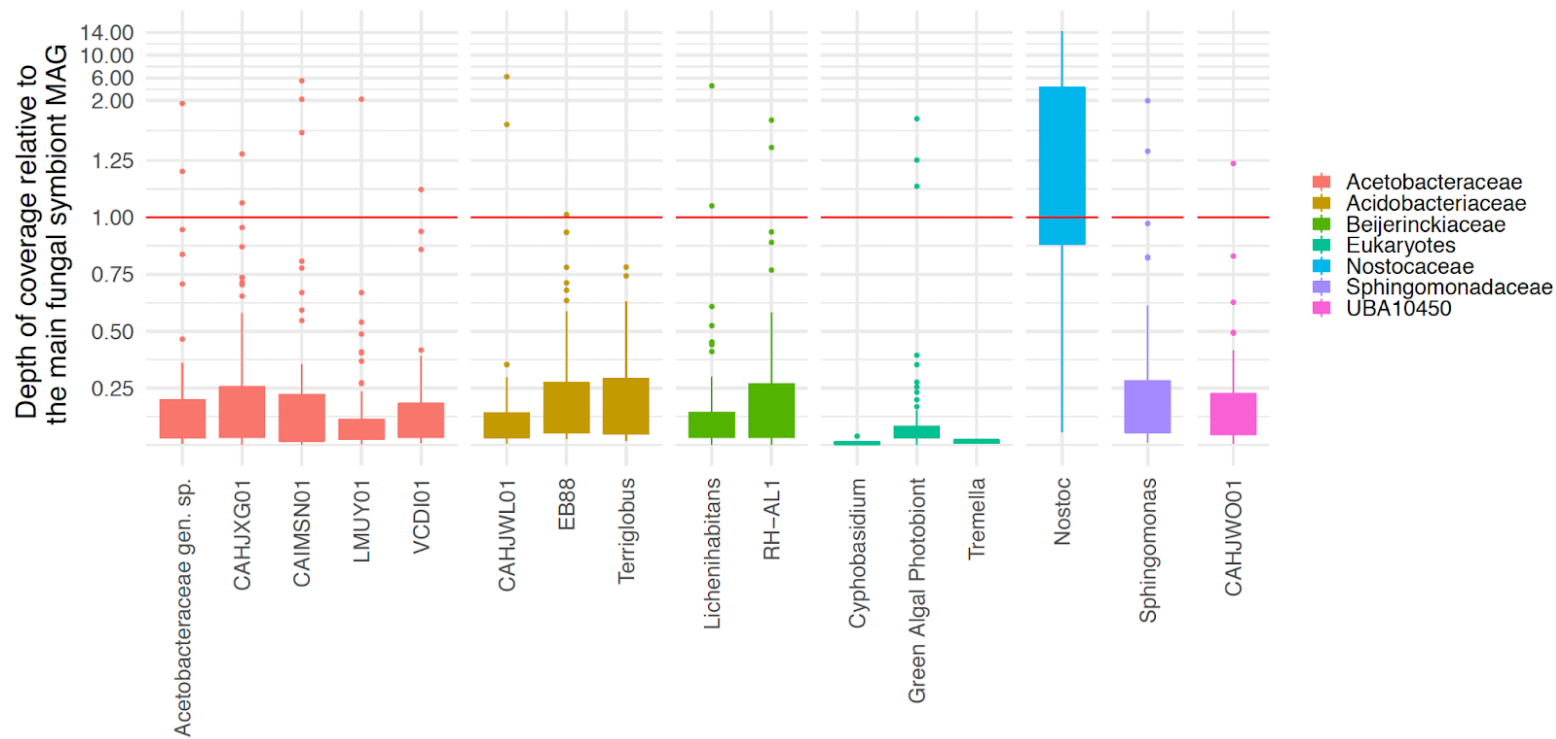


Fig. 4.11. Relative abundances of symbionts in lichen metagenomes.

The relative abundances were calculated by dividing the coverage depth of the symbiont MAG by the coverage of the main fungal symbiont MAG. Here are shown data on the 13 most frequent bacterial genera and the eukaryotes known to be stably associated with lichens. The red line shows 1:1 ratio, where the symbiont is estimated to have the same cellular abundance as the main fungal symbiont.

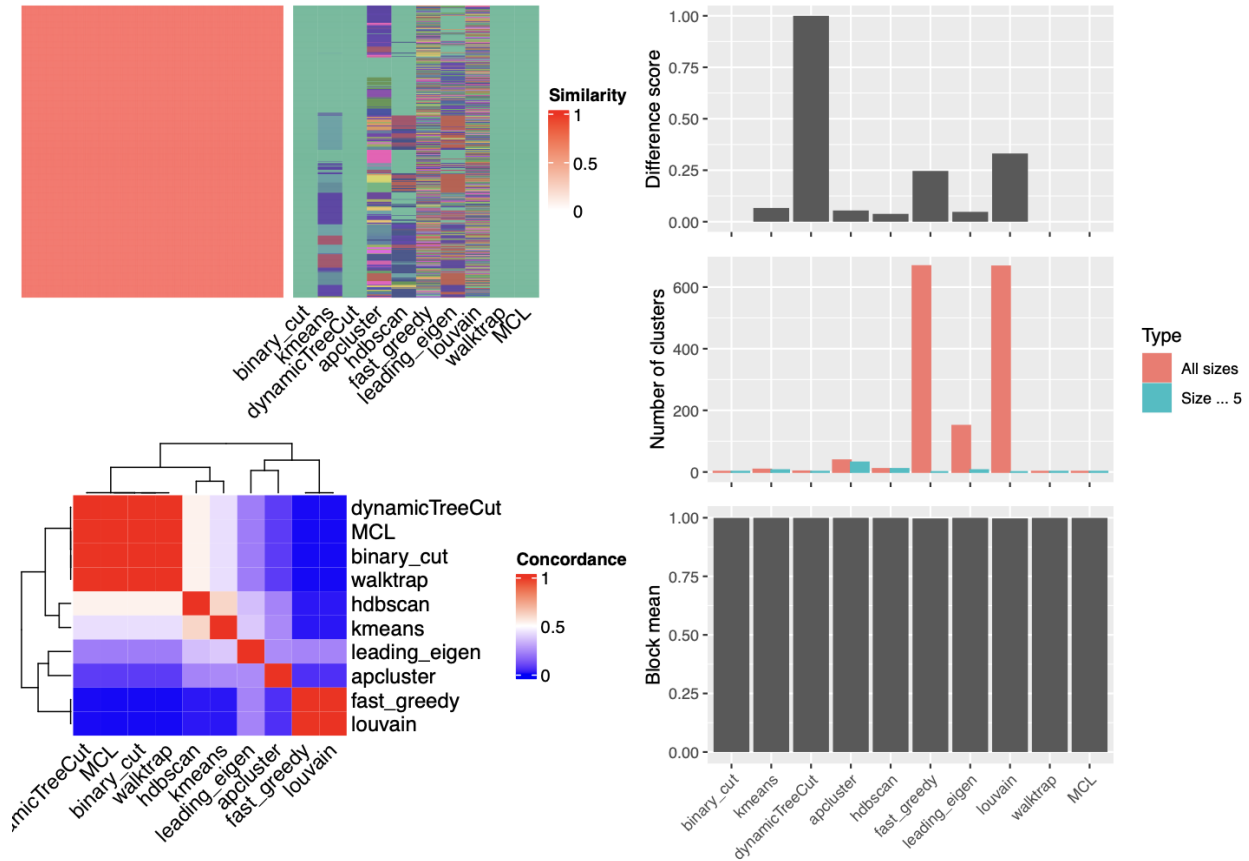


Fig. 4.12. Comparing different clustering methods for grouping bacterial MAGs based on their KEGG profiles.

We constructed the presence-absence matrix of KEGG modules in the analyzed MAGs (all bacterial MAGs that met the 90% completeness threshold). Next, we constructed the similarity matrix based on Pearson coefficients and analyzed it using ten clustering methods. The left panel shows: the heatmap of the similarity matrix with different classifications shown as bars (top) and the heatmap of pairwise concordance between the clustering methods (bottom). The right panel shows barplots for each clustering method: Difference score (top, measure of difference between the similarity metric between objects in one cluster and objects in different clusters), Number of clusters (middle), and Block mean (bottom, mean similarity values of the diagonal blocks in the similarity matrix). All the methods were applied to the similarity matrix, which was based on Pearson coefficients. The comparison was done using the SimplifyEnrichment R library.

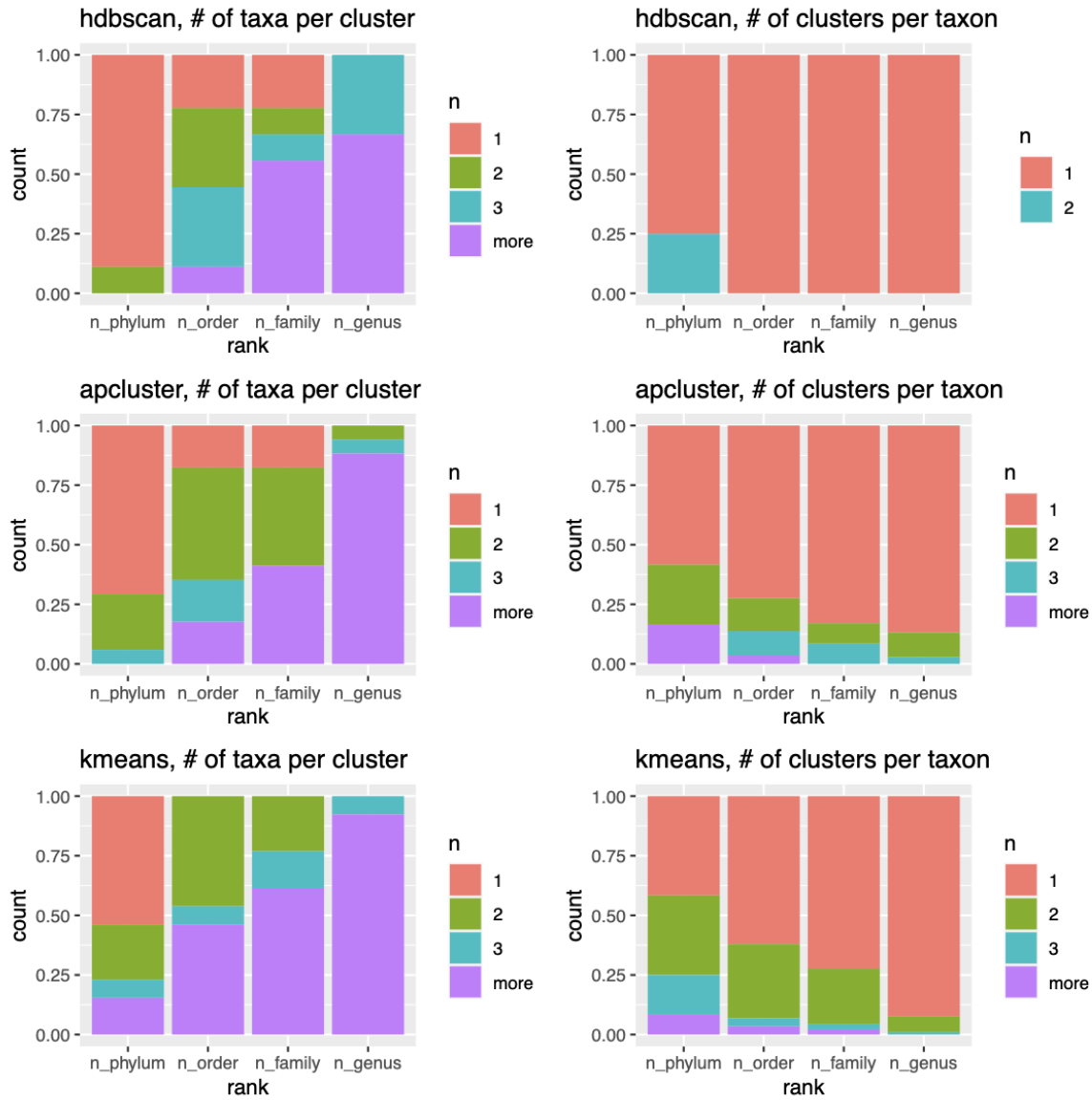


Fig. 4.13. Taxonomic coherence for the outcomes of three clustering methods: hdbscan, apcluster, and kmeans.

On the left: percentage of clusters that include 1, 2, 3, or more taxa for each taxonomic rank. On the right: percentage of taxa included in 1, 2, 3, or more different clusters for each taxonomic rank.

Tree scale: 1

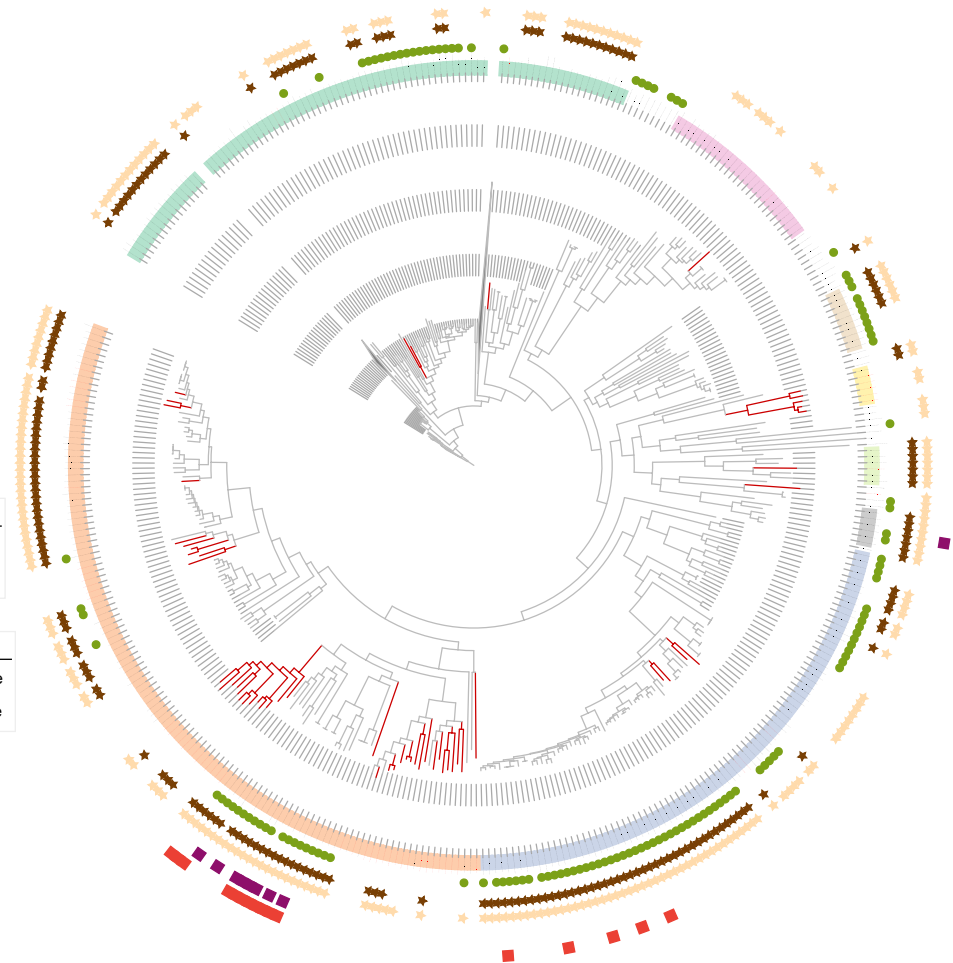
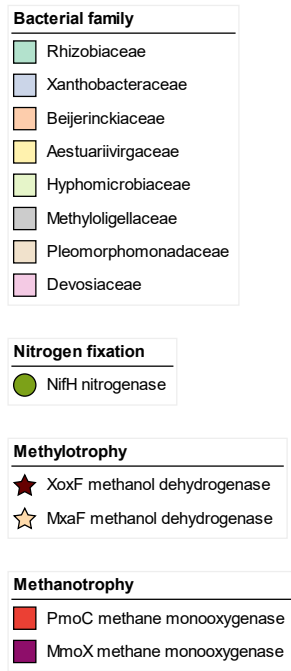


Fig. 4.15. Maximum likelihood phylogenetic tree of Rhizobiales.

The tree includes published genomes of Rhizobiales and Rhizobiales MAGs derived from lichen metagenomes (indicated in red). We generated the alignment of 120 marker genes using GTDB-Tk, and calculated the tree using IQ-TREE. The colour represents family-level taxonomic assignment. We used tblastn to search the genomes for key genes involved in nitrogen fixation and C1 metabolism. The presence of these genes is indicated with symbols. The full-size version of the tree in the graphic and Newick formats are available in FigShare (<https://doi.org/10.6084/m9.figshare.20097170.v1>).

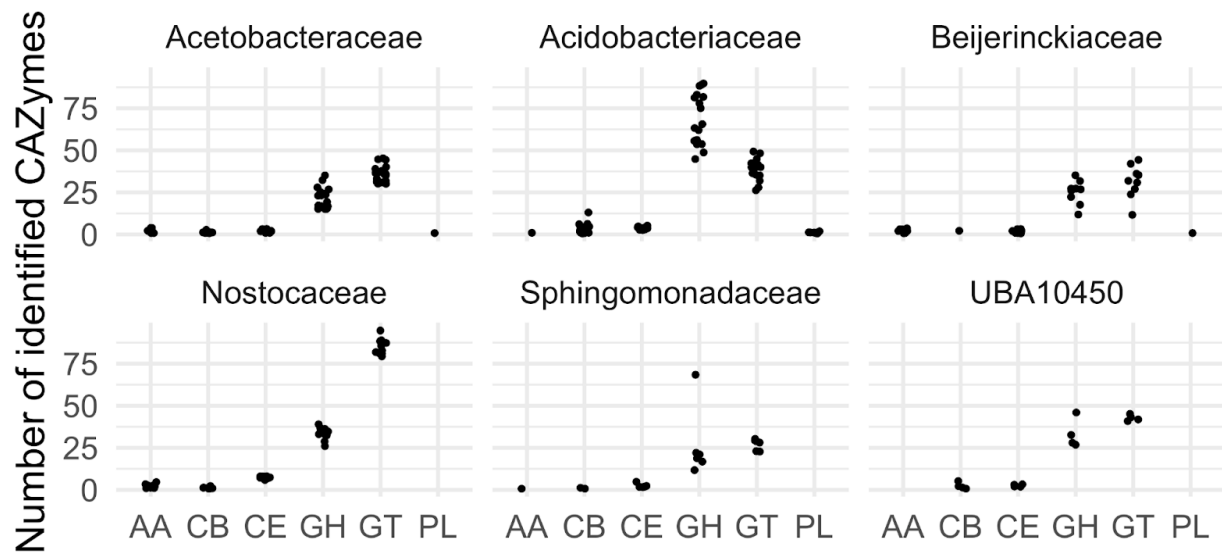


Fig. 4.16. Number of genes assigned to each CAZy class per MAG.

We annotated CAZymes in the MAGs selected for an in-depth annotation (from the 13 most frequent bacterial genera, with completeness $\geq 95\%$) using dbcan. The data here are grouped on the family level. The CAZy classes are: Auxiliary Activities (AA), Carbohydrate-Binding Modules (CB), Carbohydrate Esterases (CE), Glycoside Hydrolases (GH), Glycosyl Transferases (GT), and Polysaccharide Lyases (PL).

Chapter 5. Linking the abundance of basidiomycete yeasts to the lichen phenotype

A version of Chapter 5 is intended for publication as: Tagirdzhanova, G., Cook, J., Vinebrooke, R. & Spribille, T. Linking the abundance of basidiomycete yeasts to the lichen phenotype.

5.1. Abstract

Basidiomycete yeasts are the most recently discovered and the least studied members of the lichen symbiosis. Until now, our ability to explore their role in the symbiosis was limited due to a) our inability to re-create lichens *de novo* in the lab and b) uncluturability of the yeasts. Here, we present our method of linking individual members of the symbiosis to the lichen phenotype. We used digital droplet PCR to quantify the lichen yeasts and explored how their abundance correlates with phenotypic traits. Using *Bryoria fremontii* as our study system, we confirmed the previously suggested link between the yeast abundance and the concentration of vulpinic acid. Our exploration of whether the yeasts affect lichen water storage remain inconclusive.

5.2. Introduction

Until recently, lichens have been viewed as a symbiosis of a single fungus with one or more photosynthesizing partners (an alga or cyanobacterium). Under this scenario, the photosynthesizing partner provides the fungus with the products of photosynthesis. The fungus, in turn, creates a symbiotic body to host the algal cells and has full control over the lichen phenotype (Ahmadjian 1993). However, evidence has emerged that two or even three fungi can be stably present in a single lichen symbiosis (Spribille et al. 2016, Tuovinen et al. 2019, Tagirdzhanova et al. 2021). The “additional” fungi are basidiomycete yeasts from the classes Cystobasidiomycetes and Tremellomycetes, which are present in some lichens in addition to the

main fungal symbiont. What role the yeasts play in lichens and how they relate to other symbionts remains largely unknown.

The discovery of lichen yeasts resulted from a study into the phenotypic variation in *Bryoria fremontii* lichens (Spribille et al. 2016). Historically, *Bryoria tortuosa* and *B. fremontii* were treated as two different lichens, based on their appearance. Both lichens contain secondary metabolite called vulpinic acid — a mildly toxic yellow pigment that absorbs UV light and is derived from aromatic amino acids (Phinney et al. 2019). However, the distribution of vulpinic acid is different: it is present in *Bryoria tortuosa* throughout the thallus, while in *B. fremontii* it is restricted to the reproduction structures (Brodo & Hawksworth 1977). Velmala et al. (2009) discovered, based on a four-loci phylogeny, that the main fungal partner in both lichens was phylogenetically indistinguishable. This discovery led to lumping the two lichens together into a single species, and opened a new question: where does the phenotypic difference come from? Spribille et al. (2016) used metatranscriptomics to answer this question. They found that yellow specimens, traditionally classified as *B. tortuosa*, had higher abundance of *Cyphobasidium*, a previously undescribed basidiomycete yeast. The yeasts were present in a large variety of lichens (Spribille et al. 2016), but only in *Bryoria fremontii* did their abundance appear to be linked to the lichen phenotype. This link prompted Spribille et al. (2016) to hypothesize that the yeasts in some way participate in or enhance the biosynthesis of vulpinic acid — and therefore play a role in determining the phenotype of the symbiosis. Several constraints made it impossible to test the hypothesis experimentally. First, to this day the *Cyphobasidium* yeasts have not been isolated in culture. Second, the enzymatic pathway for vulpinic acid synthesis was, and still is, uncharacterized. Finally, at that time no genome was available for any of the symbionts, rendering generalized functional predictions difficult.

In Tagirdzhanova et al. (2021), we obtained the first genomes of two lichen yeasts — *Cyphobasidium* and *Tremella* — from the *Alectoria* lichen, a lichen symbiosis closely related to *Bryoria*. By comparing the yeast genomes to the genomes of their relatives and the main fungus genome, we generated a new set of hypotheses. First, we hypothesized that the yeasts do not contribute much to the synthesis of secondary metabolites. The secondary metabolism “arsenal” in the yeast genomes was only a fraction of that of the main fungus. However, we could not rule out that vulpinic acid is nonetheless produced by the yeasts: data from *Alectoria* (which does not contain vulpinic acid) cannot be used to settle this question. Second, we hypothesized that the yeasts produce hygroscopic polysaccharides that help the lichen to retain water.

Predictions from Spribille et al. (2016) and Tagirdzhanova et al. (2021) begged the question: how can we more accurately quantify or qualify the effects of yeasts on lichen phenotype? The standard tools and approaches used on other symbioses are inaccessible for lichens: to this day only one lichen symbiont has been successfully transformed (Park et al. 2013), lichen symbionts are notoriously hard to grow in the lab (McDonald et al. 2013), and experiments on recreating lichen symbiosis in a controlled setting have had limited success. An alternative approach is to use intact lichens sampled from nature, and to identify features of the symbiosis that are correlated with the presence and/or abundance of symbionts.

We set out to create a refined protocol for exploring correlations between symbiont abundance and phenotypic traits. First, we aimed to develop a way of measuring symbiont abundance that would be more cost-effective than costly metatranscriptomes. To this end, we experimented with quantitative PCR (qPCR), before ultimately developing a digital droplet PCR (ddPCR) protocol. Second, based on the proposed hypotheses, we created a set of measures to assess lichen phenotypes. We measured the concentration of vulpinic acid. In this study, we wanted to assess

whether treating vulpinic acid concentration as a continuous variable, as opposed to the binary presence/absence assignments of Spribille et al. (2016), would strengthen or weaken inferences. We also expanded the phenotype assessment beyond secondary metabolites, and included measuring water-holding properties of the lichen. Here, we report on the outcomes and pitfalls associated with these approaches as applied to lichen thalli gathered in nature.

5.3. Methods

5.3.1. Specimen collection and handling

In total, we collected 120 samples of *Bryoria fremontii* in 13 locations in British Columbia (Canada). To ensure that a broad range of samples were available for downstream steps, we manually categorized the samples into five categories based on colour, from “1” being bright yellow to “5” being dark brown, and “thick” to “thin” (Fig. 5.1). An initial batch was collected in Fall 2020 (“first batch”), and after it was determined that more samples were needed in certain categories (e.g. 1 and 2 and thin), more samples were collected in Spring 2021 (“second batch”) (Table 5.1).

We stored the lichen specimens air-dried. From each specimen, we took three subsamples, used for: 1) DNA extraction, 2) measuring vulpinic acid concentration, and 3) measuring water storage parameters and thallus surface area.

5.3.2. DNA extraction

All DNA extractions were done using the DNeasy Plant Mini Kit (Qiagen). We followed the standard protocol with two modifications. First, the lysis step was extended to one hour. Second, we added an extra centrifugation step during the DNA extraction. In a standard protocol, the lysate is centrifuged once (for 5 min at 14,000 rpm) before being filtered through a QIAshredder

Mini spin column. In our modification, we centrifuged the lysate twice, each time discarding the pellet and transferring the supernatant to a new tube.

5.3.3. Digital droplet PCR (ddPCR) survey

5.3.3a. Overview

To measure the abundance of symbiotic partners within *Bryoria fremontii*, we used ddPCR, a quantitative PCR-based method. Digital droplet PCR (ddPCR) is a PCR-based method used for quantification (Kokkoris et al. 2021). This method is based on splitting samples into miniscule droplets, each of which undergoes PCR amplification independently. The ratio of “positive” and “negative” droplets is then used to calculate the concentration of the target. ddPCR operates in absolute concentrations and does not rely on standard curves. Consequently, it is much less sensitive to reaction efficiency compared to qPCR and works better on low-abundance targets (Taylor et al. 2017).

Measuring absolute abundance of symbionts (i.e. number of cells per mg of lichen mass) would not be possible, since the estimates would be heavily affected by the efficiency of DNA extraction. Anecdotally, we noticed that said efficiency is highly variable and the same amount of lichen material can result in vastly different DNA yields. Instead, we measured the relative abundance of the yeasts scaled against the summed abundance of the main fungus and the alga. In total, we measured abundances of four symbionts: the main fungus (hereafter called the lecanoromycete), the algal symbiont (*Trebouxia*), and two yeasts. One was *Cyphobasidium*, which was already known to be stably present in this lichen (Spribille et al. 2016). The other was *Tremella*, which is stably associated with several lichen symbioses (Tuovinen et al. 2019, 2021, Tagirdzhanova et al. 2021), and has been occasionally reported from *Bryoria fremontii* (Lindgren et al. 2015).

To design a ddPCR survey for several non-cultured organisms that until now lacked a sequenced genome, we started by obtaining Metagenome-Assembled Genomes (MAGs) (Fig. 5.2) and identifying BUSCO genes that could serve as a target. In theory, we could have proceeded directly to designing ddPCR primers from these sequences. However, at this stage we did not know how variable the target genes are within the selected lineages. To clarify this, we added an extra screening step. We used the metagenome-derived sequences to design the first set of primers. For each target and each organism, these primers amplified a larger region within the target gene. Using these primers, we produced multiple sequences of each target, and then used them to create the final ddPCR primers. We tested the primers with qPCR.

5.3.3b. Metagenomic analysis: obtaining MAGs

We made a *Bryoria fremontii* metagenome from a sample collected in spur of Trophy Mountain Rd., British Columbia, Canada (Sample ID tort_1, Table 5.1). The sample was frozen at -80°C and pulverized with a TissueLyser II (Qiagen). We extracted DNA with DNeasy Plant Mini Kit (Qiagen), and prepared a metagenomic library using Illumina Library Prep Kit. The library was sequenced by BC Cancer on an Illumina HiSeq X machine.

The metagenomic data was filtered to remove adapters and human contamination using the READ_QC module of the metaWRAP pipeline (v1.2, Uritskiy et al., 2018). Then, we assembled the metagenome using metaSPAdes (v3.13.0, Nurk et al. 2017) and binned it with CONCOCT (Alneberg et al. 2014). We identified Metagenome-Assembled Genomes (MAGs) using BUSCO (v4.1.4, Seppey et al. 2019) in the --auto-lineage mode (Table 5.2).

From the *Bryoria fremontii* metagenome, we identified three MAGs: from the lecanoromycete fungus, the alga, and *Cyphobasidium*. To obtain the final lecanoromycete MAG, we merged

several bins (see Chapter 2). We used a custom R script to make a GC%/coverage plot and based on the plot we merged several bins to get the final MAG of the lecanoromycete fungus.

Unlike the lecanoromycete fungus and the alga, the *Cyphobasidium* MAG required an extra taxonomic analysis, since BUSCO was only able to place it on the phylum level. We confirmed the MAG identity by comparing it to the *Cyphobasidium* from *Alectoria* (Chapter 2). Their average nucleotide identity (ANI) was calculated with the EZBiocloud ANI calculator (Yoon et al. 2017), and it was only a little below the species-level threshold (ANI = 92%; Saary et al. 2022), thus we treated this MAG as Cyphobasidiales.

Tremella did not yield a MAG, but we were able to detect its rDNA in the metagenomic assembly. For that, we searched the metagenomic assembly with blastn using ITS (internal transcribed spacer) of *Tremella huuskonenii* as a query (NCBI ID: NR_159015.1). The retrieved sequence was identical to the *Tremella huuskonenii* ITS.

To obtain a *Tremella huuskonenii* MAG, we used an additional metagenome made from “galls” associated with the basidiomata of *Tremella huuskonenii* on a different *Bryoria* lichen. The metagenomic library was produced as follows: DNA was isolated from the gall as described above, the library was prepared using a NEBNext Ultra II DNA Library Prep Kit (New England BioLabs) and sequenced on an Illumina HiSeq X machine by NGX Bio (U.S.). The metagenomic data was assembled and binned as described above. The tremellomycete MAG was identified with BUSCO (Table 5.2).

5.3.3c. Selecting potential targets

Using a custom script, we prepared a list of potential single-copy genes that could serve as ddPCR targets. We selected only BUSCO genes that were present in single copy in all analyzed

MAGs. To account for the possibility that some of these genes are actually duplicated in their MAGs, but that this was unnoticed due to faulty assembly, we filtered this list in several ways. First, we excluded genes that resided on contigs whose median depth of coverage was different from that of the rest of the MAG. The cut-offs were determined manually by checking the histograms of median coverage depths. Second, we excluded the genes whose coverage was too different from the rest of their contig (relative difference >0.2). Finally, we removed all genes that were near the ends of their contigs (<200 bp away). From the remaining genes, we selected four BUSCO orthologs as potential targets: SNARE (BUSCO ID 1182451at2759), GNAT domain/ Acyl-CoA N-acyltransferase (1355894at2759), Anamorsin (1588798at2759), and Ubiquinol-cytochrome c chaperone (1428265at275).

We managed to obtain *Tremella* sequences of the selected genes from *Bryoria fremontii*, even though this metagenome did not yield a *Tremella* MAG. For that, we got the *Tremella* sequences from the *Tremella* “gall” metagenome and used them as a blastn query to search the *Bryoria fremontii* metagenomic assembly. The search resulted in several hits to unbinned low-coverage contigs; the retrieved sequences were then used to design primers.

5.3.3d. Primer design

To design the first set of primers, we gathered the target sequences from the *Bryoria fremontii* metagenome, and added orthologs from closely related MAGs: ascomycete, alga, and *Cyphobasidium* from *Alectoria* (see Chapter 2), plus *Tremella* from the “gall” metagenome. We divided the sequences by taxonomy (i.e. separated into ascomycetes, algae, *Cyphobasidium*, and *Tremella*), aligned each group individually using MAFFT (v7.427, flags --genafpair --maxiterate 10000; Katoh & Standley 2013). For each target and each organism, we made primers that amplified a region within the target gene, using Primer-BLAST (Ye et al. 2012).

Using these primers, we screened 10 DNA extractions from *Bryoria fremontii* lichens. We used the following PCR program: an initial denaturation at 95°C for 5 min, followed by 35 cycles of 95°C for 30 sec, 57°C for 30 sec, 72°C for 30 sec, and an extension of 72°C for 7 min. We used the KAPA 3G Plant PCR kit (Roche Sequencing Solutions). The amplicons were cleaned using Exonuclease I and Shrimp Alkaline Phosphatase (New England BioLabs), and then sequenced by Psomagen Inc.

We used the resulting sequences to design the final primers used for ddPCR (Table 5.3). We aligned the sequences as described above and manually created consensus sequences for each gene/organism combination. The consensus sequences were then analyzed using Primer Express (v3.0, Applied Biosystems), with default settings. We picked primer pairs that would produce amplicons 75 –150 bp long. The primers were additionally checked with Primer-BLAST, to select the most specific primer pairs. For that, we used the *Bryoria fremontii* metagenomic assembly as a database, and checked how many different regions each primer pair is predicted to amplify.

5.3.3e. qPCR

We checked the primers experimentally by qPCR. The qPCR experiment was designed following the standard guidelines (Taylor et al. 2010) and ran on a QuantStudio 3 System. Each 10 µL reaction contained 5 µL of GoTaq qPCR Master Mix (Promega), 2.5 µL of primer mix (with final primer concentration of 500 nM), and 2.5 µL of DNA. The PCR program was as follows: 95°C for 2 min, 40 cycles of 95°C for 15 sec and 60°C for 1 min. The optimal melting temperature and primer concentration were determined experimentally. Only the primer pairs that consistently showed a single peak on their melting curves were used for further analysis. Each qPCR reaction was tested in triplicate; each qPCR plate included negative controls.

5.3.3f. ddPCR

ddPCR was done on a Bio-Rad QX200 Droplet Digital PCR System. Each reaction contained 12.5 μL of QX200ddPCR EvaGreen Supermix, 2 μL of primer mix (with the final concentration of 160 nM), 1 μL of DNA, and 9.5 μL of water. The ascomycete was expected to be by far the most abundant organism, and to balance it out we diluted the DNA ten times for the reactions with the ascomycete-specific primers. For the rest of the organisms, we used undiluted DNA. We used four primer pairs, one for each organism. Each primer pair amplified a region within the single-copy SNARE gene (Table 5.3). The PCR program was as follows: 95°C for 5 min, 40 cycles of 95°C for 30 sec and 60°C for 1 min, 4°C for 5 min, 90°C for 5 min. Raw data was collected and analyzed using QuantaSoft (v1.7.4.0917). We excluded all “suspicious” runs, i.e. runs where the separation of positive and negative droplets was not clear (see Kokkoris et al. 2021; see Fig. 5.3A for a good example). To calculate the relative abundances of *Cyphobasidium* and *Tremella*, we related their number of copies per μL to the summed number of copies of the ascomycete and the alga.

5.3.4. HPLC

High-performance liquid chromatography (HPLC) analysis was performed following the protocol from Phinney et al. (2019). For each lichen sample, we freeze-dried 30 mg of the sample and ground it using a TissueLyser (Qiagen). We added 1 ml of extraction solution (80:20 acetone: methanol) for 1 hour for extraction of the vulpinic acid. After the extraction, we rinsed the samples twice with 1ml of extraction solution and filtered them using a 0.7 μm Whatman filter. The filtered samples were then dried under compressed nitrogen gas. Injection solution (100% methanol) was added to dried samples prior to injection. For each sample, an injection volume of 20 μL was run on an Agilent 1100 Series HPLC. Separation was achieved using an

Eclipse Plus C18 column (Agilent Technologies) with a flow rate of 1 ml/min. Solution A was composed of 1.5% tetrahydrofuran and 0.25% phosphoric acid in milli-Q water, and Solution B was 100% methanol (see Phinney et al. 2019, Asplund and Gauslaa 2007).

As a standard, we used a series of dilutions of a commercially available vulpinic acid (Santa Cruz Biotechnology). Vulpinic acid was identified in the samples based on the spectra and retention time matching that of the standard. The area under the spectra was used to quantify the vulpinic acid in each sample.

5.3.5. Water Storage

To assess water storage of lichen samples, we measured three characteristics: wet mass (WM), dry mass (DM), and surface area (SA). We followed the protocol from Esseen et al. (2015) with minor modifications. From each lichen thallus, we took a sample of 65–380 mg. Each sample we immersed in water until full hydration. To remove the excess water, we gently shook each sample and pressed it between two paper towels for 5 sec. Immediately after, we weighed the samples; this measurement was the wet mass. To get the dry mass, we dried the lichens at room temperature for 24 h and weighed them.

To measure the surface area, we used WinRHIZO scanner and software (v4.0B, Regent Instrument Inc.). The WinRHIZO system is designed to analyze the morphology of plant roots, but given the hair-like morphology of *Bryoria* lichens, it was ideally suited for our analysis (Fig. 5.3B). Using the default settings, we scanned each lichen sample used for the experiment and estimated its surface area.

We defined Water Holding Capacity (WHC) as $(WM - DM) / SA$. The percent water at saturation was defined as $(WM - DM) * 100 / DM$. Specific thallus mass (STM) was defined as DM / SA . For these statistics, we followed the definitions from Esseen et al. (2015).

5.3.6. Data analysis and visualization

For data manipulation and visualization, we used R (v4.1.0, R Core Team 2013) and the following libraries: dplyr (v1.0.8, Wickham et al. 2018), ggplot2 (v3.3.5, Wickham et al. 2016), and tidyr (v1.2.0, Wickham & Girlich 2022). To analyze the relationship between the relative yeast abundances and the vulpinic acid concentration or water storage parameters, we built generalized additive models, using the gam function from the MGCV library (Wood et al. 2016). To analyze the relationship between the colour of lichen samples and their characteristics (vulpinic acid concentration and relative yeast abundance) and for testing the batch effect on the WHC experiment, we used ANOVA as implemented in the CAR library (Fox & Weisberg 2019). We used ANOVA after confirming that the assumption of normality of residuals is met.

5.4. Results

5.4.1. *Cyphobasidium* and *Tremella* are ubiquitous

The lecanoromycete and alga were detected in all samples. Both yeasts were detected in nearly every lichen sample: of 120 analyzed samples, only one verifiably lacked *Cyphobasidium*, and only two lacked *Tremella*. For each organism, we excluded several ddPCR reactions, in cases where positive and negative “clouds” could not be unequivocally separated.

We used the ddPCR results to calculate the abundance ratios of lichen symbionts. In all cases, the lecanoromycete was by far the most abundant organism (Fig. 5.4). The lecanoromycete: alga ratio varied significantly between different specimens (Fig. 5.4). The median ratio was 13:1

(standard deviation 6.4). As expected, the relative abundances of both yeasts were only a fraction of that of the alga (Fig. 5.4). The lecanoromycete:yeast ratios ranged from 26:1 to 28,000:1. The lowest detected concentration of a yeast was 0.14 copies per μL , which translates into 6 genomes in total present in the ddPCR reaction prior to amplification. In 60% of the samples, *Cyphobasidium* was more abundant than *Tremella*.

The ddPCR results were largely consistent with our metagenomic analysis. Coverage depth of a MAG within a metagenome can provide a proxy for cellular abundance, and we used the *Bryoria fremontii* metagenome to validate our ddPCR results. In this metagenome, the ratio of median coverage depths of the lecanoromycete and algal MAGs is 11:1 (Table 5.2), which was close to the ddPCR estimate. Similarly, the metagenome-derived lecanoromycete:*Cyphobasidium* ratio was 57:1, and the same sample used in the ddPCR assay gave a 65:1 ratio. *Tremella* was detectable in the metagenome but did not yield a MAG, indicating that it was less abundant than *Cyphobasidium*. This inference is supported by our ddPCR results: we estimated that in the sample used for the metagenome, *Tremella* was half as abundant as *Cyphobasidium*.

5.4.2. Vulpinic acid quantity as a function of yeast abundance

As we suspected already from classifying lichen samples into groups based on colour, vulpinic acid concentration is, in fact, a continuous variable and not a binary. In the studied *Bryoria fremontii* samples, vulpinic acid concentration continuously varied from 0.01 to 13.3 $\mu\text{g/g}$.

Vulpinic acid concentration showed a weak positive correlation with the relative abundance of *Cyphobasidium* and a weak negative correlation with the relative abundance of *Tremella* (Fig. 5.5). Both trends were statistically significant ($p < 0.01$) but explained only a small fraction of the deviance (9% for *Cyphobasidium*, 14% for *Tremella*, and 22% in a model with two predictors).

In the case of *Cyphobasidium*, the trend was no longer supported after removing the outliers (two samples with relative abundance >0.02).

The relationship between vulpinic acid concentration and lichen colour turned out to be less straightforward than expected (Fig. 5.6). We confirmed that in general more yellow specimens had more vulpinic acid, but this link was not strong ($p < 0.001$, $R^2_{\text{adj}} = 0.28$). Even among the least yellow group, some specimens had much higher vulpinic acid concentration than average, and higher than some specimens in the most yellow group. Relative yeast abundances followed the same trend as outlined above: *Cyphobasidium* tended to be more abundant in yellow samples, *Tremella* tended to be less abundant (Fig. 5.6, $p < 0.01$, $R^2_{\text{adj}} = 0.17$ for *Cyphobasidium* and 0.12 for *Tremella*). These trends were stronger and did not disappear after removing the outliers.

5.4.3. Thallus morphology and water storage

We successfully measured the water storage of the lichen samples, and showed its relationship to thallus morphology, echoing Esseen et al. (2015). WHC is strongly correlated with STM, a proxy of branch thickness: with surface area being equal, lichens with thicker branches can retain more water (Fig. 5.7). Consequently, to test whether the yeast abundance correlates with water storage, we needed to exclude thallus morphology as a potential confounding factor.

While processing the first batch of lichen samples, we noticed a relationship between lichen colour and thallus morphology. Yellower samples — and lichens with higher vulpinic acid concentration — tended to have thicker branches, and consequently higher STM (Fig. 5.8). To balance the skew, we collected the second batch with the specific goal of getting thin yellow samples. The second batch indeed does not demonstrate the correlation between colour and morphology (Fig. 5.8).

We found no support for our hypothesis that higher abundance of yeasts is linked with greater water storage. Neither WHC nor percent water content at saturation were correlated with the relative abundance of the yeasts (Fig. 5.7). This was true regardless of whether we used as predictors *Cyphobasidium* abundance, *Tremella* abundance, or the total abundance of the yeasts. These results were complicated by a difference between the two batches of samples we processed. Water storage was higher in the samples we collected and processed in Fall 2020 than in Spring 2021 ($p < 0.001$, for WHC and percent water at saturation; $R^2_{\text{adj}} = 0.26$ and 0.25 respectively) (Fig. 5.7). We suspect that this difference can be attributed to a combination of two experimental factors. First, in the Fall 2020 batch, the lichen samples were immersed in water until “full hydration”, which we estimated happened after about 30 min. However, this estimation could have been mistaken. In Spring 2021, the lichen samples were immersed in water for 3 hours instead, and this batch had significantly higher water storage. After we realized this difference, we tried to correct the experiment and rerun it with standardized hydration time. Still, the effect persisted, as lichens from the first batch appeared to lose some of their dry mass. Thus, we suspect that the second factor was “shedding” caused by the handling of dry lichen specimens in the lab.

5.5. Discussion

Lichen phenotype emerges as a product of a symbiotic relationship (Ahmadjian 1993). Historically, lichens have been viewed as a binary symbiosis between a fungus and a phototroph. Under this model, the phototroph is vitally important for the symbiosis, but the fungus holds the “controlling interest” in determining how the lichen looks and behaves. All other organisms present in lichens, such as yeasts and bacteria, were viewed as external to the symbiosis and not contributing (reviewed in Spribille 2018). This view has changed recently, as more data became

available, especially through genomics and transcriptomics (Grimm et al. 2021, Tagirdzhanova et al. 2021). Yeasts and bacteria are now hypothesized to play important roles in lichens. However, to this day the framework to test these hypotheses has been lacking, mostly due to our inability to alter lichen symbiosis in a controlled setting.

Our study is the first to look into how lichen phenotype is affected by the symbionts other than the main fungus and the alga. We developed a framework that allowed us to explore how the abundance of two lichen yeasts, *Cyphobasidium* and *Tremella*, correlates with features of the lichen thalli.

5.5.1. What we learned about the lichen and its yeasts

Here, we tested two hypotheses. First, we hypothesized that *Cyphobasidium* abundance correlates with the vulpinic acid concentration. Second, we hypothesized that lichens with higher yeast abundance better hold water. In both cases, our results have opened more questions than they solved.

The original metatranscriptomic study showed that yellow lichens assigned to *Bryoria tortuosa* had more active *Cyphobasidium* cells (Spribille et al. 2016). This led us to hypothesize that the yeasts are involved in the biosynthesis of vulpinic acid, the yellow pigment in *Bryoria fremontii*. Hidden in this hypothesis is one assumption: that yellow lichens have more vulpinic acid. Based on our results, this assumption mostly holds up, but not entirely. Splitting lichens into groups based on their colour was done manually and these assignments lack precision. However, anecdotally we can say that some of the least yellow specimens had more vulpinic acid than some of the most yellow specimens. Since *Bryoria fremontii* is known to contain other pigments (Färber et al. 2014), we suspect that in these samples the yellow colour was obscured by the dark colour of the melanins. This opens three questions: 1) How does melanin concentration vary

within *Bryoria fremontii*? 2) How does melanin concentration correlates with the vulpinic acid concentration and the yeast abundance, if at all? and 3) What determines the pigment concentrations in *Bryoria fremontii*?

Cyphobasidium abundance was correlated with vulpinic acid concentration and with the lichen colour, but the trend was rather weak. This result was surprising, given the strong evidence from the original study that linked colour and yeast abundance (Spribille et al. 2016). The most likely explanation comes from one difference between the methods used. Spribille et al. (2016) used two methods, metatranscriptomics and FISH, which both measured the abundance of physiologically active cells that produce RNA. In contrast, our protocol measured symbiont abundances based on the “concentration” of their genomes, and therefore it counted all cells with intact DNA: active, inactive, and dead alike. If lichens indeed contain dead yeasts cells, as was hypothesized before (Tuovinen V. pers. comm.), their presence could obscure the patterns linking active yeast abundance to lichen traits. Whether this actually happens, remains to be tested.

Tremella has emerged as another nearly constant member of the *Bryoria fremontii* symbiosis. *Tremella* abundance was negatively correlated with vulpinic acid concentration, which could be explained by the toxicity of the substance (Emmerich et al. 1993). However, *Tremella* is ubiquitous not only in *Bryoria fremontii*, but in other lichens with vulpinic acid (Tuovinen et al. 2019). Alternatively, the causal link might be reverse: in this scenario, *Tremella* in large abundance can suppress the biosynthesis of vulpinic acid. Finally, the correlation can be caused by a confounding factor (e.g. microclimate conditions) that both the abundance of *Tremella* and vulpinic acid concentration.

We could not confirm or reject our hypothesis that the yeasts make lichens more hygroscopic. Our data showed no trends correlating WHC or percent of water at saturation with the abundance of *Cyphobasidium* and *Tremella*, either individually or together. This result can be explained by either 1) our hypothesis being incorrect, or 2) the methods not being sensitive enough to detect the pattern. Here, we followed the protocol from Esseen et al. (2015), where they showed statistically significant differences between water-retaining properties of lichen genera — but the three *Bryoria* species in their study did not differ. We cannot rule out that the effect of yeast abundance was present, but too small to be detected using this method.

The batch effect that we observed open new questions. Why did the two batches, one from Fall and one from Spring, differ in their water storage? One possibility is that this difference is entirely an artifact caused by slight differences in our experimental procedures and/or storage conditions. Alternatively, the difference can be real and caused by seasonality. As transplantation studies show, lichen water storage can change if lichens are moved to a location with different microclimate (Gauslaa & Solhaug 2001, Sonesson et al. 2007). It is, therefore, possible that seasonal changes in light and humidity can also affect lichen water storage and make lichens behave differently based on the time of the year they were collected.

5.5.2. The chicken-and-egg problem

Correlation studies like ours are the most accurate way of exploring the effect of individual symbionts on the lichen phenotype that we currently have. However, like with all correlation studies, our ability to infer causation is limited. It is important to explore the alternative explanation, i.e. that the difference in lichen phenotype affects the yeast abundance, not the other way around. While the data produced in this study cannot be used to settle this question, the metatranscriptomic study on *B. fremontii* offers some evidence (Spribille et al. 2016). They

compared *B. tortuosa* (yellow, high *Cyphobasidium* abundance) and *B. fremontii* (brown, low *Cyphobasidium* abundance), and found very little differential gene expression in the two main partners, the lecanoromycete and the alga, which makes it more likely that *Cyphobasidium* is the cause of phenotypic difference, not the other way around.

A link between symbiont abundance and lichen phenotype could result not only from a causal relationship between the two features, but also from an external factor affecting both of them. Environmental factors, such as light and humidity can affect the anatomy and physiology of a lichen, as was shown in transplantation studies (Gauslaa & Solhaug 2001, Sonesson et al. 2007). They could also, in theory, influence the composition and abundance of yeasts and bacteria. One way to better understand the relationship between the yeast abundance and the vulpinic acid concentration, is to explore what other factors play into determining the pigment profile of a lichen.

5.5.3. Strategies of measuring symbiont abundance

Lichen biologists before us have already tried to answer questions about lichens by measuring symbiont abundance. While no study before has linked lichen phenotype to yeast abundance, several studies have already explored the abundance of the alga and the lecanoromycete: alga ratio. Over the years, several vastly different methods have been used, including: 1) microscopy-based studies, i.e. counting algal cells in lichen cross-section or homogenized samples, or measuring the thickness of the algal layer (Sun & Friedmann 2005, Jairus et al. 2009, Tretiach et al. 2013), 2) estimations based on metabolite concentrations, e.g. the ratio between fungal ergosterol and algal chlorophyll (Palmqvist et al. 2002), and 3) DNA-based studies, i.e. metagenomics and qPCR (Greshake Tzovaras et al. 2020).

The toolkit available for measuring the abundance of lichen yeasts is much smaller, for several reasons. First, lichen yeasts are much less abundant than the alga, which requires the method to be sensitive. Second, in lichens the yeasts are embedded in an extracellular matrix, which renders them invisible to microscopy, unless sophisticated labeling techniques are used (Spribille et al. 2016). Finally, they are too closely related to the lecanoromycete, making it harder to find a metabolite that can be used as a proxy of their abundance (besides, the metabolite ratio method does not work well even for the alga, see Valladares et al. 1996).

Here, we explored two PCR-based methods, qPCR and ddPCR. Compared to their alternative, PCR-free metagenomics, both methods require more preparation, primarily due to primer design. Their advantage, however, is that they are more high-throughput. To measure yeast abundance via metagenomics, we would need to generate massive amounts of data for each sample, otherwise the low-abundance yeasts would not be detected (see Tagirdzhanova et al. 2021). In contrast, once a PCR assay is designed, it can be used to screen multiple samples for a fraction of the cost of one metagenome.

Designing the PCR survey was the most time-consuming part of this study, which was partially due to the steps we took to obtain the symbiont genomes. To ensure that the measurements of cellular abundances are unbiased and to exclude potential issues with gene duplication, we used single-copy genes as PCR targets, which required multi-step preparation, including metagenomic sequencing and analysis. The fact that we used single-copy genes makes our assay different from the only other study that applied qPCR to a basidiomycete fungus within a lichen. Not having a genome of *Tremella*, Bergmann & Werth (2017) used ribosomal 18S as a qPCR target, which has a variable number of copies per genome even within one species (Herrera et al. 2009). As

more genomes of lichen symbionts become available, designing an accurate qPCR or ddPCR survey will become less time consuming.

In this study, ddPCR clearly outperformed qPCR. The yeasts were present in lichens in such low abundance, that even in undiluted DNA extractions they were only a little above the detection threshold offered by qPCR, both in our experiment and in Bergmann & Werth (2017). ddPCR had no such limitation. In addition, ddPCR is independent of the reaction efficiency, which might be crucial in the case of lichen symbionts. During the screening before the primer design, we noticed large variation even in the conserved genes we selected as potential targets. For *Tremella*, it is known that multiple species often coexist within the same lichen (Tuovinen et al. 2019, 2021). In the case of qPCR, primers have to be designed in a way matching all potentially present strains, since a mutation in the primer-binding region of the target gene can lower the PCR efficiency and affect the results (Lefever et al. 2013). For the same reason, we were limited in which variety of qPCR we could use. TaqMan qPCR relies on additional oligonucleotides (the probes) that need to match the target, which would be impossible for us to design, in some cases, due to high variability of our targets. Instead, we had to use SYBR Green qPCR, which is less specific (Arikawa et al. 2008). In contrast, ddPCR results are not affected by the PCR efficiency, making the ddPCR method almost immune to strain heterogeneity.

What are the assumptions built into our approach? Here we followed a common strategy for quantifying low-abundance symbionts: measuring their abundance relative to the host (e.g., Chong & Moran 2016, Qian et al. 2018). This strategy presents the only way to standardize the raw ddPCR output — in the ideal world we would use instead the number of symbiont cells per mg of lichen, but in reality these numbers are too noisy due to the variable efficiency of DNA extraction. Using relative abundance relies on one assumption: that the cellular abundance of the

lecanoromycete and the alga have a linear relationship with the biomass. But what if they do not? In non-lichen fungi, the genome copy number does not always reflect biomass, which is especially true for fungi that form multicellular structures (Tellenbach et al. 2010). While no such study has been done on lichens, we know that the size of algal cells and hyphal compartments of the lecanoromycete varies within one thallus (Honegger 1993), which suggests that in lichens the genome count and biomass do not correlate perfectly either. Future studies will determine to which extent this variability affects the estimates of abundance.

5.5.4. Outlook

This study offers the first attempt to study the role of lichen yeasts by exploring how their abundance correlates with traits exhibited on the level of the symbiotic body. For that, we designed a ddPCR-based survey and screened lichen samples collected in nature. ddPCR emerged as a promising tool for characterizing lichen symbiosis, as it allowed us to process a large number of samples, and to quantify the low-abundance members of the symbiosis. We suspect that several factors might affect the accuracy of a ddPCR survey on lichens, chiefly the non-direct link between genome count and biomass in the dominant lichen symbionts, and the impact of physiologically inactive cells. One potential avenue for future research would be to expand this protocol and measure the abundance of physiologically active cells (e.g. by performing ddPCR on cDNA reverse-transcribed from an RNA extraction).

References

Ahmadjian, V. (1993). *The lichen symbiosis*. John Wiley & Sons.

Alneberg, J., Bjarnason, B. S., De Bruijn, I., Schirmer, M., Quick, J., Ijaz, U. Z., ... & Quince, C. (2014). Binning metagenomic contigs by coverage and composition. *Nature Methods*, *11*(11), 1144–1146.

Arikawa, E., Sun, Y., Wang, J., Zhou, Q., Ning, B., Dial, S. L., ... & Yang, J. (2008). Cross-platform comparison of SYBR® Green real-time PCR with TaqMan PCR, microarrays and other gene expression measurement technologies evaluated in the MicroArray Quality Control (MAQC) study. *BMC Genomics*, *9*(1), 1-12.

Asplund, J., & Gauslaa, Y. (2007). Content of secondary compounds depends on thallus size in the foliose lichen *Lobaria pulmonaria*. *The Lichenologist*, *39*(3), 273–278.

Bergmann, T. C., & Werth, S. (2017). Intrathalline distribution of two lichenicolous fungi on *Lobaria* hosts—an analysis based on quantitative real-time PCR. *Herzogia*, *30*(1), 253–271.

Brodo, I. M. & Hawksworth, D. L. (1977) *Alectoria* and allied genera in North America. *Opera Botanica*, *42*, 1–164.

Chong, R. A., & Moran, N. A. (2016). Intraspecific genetic variation in hosts affects regulation of obligate heritable symbionts. *Proceedings of the National Academy of Sciences*, *113*(46), 13114–13119.

Dykstra, H. R., Weldon, S. R., Martinez, A. J., White, J. A., Hopper, K. R., Heimpel, G. E., ... & Oliver, K. M. (2014). Factors limiting the spread of the protective symbiont *Hamiltonella defensa* in *Aphis craccivora* aphids. *Applied and Environmental Microbiology*, *80*(18), 5818–5827.

Emmerich, R., Giez, I., Lange, O. L., & Proksch, P. (1993). Toxicity and antifeedant activity of lichen compounds against the polyphagous herbivorous insect *Spodoptera littoralis*.

Phytochemistry, 33(6), 1389–1394.

Esseen, P. A., Olsson, T., Coxson, D., & Gauslaa, Y. (2015). Morphology influences water storage in hair lichens from boreal forest canopies. *Fungal Ecology*, 18, 26–35.

Färber, L., Solhaug, K. A., Esseen, P. A., Bilger, W., & Gauslaa, Y. (2014). Sunscreening fungal pigments influence the vertical gradient of pendulous lichens in boreal forest canopies. *Ecology*, 95(6), 1464–1471.

Fox, J. & Weisberg, S. (2019) *An R companion to applied regression, 3rd ed.* Sage, Thousand Oaks.

Gauslaa, Y., & Solhaug, K. A. (2001). Fungal melanins as a sun screen for symbiotic green algae in the lichen *Lobaria pulmonaria*. *Oecologia*, 126(4), 462–471.

Greshake Tzovaras, B., Segers, F. H., Bicker, A., Dal Grande, F., Otte, J., Anvar, S. Y., ... & Ebersberger, I. (2020). What is in *Umbilicaria pustulata*? A metagenomic approach to reconstruct the holo-genome of a lichen. *Genome Biology and Evolution*, 12(4), 309–324.

Grimm, M., Grube, M., Schiefelbein, U., Zühlke, D., Bernhardt, J., & Riedel, K. (2021). The lichens' microbiota, still a mystery?. *Frontiers in Microbiology*, 12, 714.

Herrera, M. L., Vallor, A. C., Gelfond, J. A., Patterson, T. F., & Wickes, B. (2009). Strain-dependent variation in 18S ribosomal DNA copy numbers in *Aspergillus fumigatus*. *Journal of Clinical Microbiology*, 47(5), 1325–1332.

Honegger, R. (1993). Developmental biology of lichens. *New Phytologist*, 125(4), 659–677.

- Jairus, K., Lõhmus, A., & Lõhmus, P. (2009). Lichen acclimatization on retention trees: a conservation physiology lesson. *Journal of Applied Ecology*, *46*(4), 930–936.
- Katoh, K., & Standley, D. M. (2013). MAFFT multiple sequence alignment software version 7: improvements in performance and usability. *Molecular Biology and Evolution*, *30*(4), 772–780.
- Kokkoris, V., Vukicevich, E., Richards, A., Thomsen, C., & Hart, M. M. (2021). Challenges using droplet digital PCR for environmental samples. *Applied Microbiology*, *1*(1), 74–88.
- Lefever, S., Pattyn, F., Hellemans, J., & Vandesompele, J. (2013). Single-nucleotide polymorphisms and other mismatches reduce performance of quantitative PCR assays. *Clinical Chemistry*, *59*(10), 1470–1480.
- Lindgren, H., Diederich, P., Goward, T., & Myllys, L. (2015). The phylogenetic analysis of fungi associated with lichenized ascomycete genus *Bryoria* reveals new lineages in the Tremellales including a new species *Tremella huuskonenii* hyperparasitic on *Phacopsis huuskonenii*. *Fungal Biology*, *119*(9), 844–856.
- McDonald, T. R., Gaya, E., & Lutzoni, F. (2013). Twenty-five cultures of lichenizing fungi available for experimental studies on symbiotic systems. *Symbiosis*, *59*(3), 165–171.
- Nurk, S., Meleshko, D., Korobeynikov, A., & Pevzner, P. A. (2017). metaSPAdes: a new versatile metagenomic assembler. *Genome Research*, *27*(5), 824–834.
- Palmqvist, K., Dahlman, L., Valladares, F., Tehler, A., Sancho, L. G., & Mattsson, J. E. (2002). CO₂ exchange and thallus nitrogen across 75 contrasting lichen associations from different climate zones. *Oecologia*, *133*(3), 295–306.

- Park, S. Y., Jeong, M. H., Wang, H. Y., Kim, J. A., Yu, N. H., Kim, S., ... & Hur, J. S. (2013). *Agrobacterium tumefaciens*-mediated transformation of the lichen fungus, *Umbilicaria muehlenbergii*. *PLoS One*, 8(12), e83896.
- Phinney, N. H., Gauslaa, Y., & Solhaug, K. A. (2019). Why chartreuse? The pigment vulpinic acid screens blue light in the lichen *Letharia vulpina*. *Planta*, 249(3), 709–718.
- Qian, L., Jia, F., Jingxuan, S., Manqun, W., & Julian, C. (2018). Effect of the secondary symbiont *Hamiltonella defensa* on fitness and relative abundance of *Buchnera aphidicola* of wheat aphid, *Sitobion miscanthi*. *Frontiers in Microbiology*, 9, 582.
- R Core Team (2013). R: A language and environment for statistical computing.
- Saary, P., Kale, V., & Finn, R. (2022). Large-scale analysis reveals the distribution of novel cellular microbes across multiple biomes and kingdoms.
- Sepey, M., Manni, M., & Zdobnov, E. M. (2019). BUSCO: assessing genome assembly and annotation completeness. In *Gene Prediction* (pp. 227–245). Humana, New York, NY.
- Sonesson, M., Sveinbjörnsson, B., Tehler, A., & Carlsson, B. Å. (2007). A comparison of the physiology, anatomy and ribosomal DNA in alpine and subalpine populations of the lichen *Nephroma arcticum*—the effects of an eight-year transplant experiment. *The Bryologist*, 110(2), 244–253.
- Spribille, T. (2018). Relative symbiont input and the lichen symbiotic outcome. *Current Opinion in Plant Biology*, 44, 57–63.
- Spribille, T., Tuovinen, V., Resl, P., Vanderpool, D., Wolinski, H., Aime, M. C., ... & McCutcheon, J. P. (2016). Basidiomycete yeasts in the cortex of ascomycete macrolichens. *Science*, 353(6298), 488–492.

- Sun, H. J., & Friedmann, E. I. (2005). Communities adjust their temperature optima by shifting producer-to-consumer ratio, shown in lichens as models: II. Experimental verification. *Microbial Ecology*, 49(4), 528–535.
- Tagirdzhanova, G., Saary, P., Tingley, J. P., Díaz-Escandón, D., Abbott, D. W., Finn, R. D., & Spribille, T. (2021). Predicted input of uncultured fungal symbionts to a lichen symbiosis from metagenome-assembled genomes. *Genome Biology and Evolution*, 13(4), evab047.
- Taylor, S. C., Laperriere, G., & Germain, H. (2017). Droplet Digital PCR versus qPCR for gene expression analysis with low abundant targets: from variable nonsense to publication quality data. *Scientific Reports*, 7(1), 1–8.
- Taylor, S., Wakem, M., Dijkman, G., Alsarraj, M., & Nguyen, M. (2010). A practical approach to RT-qPCR—publishing data that conform to the MIQE guidelines. *Methods*, 50(4), S1–S5.
- Tellenbach, C., Grünig, C. R., & Sieber, T. N. (2010). Suitability of quantitative real-time PCR to estimate the biomass of fungal root endophytes. *Applied and Environmental Microbiology*, 76(17), 5764–5772.
- Tretiach, M., Bertuzzi, S., Candotto Carniel, F., & Virgilio, D. (2013). Seasonal acclimation in the epiphytic lichen *Parmelia sulcata* is influenced by change in photobiont population density. *Oecologia*, 173(3), 649–663.
- Tuovinen, V., Ekman, S., Thor, G., Vanderpool, D., Spribille, T., & Johannesson, H. (2019). Two basidiomycete fungi in the cortex of wolf lichens. *Current Biology*, 29(3), 476–483.
- Tuovinen, V., Millanes, A. M., Freire-Rallo, S., Rosling, A., & Wedin, M. (2021). *Tremella macrobasidiata* and *Tremella variaie* have abundant and widespread yeast stages in *Lecanora* lichens. *Environmental Microbiology*, 23(5), 2484–2498.

- Uritskiy, G. V., DiRuggiero, J., & Taylor, J. (2018). MetaWRAP—a flexible pipeline for genome-resolved metagenomic data analysis. *Microbiome*, *6*(1), 1–13.
- Valladares, F., Sancho, L. G., & Ascaso, C. (1996). Functional analysis of the intrathalline and intracellular chlorophyll concentrations in the lichen family Umbilicariaceae. *Annals of Botany*, *78*(4), 471–477.
- Velmala, S., Myllys, L., Halonen, P., Goward, T., & Teuvo, A. H. T. I. (2009). Molecular data show that *Bryoria fremontii* and *B. tortuosa* (Parmeliaceae) are conspecific. *The Lichenologist*, *41*(3), 231–242.
- Wickham, H. (2016) *ggplot2: Elegant Graphics for Data Analysis*. Springer-Verlag New York.
- Wickham, H. & Girlich, M. (2022). *tidyr: Tidy Messy Data*. R package version 1.2.0. <https://CRAN.R-project.org/package=tidyr>
- Wickham, H., François, R., Henry, L., & Müller, K. (2018). *Dplyr: A grammar of data manipulation* (R package v1.0.8). <https://CRAN.R-project.org/package=dplyr>
- Wood, S. N., Pya, N., & Säfken, B. (2016). Smoothing parameter and model selection for general smooth models. *Journal of the American Statistical Association*, *111*(516), 1548–1563.
- Ye, J., Coulouris, G., Zaretskaya, I., Cutcutache, I., Rozen, S., & Madden, T. L. (2012). Primer-BLAST: a tool to design target-specific primers for polymerase chain reaction. *BMC Bioinformatics*, *13*(1), 1–11.
- Yoon, S. H., Ha, S. M., Lim, J., Kwon, S., & Chun, J. (2017). A large-scale evaluation of algorithms to calculate average nucleotide identity. *Antonie Van Leeuwenhoek*, *110*(10), 1281–1286.

Table 5.1. Specimens of *Bryoria fremontii* used in the analysis

Thallus ID	Type (by color)	Province	location name	Lat	Long	Batch
tort_1	1	British Columbia	spur of Trophy Mountain Rd.	51.78415°N	119.97601°W	Fall 2020
tort_2	1	British Columbia	spur of Trophy Mountain Rd.	51.78415°N	119.97601°W	Fall 2020
tort_3	1	British Columbia	spur of Trophy Mountain Rd.	51.78415°N	119.97601°W	Fall 2020
tort_4	5	British Columbia	McCorvie Lakes FS Rd about 300 m off Hwy. 5	51.59256°N	119.85643°W	Fall 2020
tort_5	5	British Columbia	McCorvie Lakes FS Rd about 300 m off Hwy. 5	51.59256°N	119.85643°W	Fall 2020
tort_6	5	British Columbia	McCorvie Lake upland	51.61888°N	119.79395°W	Fall 2020
tort_7	1	British Columbia	spur of Trophy Mountain Rd.	51.78415°N	119.97601°W	Fall 2020
tort_8	2	British Columbia	spur of Trophy Mountain Rd.	51.78415°N	119.97601°W	Fall 2020
tort_9	2	British Columbia	spur of Trophy Mountain Rd.	51.78415°N	119.97601°W	Fall 2020
tort_10	2	British Columbia	spur of Trophy Mountain Rd.	51.78415°N	119.97601°W	Fall 2020
tort_11	2	British Columbia	spur of Trophy Mountain Rd.	51.78415°N	119.97601°W	Fall 2020
tort_12	2	British Columbia	McCorvie Lakes FS Rd about 300 m off Hwy. 5	51.59256°N	119.85643°W	Fall 2020
tort_13	2	British Columbia	McCorvie Lakes FS Rd about 300 m off Hwy. 5	51.59256°N	119.85643°W	Fall 2020
tort_14	2	British Columbia	spur of Trophy Mountain Rd.	51.78415°N	119.97601°W	Fall 2020
tort_15	2	British Columbia	McCorvie Lakes FS Rd about 300 m off Hwy. 5	51.59256°N	119.85643°W	Fall 2020
tort_16	2	British Columbia	spur of Trophy Mountain Rd.	51.78415°N	119.97601°W	Fall 2020
tort_17	2	British Columbia	McCorvie Lakes FS Rd about 300 m off Hwy. 5	51.59256°N	119.85643°W	Fall 2020
tort_18	2	British Columbia	spur of Trophy Mountain Rd.	51.78415°N	119.97601°W	Fall 2020
tort_19	2	British Columbia	spur of Trophy Mountain Rd.	51.78415°N	119.97601°W	Fall 2020
tort_20	2	British Columbia	spur of Trophy Mountain Rd.	51.78415°N	119.97601°W	Fall 2020
tort_21	2	British Columbia	spur of Trophy Mountain Rd.	51.78415°N	119.97601°W	Fall 2020

tort_22	2	British Columbia	McCorvie Lake upland	51.61888°N	119.79395°W	Fall 2020
tort_23	2	British Columbia	spur of Trophy Mountain Rd. McCorvie Lakes FS Rd about 300 m off	51.78415°N	119.97601°W	Fall 2020
tort_24	2	British Columbia	Hwy. 5 McCorvie Lakes FS Rd about 300 m off	51.59256°N	119.85643°W	Fall 2020
tort_25	2	British Columbia	Hwy. 5	51.59256°N	119.85643°W	Fall 2020
tort_26	2	British Columbia	spur of Trophy Mountain Rd.	51.78415°N	119.97601°W	Fall 2020
tort_27	3	British Columbia	spur of Trophy Mountain Rd.	51.78415°N	119.97601°W	Fall 2020
tort_28	3	British Columbia	Eakin Creek, W of Little Fort	51.449484°N	120.219359°W	Fall 2020
tort_29	3	British Columbia	spur of Trophy Mountain Rd. McCorvie Lakes FS Rd about 300 m off	51.78415°N	119.97601°W	Fall 2020
tort_30	3	British Columbia	Hwy. 5 McCorvie Lakes FS Rd about 300 m off	51.59256°N	119.85643°W	Fall 2020
tort_31	3	British Columbia	Hwy. 5 McCorvie Lakes FS Rd about 300 m off	51.59256°N	119.85643°W	Fall 2020
tort_32	3	British Columbia	Hwy. 5	51.59256°N	119.85643°W	Fall 2020
tort_33	3	British Columbia	McCorvie Lake upland	51.61888°N	119.79395°W	Fall 2020
tort_34	3	British Columbia	spur of Trophy Mountain Rd.	51.78415°N	119.97601°W	Fall 2020
tort_35	3	British Columbia	spur of Trophy Mountain Rd.	51.78415°N	119.97601°W	Fall 2020
tort_36	3	British Columbia	spur of Trophy Mountain Rd.	51.78415°N	119.97601°W	Fall 2020
tort_37	3	British Columbia	spur of Trophy Mountain Rd.	51.78415°N	119.97601°W	Fall 2020
tort_38	3	British Columbia	spur of Trophy Mountain Rd.	51.78415°N	119.97601°W	Fall 2020
tort_39	3	British Columbia	spur of Trophy Mountain Rd. McCorvie Lakes FS Rd about 300 m off	51.78415°N	119.97601°W	Fall 2020
tort_40	3	British Columbia	Hwy. 5 McCorvie Lakes FS Rd about 300 m off	51.59256°N	119.85643°W	Fall 2020
tort_41	3	British Columbia	Hwy. 5	51.59256°N	119.85643°W	Fall 2020
tort_42	3	British Columbia	spur of Trophy Mountain Rd.	51.78415°N	119.97601°W	Fall 2020
tort_43	3	British Columbia	spur of Trophy Mountain Rd.	51.78415°N	119.97601°W	Fall 2020
tort_44	3	British Columbia	spur of Trophy Mountain Rd.	51.78415°N	119.97601°W	Fall 2020
tort_45	3	British Columbia	spur of Trophy Mountain Rd.	51.78415°N	119.97601°W	Fall 2020

tort_46	3	British Columbia	spur of Trophy Mountain Rd.	51.78415°N	119.97601°W	Fall 2020
tort_47	3	British Columbia	spur of Trophy Mountain Rd.	51.78415°N	119.97601°W	Fall 2020
tort_48	3	British Columbia	spur of Trophy Mountain Rd.	51.78415°N	119.97601°W	Fall 2020
tort_49	3	British Columbia	spur of Trophy Mountain Rd.	51.78415°N	119.97601°W	Fall 2020
tort_50	3	British Columbia	spur of Trophy Mountain Rd. McCorvie Lakes FS Rd about 300 m off	51.78415°N	119.97601°W	Fall 2020
tort_51	3	British Columbia	Hwy. 5	51.59256°N	119.85643°W	Fall 2020
tort_52	4	British Columbia	McCorvie Lake upland	51.61888°N	119.79395°W	Fall 2020
tort_53	4	British Columbia	spur of Trophy Mountain Rd.	51.78415°N	119.97601°W	Fall 2020
tort_54	4	British Columbia	McCorvie Lake upland	51.61888°N	119.79395°W	Fall 2020
tort_55	4	British Columbia	spur of Trophy Mountain Rd.	51.78415°N	119.97601°W	Fall 2020
tort_56	4	British Columbia	McCorvie Lake upland	51.61888°N	119.79395°W	Fall 2020
tort_57	4	British Columbia	spur of Trophy Mountain Rd.	51.78415°N	119.97601°W	Fall 2020
tort_58	4	British Columbia	spur of Trophy Mountain Rd. McCorvie Lakes FS Rd about 300 m off	51.78415°N	119.97601°W	Fall 2020
tort_59	4	British Columbia	Hwy. 5	51.59256°N	119.85643°W	Fall 2020
tort_60	4	British Columbia	McCorvie Lake upland McCorvie Lakes FS Rd about 300 m off	51.61888°N	119.79395°W	Fall 2020
tort_61	4	British Columbia	Hwy. 5 McCorvie Lakes FS Rd about 300 m off	51.59256°N	119.85643°W	Fall 2020
tort_62	4	British Columbia	Hwy. 5	51.59256°N	119.85643°W	Fall 2020
tort_63	4	British Columbia	McCorvie Lake upland	51.61888°N	119.79395°W	Fall 2020
tort_64	4	British Columbia	Eakin Creek, W of Little Fort	51.449484°N	120.219359°W	Fall 2020
tort_65	4	British Columbia	Eakin Creek, W of Little Fort	51.449484°N	120.219359°W	Fall 2020
tort_66	4	British Columbia	spur of Trophy Mountain Rd. McCorvie Lakes FS Rd about 300 m off	51.78415°N	119.97601°W	Fall 2020
tort_67	4	British Columbia	Hwy. 5	51.59256°N	119.85643°W	Fall 2020
tort_68	4	British Columbia	McCorvie Lake upland	51.61888°N	119.79395°W	Fall 2020
tort_69	4	British Columbia	spur of Trophy Mountain Rd.	51.78415°N	119.97601°W	Fall 2020
tort_70	4	British Columbia	McCorvie Lake upland	51.61888°N	119.79395°W	Fall 2020
tort_71	5	British Columbia	McCorvie Lake upland McCorvie Lakes FS Rd about 300 m off	51.61888°N	119.79395°W	Fall 2020
tort_72	5	British Columbia	Hwy. 5	51.59256°N	119.85643°W	Fall 2020

tort_73	5	British Columbia	McCorvie Lakes FS Rd about 300 m off Hwy. 5	51.59256°N	119.85643°W	Fall 2020
tort_74	5	British Columbia	McCorvie Lake upland	51.61888°N	119.79395°W	Fall 2020
tort_75	5	British Columbia	spur of Trophy Mountain Rd.	51.78415°N	119.97601°W	Fall 2020
tort_76	5	British Columbia	Eakin Creek, W of Little Fort McCorvie Lakes FS Rd about 300 m off	51.449484°N	120.219359°W	Fall 2020
tort_77	5	British Columbia	Hwy. 5	51.59256°N	119.85643°W	Fall 2020
tort_78	5	British Columbia	McCorvie Lake upland	51.61888°N	119.79395°W	Fall 2020
tort_79	5	British Columbia	McCorvie Lake upland	51.61888°N	119.79395°W	Fall 2020
tort_80	5	British Columbia	Eakin Creek, W of Little Fort	51.449484°N	120.219359°W	Fall 2020
tort_81	5	British Columbia	McCorvie Lake upland McCorvie Lakes FS Rd about 300 m off	51.61888°N	119.79395°W	Fall 2020
tort_82	5	British Columbia	Hwy. 5	51.59256°N	119.85643°W	Fall 2020
tort_83	5	British Columbia	Avola talus slope	51.80943°N	119.30175°W	Spring 2021
tort_84	4	British Columbia	Moosehouse cabin	51.90696°N	120.02548°W	Spring 2021
tort_85	4	British Columbia	Moosehouse cabin	51.90696°N	120.02548°W	Spring 2021
tort_86	4	British Columbia	Tranquille River crossing	50.81962°N	120.58024°W	Spring 2021
tort_87	4	British Columbia	Tranquille River crossing	50.81962°N	120.58024°W	Spring 2021
tort_88	3	British Columbia	Tranquille River crossing	50.81962°N	120.58024°W	Spring 2021
tort_89	3	British Columbia	Tranquille River crossing	50.81962°N	120.58024°W	Spring 2021
tort_90	2	British Columbia	Tranquille River crossing	50.81962°N	120.58024°W	Spring 2021
tort_91	3	British Columbia	Moosehouse cabin	51.90696°N	120.02548°W	Spring 2021
tort_92	4	British Columbia	Moosehouse cabin	51.90696°N	120.02548°W	Spring 2021
tort_93	4	British Columbia	Moosehouse cabin	51.90696°N	120.02548°W	Spring 2021
tort_94	3	British Columbia	Tranquille River crossing	50.81962°N	120.58024°W	Spring 2021
tort_95	3	British Columbia	Tranquille River crossing	50.81962°N	120.58024°W	Spring 2021
tort_96	3	British Columbia	Tranquille River crossing	50.81962°N	120.58024°W	Spring 2021
tort_97	2	British Columbia	Tranquille River crossing	50.81962°N	120.58024°W	Spring 2021
tort_98	3	British Columbia	S of Chu Chua	51.28389°N	120.15142°W	Spring 2021
tort_99	3	British Columbia	S of Chu Chua	51.28389°N	120.15142°W	Spring 2021
tort_100	4	British Columbia	About 550 m N of Moosehouse cabin	51.91197°N	120.02750°W	Spring 2021
tort_101	2	British Columbia	S of Chu Chua	51.30561°N	120.15222°W	Spring 2021
tort_102	1	British Columbia	S of Chu Chua	51.30561°N	120.15222°W	Spring 2021

tort_103	3	British Columbia	S of Chu Chua	51.30561°N	120.15222°W	Spring 2021
tort_104	4	British Columbia	S of Chu Chua	51.28389°N	120.15142°W	Spring 2021
tort_105	2	British Columbia	S of Chu Chua	51.30561°N	120.15222°W	Spring 2021
tort_106	2	British Columbia	S of Chu Chua	51.28389°N	120.15142°W	Spring 2021
tort_107	3	British Columbia	S of Chu Chua	51.30561°N	120.15222°W	Spring 2021
tort_108	3	British Columbia	McCorvie Lakes FS Rd about 300 m off Hwy. 5	51.59252°N	119.85665°W	Spring 2021
tort_109	1	British Columbia	McCorvie Lakes FS Rd about 300 m off Hwy. 5	51.59252°N	119.85665°W	Spring 2021
tort_110	5	British Columbia	Moosehouse cabin	51.90696°N	120.02548°W	Spring 2021
tort_111	3	British Columbia	S of Chu Chua	51.30561°N	120.15222°W	Spring 2021
tort_112	3	British Columbia	S of Chu Chua	51.28389°N	120.15142°W	Spring 2021
tort_113	2	British Columbia	S of Chu Chua	51.30561°N	120.15222°W	Spring 2021
tort_114	3	British Columbia	S of Chu Chua	51.30561°N	120.15222°W	Spring 2021
tort_115	3	British Columbia	S of Chu Chua	51.30561°N	120.15222°W	Spring 2021
tort_116	3	British Columbia	S of Chu Chua	51.30561°N	120.15222°W	Spring 2021
tort_117	4	British Columbia	S of Chu Chua	51.28389°N	120.15142°W	Spring 2021
tort_118	4	British Columbia	About 550 m N of Moosehouse cabin	51.91197°N	120.02750°W	Spring 2021
tort_119	2	British Columbia	S of Chu Chua	51.30561°N	120.15222°W	Spring 2021
tort_120	5	British Columbia	Hwy 5 near Blue River bridge	52.009265°N	119.336278°W	Spring 2021

Table 5.2. Metagenome-assembled genomes used for designing the ddPCR survey.

Organism	Lineage	Metagenome description	BUSCO completeness score	BUSCO contamination score	Median Coverage Depth in <i>Bryoria fremontii</i> metagenome
Main fungus	Ascomycota	<i>Bryoria fremontii</i>	96.40%	0.10%	418.4
alga	Chlorophyta	<i>Bryoria fremontii</i>	94.70%	0.90%	39.5
<i>Cyphobasidium</i>	Cyphobasidiales	<i>Bryoria fremontii</i>	72.40%	0.10%	7.4
<i>Tremella</i>	Tremellomycetes	<i>Tremella</i> gall on <i>Bryoria</i> sp.	81.90%	0.10%	NA

Table 5.3. Oligonucleotide primers used for PCR.

ID	Gene description	Species	Sequence	Used for
ubiq_alg_f1	Ubiquinol-cytochrome c chaperone	alga	GAGACAATGTCCTGCCTTGC	additional screening
ubiq_alg_r1	Ubiquinol-cytochrome c chaperone	alga	GCATTACTGACCCCCACCAA	additional screening
ubiq_cypho_f1	Ubiquinol-cytochrome c chaperone	<i>Cyphobasidium</i>	ACGCGCAACTTCTGACTACT	additional screening
ubiq_cypho_r1	Ubiquinol-cytochrome c chaperone	<i>Cyphobasidium</i>	TAAGGCCCTCGTCATAGCCT	additional screening
ubiq_lec_f1	Ubiquinol-cytochrome c chaperone	ascomycete	CTCAATTGCAAAGGAGCTTCACA	additional screening
ubiq_lec_r1	Ubiquinol-cytochrome c chaperone	ascomycete	TCCACATTTTCATCCGCCTTGA	additional screening
anam_alg_f1	Anamorsin	alga	GGCAGCTCCCTCGAGAATAC	additional screening
anam_alg_r1	Anamorsin	alga	AATCCAACAAACTTGGCCGC	additional screening
anam_cypho_f1	Anamorsin	<i>Cyphobasidium</i>	ATCACGTAAGAGCTCGCCAC	additional screening
anam_cypho_r1	Anamorsin	<i>Cyphobasidium</i>	AGCTCTGCTTATCACGCTCC	additional screening
anam_lec_f1	Anamorsin	ascomycete	TCCAAATGCTCGATCGCCT	additional screening
anam_lec_r1	Anamorsin	ascomycete	TTACAAGCACGCCGACGTTT	additional screening
snare_alg_f1	SNARE	alga	AGCGGTGCTGAAGCCTATTT	additional screening
snare_alg_r1	SNARE	alga	GTGCAACAAAGCACTGTGGA	additional screening
snare_cypho_f2	SNARE	<i>Cyphobasidium</i>	ATCTTATGGCGTGAACCGCA	additional screening
snare_cypho_r2	SNARE	<i>Cyphobasidium</i>	ACGAAGTTCTAGCTAGCCGC	additional screening
snare_lec_f1	SNARE	ascomycete	ACCTGGAGAAGTTGCACCAAA	additional screening
snare_lec_r1	SNARE	ascomycete	GATGATTCCCTGCGCGATGT	additional screening
gnat_alg_f1	GNAT domain/ Acyl-CoA N-acyltransferase	alga	GTTGGGATACTACAGCGGGG	additional screening

gnat_alg_r1	GNAT domain/ Acyl-CoA N-acyltransferase	alga	CCATATAGGTCGCGGTTCCC	additional screening
gnat_cypho_f1	GNAT domain/ Acyl-CoA N-acyltransferase	<i>Cyphobasidium</i>	GGGTCGAGCCATATCTTGCG	additional screening
gnat_cypho_r1	GNAT domain/ Acyl-CoA N-acyltransferase	<i>Cyphobasidium</i>	AGAAGAGAAGCGCTACTGGC	additional screening
gnat_lec_f1	GNAT domain/ Acyl-CoA N-acyltransferase	ascomycete	TGGGCAAAGTCGAGGAAGACC	additional screening
gnat_lec_r1	GNAT domain/ Acyl-CoA N-acyltransferase	ascomycete	GCTTCCGCATATCAAATGCATCC	additional screening
gnat_trem_f4	GNAT domain/ Acyl-CoA N-acyltransferase	<i>Tremella</i>	TGATAGCGAAACACGAGCCC	additional screening
gnat_trem_r4	GNAT domain/ Acyl-CoA N-acyltransferase	<i>Tremella</i>	ACTCGACGACCCTTCGAAAC	additional screening
anam_trem_f3	Anamorsin	<i>Tremella</i>	GCGGCAGATCCCTTCTCACT	additional screening
anam_trem_r3	Anamorsin	<i>Tremella</i>	CTGTACCTTCTACCCGGCTT	additional screening
snare_trem_f5	SNARE	<i>Tremella</i>	ACCTTGAAAGGCGCGGATAG	additional screening
snare_trem_r5	SNARE	<i>Tremella</i>	CGACCGGTGTTCGCTTGATA	additional screening
ubiq_trem_f4	Ubiquinol-cytochrome c chaperone	<i>Tremella</i>	AGCTGCTCAACCACTTTTTTCG	additional screening
ubiq_trem_r4	Ubiquinol-cytochrome c chaperone	<i>Tremella</i>	GTCCCCACGCCCTATATTC	additional screening
Qsnare_alg_f1	SNARE	alga	AACCGGTTGAGGCAGAAGAGT	ddPCR
Qsnare_alg_r1	SNARE	alga	AGAGCCTCTCGCCCCTAGTC	ddPCR
Qsnare_cypho_f1	SNARE	<i>Cyphobasidium</i>	CAAGCTGACATTGATCTACACTGAATAG	ddPCR
Qsnare_cypho_r1	SNARE	<i>Cyphobasidium</i>	GGAECTCTTGTCGCTGAAGGA	ddPCR
Qsnare_lec_f1	SNARE	ascomycete	GGTGTGAGTGCAGCAGATGAAA	ddPCR
Qsnare_lec_r1	SNARE	ascomycete	CTGYTTCTTCTGAATCCTGCA	ddPCR
Qsnare_trem_f1	SNARE	<i>Tremella</i>	CGATCGGCATAGACCTGAATATC	ddPCR
Qsnare_trem_r1	SNARE	<i>Tremella</i>	CCGCCAATTCTGAGATGGA	ddPCR



Fig. 5.1. Specimens of *B. fremontii*.

Two specimens from the opposite sides of the colour spectrum: yellow *B. tortuosa* on the left and brown *B. fremontii* on the right.

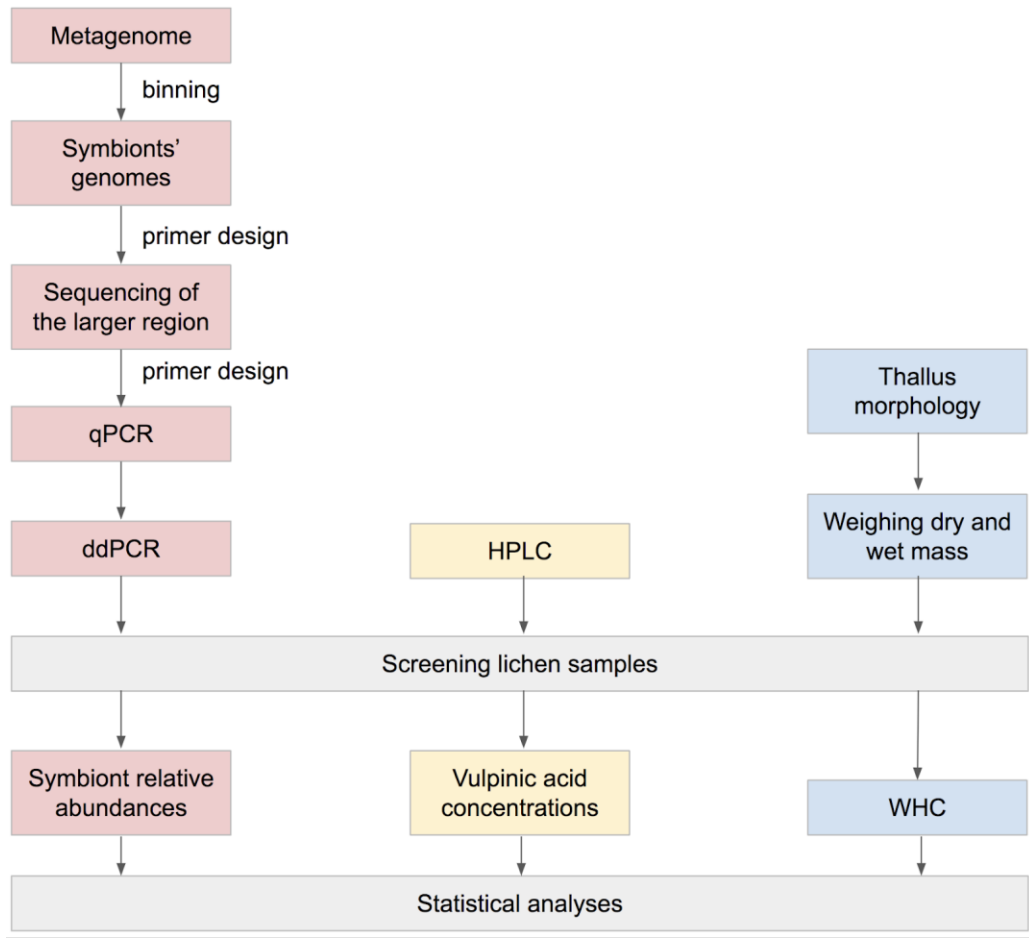


Fig. 5.2. Study design.

The flowchart shows the three components of the study — measuring symbiont abundance, measuring vulpinic acid concentration, and assessing water holding capacity (WHC) of lichen samples — followed by the data analysis.

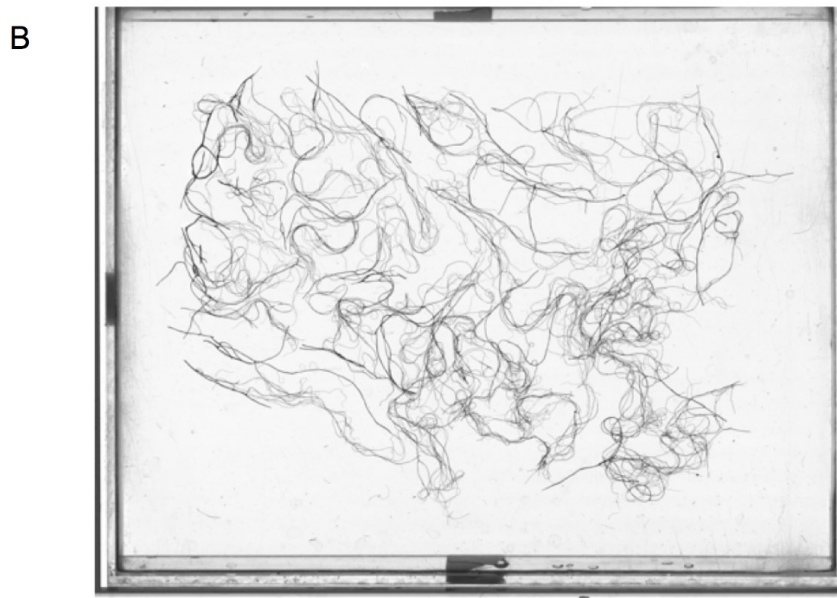
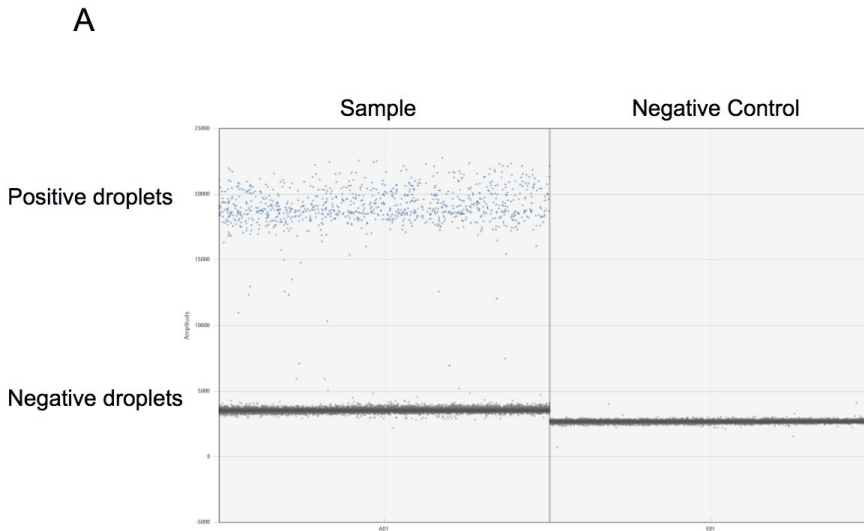


Fig. 5.3. Examples of images created during the data generation steps.

A. Output of a ddPCR run. Scatterplots show droplets positioned based on their fluorescence level. The sample (on the left) has both a positive cloud — i.e. droplets where amplification took place — and a negative cloud. The negative control (on the right) has only a negative cloud. B. Scan of a lichen sample created using a WinRhizo Scanner. We analyzed the images using WinRhizo Software in order to estimate the surface area of a lichen sample.

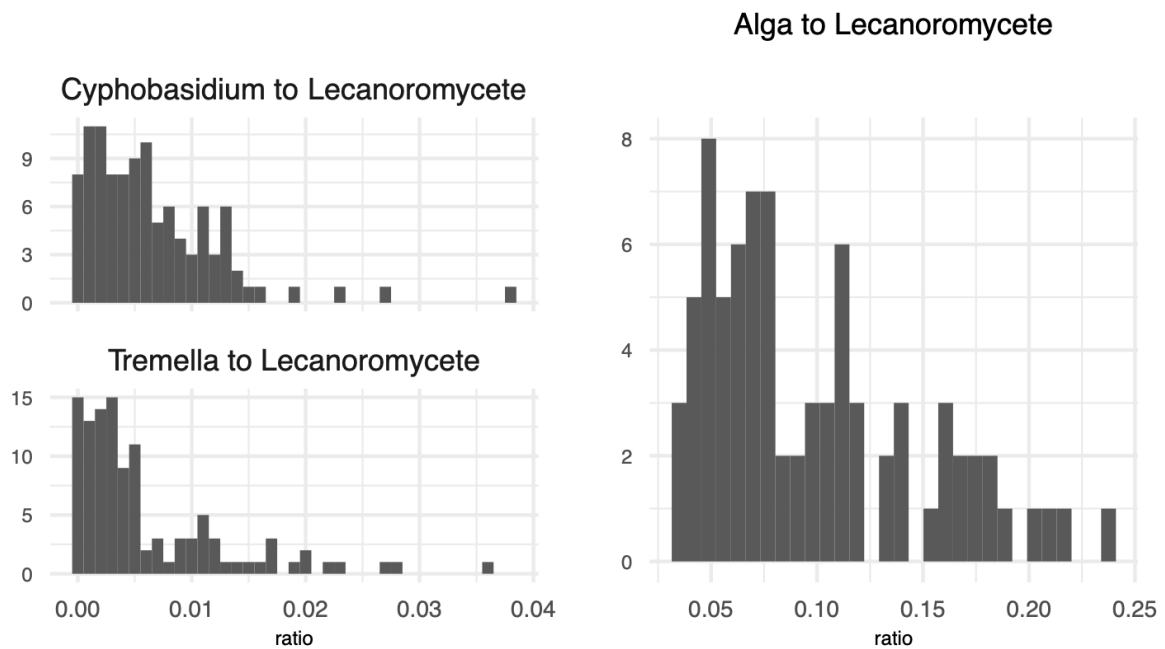


Fig. 5.4. Histograms of the relative abundances of lichen symbionts.

For each of the three symbionts (the alga, *Cyphobasidium*, and *Tremella*) in each lichen sample, we calculated their relative abundance by dividing the absolute abundance by the abundance of the lecanoromycete.

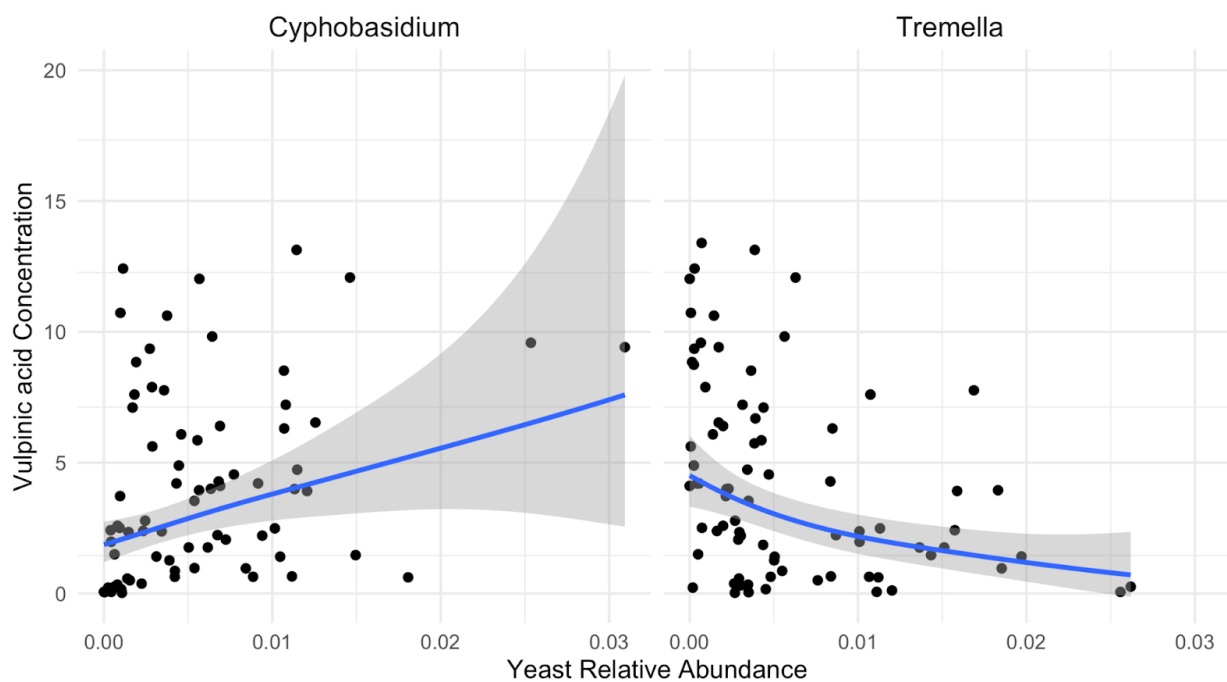


Fig. 5.5. The relationship between yeast relative abundance and vulpinic acid concentration.

Each dot represents a lichen sample, positioned based on the relative abundance of a yeast and vulpinic acid concentration. To analyze the relationship between the yeast abundance and vulpinic acid concentration, we built a GAM model, using relative abundances of *Cyphobasidium* and *Tremella* as predictors. The model predictions are indicated on the scatter plot with a line. Both relationships were statistically significant (p value for *Cyphobasidium* < 0.05, for *Tremella* < 0.005, the model explained 22% of deviance).

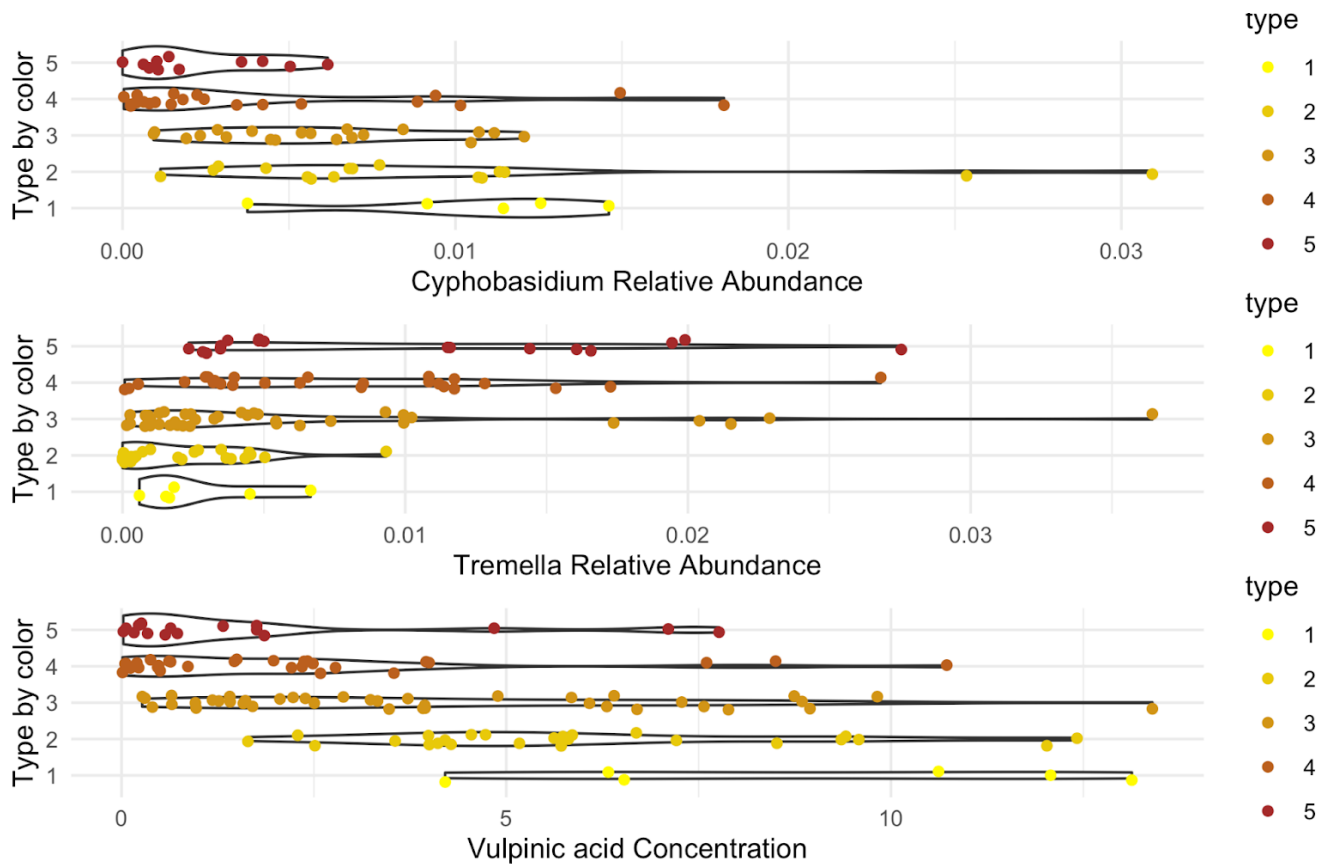


Fig. 5.6. The relationship between lichen colour type and other characteristics of a lichen sample.

We classified lichen samples into 5 “types” based on colour, from “1” being bright yellow to “5” being dark brown. This graph shows how the type by colour relates to other characteristics: relative abundance of *Cyphobasidium* and *Tremella*, and vulpinic acid concentration. The sample types differed significantly as confirmed by ANOVA (top plot: $p < 0.001$, $R^2_{\text{adj}} = 0.17$; middle plot: $p < 0.001$, $R^2_{\text{adj}} = 0.12$; bottom plot: $p < 0.001$, $R^2_{\text{adj}} = 0.28$).

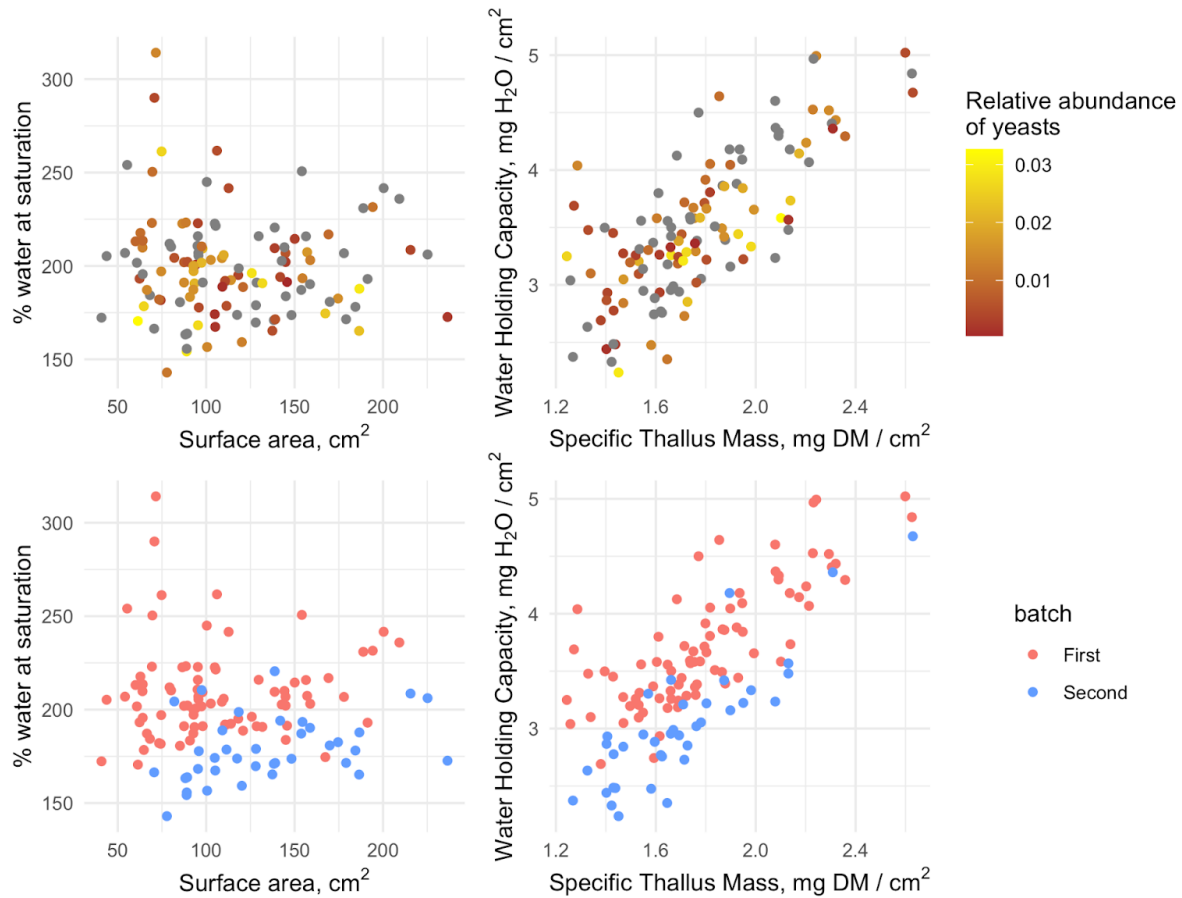


Fig. 5.7. Water storage characteristics of *B. fremontii* in relation to the relative yeast abundance and batch effect.

Each dot represents a lichen sample. The scatter plots show the relationship between water storage and morphology characteristics: On the left, percent water at saturation as a function of surface area. On the right, WHC as a function of STM. In the top row, the dots are coloured based on the yeast relative abundance (calculated as a sum of relative abundances of *Cyphobasidium* and *Tremella*). In the bottom row, the dots are coloured based on what batch they belong to. While the yeast relative abundance does not appear to influence water storage, two batches differed in their water storage characteristics ($p < 0.001$, for WHC and percent water at saturation; $R^2_{\text{adj}} = 0.26$ and 0.25 respectively).

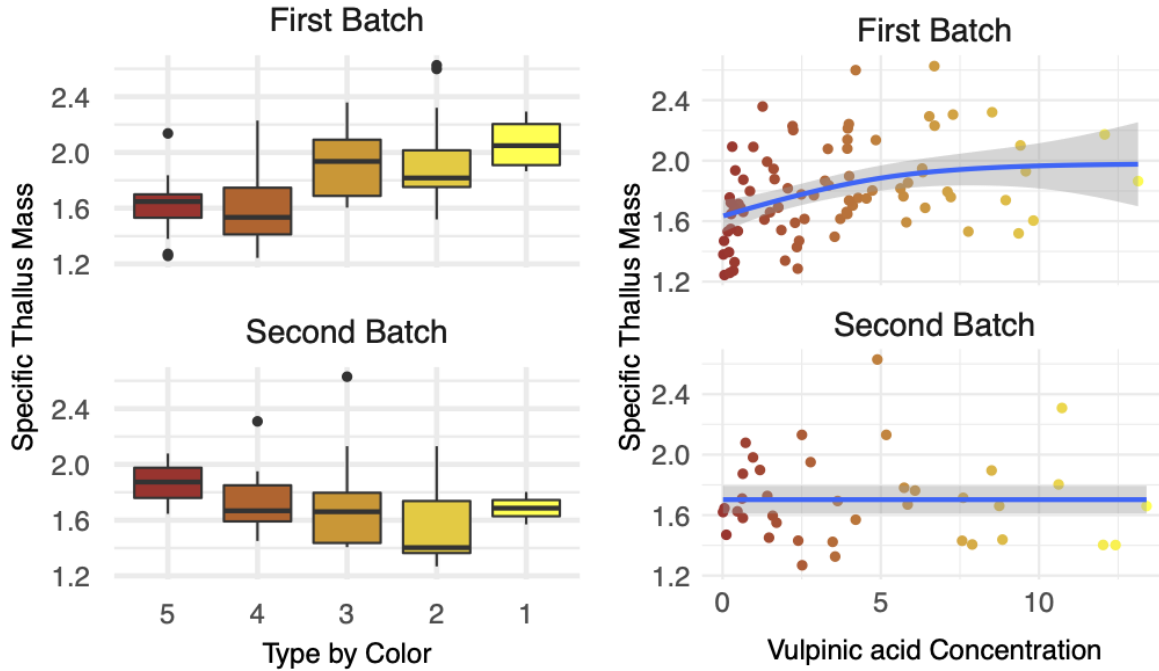


Fig. 5.8. The relationship between sample STM and its colour and vulpinic acid concentration, in the two analyzed batches.

The boxplots on the left show the relationship between type by colour and STM. The scatter plots on the right show the relationship between vulpinic acid concentration and STM. In the first batch, STM appeared linked to the colour of the lichen and to its vulpinic acid concentration: more yellow samples had higher STM. In practice, this meant that yellow samples tended to have thicker branches. For the second batch, we specifically collected lichens to balance our sample. This goal was achieved, as STM does not appear linked to the other characteristics.

Chapter 6. General Conclusions

Lichens are an outcome of a symbiotic relationship that involves fungi, unicellular algae and bacteria. A unique feature of lichen symbioses is their architectures, which can have remarkably complex structure, and which arise as a result of interactions between symbionts (Sanders 2001). Each lichen symbiosis possesses a set of phenotypic characteristics: morphological — the shape of lobes or branches, the branching pattern, the presence of vegetative reproduction structures — as well as ecological and chemical (Honegger 1993). These characteristics only emerge in symbiosis, as none of the isolated partners is capable of creating an architecture similar to lichens on its own. To understand how lichen phenotype arises, one needs to understand the flow of goods and services in lichens.

The overarching goal of my thesis was to reconstruct the flow of goods and services in lichens using culture-free methods. I focused on two main questions: who's there and what do they do?

Who's there?

What constitutes a lichen? Schwendener (1869) discovered that lichens consist of fungal and algal cells. The symbiotic hypothesis caused a decades-long controversy, before ultimately being accepted as a fact (Honegger 2000). Now, the question of what organisms constitute a lichen is open again. Sequencing-based techniques such as metabarcoding allowed biologists to detect a plethora of organisms present in lichens, in addition to the main two partners, the main fungus and the phototroph (Grimm et al. 2021). Whether these organisms are an integral part of the symbiosis or something external to it is still debated.

My thesis focuses on the newly discovered lichen symbionts, bacteria and yeasts. Here, I demonstrate that bacterial communities are highly structured and contain bacterial lineages that

are nearly universal and might be stable members of lichen symbioses. My results also expand what we know about basidiomycete yeasts in lichens. One of the yeasts, *Tremella*, was previously known to be stably present in two lichen genera (Tuovinen et al. 2019, 2021). Now, I show it to be ubiquitous in the two lichen symbioses that I used as model systems (*Alectoria sarmentosa* in Chapter 2 and *Bryoria fremontii* in Chapter 5). In addition, I detected both *Tremella* and *Cyphobasidium* basidiomycetes in a variety of lichen symbioses, including symbioses they have not been reported from previously (Chapter 4).

At first glance, the composition of a lichen symbiosis does not tell us much about how the lichen functions. However, closing the ‘who’s there’ knowledge gap is essential for future functional studies. To design experiments that will clarify how symbiotic traits emerge, we need to consider all potentially involved parties, including the yeasts and bacteria.

What do they do?

To understand how lichen phenotypes emerge, we need to reconstruct the flow of goods and services and understand the contributions of individual partners. In this thesis, I made predictions based on my analysis of the lichen symbionts’ genomes (Chapters 2–4), and later tested some of these hypotheses (Chapter 5). I predicted that yeasts and bacteria contribute to the lichen symbiosis in several ways: 1) by participating in making the extracellular matrix that glues cells into the lichen shape, 2) by scavenging nutrients, 3) by producing vitamins.

While I proposed ways in which yeasts and bacteria might be integrated into the lichen symbiosis, it is important to remember the major knowledge gaps surrounding the flow of goods and services in lichens. While most studies agree that the “basis” of symbiosis lies in the flux of sugars or sugar alcohols produced by the photosynthetic partner, the function of these metabolites remains unclear. Spribille et al. (2022) discussed two alternative hypotheses: that

sugar alcohols serve as a carbon source, or that they ensure that lichens survive desiccation. My results do not offer a way to discriminate between the two hypotheses.

Are the yeasts and bacteria necessary for the lichen symbiosis?

Hard to tell. One reason why generalizing is not possible here is the nature of the lichen symbiosis. Lichen symbioses are open systems, where symbionts can be acquired horizontally and symbiotic turnover is frequent (Sanders & Lücking 2002, Dal Grande et al. 2012, Medeiros et al. 2021, Leiva et al. 2021, Chapter 4). This openness makes lichens different from many well-studied symbiotic systems, e.g. bacterial endosymbionts of insects. It also makes it harder to demonstrate the contribution of individual symbionts. In closed symbioses, the partners are locked together, and over time they shed all superfluous functions and, often, develop tight metabolic interdependence (Husnik & Keeling 2019, Perreau & Moran 2022), which can be demonstrated in the form of mosaic pathways (e.g. Bublitz et al. 2019). In contrast, open symbioses often exchange symbionts with their environment or with other symbioses, which leads to lower specificity and a higher chance of acquiring new functions from the outside (Perreau & Moran 2022). In addition, horizontal gene transfer between symbiotic bacteria is frequent in open symbioses, which further complicates the question of contribution of each lineage.

In lichens, one can hardly expect the level of metabolic integration typical for intracellular symbioses. In Chapter 3, I examined a previously made hypothesis that lichen fungi depend on their algal partners for ATP (Pogoda et al. 2018), and conclusively demonstrated that the proposed mechanism is not valid. Similarly, neither of the main lichen symbionts is likely to have such a tight relationship with lichen bacteria and yeasts. This however does not mean that yeasts and bacteria are unnecessary — only that the mechanisms of their contribution are more

complex and harder to demonstrate. In such complex and “fluid” system as a lichen thallus, it might be beneficial to focus on functions and metabolic processes within a lichen (“the song”), and not on individual symbionts (“the singers”), which might come and go, and gain and lose functions (Doolittle & Booth 2017).

Why culture-free methods?

I used culture-free methods because they allowed us to interrogate lichens in all their complexity. Our abilities to perform culture-based experiments are limited: not every lichen symbiont has been cultured so far, and the ones that have been cultured are hard to handle (McDonald et al. 2013). More importantly, lichen symbiosis is still a black box, and we know very little about what happens inside it, which makes it hard to design experiments.

To look inside the black box, I used metagenomic data. Data-driven approaches may not be as good at producing ironclad evidence as hypothesis-driven approaches, but they have a crucial advantage: they allow us to go into uncharted territory (Kell & Oliver 2004). While hypothesis-driven research is great at settling known unknowns, data-driven research can explore unknown unknowns. Metagenomic data allowed me to take an unbiased look into the composition of lichen symbioses and explore the functional potential of the symbionts (Chapters 2 and 4). In these explorations, we found some unexpected results, and formulated hypotheses about the role of lichen yeasts and bacteria. These hypotheses are one of the main outcomes of my thesis.

Another important outcome is the genomes of lichen symbionts. These genomes are (or will be) publicly available for future research, and can be used for further interrogation.

In other parts of my thesis (Chapters 3 and 5), I moved from data exploration to testing hypotheses. Here too, I used culture-free methods. In Chapter 5, I describe a framework I developed for testing how lichen symbionts influence the lichen phenotype, i.e. features of the

lichen as a whole. To achieve this goal, I used intact lichen samples from nature — since recreating lichens in the lab is borderline impossible, only this way we could observe how lichen phenotype changes as a function of the symbiont composition. The hypotheses that I tested using this approach were based on previous, data-driven studies (Spribille et al. 2016, Chapter 2). The interplay between data exploration and hypothesis testing is recognized as an effective strategy in general (Kell & Oliver 2004), and it worked well for exploring lichen symbiosis.

Fuzzy terminology

My results highlight that lichen symbionts do not always fit the terminology used to describe them. Traditionally, the two main partners in the symbiosis have been referred to as mycobiont and photobiont — the main fungus and the phototrophic partner respectively. All other organisms present in a lichen were called lichenicolous or endolichenic (Honegger 2001). All these terms rely on assumptions that do not always hold true. The terms mycobiont and photobiont, as applied to the two main partners, ignore the possibility that other fungi and other phototrophs can be present. This possibility, however, is very real. Here, I confirmed that many lichens contain not one but many different fungi (Chapters 2 and 5), and hypothesized that some lichens might contain phototrophic bacteria in addition to the main phototroph (Chapter 4). The terms lichenicolous and endolichenic assume that these organisms are external to the symbiosis (growing on lichens, therefore not part of the lichen), which also might not be accurate.

In recent years, lichen researchers began using terminology “borrowed” from the studies of animal microbial communities: e.g. lichen microbiome, lichen as a holobiont, etc.

(Aschenbrenner et al. 2014, Grimm et al. 2021). These terms, however, ignore an important difference between animals and lichens. While animal microbiome is well separated from its host, which is a genetically uniform, multicellular organism, in lichens such separation is

problematic. What is a “host” in lichens? Different studies appear to have different answers, calling the host either the main fungal partner (e.g. Rolshausen et al. 2022) or both main partners together (e.g. Grube et al. 2012). To make the matter even more confusing, in older literature the photosynthetic partner was called the host, as it was believed that the main fungus parasitizes it (Fink 1914). The way the terms “lichen microbiota” and “lichen microbiome” are used typically excludes cyanobacteria, but often includes yeasts (e.g. Allen & Lendemer 2022). The line separating the host and the microbiome is inevitably fuzzy in lichens, which are a product of symbiosis.

Knowing how little we actually know about lichens, it might be beneficial to shift our focus away from labels and onto functions and actual metabolic processes.

Outlook

My thesis has opened more new questions than closed the existing ones. Most results presented here come from analyzing genomes, and are, to some extent, tentative. Several avenues of research can be used to test the hypotheses I presented here. First, correlation studies similar to the study presented in Chapter 5 can provide some understanding of how the presence/absence and abundance of symbionts affect the lichen phenotype. Second, metatranscriptomics and metaproteomics applied to intact lichen thalli can help determine whether the genes and pathways I identified in the symbiont genomes are actually expressed in symbiosis. Finally, culture-based methods can be used to follow up on specific symbiotic lineages. Previously, co-culturing experiments provided some information about how the main fungus and the alga interact (Armaleo et al. 2019). Even though culture-based approaches inevitably limit us to those symbionts that have been isolated in culture, adding yeasts and bacteria to co-culturing experiments has a yet unexplored potential.

The results presented in this thesis call for rethinking of the place yeasts and bacteria play in lichens. Integrating these symbionts into the study of the lichen symbiosis can help us to understand how lichen symbioses work — and consequently to bring us closer to knowing how complexity arises in evolution.

References

Allen, J. L., & Lendemer, J. C. (2022). A call to reconceptualize lichen symbioses. *Trends in Ecology & Evolution*, *37*(7), 582–589.

Armaleo, D., Müller, O., Lutzoni, F., Andrésson, Ó. S., Blanc, G., Bode, H. B., ... & Xavier, B. B. (2019). The lichen symbiosis re-viewed through the genomes of *Cladonia grayi* and its algal partner *Asterochloris glomerata*. *BMC Genomics*, *20*(1), 1–33.

Aschenbrenner, I. A., Cardinale, M., Berg, G., & Grube, M. (2014). Microbial cargo: do bacteria on symbiotic propagules reinforce the microbiome of lichens?. *Environmental Microbiology*, *16*(12), 3743–3752.

Bublitz, D. C., Chadwick, G. L., Magyar, J. S., Sandoz, K. M., Brooks, D. M., Mesnage, S., ... & McCutcheon, J. P. (2019). Peptidoglycan production by an insect-bacterial mosaic. *Cell*, *179*(3), 703–712.

Dal Grande, F., Widmer, I., Wagner, H. H., & Scheidegger, C. (2012). Vertical and horizontal photobiont transmission within populations of a lichen symbiosis. *Molecular Ecology*, *21*(13), 3159–3172.

Doolittle, W. F., & Booth, A. (2017). It's the song, not the singer: an exploration of holobiosis and evolutionary theory. *Biology & Philosophy*, *32*(1), 5–24.

- Fink, B. (1914). The relation of the lichen to its algal host. *Transactions of the American Microscopical Society*, 33(1), 5–10.
- Grimm, M., Grube, M., Schiefelbein, U., Zühlke, D., Bernhardt, J., & Riedel, K. (2021). The lichens' microbiota, still a mystery?. *Frontiers in Microbiology*, 12, 714.
- Grube, M., Köberl, M., Lackner, S., Berg, C., & Berg, G. (2012). Host–parasite interaction and microbiome response: effects of fungal infections on the bacterial community of the Alpine lichen *Solorina crocea*. *FEMS Microbiology Ecology*, 82(2), 472–481.
- Honegger, R. (1993). Developmental biology of lichens. *New Phytologist*, 125(4), 659–677.
- Honegger, R. (2000). Simon Schwendener (1829-1919) and the dual hypothesis of lichens. *The Bryologist*, 103(2), 307–313.
- Honegger, R. (2001). The symbiotic phenotype of lichen-forming ascomycetes. In *Fungal associations* (pp. 165–188). Springer, Berlin, Heidelberg.
- Husnik, F., & Keeling, P. J. (2019). The fate of obligate endosymbionts: reduction, integration, or extinction. *Current Opinion in Genetics & Development*, 58, 1–8.
- Kell, D. B., & Oliver, S. G. (2004). Here is the evidence, now what is the hypothesis? The complementary roles of inductive and hypothesis-driven science in the post-genomic era. *Bioessays*, 26(1), 99–105.
- Leiva, D., Fernández-Mendoza, F., Acevedo, J., Carú, M., Grube, M., & Orlando, J. (2021). The bacterial community of the foliose macro-lichen *Peltigera frigida* is more than a mere extension of the microbiota of the subjacent substrate. *Microbial Ecology*, 81(4), 965–976.

- McDonald, T. R., Gaya, E., & Lutzoni, F. (2013). Twenty-five cultures of lichenizing fungi available for experimental studies on symbiotic systems. *Symbiosis*, *59*(3), 165–171.
- Medeiros, I. D., Mazur, E., Miadlikowska, J., Flakus, A., Rodriguez-Flakus, P., Cieślak, E., ... & Lutzoni, F. (2021). Turnover of lecanoroid mycobionts and their Trebouxia photobionts along an elevation gradient in Bolivia highlights the role of environment in structuring the lichen symbiosis. *Frontiers in Microbiology*, *3859*.
- Perreau, J., & Moran, N. A. (2022). Genetic innovations in animal–microbe symbioses. *Nature Reviews Genetics*, *23*(1), 23–39.
- Pogoda, C. S., Keepers, K. G., Lendemer, J. C., Kane, N. C., & Tripp, E. A. (2018). Reductions in complexity of mitochondrial genomes in lichen-forming fungi shed light on genome architecture of obligate symbioses. *Molecular Ecology*, *27*(5), 1155–1169.
- Rolshausen, G., Dal Grande, F., Otte, J., & Schmitt, I. (2022). Lichen holobionts show compositional structure along elevation. *Molecular Ecology*.
- Sanders, W. B. (2001). Lichens: The Interface between Mycology and Plant Morphology: Whereas most other fungi live as an absorptive mycelium inside their food substrate, the lichen fungi construct a plant-like body within which photosynthetic algal symbionts are cultivated. *Bioscience*, *51*(12), 1025–1035.
- Sanders, W. B., & Lücking, R. (2002). Reproductive strategies, relichenization and thallus development observed in situ in leaf-dwelling lichen communities. *New Phytologist*, *155*(3), 425–435.
- Schwendener, S. (1869). Die Algentypen der Flechtengonidien. Basel, Switzerland: Universitaetsbuchdruckerei.

Spribile, T., Resl, P., Stanton, D. E., & Tagirdzhanova, G. (2022). Evolutionary biology of lichen symbioses. *New Phytologist*, 234(5), 1566–1582.

Spribile, T., Tuovinen, V., Resl, P., Vanderpool, D., Wolinski, H., Aime, M. C., ... & McCutcheon, J. P. (2016). Basidiomycete yeasts in the cortex of ascomycete macrolichens. *Science*, 353(6298), 488–492.

Tuovinen, V., Ekman, S., Thor, G., Vanderpool, D., Spribile, T., & Johannesson, H. (2019). Two basidiomycete fungi in the cortex of wolf lichens. *Current Biology*, 29(3), 476–483.

Tuovinen, V., Millanes, A. M., Freire-Rallo, S., Rosling, A., & Wedin, M. (2021). *Tremella macrobasidiata* and *Tremella varia*e have abundant and widespread yeast stages in *Lecanora* lichens. *Environmental Microbiology*, 23(5), 2484–2498.

Bibliography

- Abdel-Hameed, M., Bertrand, R. L., Piercey-Normore, M. D., Sorensen, J. L. (2016). Putative identification of the usnic acid biosynthetic gene cluster by *de novo* whole-genome sequencing of a lichen-forming fungus. *Fungal Biol.* 120(3), 306–316.
- Adrio, J. L. (2017). Oleaginous yeasts: promising platforms for the production of oleochemicals and biofuels. *Biotechnol Bioeng.* 114(9), 1915–1920.
- Ahmadjian, V. (1993). *The lichen symbiosis*. New York: John Wiley & Sons.
- Allen, J. L., & Lendemer, J. C. (2022). A call to reconceptualize lichen symbioses. *Trends in Ecology & Evolution*, 37(7), 582–589.
- Almendras, K., García, J., Carú, M., & Orlando, J. (2018). Nitrogen-fixing bacteria associated with *Peltigera cyanolichens* and *Cladonia chlorolichens*. *Molecules*, 23(12), 3077.
- Alneberg, J., Bjarnason, B. S., De Bruijn, I., Schirmer, M., Quick, J., Ijaz, U. Z., ... & Quince, C. (2014). Binning metagenomic contigs by coverage and composition. *Nature Methods*, 11(11), 1144–1146.
- Altschul, S. F., Gish, W., Miller, W., Myers, E. W., & Lipman, D. J. (1990). Basic local alignment search tool. *Journal of Molecular Biology*, 215(3), 403–410.
- Aramaki, T., Blanc-Mathieu, R., Endo, H., Ohkubo, K., Kanehisa, M., Goto, S., & Ogata, H. (2020). KofamKOALA: KEGG ortholog assignment based on profile HMM and adaptive score threshold. *Bioinformatics*, 36(7), 2251–2252.
- Arikawa, E., Sun, Y., Wang, J., Zhou, Q., Ning, B., Dial, S. L., ... & Yang, J. (2008). Cross-platform comparison of SYBR® Green real-time PCR with TaqMan PCR, microarrays and other

gene expression measurement technologies evaluated in the MicroArray Quality Control (MAQC) study. *BMC Genomics*, *9*(1), 1-12.

Armaleo, D., Müller, O., Lutzoni, F., Andrésson, Ó. S., Blanc, G., Bode, H. B., ... & Xavier, B. B. (2019). The lichen symbiosis re-viewed through the genomes of *Cladonia grayi* and its algal partner *Asterochloris glomerata*. *BMC Genomics*, *20*(1), 1–33.

Aschenbrenner, I. A., Cardinale, M., Berg, G., & Grube, M. (2014). Microbial cargo: do bacteria on symbiotic propagules reinforce the microbiome of lichens?. *Environmental Microbiology*, *16*(12), 3743–3752.

Aschenbrenner, I. A., Cernava, T., Berg, G., & Grube, M. (2016). Understanding microbial multi-species symbioses. *Frontiers in Microbiology*, *7*, 180.

Aschenbrenner, I. A., Cernava, T., Erlacher, A., Berg, G., & Grube, M. (2017). Differential sharing and distinct co-occurrence networks among spatially close bacterial microbiota of bark, mosses and lichens. *Molecular Ecology*, *26*(10), 2826–2838.

Asplund, J., & Gauslaa, Y. (2007). Content of secondary compounds depends on thallus size in the foliose lichen *Lobaria pulmonaria*. *The Lichenologist*, *39*(3), 273–278.

Assié, A., Leisch, N., Meier, D. V., Gruber-Vodicka, H., Tegetmeyer, H. E., Meyerdierks, A., ... & Petersen, J. M. (2020). Horizontal acquisition of a patchwork Calvin cycle by symbiotic and free-living Campylobacterota (formerly Epsilonproteobacteria). *The ISME journal*, *14*(1), 104–122.

Aylward, F.O. (2018). Introduction to calculating dN/dS ratios with codeml. *protocols.io* doi: <https://dx.doi.org/10.17504/protocols.io.qhwdt7e>

- Bates, S. T., Cropsey, G. W., Caporaso, J. G., Knight, R., & Fierer, N. (2011). Bacterial communities associated with the lichen symbiosis. *Applied and Environmental Microbiology*, 77(4), 1309–1314.
- Becquer, A., Trap, J., Irshad, U., Ali, M. A., Claude, P. (2014). From soil to plant, the journey of P through trophic relationships and ectomycorrhizal association. *Front Plant Sci.* 5, 548.
- Bendtsen, J. D., Nielsen, H., von Heijne, G., Brunak, S. (2004). Improved prediction of signal peptides: signalP 3.0. *J Mol Biol.* 340(4), 783–795.
- Bengtsson-Palme, J., Hartmann, M., Eriksson, K. M., Pal, C., Thorell, K., Larsson, D. G. J., & Nilsson, R. H. (2015). METAXA2: improved identification and taxonomic classification of small and large subunit rRNA in metagenomic data. *Molecular Ecology Resources*, 15(6), 1403–1414.
- Beopoulos, A., et al. (2009). *Yarrowia lipolytica* as a model for bio-oil production. *Prog Lipid Res.* 48(6), 375–387.
- Bergmann, T. C., & Werth, S. (2017). Intrathalline distribution of two lichenicolous fungi on *Lobaria* hosts—an analysis based on quantitative real-time PCR. *Herzogia*, 30(1), 253–271.
- Bertrand, R. L., Abdel-Hameed, M., Sorensen, J. L. (2018). Lichen biosynthetic gene clusters. Part I. Genome sequencing reveals a rich biosynthetic potential. *J Nat Prod.* 81(4), 723–731.
- Blanch, M., Blanco, Y., Fontaniella, B., Legaz, M. E., & Vicente, C. (2001). Production of phenolics by immobilized cells of the lichen *Pseudevernia furfuracea*: the role of epiphytic bacteria. *International Microbiology*, 4(2), 89–92.
- Blin, K., et al. (2019). AntiSMASH 5.0: updates to the secondary metabolite genome mining pipeline. *Nucleic Acids Res.* 47(W1), W81–W87.

- Blin, K., Shaw, S., Kloosterman, A. M., Charlop-Powers, Z., van Wezel, G. P., Medema, M. H., & Tilmann, W. (2021). antismash 6.0. *Nucleic Acids Research*.
- Bodenhofer, U., Kothmeier, A., & Hochreiter, S. (2011). APCluster: an R package for affinity propagation clustering. *Bioinformatics*, 27(17), 2463–2464.
- Borges-Walmsley, M. I., Walmsley, A. R. (2000). cAMP signalling in pathogenic fungi: control of dimorphic switching and pathogenicity. *Trends Microbiol.* 8(3), 133–141.
- Bowers, R. M., et al. (2017). Minimum information about a single amplified genome (MISAG) and a metagenome-assembled genome (MIMAG) of bacteria and archaea. *Nat Biotechnol.* 35(8), 725–731.
- Brodo, I., Hawksworth, D. L. (1977). *Alectoria* and allied genera in North America. *Opera Bot.* 42, 1–164.
- Brune, A. (2014). Symbiotic digestion of lignocellulose in termite guts. *Nature Reviews Microbiology*, 12(3), 168–180.
- Bublitz, D.C., Chadwick, G.L., Magyar, J.S., Sandoz, K.M., Brooks, D.M., Mesnage, S., ... McCutcheon, J.P. (2019). Peptidoglycan production by an insect-bacterial mosaic. *Cell*, 179(3), 703–712.
- Buchfink, B., Xie, C., Huson, D. H. (2015). Fast and sensitive protein alignment using DIAMOND. *Nat Methods*. 12(1), 59–60.
- Burton, R. A., Gidley, M. J., Fincher, G. B. (2010). Heterogeneity in the chemistry, structure and function of plant cell walls. *Nat Chem Biol.* 6(10), 724–732.
- Bushnell, B. (2014). BBMap: a fast, accurate, splice-aware aligner. Berkeley (CA): Ernest Orlando Lawrence Berkeley National Laboratory.

Camacho, C., Coulouris, G., Avagyan, V., Ma, N., Papadopoulos, J., Bealer, K., & Madden, T. L. (2009). BLAST+: architecture and applications. *BMC Bioinformatics*, *10*(1), 421.

Capella-Gutiérrez, S., Silla-Martínez, J. M., Gabaldón, T. (2009). trimAl: a tool for automated alignment trimming in large-scale phylogenetic analyses. *Bioinformatics* *25*(15), 1972–1973.

Cardinale, M., Grube, M., Castro Jr, J. V., Müller, H., & Berg, G. (2012). Bacterial taxa associated with the lung lichen *Lobaria pulmonaria* are differentially shaped by geography and habitat. *FEMS Microbiology Letters*, *329*(2), 111–115.

Cardinale, M., Vieira de Castro Jr, J., Müller, H., Berg, G., & Grube, M. (2008). In situ analysis of the bacterial community associated with the reindeer lichen *Cladonia arbuscula* reveals predominance of Alphaproteobacteria. *FEMS Microbiology Ecology*, *66*(1), 63–71.

Casadevall, A., & Pirofski, L. A. (2014). Microbiology: ditch the term pathogen. *Nature*, *516*(7530), 165–166.

Cavanaugh, C. M. (1983). Symbiotic chemoautotrophic bacteria in marine invertebrates from sulphide-rich habitats. *Nature*, *302*(5903), 58–61.

Cengia Sambo, M. (1926). Ancora della polysimbiosi nei licheni ad alghe cianoficee. 1. Batteri simbiotici. *Atti della Società Italiana di Scienze Naturali e del Museo Civico di Storia Naturale in Milano*, *64*, 191–195.

Centeno, D. C., Hell, A. F., Braga, M. R., del Campo, E. M., Casano, L. M. (2016). Contrasting strategies used by lichen microalgae to cope with desiccation-rehydration stress revealed by metabolite profiling and cell wall analysis. *Environ Microbiol.* *18*(5), 1546–1560.

- Černajová, I., Škaloud, P. (2019). The first survey of Cystobasidiomycete yeasts in the lichen genus *Cladonia*; with the description of *Lichenozyma pisutiana* gen. nov., sp. nov. *Fungal Biol.* 123(9), 625–637.
- Cernava, T., Aschenbrenner, I. A., Soh, J., Sensen, C. W., Grube, M., & Berg, G. (2019). Plasticity of a holobiont: desiccation induces fasting-like metabolism within the lichen microbiota. *The ISME journal*, 13(2), 547–556.
- Cernava, T., Erlacher, A., Aschenbrenner, I. A., Krug, L., Lassek, C., Riedel, K., ... & Berg, G. (2017). Deciphering functional diversification within the lichen microbiota by meta-omics. *Microbiome*, 5(1), 1–13.
- Chang, H. X., Yendrek, C. R., Caetano-Anolles, G., Hartman, G. L. (2016). Genomic characterization of plant cell wall degrading enzymes and in silico analysis of xylanases and polygalacturonases of *Fusarium virguliforme*. *BMC Microbiol.* 16(1), 147.
- Chaumeil, P. A., Mussig, A. J., Hugenholtz, P., & Parks, D. H. (2020). GTDB-Tk: a toolkit to classify genomes with the Genome Taxonomy Database. *Bioinformatics*, 36(6), 1925–1927.
- Chen, E. C. H., et al. (2018). High intraspecific genome diversity in the model arbuscular mycorrhizal symbiont *Rhizophagus irregularis*. *New Phytol.* 220(4), 1161–1171.
- Chen, S., Zhou, Y., Chen, Y., & Gu, J. (2018). fastp: an ultra-fast all-in-one FASTQ preprocessor. *Bioinformatics*, 34(17), i884–i890.
- Chomiccki, G., Kiers, E. T., & Renner, S. S. (2020). The evolution of mutualistic dependence. *Annu. Rev. Ecol. Evol. Syst.* 51(1), 409–432.

Chong, R. A., & Moran, N. A. (2016). Intraspecific genetic variation in hosts affects regulation of obligate heritable symbionts. *Proceedings of the National Academy of Sciences*, *113*(46), 13114–13119.

Cissé, O. H., Stajich, J. E. (2019). FGMP: assessing fungal genome completeness. *BMC Bioinformatics* *20*(1), 184.

Cornet, L., Magain, N., Baurain, D., & Lutzoni, F. (2021). Exploring syntenic conservation across genomes for phylogenetic studies of organisms subjected to horizontal gene transfers: A case study with Cyanobacteria and cyanolichens. *Molecular Phylogenetics and Evolution*, *162*, 107100.

Crittenden, P. D., David, J. C., Hawksworth, D. L., & Campbell, F. S. (1995). Attempted isolation and success in the culturing of a broad spectrum of lichen-forming and lichenicolous fungi. *New Phytologist*, *130*(2), 267–297.

Croft, M. T., Lawrence, A. D., Raux-Deery, E., Warren, M. J., & Smith, A. G. (2005). Algae acquire vitamin B12 through a symbiotic relationship with bacteria. *Nature*, *438*(7064), 90–93.

Csardi, G., & Nepusz, T. (2006). The igraph software package for complex network research. *InterJournal, complex systems*, *1695*(5), 1–9.

Dal Grande, F., Widmer, I., Wagner, H. H., & Scheidegger, C. (2012). Vertical and horizontal photobiont transmission within populations of a lichen symbiosis. *Molecular Ecology*, *21*(13), 3159–3172.

de Baets, S., Vandamme, E. J. (2001). Extracellular *Tremella* polysaccharides: structure, properties and applications. *Biotechnol Lett.* *23*(17), 1361–1366.

De Bary, A. (1879). Die erscheinung der symbiose. In Die Erscheinung der Symbiose. De Gruyter.

Delmont, T. O., et al. (2018). Nitrogen-fixing populations of Planctomycetes and Proteobacteria are abundant in surface ocean metagenomes. *Nat Microbiol.* 3(7), 804–813.

Deorowicz, S., Debudaj-Grabysz, A., & Gudyś, A. (2016). FAMSA: Fast and accurate multiple sequence alignment of huge protein families. *Scientific Reports*, 6(1), 1–13.

Déquard-Chablat, M., Sellem, C. H., Golik, P., Bidard, F., Martos, A., Bietenhader, M., ... & Contamine, V. (2011). Two nuclear life cycle–regulated genes encode interchangeable subunits of mitochondrial ATP synthase in *Podospora anserina*. *Molecular Biology and Evolution*, 28(7), 2063-2075.

Doering, T. L. (2009). How sweet it is! Cell wall biogenesis and polysaccharide capsule formation in *Cryptococcus neoformans*. *Annu Rev Microbiol.* 63, 223–247.

Doolittle, W. F., & Booth, A. (2017). It's the song, not the singer: an exploration of holobiosis and evolutionary theory. *Biology & Philosophy*, 32(1), 5–24.

Drew, E. A., & Smith, D. C. (1967). Studies in the physiology of lichens: VIII. Movement of glucose from alga to fungus during photosynthesis in the thallus of *Peltigera polydactyla*. *New Phytologist*, 66(3), 389–400.

Dubovenko, A. G., et al. (2010). Trypsin-like proteins of the fungi as possible markers of pathogenicity. *Fungal Biol.* 114(2–3), 151–159.

Dykstra, H. R., Weldon, S. R., Martinez, A. J., White, J. A., Hopper, K. R., Heimpel, G. E., ... & Oliver, K. M. (2014). Factors limiting the spread of the protective symbiont *Hamiltonella*

defensa in *Aphis craccivora* aphids. *Applied and Environmental Microbiology*, 80(18), 5818–5827.

Ebert, D. (2013). The epidemiology and evolution of symbionts with mixed-mode transmission. *Annual Review of Ecology, Evolution, and Systematics*, 44, 623–643.

Eddy, S. R. (2011). Accelerated profile HMM searches. *PLoS Comput Biol.* 7(10), e1002195.

Edgar, R. C. (2004). MUSCLE: multiple sequence alignment with high accuracy and high throughput. *Nucleic Acids Res.* 32(5), 1792–1797.

El-Gebali, S., et al. (2019). The Pfam protein families database in 2019. *Nucleic Acids Res.* 47(D1), D427–D432.

Emmerich, R., Giez, I., Lange, O. L., & Proksch, P. (1993). Toxicity and antifeedant activity of lichen compounds against the polyphagous herbivorous insect *Spodoptera littoralis*. *Phytochemistry*, 33(6), 1389–1394.

Emms, D. M., Kelly, S. (2018). STAG: species tree inference from all genes. *bioRxiv*. Available from: 10.1101/267914.

Emms, D. M., Kelly, S. (2019). OrthoFinder: phylogenetic orthology inference for comparative genomics. *Genome Biol.* 20(1), 238.

Engel, P., Bartlett, K. D., & Moran, N. A. (2015). The bacterium *Frischella perrara* causes scab formation in the gut of its honeybee host. *MBio*, 6(3), e00193-15.

Epskamp, S., Cramer, A. O., Waldorp, L. J., Schmittmann, V. D., & Borsboom, D. (2012). qgraph: Network visualizations of relationships in psychometric data. *Journal of Statistical Software*, 48, 1–18.

- Erlacher, A., Cernava, T., Cardinale, M., Soh, J., Sensen, C. W., Grube, M., & Berg, G. (2015). Rhizobiales as functional and endosymbiotic members in the lichen symbiosis of *Lobaria pulmonaria* L. *Frontiers in Microbiology*, *6*, 53.
- Esseen, P. A., Olsson, T., Coxson, D., & Gauslaa, Y. (2015). Morphology influences water storage in hair lichens from boreal forest canopies. *Fungal Ecology*, *18*, 26–35.
- Eymann, C., Lassek, C., Wegner, U., Bernhardt, J., Fritsch, O. A., Fuchs, S., ... & Riedel, K. (2017). Symbiotic interplay of fungi, algae, and bacteria within the lung lichen *Lobaria pulmonaria* L. Hoffm. as assessed by state-of-the-art metaproteomics. *Journal of Proteome Research*, *16*(6), 2160–2173.
- Fan, H., et al. (2014). Functional analysis of a subtilisin-like serine protease gene from biocontrol fungus *Trichoderma harzianum*. *J Microbiol.* *52*(2), 129–138.
- Färber, L., Solhaug, K. A., Esseen, P. A., Bilger, W., & Gauslaa, Y. (2014). Sunscreening fungal pigments influence the vertical gradient of pendulous lichens in boreal forest canopies. *Ecology*, *95*(6), 1464–1471.
- Fink, B. (1914). The relation of the lichen to its algal host. *Transactions of the American Microscopical Society*, *33*(1), 5–10.
- Fox, J. & Weisberg, S. (2019) *An R companion to applied regression, 3rd ed.* Sage, Thousand Oaks.
- Frank, A.B. 1877. Über die biologischen Verhältnisse des Thallus einiger Krustenflechten Beitr. *Biol. Pflanz.* *2*, 123–200.
- Frey, K., & Pucker, B. (2020). Animal, Fungi, and Plant Genome Sequences Harbor Different Non-Canonical Splice Sites. *Cells*, *9*(2), 458.

Funk, E. R., Adams, A. N., Spotten, S. M., Van Hove, R. A., Whittington, K. T., Keepers, K. G., ... & Kane, N. C. (2018). The complete mitochondrial genomes of five lichenized fungi in the genus *Usnea* (Ascomycota: Parmeliaceae). *Mitochondrial DNA Part B*, 3(1), 305–308.

Garber, A. I., Neelson, K. H., Okamoto, A., McAllister, S. M., Chan, C. S., Barco, R. A., & Merino, N. (2020). FeGenie: a comprehensive tool for the identification of iron genes and iron gene neighborhoods in genome and metagenome assemblies. *Frontiers in Microbiology*, 37.

García-Angulo, V. A. (2017). Overlapping riboflavin supply pathways in bacteria. *Critical Reviews in Microbiology*, 43(2), 196–209.

Gauslaa, Y., & Solhaug, K. A. (2001). Fungal melanins as a sun screen for symbiotic green algae in the lichen *Lobaria pulmonaria*. *Oecologia*, 126(4), 462–471.

Geshi, N., Harholt, J., Sakuragi, Y., Jensen, J. K., Scheller, H. V. (2018). Glycosyltransferases of the GT47 family. In: *Annual plant reviews online*. p. 265–283.

Gołębiewski, M., & Tretyn, A. (2020). Generating amplicon reads for microbial community assessment with next-generation sequencing. *Journal of Applied Microbiology*, 128(2), 330–354.

Goodenough, U., & Roth, R. (2021). Lichen 5. Medullary and bacterial biofilm layers. *Algal Research*, 58, 102333.

Greshake Tzovaras, B., Segers, F. H., Bicker, A., Dal Grande, F., Otte, J., Anvar, S. Y., ... & Ebersberger, I. (2020). What is in *Umbilicaria pustulata*? A metagenomic approach to reconstruct the holo-genome of a lichen. *Genome Biology and Evolution*, 12(4), 309–324.

Grewe, F., Ametrano, C., Widhelm, T. J., Leavitt, S., Distefano, I., Polyiam, W., ... & Lumbsch, H. T. (2020). Using target enrichment sequencing to study the higher-level phylogeny of the largest lichen-forming fungi family: Parmeliaceae (Ascomycota). *IMA Fungus*, 11(1), 1–11.

- Grijpstra, J. (2008). Capsule biogenesis in *Cryptococcus neoformans*. Utrecht, The Netherlands: Utrecht University.
- Grimm, M., Grube, M., Schiefelbein, U., Zühlke, D., Bernhardt, J., & Riedel, K. (2021). The lichens' microbiota, still a mystery?. *Frontiers in Microbiology*, *12*, 714.
- Grube, M., & Berg, G. (2009). Microbial consortia of bacteria and fungi with focus on the lichen symbiosis. *Fungal Biology Reviews*, *23*(3), 72–85.
- Grube, M., Cernava, T., Soh, J., Fuchs, S., Aschenbrenner, I., Lassek, C., ... & Berg, G. (2015). Exploring functional contexts of symbiotic sustain within lichen-associated bacteria by comparative omics. *The ISME journal*, *9*(2), 412–424.
- Grube, M., Köberl, M., Lackner, S., Berg, C., & Berg, G. (2012). Host–parasite interaction and microbiome response: effects of fungal infections on the bacterial community of the Alpine lichen *Solorina crocea*. *FEMS Microbiology Ecology*, *82*(2), 472–481.
- Gruber-Vodicka, H. R., Seah, B. K., & Pruesse, E. (2020). phyloFlash: rapid small-subunit rRNA profiling and targeted assembly from metagenomes. *Msystems*, *5*(5), e00920–20.
- Gu, Z., & Hübschmann, D. (2021). simplifyEnrichment: an R/Bioconductor package for clustering and visualizing functional enrichment results. *bioRxiv*, doi.org/10.1101/2020.10.27.312116.
- Gu, Z., Eils, R., & Schlesner, M. (2016). Complex heatmaps reveal patterns and correlations in multidimensional genomic data. *Bioinformatics*, *32*(18), 2847–2849.
- Gu, Z., Gu, L., Eils, R., Schlesner, M., & Brors, B. (2014). Circlize implements and enhances circular visualization in R. *Bioinformatics*, *30*(19), 2811–2812.

- Gurevich, A., Saveliev, V., Vyahhi, N., Tesler, G. (2013). QCAST: quality assessment tool for genome assemblies. *Bioinformatics* 29(8), 1072–1075.
- Haas, B. J., Salzberg, S. L., Zhu, W., Pertea, M., Allen, J. E., Orvis, J., ... & Wortman, J. R. (2008). Automated eukaryotic gene structure annotation using EVIDENCEModeler and the Program to Assemble Spliced Alignments. *Genome Biology*, 9(1), R7.
- Haferkamp, I., Schmitz-Esser, S., Wagner, M., Neigel, N., Horn, M., & Neuhaus, H. E. (2006). Tapping the nucleotide pool of the host: novel nucleotide carrier proteins of *Protochlamydia amoebophila*. *Molecular Microbiology*, 60(6), 1534–1545.
- Hale Jr, M. E. (1958). Vitamin requirements of three lichen fungi. *Bulletin of the Torrey Botanical Club*, 182–187.
- Hammer, T. J., Sanders, J. G., & Fierer, N. (2019). Not all animals need a microbiome. *FEMS Microbiology Letters*, 366(10), fnz117.
- Harada, J., Mizoguchi, T., Tsukatani, Y., Yokono, M., Tanaka, A., & Tamiaki, H. (2014). Chlorophyllide a oxidoreductase works as one of the divinyl reductases specifically involved in bacteriochlorophyll a biosynthesis. *Journal of Biological Chemistry*, 289(18), 12716–12726.
- Haridas, S., et al. (2020). 101 Dothideomycetes genomes: a test case for predicting lifestyles and emergence of pathogens. *Stud Mycol.* 96, 141–153.
- Heinz, E., Williams, T. A., Nakjang, S., Noël, C. J., Swan, D. C., Goldberg, A. V., ... & Bernhardt, J. (2012). The genome of the obligate intracellular parasite *Trachipleistophora hominis*: new insights into microsporidian genome dynamics and reductive evolution. *PLoS Pathog*, 8(10), e1002979.

- Helliwell, K. E., Wheeler, G. L., Leptos, K. C., Goldstein, R. E., & Smith, A. G. (2011). Insights into the evolution of vitamin B12 auxotrophy from sequenced algal genomes. *Molecular Biology and Evolution*, *28*(10), 2921–2933.
- Henkel, P. A., Yuzhakova, L. A. (1936). Azotfiksiruyuschie bakterii v lishaynikah [nitrogen-fixing bacteria in lichens]. *Izv Biol Inst Permsk Gos Univ*, *10*, 9–10.
- Henry, C., et al. (2016). Biosynthesis of cell wall mannan in the conidium and the mycelium of *Aspergillus fumigatus*. *Cell Microbiol.* *18*(12), 1881–1891.
- Herrera, M. L., Vallor, A. C., Gelfond, J. A., Patterson, T. F., & Wickes, B. (2009). Strain-dependent variation in 18S ribosomal DNA copy numbers in *Aspergillus fumigatus*. *Journal of Clinical Microbiology*, *47*(5), 1325–1332.
- Herridge, D. F., Peoples, M. B., & Boddey, R. M. (2008). Global inputs of biological nitrogen fixation in agricultural systems. *Plant and Soil*, *311*(1), 1–18.
- Hodkinson, B. P., & Lutzoni, F. (2009). A microbiotic survey of lichen-associated bacteria reveals a new lineage from the Rhizobiales. *Symbiosis*, *49*(3), 163–180.
- Hodkinson, B. P., Gottel, N. R., Schadt, C. W., & Lutzoni, F. (2012). Photoautotrophic symbiont and geography are major factors affecting highly structured and diverse bacterial communities in the lichen microbiome. *Environmental Microbiology*, *14*(1), 147–161.
- Honegger, R. (1993). Developmental biology of lichens. *New Phytologist*, *125*(4), 659–677.
- Honegger, R. (2000). Simon Schwendener (1829–1919) and the dual hypothesis of lichens. *The Bryologist*, *103*(2), 307–313.
- Honegger, R. (2001). The symbiotic phenotype of lichen-forming ascomycetes. In *Fungal Associations* (pp. 165–188). Springer, Berlin, Heidelberg.

- Honegger, R., Bartnicki-Garcia, S. (1991). Cell wall structure and composition of cultured mycobionts from the lichens *Cladonia macrophylla*, *Cladonia caespiticia*, and *Physcia stellaris* (Lecanorales, Ascomycetes). *Mycol Res.* 95(8), 905–914.
- Honegger, R., Brunner, U. (1981). Sporopollenin in the cell walls of *Coccomyxa* and *Myrmecia* phycobionts of various lichens: an ultrastructural and chemical investigation. *Can J Bot.* 59(12), 2713–2734.
- Horton, P., et al. (2007). WoLF PSORT: protein localization predictor. *Nucleic Acids Res.* 35(Web Server issue), W585–W587.
- Huang, L., et al. (2018). DbCAN-seq: a database of carbohydrate-active enzyme (CAZyme) sequence and annotation. *Nucleic Acids Res.* 46(D1), D516–D521.
- Huerta-Cepas, J., et al. (2017). Fast genome-wide functional annotation through orthology assignment by eggNOG-mapper. *Mol Biol Evol.* 34(8), 2115–2122.
- Hurtado, C. A. R., Rachubinski, R. A. (1999). Mhy1 encodes a c2h2-type zinc finger protein that promotes dimorphic transition in the yeast *Yarrowia lipolytica*. *J Bacteriol.* 181(10), 3051–3057.
- Husnik, F., & Keeling, P. J. (2019). The fate of obligate endosymbionts: reduction, integration, or extinction. *Current Opinion in Genetics & Development*, 58, 1–8.
- Husnik, F., Tashyreva, D., Boscaro, V., George, E. E., Lukeš, J., & Keeling, P. J. (2021). Bacterial and archaeal symbioses with protists. *Current Biology*, 31(13), R862–R877.
- Iskina, R. E. (1938). K voprosu ob azotfiksiruyushchikh bakteriyakh v lishaynikakh (On the question of nitrogen-fixing bacteria in lichens). *Izvestiya Permskogo Nauchno-Issledovatel'skogo Instituta*, 11, 133–140.

- Jaffe, A. L., Konno, M., Kawasaki, Y., Kataoka, C., Béjà, O., Kandori, H., ... & Banfield, J. F. (2022). Saccharibacteria harness light energy using Type-1 rhodopsins that may rely on retinal sourced from microbial hosts. *The ISME Journal*, 1–4.
- Jairus, K., Lõhmus, A., & Lõhmus, P. (2009). Lichen acclimatization on retention trees: a conservation physiology lesson. *Journal of Applied Ecology*, 46(4), 930–936.
- Jeong, M. H., Park, S. Y., Kim, J. A., Cheong, Y. H., Hur, J. S. (2015). RDS1 involved in yeast-to-mycelium transition in lichen-forming fungus *Umbilicaria muehlenbergii*. *Korean Mycol Soc News*. 27(2), 93.
- Jiang, D. F., Wang, H. Y., Si, H. L., Zhao, L., Liu, C. P., & Zhang, H. (2017). Isolation and culture of lichen bacteriobionts. *The Lichenologist*, 49(2), 175–181.
- Jiang, X., Zerfaß, C., Feng, S., Eichmann, R., Asally, M., Schäfer, P., & Soyer, O. S. (2018). Impact of spatial organization on a novel auxotrophic interaction among soil microbes. *The ISME journal*, 12(6), 1443–1456.
- Johansson, O., Olofsson, J., Giesler, R., Palmqvist, K. (2011). Lichen responses to nitrogen and phosphorus additions can be explained by the different symbiont responses. *New Phytol.* 191(3), 795–805.
- Jones, D. R., et al. (2018). SACCHARIS: an automated pipeline to streamline discovery of carbohydrate active enzyme activities within polyspecific families and *de novo* sequence datasets. *Biotechnol Biofuels*. 11, 27.
- Jones, P., et al. (2014). InterProScan 5: genome-scale protein function classification. *Bioinformatics* 30(9), 1236–1240.

- Joneson, S., Armaleo, D., Lutzoni, F. (2011). Fungal and algal gene expression in early developmental stages of lichen-symbiosis. *Mycologia* 103(2), 291–306.
- Jousset, A., Bienhold, C., Chatzinotas, A., Gallien, L., Gobet, A., Kurm, V., ... & Hol, W. H. (2017). Where less may be more: how the rare biosphere pulls ecosystems strings. *The ISME journal*, 11(4), 853–862.
- Kadosh, D., Johnson, A. D. (2001). Rfg1, a protein related to the *Saccharomyces cerevisiae* hypoxic regulator Rox1, controls filamentous growth and virulence in *Candida albicans*. *Mol Cell Biol*. 21(7), 2496–2505.
- Kanehisa, M., Goto, S., Kawashima, S., & Nakaya, A. (2002). The KEGG databases at GenomeNet. *Nucleic Acids Research*, 30(1), 42–46.
- Kang, D. D., Li, F., Kirton, E., Thomas, A., Egan, R., An, H., & Wang, Z. (2019). MetaBAT 2: an adaptive binning algorithm for robust and efficient genome reconstruction from metagenome assemblies. *PeerJ*, 7, e7359.
- Kardish, N., Kessel, M., & Galun, M. (1989). Characterization of symbiotic and cultured Nostoc of the lichen *Nephroma laevigatum* Ach. *Symbiosis*, 7, 257–266
- Karimi, E., et al. (2018). Metagenomic binning reveals versatile nutrient cycling and distinct adaptive features in alphaproteobacterial symbionts of marine sponges. *FEMS Microbiol Ecol*. 94(6), fyy074.
- Karunakaran, R., Ebert, K., Harvey, S., Leonard, M. E., Ramachandran, V., & Poole, P. S. (2006). Thiamine is synthesized by a salvage pathway in *Rhizobium leguminosarum* bv. viciae strain 3841. *Journal of Bacteriology*, 188(18), 6661–6668.

Katoh, K., & Standley, D. M. (2013). MAFFT multiple sequence alignment software version 7: improvements in performance and usability. *Molecular Biology and Evolution*, 30(4), 772–780.

Katoh, K., Misawa, K., Kuma, K. I., & Miyata, T. (2002). MAFFT: a novel method for rapid multiple sequence alignment based on fast Fourier transform. *Nucleic Acids Research*, 30(14), 3059–3066.

Keeling, P. J., & McCutcheon, J. P. (2017). Endosymbiosis: the feeling is not mutual. *Journal of Theoretical Biology*, 434, 75–79.

Keepers, K. G. (2021). *Harnessing Genomic and Bioinformatic Tools to Inform Conservation Decisions of Species that Are Vulnerable to Human-Driven Impacts of Climate Change* (Doctoral dissertation, University of Colorado at Boulder).

Kell, D. B., & Oliver, S. G. (2004). Here is the evidence, now what is the hypothesis? The complementary roles of inductive and hypothesis-driven science in the post-genomic era. *Bioessays*, 26(1), 99–105.

Kielak, A. M., Barreto, C. C., Kowalchuk, G. A., Van Veen, J. A., & Kuramae, E. E. (2016). The ecology of Acidobacteria: moving beyond genes and genomes. *Frontiers in Microbiology*, 7, 744.

Kielak, A. M., Castellane, T. C., Campanharo, J. C., Colnago, L. A., Costa, O. Y., Corradi da Silva, M. L., ... & Kuramae, E. E. (2017). Characterization of novel Acidobacteria exopolysaccharides with potential industrial and ecological applications. *Scientific Reports*, 7(1), 1–11.

- Klindworth, A., Pruesse, E., Schweer, T., Peplies, J., Quast, C., Horn, M., & Glöckner, F. O. (2013). Evaluation of general 16S ribosomal RNA gene PCR primers for classical and next-generation sequencing-based diversity studies. *Nucleic Acids Research*, *41*(1), e1.
- Kokkoris, V., Vukicevich, E., Richards, A., Thomsen, C., & Hart, M. M. (2021). Challenges using droplet digital PCR for environmental samples. *Applied Microbiology*, *1*(1), 74–88.
- Kombrink, A., Thomma, B. P. H. J. (2013). LysM effectors: secreted proteins supporting fungal life. *PLoS Pathog.* *9*(12), e1003769.
- Kono, M., Kon, Y., Ohmura, Y., Satta, Y., Terai, Y. (2020). In vitro resynthesis of lichenization reveals the genetic background of symbiosis-specific fungal–algal interaction in *Usnea hakonensis*. *BMC Genomics* *21*(1), 671.
- Korf, I. (2004). Gene finding in novel genomes. *BMC bioinformatics*, *5*(1), 59.
- Koumandou, V. L., & Kossida, S. (2014). Evolution of the F₀F₁ ATP synthase complex in light of the patchy distribution of different bioenergetic pathways across prokaryotes. *PLoS Comput Biol*, *10*(9), e1003821.
- Krogh, A., Larsson, B., von Heijne, G., Sonnhammer, E. L. L. (2001). Predicting transmembrane protein topology with a hidden Markov model: application to complete genomes. *J Mol Biol.* *305*(3), 567–580.
- Kues, U., Ruhl, M. (2011). Multiple multi-copper oxidase gene families in basidiomycetes—what for? *Curr Genomics.* *12*(2), 72–94.
- Lanfear, R., Calcott, B., Ho, S. Y. W., Guindon, S. (2012). PartitionFinder: combined selection of partitioning schemes and substitution models for phylogenetic analyses. *Mol Biol Evol.* *29*(6), 1695–1701.

- Langmead, B., Salzberg, S. L. (2012). Fast gapped-read alignment with Bowtie 2. *Nat Methods*. 9(4), 357–359.
- Le, S. Q., Gascuel, O. (2008). An improved general amino acid replacement matrix. *Mol Biol Evol*. 25(7), 1307–1320.
- Leal, J. A., Prieto, A., Bernabé, M., Hawksworth, D. L. (2010). An assessment of fungal wall heteromannans as a phylogenetically informative character in ascomycetes. *FEMS Microbiol Rev*. 34(6), 986–1014.
- Leandro, M. J., Fonseca, C., Gonçalves, P. (2009). Hexose and pentose transport in ascomycetous yeasts: an overview. *FEMS Yeast Res*. 9(4), 511–525.
- Lee, I. R., Chow, E. W., Morrow, C. A., Djordjevic, J. T., Fraser, J. A. (2011). Nitrogen metabolite repression of metabolism and virulence in the human fungal pathogen *Cryptococcus neoformans*. *Genetics* 188(2), 309–323.
- Lefever, S., Pattyn, F., Hellemans, J., & Vandesompele, J. (2013). Single-nucleotide polymorphisms and other mismatches reduce performance of quantitative PCR assays. *Clinical Chemistry*, 59(10), 1470–1480.
- Leiva, D., Fernández-Mendoza, F., Acevedo, J., Carú, M., Grube, M., & Orlando, J. (2021). The bacterial community of the foliose macro-lichen *Peltigera frigida* is more than a mere extension of the microbiota of the subjacent substrate. *Microbial Ecology*, 81(4), 965–976.
- Lendemmer, J. C., Keepers, K. G., Tripp, E. A., Pogoda, C. S., McCain, C. M., & Kane, N. C. (2019). A taxonomically broad metagenomic survey of 339 species spanning 57 families suggests cystobasidiomycete yeasts are not ubiquitous across all lichens. *American Journal of Botany*, 106(8), 1090–1095.

- Lenova, L. I., Blum, O. B. (1983). K voprosu o tret'em komponente lishaynikov (On the question of the third component of lichens). *Bot Zhurn.* 68, 21–28.
- Lesage, G., et al. (2004). Analysis of β -1,3-glucan assembly in *Saccharomyces cerevisiae* using a synthetic interaction network and altered sensitivity to caspofungin. *Genetics* 167(1), 35–49.
- Lesage, G., et al. (2005). An interactional network of genes involved in chitin synthesis in *Saccharomyces cerevisiae*. *BMC Genet.* 6(1), 8.
- Letunic, I., & Bork, P. (2007). Interactive Tree Of Life (iTOL): an online tool for phylogenetic tree display and annotation. *Bioinformatics*, 23(1), 127–128.
- Letunic, I., Bork, P. (2019). Interactive Tree of Life (iTOL) v4: recent updates and new developments. *Nucleic Acids Res.* 47(W1), W256–W259.
- Levy Karin, E., Mirdita, M., Söding, J. (2020). MetaEuk—sensitive, high-throughput gene discovery, and annotation for large-scale eukaryotic metagenomics. *Microbiome* 8(1), 1–15.
- Li, H., & Durbin, R. (2009). Fast and accurate short read alignment with Burrows–Wheeler transform. *Bioinformatics*, 25(14), 1754–1760.
- Li, H., et al. (2009). The Sequence Alignment/Map format and SAMtools. *Bioinformatics* 25(16), 2078–2079.
- Liba, C. M., Ferrara, F. I. D. S., Manfio, G. P., Fantinatti-Garboggini, F., Albuquerque, R. C., Pavan, C., ... & Barbosa, H. R. (2006). Nitrogen-fixing chemo-organotrophic bacteria isolated from cyanobacteria-deprived lichens and their ability to solubilize phosphate and to release amino acids and phytohormones. *Journal of Applied Microbiology*, 101(5), 1076–1086.

- Lindgren, H., Diederich, P., Goward, T., & Myllys, L. (2015). The phylogenetic analysis of fungi associated with lichenized ascomycete genus *Bryoria* reveals new lineages in the Tremellales including a new species *Tremella huuskonenii* hyperparasitic on *Phacopsis huuskonenii*. *Fungal Biology*, 119(9), 844–856.
- Liu, L., Zhang, Z., et al. (2015). Bioinformatical analysis of the sequences, structures and functions of fungal polyketide synthase product template domains. *Sci Rep.* 5, 10463.
- Liu, X.-Z., Wang, Q.-M., et al. (2015). Phylogeny of tremellomycetous yeasts and related dimorphic and filamentous basidiomycetes reconstructed from multiple gene sequence analyses. *Stud Mycol.* 81, 1–26.
- Lomsadze, A., Burns, P. D., Borodovsky, M. (2014). Integration of mapped RNA-Seq reads into automatic training of eukaryotic gene finding algorithm. *Nucleic Acids Res.* 42(15), e119.
- Louca, S., Parfrey, L. W., & Doebeli, M. (2016). Decoupling function and taxonomy in the global ocean microbiome. *Science*, 353(6305), 1272–1277.
- Maciá-Vicente, J. G., Jansson, H. B., Talbot, N. J., & Lopez-Llorca, L. V. (2009). Real-time PCR quantification and live-cell imaging of endophytic colonization of barley (*Hordeum vulgare*) roots by *Fusarium equiseti* and *Pochonia chlamydosporia*. *New Phytologist*, 182(1), 213-228.
- Majoros, W. H., Pertea, M., & Salzberg, S. L. (2004). TigrScan and GlimmerHMM: two open source ab initio eukaryotic gene-finders. *Bioinformatics*, 20(16), 2878–2879.
- Margulis, L. (1981). Symbiosis in cell evolution: Life and its environment on the early earth.
- Margulis, L., & Fester, R. (Editors). 1991. Symbiosis as a source of evolutionary innovation, speciation and morphogenesis. MIT Press, Cambridge

- Mark, K., et al. (2020). Contrasting co-occurrence patterns of photobiont and cystobasidiomycete yeast associated with common epiphytic lichen species. *New Phytol.* 227(5), 1362–1375.
- Martinou, A., Koutsioulis, D., Bouriotis, V. (2003). Cloning and expression of a chitin deacetylase gene (CDA2) from *Saccharomyces cerevisiae* in *Escherichia coli*: purification and characterization of the cobalt-dependent recombinant enzyme. *Enzyme Microb Tech.* 32(6), 757–763.
- Matsuura, Y., et al. (2018). Recurrent symbiont recruitment from fungal parasites in cicadas. *Proc Natl Acad Sci USA.* 115(26), E5970–E5979.
- McCutcheon, J. P., McDonald, B. R., & Moran, N. A. (2009). Convergent evolution of metabolic roles in bacterial co-symbionts of insects. *Proceedings of the National Academy of Sciences*, 106(36), 15394–15399.
- McDonald, T. R., Gaya, E., & Lutzoni, F. (2013). Twenty-five cultures of lichenizing fungi available for experimental studies on symbiotic systems. *Symbiosis*, 59(3), 165–171.
- McDonald, T. R., Mueller, O., Dietrich, F. S., & Lutzoni, F. (2013). High-throughput genome sequencing of lichenizing fungi to assess gene loss in the ammonium transporter/ammonia permease gene family. *BMC Genomics*, 14(1), 1–14.
- McFall-Ngai, M., Hadfield, M. G., Bosch, T. C., Carey, H. V., Domazet-Lošo, T., Douglas, A. E., ... & Wernegreen, J. J. (2013). Animals in a bacterial world, a new imperative for the life sciences. *Proceedings of the National Academy of Sciences*, 110(9), 3229–3236.
- Medeiros, I. D., Mazur, E., Miadlikowska, J., Flakus, A., Rodriguez-Flakus, P., Cieślak, E., ... & Lutzoni, F. (2021). Turnover of lecanoroid mycobionts and their *Trebouxia* photobionts along an

elevation gradient in Bolivia highlights the role of environment in structuring the lichen symbiosis. *Frontiers in Microbiology*, 3859.

Millanes, A. M., Diederich, P., Ekman, S., Wedin, M. (2011). Phylogeny and character evolution in the jelly fungi (Tremellomycetes, Basidiomycota, Fungi). *Mol Phylogenet Evol.* 61(1), 12–28.

Millanes, A. M., Diederich, P., Wedin, M. (2016). *Cyphobasidium* gen. nov., a new lichen-inhabiting lineage in the Cystobasidiomycetes (Pucciniomycotina, Basidiomycota, Fungi). *Fungal Biol.* 120(11), 1468–1477.

Millanes, A. M., Truong, C., Westberg, M., Diederich, P., Wedin, M. (2014). Host switching promotes diversity in host-specialized mycoparasitic fungi: uncoupled evolution in the *Biatoropsis-Usnea* system. *Evolution* 68(6), 1576–1593.

Millbank, J. W., & Kershaw, K. A. (1970). Nitrogen metabolism in lichens: III. Nitrogen fixation by internal cephalodia in *Lobaria pulmonaria*. *New Phytologist*, 69(2), 595–597.

Miller, M. A., Pfeiffer, W., Schwartz, T. (2010). Creating the CIPRES science gateway for inference of large phylogenetic trees. In: *2010 Gateway Computing Environments Workshop, GCE 2010*. p. 1–8.

Modenesi, P., Vanzo, C. (1986). The cortical surfaces in *Parmelia saxatilis* and *P. caperata*: a histochemical approach. *The Lichenologist* 18(4), 329–338.

Moriya, Y., Itoh, M., Okuda, S., Yoshizawa, A. C., Kanehisa, M. (2007). KAAS: an automatic genome annotation and pathway reconstruction server. *Nucleic Acids Res.* 35(Web Server issue), W182–W185.

Murad, A. M. A., et al. (2001). NRG1 represses yeast–hypha morphogenesis and hypha-specific gene expression in *Candida albicans*. *EMBO J.* 20(17), 4742–4752.

- Murali, A., Bhargava, A., & Wright, E. S. (2018). IDTAXA: a novel approach for accurate taxonomic classification of microbiome sequences. *Microbiome*, 6(1), 1–14.
- Nagy, L. G., Kovács, G. M., & Krizsán, K. (2018). Complex multicellularity in fungi: evolutionary convergence, single origin, or both?. *Biological Reviews*, 93(4), 1778–1794.
- Nakamura, A. M., Nascimento, A. S., Polikarpov, I. (2017). Structural diversity of carbohydrate esterases. *Biotechnol Res Innov.* 1(1), 35–51.
- Nash, T. H. (Ed.). (1996). *Lichen biology*. Cambridge University Press.
- Nguyen, L. T., Schmidt, H. A., Von Haeseler, A., & Minh, B. Q. (2015). IQ-TREE: a fast and effective stochastic algorithm for estimating maximum-likelihood phylogenies. *Molecular Biology and Evolution*, 32(1), 268–274.
- Noh, H. J., Baek, K., Hwang, C. Y., Shin, S. C., Hong, S. G., & Lee, Y. M. (2019). *Lichenihabitans psoromatis* gen. nov., sp. nov., a member of a novel lineage (Lichenihabitaceae fam. nov.) within the order of Rhizobiales isolated from Antarctic lichen. *International Journal of Systematic and Evolutionary Microbiology*, 69(12), 3837–3842.
- Nurk, S., Meleshko, D., Korobeynikov, A., & Pevzner, P. A. (2017). metaSPAdes: a new versatile metagenomic assembler. *Genome Research*, 27(5), 824–834.
- Oberwinkler, F. (2017). Yeasts in Pucciniomycotina. *Mycol Progress*. 16(9):831–856.
- Oksanen, J., Blanchet, F. G., Friendly, M., Kindt, R., Legendre, P., McGlinn, D., Minchin, P. R., O'Hara, R. B., Simpson, G. L., Solymos, P., Stevens, M. H. H., Szoecs E., Wagner, H. (2020). vegan: Community Ecology Package. R package version 2.5-7. <https://CRAN.R-project.org/package=vegan>

- Olm, M. R., Brown, C. T., Brooks, B., & Banfield, J. F. (2017). dRep: a tool for fast and accurate genomic comparisons that enables improved genome recovery from metagenomes through de-replication. *The ISME journal*, *11*(12), 2864–2868.
- Overmann, J., Abt, B., & Sikorski, J. (2017). Present and future of culturing bacteria. *Annual Review of Microbiology*, *71*, 711–730.
- Palmqvist, K., Dahlman, L., Valladares, F., Tehler, A., Sancho, L. G., & Mattsson, J. E. (2002). CO₂ exchange and thallus nitrogen across 75 contrasting lichen associations from different climate zones. *Oecologia*, *133*(3), 295–306.
- Pankratov, T. A., Grouzdev, D. S., Patutina, E. O., Kolganova, T. V., Suzina, N. E., & Berestovskaya, J. J. (2020). *Lichenibacterium ramalinae* gen. nov, sp. nov., *Lichenibacterium minor* sp. nov., the first endophytic, beta-carotene producing bacterial representatives from lichen thalli and the proposal of the new family Lichenibacteriaceae within the order Rhizobiales. *Antonie van Leeuwenhoek*, *113*(4), 477–489.
- Pankratov, T. A., Nikitin, P. A., & Patutina, E. O. (2022). Genome Analysis of Two Lichen Bacteriobionts, *Lichenibacterium ramalinae* and *Lichenibacterium minor*: Toxin–Antitoxin Systems and Secretion Proteins. *Microbiology*, *91*(2), 160–172.
- Pankratov, T. A., Serkebaeva, Y. M., Kulichevskaya, I. S., Liesack, W., & Dedysh, S. N. (2008). Substrate-induced growth and isolation of Acidobacteria from acidic *Sphagnum* peat. *The ISME Journal*, *2*(5), 551–560.
- Paradis, E., & Schliep, K. (2019). ape 5.0: an environment for modern phylogenetics and evolutionary analyses in R. *Bioinformatics*, *35*(3), 526–528.

- Park, S. Y., et al. (2013). *Agrobacterium tumefaciens*-mediated transformation of the lichen fungus, *Umbilicaria muehlenbergii*. *PLoS One* 8(12), e83896.
- Parks, D. H., Imelfort, M., Skennerton, C. T., Hugenholtz, P., & Tyson, G. W. (2015). CheckM: assessing the quality of microbial genomes recovered from isolates, single cells, and metagenomes. *Genome Research*, 25(7), 1043–1055.
- Pellegrin, C., Morin, E., Martin, F. M., Veneault-Fourrey, C. (2015). Comparative analysis of secretomes from ectomycorrhizal fungi with an emphasis on small-secreted proteins. *Front Microbiol.* 6, 1278.
- Pereira, I., Madeira, A., Prista, C., Loureiro-Dias, M. C., Leandro, M. J. (2014). Characterization of new polyol/H⁺ symporters in *Debaryomyces hansenii*. *PLoS One* 9(2), e88180.
- Perreau, J., & Moran, N. A. (2022). Genetic innovations in animal–microbe symbioses. *Nature Reviews Genetics*, 23(1), 23–39.
- Philippe, G., et al. (2020). Cutin and suberin: assembly and origins of specialized lipidic cell wall scaffolds. *Curr Opin Plant Biol.* 55, 11–20.
- Phinney, N. H., Gauslaa, Y., & Solhaug, K. A. (2019). Why chartreuse? The pigment vulpinic acid screens blue light in the lichen *Letharia vulpina*. *Planta*, 249(3), 709–718.
- Pogoda, C. S., Keepers, K. G., Lendemer, J. C., Kane, N. C., & Tripp, E. A. (2018). Reductions in complexity of mitochondrial genomes in lichen-forming fungi shed light on genome architecture of obligate symbioses. *Molecular Ecology*, 27(5), 1155–1169.
- Pogoda, C. S., Keepers, K. G., Nadiadi, A. Y., Bailey, D. W., Lendemer, J. C., Tripp, E. A., & Kane, N. C. (2019). Genome streamlining via complete loss of introns has occurred multiple times in lichenized fungal mitochondria. *Ecology and Evolution*, 9(7), 4245–4263.

- Price, M. N., Dehal, P. S., Arkin, A. P. (2010). FastTree 2—Approximately maximum-likelihood trees for large alignments. *PLoS One* 5(3), e9490.
- Puri, K. M., Butardo, V., & Sumer, H. (2021). Evaluation of natural endosymbiosis for progress towards artificial endosymbiosis. *Symbiosis*, 84, 1–17
- Qian, L., Jia, F., Jingxuan, S., Manqun, W., & Julian, C. (2018). Effect of the secondary symbiont *Hamiltonella defensa* on fitness and relative abundance of *Buchnera aphidicola* of wheat aphid, *Sitobion miscanthi*. *Frontiers in Microbiology*, 9, 582.
- R Core Team (2013). R: A language and environment for statistical computing.
- Rawlings, N. D., et al. (2018). The MEROPS database of proteolytic enzymes, their substrates and inhibitors in 2017 and a comparison with peptidases in the PANTHER database. *Nucleic Acids Res.* 46(D1), D624–D632.
- Resl, P., Bujold, A. R., Tagirdzhanova, G., Meidl, P., Freire Rallo, S., Kono, M., ... & Spribille, T. (2022). Large differences in carbohydrate degradation and transport potential among lichen fungal symbionts. *Nature Communications*, 13(1), 1–13.
- Revell, L. J. (2012). phytools: An R package for phylogenetic comparative biology (and other things). *Methods Ecol. Evol.* 3, 217–223.
- Richardson, D. H. S., & Smith, D. C. (1968). Lichen physiology: X. The isolated algal and fungal symbionts of *Xanthoria aureola*. *New Phytologist*, 67(1), 69–77.
- Richly, E., & Leister, D. (2004). NUMTs in sequenced eukaryotic genomes. *Molecular Biology and Evolution*, 21(6), 1081–1084.
- Rigden, D. J. (2008). The histidine phosphatase superfamily: structure and function. *Biochem J.* 409(2), 333–348.

- Rolshausen, G., Dal Grande, F., Otte, J., & Schmitt, I. (2022). Lichen holobionts show compositional structure along elevation. *Molecular Ecology*.
- Ruby, E. G., & McFall-Ngai, M. J. (1992). A squid that glows in the night: development of an animal-bacterial mutualism. *Journal of Bacteriology*, *174*(15), 4865–4870.
- Saary, P., Kale, V., & Finn, R. (2022). Large-scale analysis reveals the distribution of novel cellular microbes across multiple biomes and kingdoms. In prep.
- Saary, P., Mitchell, A. L., & Finn, R. D. (2020). Estimating the quality of eukaryotic genomes recovered from metagenomic analysis with EukCC. *Genome Biology*, *21*(1), 1–21.
- Sanders, W. B. (2001). Lichens: The Interface between Mycology and Plant Morphology: Whereas most other fungi live as an absorptive mycelium inside their food substrate, the lichen fungi construct a plant-like body within which photosynthetic algal symbionts are cultivated. *Bioscience*, *51*(12), 1025–1035.
- Sanders, W. B., & Lücking, R. (2002). Reproductive strategies, relichenization and thallus development observed in situ in leaf-dwelling lichen communities. *New Phytologist*, *155*(3), 425–435.
- Sanz-Martín, J. M., et al. (2016). A highly conserved metalloprotease effector enhances virulence in the maize anthracnose fungus *Colletotrichum graminicola*. *Mol Plant Pathol*. *17*(7), 1048–1062.
- Sapp, J. (2010). On the Origin of Symbiosis. In *Symbioses and Stress* (pp. 3–18). Springer, Dordrecht.
- Schliep, K. P. (2011). phangorn: phylogenetic analysis in R. *Bioinformatics*, *27*(4), 592–593.

- Schneider, T., Schmid, E., de Castro Jr, J. V., Cardinale, M., Eberl, L., Grube, M., ... & Riedel, K. (2011). Structure and function of the symbiosis partners of the lung lichen (*Lobaria pulmonaria* L. Hoffm.) analyzed by metaproteomics. *Proteomics*, *11*(13), 2752–2756.
- Schroeckh, V., et al. (2009). Intimate bacterial-fungal interaction triggers biosynthesis of archetypal polyketides in *Aspergillus nidulans*. *Proc Natl Acad Sci USA*. *106*(34), 14558–14563.
- Schwendener, S. (1869). Die Algentypen der Flechtengonidien. Basel, Switzerland: Universitaetsbuchdruckerei.
- Schwendener, S. (1869). Die Algentypen der Flechtengonidien. Basel, Switzerland: Universitaetsbuchdruckerei.
- Seemann, T. (2014). Prokka: rapid prokaryotic genome annotation. *Bioinformatics*, *30*(14), 2068–2069.
- Sepey, M., Manni, M., & Zdobnov, E. M. (2019). BUSCO: assessing genome assembly and annotation completeness. In M. Kollmar (Ed.) *Gene Prediction* (pp. 227–4245). New York, NY: Humana.
- Sitepu, I. R., et al. (2014). Oleaginous yeasts for biodiesel: current and future trends in biology and production. *Biotechnol Adv*. *32*(7), 1336–1360.
- Smith, D. C. (1979). Is a lichen a good model of interactions in nutrient-limited environments? In: Shilo M, ed. *Strategies of microbial life in extreme environments: report of the Dahlem Workshop on Strategy of Life in Extreme Environments, Berlin, 1978, November 20–24*. Weinheim, Germany: Verlag Chemie, 291–301.
- Smith, D. C., & Douglas, A. E. (1987). *The Biology of Symbiosis* London: Edward Arnold.

Smith, S. E., Jakobsen, I., Grønlund, M., Smith, F. A. (2011). Roles of arbuscular mycorrhizas in plant phosphorus nutrition: interactions between pathways of phosphorus uptake in arbuscular mycorrhizal roots have important implications for understanding and manipulating plant phosphorus acquisition. *Plant Physiol.* 156(3), 1050–1057.

Sonesson, M., Sveinbjörnsson, B., Tehler, A., & Carlsson, B. Å. (2007). A comparison of the physiology, anatomy and ribosomal DNA in alpine and subalpine populations of the lichen *Nephroma arcticum*—the effects of an eight-year transplant experiment. *The Bryologist*, 110(2), 244–253.

Sperschneider, J., Dodds, P. N., Gardiner, D. M., Singh, K. B., Taylor, J. M. (2018). Improved prediction of fungal effector proteins from secretomes with EffectorP 2.0. *Mol Plant Pathol.* 19(9), 2094–2110.

Spribille, T. (2018). Relative symbiont input and the lichen symbiotic outcome. *Current Opinion in Plant Biology*, 44, 57–63.

Spribille, T., Resl, P., Stanton, D. E., & Tagirdzhanova, G. (2022). Evolutionary biology of lichen symbioses. *New Phytologist*, 234(5), 1566–1582.

Spribille, T., Tagirdzhanova, G., Goyette, S., Tuovinen, V., Case, R., & Zandberg, W. F. (2020). 3D biofilms: in search of the polysaccharides holding together lichen symbioses. *FEMS Microbiology Letters*, 367(5), fnaa023.

Spribille, T., Tuovinen, V., Resl, P., Vanderpool, D., Wolinski, H., Aime, M. C., ... & McCutcheon, J. P. (2016). Basidiomycete yeasts in the cortex of ascomycete macrolichens. *Science*, 353(6298), 488–492.

- Stamatakis, A. (2014). RAxML version 8: a tool for phylogenetic analysis and post-analysis of large phylogenies. *Bioinformatics* 30(9), 1312–1313.
- Stanke, M., Steinkamp, R., Waack, S., & Morgenstern, B. (2004). AUGUSTUS: a web server for gene finding in eukaryotes. *Nucleic Acids Research*, 32(suppl_2), W309–W312.
- Stewart, C. R. A., Lendemer, J. C., Keepers, K. G., Pogoda, C. S., Kane, N. C., McCain, C. M., & Tripp, E. A. (2018). *Lecanora markjohnstonii* (Lecanoraceae, lichenized Ascomycetes), a new sorediate crustose lichen from the southeastern United States. *The Bryologist*, 121(4), 498–512.
- Sudbery, P. E. (2011). Growth of *Candida albicans* hyphae. *Nat Rev Microbiol.* 9(10), 737–748.
- Sun, H. J., & Friedmann, E. I. (2005). Communities adjust their temperature optima by shifting producer-to-consumer ratio, shown in lichens as models: II. Experimental verification. *Microbial Ecology*, 49(4), 528–535.
- Suyama, M., Torrents, D., & Bork, P. (2006). PAL2NAL: robust conversion of protein sequence alignments into the corresponding codon alignments. *Nucleic Acids Research*, 34(suppl_2), W609–W612.
- Tagirdzhanova, G., Saary, P., Tingley, J. P., Díaz-Escandón, D., Abbott, D. W., Finn, R. D., & Spribille, T. (2021). Predicted input of uncultured fungal symbionts to a lichen symbiosis from metagenome-assembled genomes. *Genome Biology and Evolution*, 13(4), evab047.
- Takashima, M., Hamamoto, M., Nakase, T. (2000). Taxonomic significance of fucose in the class urediniomycetes: distribution of fucose in cell wall and phylogeny of urediniomycetous yeasts. *Syst Appl Microbiol.* 23(1), 63–70.
- Tang, K., Liu, Y., Zeng, Y., Feng, F., Jin, K., & Yuan, B. (2021a). An Aerobic Anoxygenic Phototrophic Bacterium Fixes CO₂ via the Calvin-Benson-Bassham Cycle. *bioRxiv*.

- Tang, K., Yuan, B., Jia, L., Pan, X., Feng, F., & Jin, K. (2021b). Spatial and temporal distribution of aerobic anoxygenic phototrophic bacteria: key functional groups in biological soil crusts. *Environmental Microbiology*, *23*(7), 3554–3567.
- Taş, N., de Jong, A. E., Li, Y., Trubl, G., Xue, Y., & Dove, N. C. (2021). Metagenomic tools in microbial ecology research. *Current Opinion in Biotechnology*, *67*, 184–191.
- Taylor, S. C., Laperriere, G., & Germain, H. (2017). Droplet Digital PCR versus qPCR for gene expression analysis with low abundant targets: from variable nonsense to publication quality data. *Scientific Reports*, *7*(1), 1–8.
- Taylor, S., Wakem, M., Dijkman, G., Alsarraj, M., & Nguyen, M. (2010). A practical approach to RT-qPCR—publishing data that conform to the MIQE guidelines. *Methods*, *50*(4), S1–S5.
- Tellenbach, C., Grünig, C. R., & Sieber, T. N. (2010). Suitability of quantitative real-time PCR to estimate the biomass of fungal root endophytes. *Applied and Environmental Microbiology*, *76*(17), 5764–5772.
- The UniProt Consortium. (2019). UniProt: a worldwide hub of protein knowledge. The UniProt Consortium. *Nucleic Acids Res.* *47*(D1), D506–D515.
- Tretiach, M., Bertuzzi, S., Candotto Carniel, F., & Virgilio, D. (2013). Seasonal acclimation in the epiphytic lichen *Parmelia sulcata* is influenced by change in photobiont population density. *Oecologia*, *173*(3), 649–663.
- Tuovinen, V., Ekman, S., Thor, G., Vanderpool, D., Spribille, T., & Johannesson, H. (2019). Two basidiomycete fungi in the cortex of wolf lichens. *Current Biology*, *29*(3), 476–483.

- Tuovinen, V., Millanes, A. M., Freire-Rallo, S., Rosling, A., Wedin, M. (2021). *Tremella macrobasidiata* and *Tremella varia*e have abundant and widespread yeast stages in *Lecanora* lichens. *Environ Microbiol.* doi: 10.1111/1462-2920.15455.
- Uritskiy, G. V., DiRuggiero, J., & Taylor, J. (2018). MetaWRAP—a flexible pipeline for genome-resolved metagenomic data analysis. *Microbiome*, 6(1), 1–13.
- Valladares, F., Sancho, L. G., & Ascaso, C. (1996). Functional analysis of the intrathalline and intracellular chlorophyll concentrations in the lichen family Umbilicariaceae. *Annals of Botany*, 78(4), 471–477.
- Van Arnem, E. B., Currie, C. R., & Clardy, J. (2018). Defense contracts: molecular protection in insect-microbe symbioses. *Chemical Society Reviews*, 47(5), 1638–1651.
- van der Heijden, M. G., Martin, F. M., Selosse, M. A., & Sanders, I. R. (2015). Mycorrhizal ecology and evolution: the past, the present, and the future. *New Phytologist*, 205(4), 1406–1423.
- Velmala, S., Myllys, L., Halonen, P., Goward, T., & Teuvo, A. H. T. I. (2009). Molecular data show that *Bryoria fremontii* and *B. tortuosa* (Parmeliaceae) are conspecific. *The Lichenologist*, 41(3), 231–242.
- Volpiano, C. G., Sant’Anna, F. H., Ambrosini, A., de São José, J. F. B., Beneduzi, A., Whitman, W. B., ... & Passaglia, L. M. P. (2021). Genomic metrics applied to Rhizobiales (Hyphomicrobiales): species reclassification, identification of unauthentic genomes and false type strains. *Frontiers in Microbiology*, 12, 614957.

- von Meijenfeldt, F. A., Arkhipova, K., Cambuy, D. D., Coutinho, F. H., & Dutilh, B. E. (2019). Robust taxonomic classification of uncharted microbial sequences and bins with CAT and BAT. *Genome Biology*, *20*(1), 1–14.
- Wang, L. G., Lam, T. T. Y., Xu, S., Dai, Z., Zhou, L., Feng, T., ... & Yu, G. (2020a). Treeio: an R package for phylogenetic tree input and output with richly annotated and associated data. *Molecular Biology and Evolution*, *37*(2), 599–603.
- Wang, S., Meade, A., Lam, H. M., & Luo, H. (2020b). Evolutionary timeline and genomic plasticity underlying the lifestyle diversity in Rhizobiales. *Msystems*, *5*(4), e00438–20.
- Wang, Y., Coleman-Derr, D., Chen, G., Gu, Y. Q. (2015). OrthoVenn: a web server for genome wide comparison and annotation of orthologous clusters across multiple species. *Nucleic Acids Res.* *43*(W1), W78–W84.
- Wang, Y., Wei, X., Bian, Z., Wei, J., Xu, J.-R. (2020). Coregulation of dimorphism and symbiosis by cyclic AMP signaling in the lichenized fungus *Umbilicaria muhlenbergii*. *Proc Natl Acad Sci USA*. *117*(38), 23847–23858.
- West, N. J., Parrot, D., Fayet, C., Grube, M., Tomasi, S., & Suzuki, M. T. (2018). Marine cyanolichens from different littoral zones are associated with distinct bacterial communities. *PeerJ*, *6*, e5208.
- West, P. T., Probst, A. J., Grigoriev, I. V., Thomas, B. C., Banfield, J. F. (2018). Genome-reconstruction for eukaryotes from complex natural microbial communities. *Genome Res.* *28*(4), 569–580.
- Wickham, H. (2016) ggplot2: Elegant Graphics for Data Analysis. Springer-Verlag New York.

Wickham, H. & Girlich, M. (2022). tidyr: Tidy Messy Data. R package version 1.2.0.

<https://CRAN.R-project.org/package=tidyr>

Wickham, H. & Seidel, D. (2020). scales: Scale Functions for Visualization. R package version 1.1.1. <https://CRAN.R-project.org/package=scales>

Wickham, H., François, R., Henry, L., & Müller, K. (2018). Dplyr: A grammar of data manipulation (R package v1.0.8). <https://CRAN.R-project.org/package=dplyr>

Wohlfahrt, G., Amelynck, C., Ammann, C., Arneth, A., Bamberger, I., Goldstein, A. H., ... & Schoon, N. (2015). An ecosystem-scale perspective of the net land methanol flux: synthesis of micrometeorological flux measurements. *Atmospheric Chemistry and Physics*, 15(13), 7413–7427.

Wolfe, S. A., Nekludova, L., Pabo, C. O. (2000). DNA recognition by Cys2His2 zinc finger proteins. *Annu Rev Biophys Biomol Struct.* 29, 183–212.

Wood, S. N., Pya, N., & Säfken, B. (2016). Smoothing parameter and model selection for general smooth models. *Journal of the American Statistical Association*, 111(516), 1548–1563.

Wright, E. S. (2016). Using DECIPHER v2. 0 to analyze big biological sequence data in R. *R J.*, 8(1), 352.

Wyatt, G. A., Kiers, E. T., Gardner, A., & West, S. A. (2014). A biological market analysis of the plant-mycorrhizal symbiosis. *Evolution*, 68(9), 2603–2618.

Yang, Z. (2007). PAML 4: phylogenetic analysis by maximum likelihood. *Molecular Biology and Evolution*, 24(8), 1586–1591.

- Ye, J., Coulouris, G., Zaretskaya, I., Cutcutache, I., Rozen, S., & Madden, T. L. (2012). Primer-BLAST: a tool to design target-specific primers for polymerase chain reaction. *BMC Bioinformatics*, *13*(1), 1–11.
- Yellowlees, D., Rees, T. A. V., & Leggat, W. (2008). Metabolic interactions between algal symbionts and invertebrate hosts. *Plant, Cell & Environment*, *31*(5), 679–694.
- Yoon, S. H., Ha, S. M., Lim, J., Kwon, S., & Chun, J. (2017). A large-scale evaluation of algorithms to calculate average nucleotide identity. *Antonie Van Leeuwenhoek*, *110*(10), 1281–1286.
- Yoshimura, I., Yamamoto, Y., Nakano, T., & Finnie, J. (2002). Isolation and culture of lichen photobionts and mycobionts. In I. C. Kranner, R. P. Beckett & A. K. Varma (Eds.), *Protocols in Lichenology* (pp. 3–33). Berlin, Heidelberg: Springer.
- Yurkov, V. V., & Beatty, J. T. (1998). Aerobic anoxygenic phototrophic bacteria. *Microbiology and Molecular Biology Reviews*, *62*(3), 695–724.
- Yurkov, V., & Csotonyi, J. T. (2009). New light on aerobic anoxygenic phototrophs. In *The purple phototrophic bacteria* (pp. 31–55). Springer, Dordrecht.
- Zaheer, R., Noyes, N., Polo, R. O., Cook, S. R., Marinier, E., Van Domselaar, G., ... & McAllister, T. A. (2018). Impact of sequencing depth on the characterization of the microbiome and resistome. *Scientific Reports*, *8*(1), 1–11.
- Zaragoza, O., et al. (2009). The capsule of the fungal pathogen *Cryptococcus neoformans*. *Adv Appl Microbiol.* *68*, 133–216.
- Zhang, C., Rabiee, M., Sayyari, E., Mirarab, S. (2018). ASTRAL-III: polynomial time species tree reconstruction from partially resolved gene trees. *BMC Bioinformatics* *19*(Suppl 6), 153.

Zilber-Rosenberg, I., & Rosenberg, E. (2008). Role of microorganisms in the evolution of animals and plants: the hologenome theory of evolution. *FEMS Microbiology Reviews*, 32(5), 723–735.

Zoccarato, L., Sher, D., Miki, T., Segrè, D., & Grossart, H. P. (2022). A comparative whole-genome approach identifies bacterial traits for marine microbial interactions. *Communications Biology*, 5(1), 1–13.

Zuccaro, A., et al. (2011). Endophytic life strategies decoded by genome and transcriptome analyses of the mutualistic root symbiont *Piriformospora indica*. *PLoS Pathog.* 7(10), e1002290.